

# EARLY IRON PRODUCTION IN THE LEVANT

SMELTING AND SMITHING AT EARLY 1<sup>ST</sup> MILLENNIUM BC TELL HAMMEH, JORDAN,  
AND TEL BETH-SHEMESH, ISRAEL

HARALD ALEXANDER VELDHIJZEN

Thesis submitted to the University of London  
for the degree of Doctor of Philosophy

Institute of Archaeology,  
University College London

AUGUST 2005



UMI Number: U593473

All rights reserved

INFORMATION TO ALL USERS

The quality of this reproduction is dependent upon the quality of the copy submitted.

In the unlikely event that the author did not send a complete manuscript and there are missing pages, these will be noted. Also, if material had to be removed, a note will indicate the deletion.



UMI U593473

Published by ProQuest LLC 2013. Copyright in the Dissertation held by the Author.  
Microform Edition © ProQuest LLC.

All rights reserved. This work is protected against  
unauthorized copying under Title 17, United States Code.



ProQuest LLC  
789 East Eisenhower Parkway  
P.O. Box 1346  
Ann Arbor, MI 48106-1346



## ABSTRACT

The use of iron in the Near East is first attested by the sporadic occurrence of iron artefacts during the Bronze Age. By the end of the Late Bronze Age, however, use of iron metal gradually increases to such a level that one can assume a reasonably regular production of iron metal from terrestrial ores by smelting. However, very few iron metallurgical workshops or installations have been discovered in the Near East thus far. Of these, most are apparently related to secondary smithing, and very few if any have clear evidence for iron smelting.

Recent fieldwork at Tell Hammeh, Jordan, identified a major iron smelting operation dated to ca. 930 Cal BC. Excavations in 2001 and 2003 at Tel Beth-Shemesh, Israel, uncovered remains of a full-scale smithing operation, dating to ca. 900 Cal BC. Dedicated excavation techniques were developed and refined for both sites, aiming at optimal recovery of both technological and archaeological information. The excavated materials were comprehensively analysed using relevant scientific analytical techniques, which included the development and application of a calibration method for quantitative bulk chemical analysis of iron-rich materials by XRF.

Combining laboratory data and fieldwork, this thesis explores the particular lime-rich and iron-oxide-poor nature of the Hammeh slags as a function of the composition of the local ore and the sacrificial contribution of technical ceramics (tuyères and furnace wall). Furthermore, it compares the smelting operations at Tell Hammeh with the smithing at Tel Beth-Shemesh, both in terms of their respective archaeological contexts as well as of their technological residues. This aims at the identification and reconstruction of the *chaîne opératoire* of the technologies at both sites.

The reconstructed technological processes are discussed in terms of their place in the socio-economic and cultural context of the early first millennium BC of the Levant. Beyond providing new data about early iron metallurgy, the integrated archaeological and laboratory approach, the excavation methods applied, the analytical methodology, as well as the archaeometric data presented here may serve as a model for the excavation, interpretation, or comparison of future (and previous) discoveries of iron metallurgy in the Near East.

# TABLE OF CONTENTS

<b>ABSTRACT .....</b>	<b>2</b>
<b>TABLE OF CONTENTS .....</b>	<b>3</b>
<b>LIST OF FIGURES .....</b>	<b>7</b>
<b>LIST OF TABLES .....</b>	<b>12</b>
<b>ACKNOWLEDGEMENTS .....</b>	<b>15</b>
AFFILIATIONS .....	15
ACKNOWLEDGMENTS .....	16
<b>CHAPTER 1: INTRODUCTION .....</b>	<b>17</b>
INTRODUCTION .....	17
AIMS AND OBJECTIVES .....	19
<i>Introduction</i> .....	19
<i>Three Areas of Interest</i> .....	20
<i>Objectives and Context</i> .....	20
<b>CHAPTER 2: THE SOCIAL CONTEXT OF TECHNOLOGY .....</b>	<b>23</b>
INTRODUCTION .....	23
TRADITIONS IN THINKING ABOUT TECHNOLOGY .....	24
<i>The French-European Tradition</i> .....	24
<i>The Anglo-American Tradition</i> .....	26
<i>Recent Development: Agency and Practice Theory</i> .....	30
DEFINITIONS OF TECHNOLOGY .....	32
RELEVANT CONCEPTS .....	34
<i>The Concept of the Chaîne opératoire</i> .....	34
<i>The Concept of Technological Style</i> .....	36
<i>Organisation of Production</i> .....	38
THE ETHNOGRAPHY OF AFRICAN METALLURGY .....	41
DISCUSSION AND CONCLUSION .....	42
<b>CHAPTER 3: A BRIEF TECHNOLOGY AND HISTORY OF IRON .....</b>	<b>45</b>
INTRODUCTION .....	45
MAKING IRON METAL; SMELTING AND SMITHING TECHNOLOGY .....	46
<i>Basic Information on Iron</i> .....	47
<i>Summary of Bloomery Iron Smelting and Smithing Technology</i> .....	47
<i>Ore</i> .....	49
<i>Mineral Dressing</i> .....	51
Comminution .....	51
Roasting .....	52
<i>Smelting</i> .....	52
<i>Primary Smithing</i> .....	56
<i>Secondary Smithing</i> .....	57
THE EARLY HISTORY OF IRON METAL IN THE NEAR EAST .....	58
<i>Introduction</i> .....	58
<i>The Chronology of Iron Artefacts</i> .....	59
Before 3000 BC .....	60
The Early Bronze Age (ca. 3000-2000 BC) .....	60
The Middle Bronze Age (ca. 2000-1600 BC) .....	61
The Late Bronze Age (ca. 1600-1150 BC) .....	61
The Early Iron Age / Iron Age I (ca. 1150-1000 BC) .....	62
The Full Iron Age / Iron Age II (ca. 1000-586 BC) .....	62
<i>Ideas on the Origin and Spread of Iron Technology in the Near East</i> .....	63
Introduction .....	63
Anatolia .....	64
Cyprus/Greece .....	64
Assyria .....	65

Iran.....	65
Levant.....	66
Discussion .....	67
<i>Evidence for Iron Production in the Near East and Mediterranean World</i> .....	67
SUMMARY.....	72
<b>CHAPTER 4: THE ARCHAEOLOGY OF TELL HAMMEH.....</b>	<b>74</b>
INTRODUCTION .....	74
THE LOCATION OF TELL HAMMEH.....	75
RESOURCES FOR IRON PRODUCTION.....	77
<i>Ore</i> .....	77
<i>Clay</i> .....	78
<i>Fuel</i> .....	79
<i>Water</i> .....	80
<i>Wind</i> .....	80
EXCAVATION HISTORY.....	80
<i>The 1994 Survey</i> .....	80
<i>The 1996 Rescue Excavation</i> .....	81
<i>The 1997 Rescue Excavation</i> .....	82
THE 2000 SEASON.....	83
<i>Aims of the 2000 Season</i> .....	83
<i>Excavation Method: Laying out a Grid and Squares</i> .....	84
<i>Collection and Registration in the Field</i> .....	85
<i>The Furnace Structures</i> .....	86
<i>Interpretation of the 2000 Excavation</i> .....	89
<i>The 2001 Sampling Season</i> .....	90
CHRONOLOGICAL FRAMEWORK.....	91
<i>Periods Present on Tell Hammeh</i> .....	91
<i>Dating the Iron Production</i> .....	92
<i>The Socio-Economic Context of the Iron Production</i> .....	95
SUMMARY AND INTERPRETATIONS.....	97
<b>CHAPTER 5: THE ARCHAEOLOGY OF TEL BETH-SHEMESH .....</b>	<b>101</b>
THE LOCATION OF TEL BETH-SHEMESH.....	101
THE EXCAVATION HISTORY OF TEL BETH-SHEMESH .....	102
EXCAVATING THE BETH-SHEMESH SMITHY .....	104
AIM OF THE METALLURGICAL EXCAVATION APPROACH.....	105
THE METALLURGICAL EXCAVATION TECHNIQUES.....	105
THE METALLURGICAL ASSEMBLAGE AT BETH-SHEMESH .....	108
SUMMARY.....	109
<b>CHAPTER 6: ANALYTICAL METHODS AND METHODOLOGY.....</b>	<b>111</b>
INTRODUCTION .....	111
SAMPLE SELECTION AND PREPARATION .....	112
<i>Sample Selection</i> .....	112
<i>Sample Preparation</i> .....	113
Introduction.....	113
Cutting.....	113
Mounting.....	114
Grinding and Polishing .....	114
Milling .....	115
Pelletising.....	116
MACROSCOPIC ANALYSIS.....	116
MINERALOGICAL ANALYSIS .....	117
<i>Optical Microscopy</i> .....	117
<i>X-Ray Diffraction (XRD)</i> .....	117
<i>Back Scatter Electron Imaging (BSE)</i> .....	119
CHEMICAL ANALYSIS.....	120
<i>X-Ray Fluorescence Spectrometry (XRF)</i> .....	120

<i>Scanning Electron Microscope- Energy Dispersive Spectrometry (SEM-EDS)</i> .....	120
<i>Electron Probe Micro Analysis (EPMA)</i> .....	122
STATISTICAL ANALYSIS.....	123
<i>Principal Component Analysis (PCA)</i> .....	123
<b>CHAPTER 7: DEVELOPMENT OF ‘SLAG_FUN’, AN ANALYTICAL (P)ED-XRF METHOD FOR IRON-RICH MATERIALS.....</b>	<b>125</b>
INTRODUCTION .....	125
X-RAY FLUORESCENCE SPECTROMETRY (ED-XRF AND WD-XRF).....	125
POLARISING ENERGY DISPERSIVE X-RAY FLUORESCENCE ((P)ED-XRF) .....	126
THE SPECTRO X-LAB PRO 2000 (P)ED-XRF CALIBRATION METHODS.....	129
DESIGN AND DEVELOPMENT OF THE ‘SLAG_FUN’ METHOD .....	131
<i>Measurement Settings</i> .....	131
<i>Deconvolution Settings</i> .....	134
<i>Evaluation Settings</i> .....	134
CERTIFIED REFERENCE MATERIALS (CRMs).....	135
<i>Selection and Preparation</i> .....	135
<i>Installing the Standards</i> .....	138
TESTING AND APPLICATION OF THE ‘SLAG_FUN’ METHOD .....	138
CONCLUSIONS.....	143
<b>CHAPTER 8: ANALYSIS OF THE HAMMEH MATERIAL.....</b>	<b>146</b>
INTRODUCTION .....	146
THE MUGHARET AL-WARDA ORE.....	147
<i>Location and Previous Study of the Ore Source</i> .....	147
<i>Further Characterisation of the Ore</i> .....	148
<i>Discarded Ore</i> .....	150
<i>Summary</i> .....	151
THE TUYÈRES .....	152
<i>Introduction</i> .....	152
<i>Quantities and Scale of Operation</i> .....	152
<i>Sampling of the Tuyères</i> .....	153
<i>Shape</i> .....	154
<i>Bore</i> .....	155
<i>Angle</i> .....	156
<i>Length</i> .....	156
<i>Standardisation</i> .....	159
<i>Melting of the Ceramic</i> .....	159
<i>Chemical Composition of the Tuyères and the Local Clay</i> .....	160
<i>Other Square Section Tuyères in the Near East</i> .....	161
<i>Summary and Discussion</i> .....	162
THE SLAG .....	164
<i>Introduction</i> .....	164
<i>Quantities and Scale of Operation</i> .....	165
<i>Classification and Sampling</i> .....	166
<i>Analysis of the Slag Groups</i> .....	170
Furnace Slags (Incompletely Reduced Ore).....	170
Furnace Bottom Slag.....	174
Tap Slags.....	175
Technical ‘Ceramic-rich’ Slags .....	183
Primary Smithing Slags.....	186
<i>Discussions</i> .....	188
Sulphur in the Slag .....	188
Trace Elements and Relations between Materials.....	190
Efficiency of the Process.....	191
Principal Component Analysis.....	192
<i>Summary</i> .....	194
THE CHARCOAL.....	197
THE METAL ARTIFACTS .....	199

TECHNICAL CERAMICS AND FUEL ASH IN THE FORMATION OF SLAG .....	201
<i>Introduction</i> .....	201
<i>Mass Balance Calculations</i> .....	203
<i>Comparison of Warda Ore and Hammeh Slag</i> .....	204
<i>Contribution of Technical Ceramic to Hammeh Slag Formation</i> .....	208
<i>Remaining Discrepancies</i> .....	213
INTERPRETATIONS AND CONCLUSIONS.....	214
<b>CHAPTER 9: ANALYSIS OF THE BETH-SHEMESH MATERIAL .....</b>	<b>217</b>
INTRODUCTION .....	217
FORMATION AND ANALYSIS OF THE SLAG .....	217
SPATIAL PATTERNS OF THE HAMMERSCALE AND SLAG PRILLS.....	225
THE TUYÈRES .....	230
IRON AND COPPER (ALLOY) ARTEFACTS.....	231
INTERPRETATIONS AND CONCLUSIONS.....	231
<b>CHAPTER 10: INTERPRETATIONS AND CONCLUSIONS.....</b>	<b>234</b>
INTRODUCTION .....	234
RECONSTRUCTION OF TECHNOLOGY.....	235
<i>Iron Smelting at Tell Hammeh (az-Zarqa)</i> .....	235
<i>Iron Smithing at Tel Beth-Shemesh</i> .....	239
<i>Comparing Smelting and Smithing</i> .....	241
THE PLACE OF HAMMEH AND BETH-SHEMESH IN THE HISTORY OF IRON .....	243
ORGANISATION OF PRODUCTION AND TECHNOLOGICAL CHOICES.....	244
ORIGINAL CONTRIBUTIONS AND SUGGESTIONS FOR FUTURE RESEARCH .....	245
<b>APPENDIX 1. BULK CHEMICAL ANALYSES.....</b>	<b>248</b>
<b>APPENDIX 2. SEM-EDS ANALYSES.....</b>	<b>265</b>
<b>APPENDIX 3. PRINCIPAL COMPONENT ANALYSES .....</b>	<b>275</b>
PCA SCORES AND LOADING VECTOR VALUES OF THE HAMMEH SYSTEM.....	276
PCA SCORES AND LOADING VECTOR VALUES OF THE HAMMEH SYSTEM.....	276
PCA SCORES AND LOADING VECTOR VALUES OF THE BETH-SHEMESH SECONDARY SMITHING SLAGS COMPARED WITH THE HAMMEH TAP AND PRIMARY SMITHING SLAGS.....	278
<b>APPENDIX 4. GLOSSARY OF THE MATERIAL SCIENCE OF IRON .....</b>	<b>280</b>
<b>REFERENCES .....</b>	<b>299</b>

## LIST OF FIGURES

Figure 1. Flow chart of the integrated process of pre-industrial iron production. The chart shows four stages (black labels) of a generic <i>chaîne opératoire</i> (central column). Materials entering the process are in the left column, those produced are in the right column. Activities are in italics, materials used and produced in regular case. The chart does not represent processes that move ‘upwards’ such as repair or reworking of objects.....	50
Figure 2. Theoretical model of a bloomery iron shaft furnace. The drawing shows various stages of the smelting process. The physical breaking up of the ore, the formation of slag, and the transportation of metal particles by the slag are schematically shown on the left. Ranges of furnace temperatures, the formation of an iron bloom near tuyère level, the deposition of slag at the bottom of the furnace as well potential tapping of the slag, and melting of furnace wall and/or tuyère ceramic are indicated in the furnace itself. The chemical reactions taking place at the various locations and temperature zones of the furnace are indicated on the right (from Pleiner 2000, 134, Fig. 33).....	55
Figure 3. Map of the southern Levant, indicating the location of Tell Hammeh (az-Zarqa) and several of the major sites in the Jordan Valley. ....	76
Figure 4. View of Tell Hammeh, seen from the south. The Zarqa River is visible in the foreground. The tell itself clearly shows the bulldozer cut around its southern and eastern side.....	77
Figure 5. Plan of Tell Hammeh, showing the 1996 and 1997 squares in grey, and the 2000 squares in red (based on the survey of the Tell by Muwafaq Bataineh, Yarmouk University) .....	86
Figure 6. Plan of square A/B7 near the end of excavation, showing tuyère fragments in green, possible furnace wall material in orange, larger slag pieces in black, scarce pottery in pink, and the 75 x 75 cm grid in blue. Empty grids were either excavated before the drawing was made (e.g. F4), or have not been fully excavated (row D). ....	88
Figure 7. AMS <sup>14</sup> C calibration curve for sample IPAB7.118 (source: Beta Analytical) .....	94
Figure 8. AMS <sup>14</sup> C Calibration curve for sample IPAB7.157 (source: Beta Analytical) .....	95
Figure 9. Map of the Southern Levant, showing the location of Beth-Shemesh.....	101
Figure 10. Plan of Tel Beth-Shemesh, showing the areas excavated by MacKenzie (1911-1912), Grant (1928-1933), and Tel Aviv University (grey and black), indicating the location of the iron workshop. Drawing by S. Bunimovitz and Z. Lederman. ....	103
Figure 11. Possible iron billet found in square E/T49. Exact stratigraphic relation to the smithy unclear. ....	104
Figure 12. Meitar Lederman dragging a magnet above the surface of a grid in E/T48 to recover hammerscale.....	106
Figure 13. Plan of square E/T48, showing the grid system in light blue, various partial potential hearth structures in dark red, stone wall in grey and concentrations of ash bordered within grey. The blue border in the north of the square indicates a row of pits, or potentially a sequence of hearth structures that was excavated in the 2001 season.....	107
Figure 14. Shows the principle of Bragg's Law, where incident beam angle equals the diffracted beam angle. Image after MATTER (MATTER 2000).....	118
Figure 15. Schematic view of the incident electron beam and reflected primary and secondary electrons in a Scanning Electron Microscope (SEM). ....	121
Figure 16. The principle of polarisation (P)ED-XRF, showing the orientation of secondary target and sample in relation to the beam.....	127
Figure 17. The effect of background noise reduction by (P)ED-XRF, compared to (standard) ED-XRF and WD-XRF (after Schramm undated b, 10, figure 7).....	128
Figure 18. X-Lab Pro method development. Showing the ‘Slag_fun’ development screen with the CRMs in the background. The cascading boxes show the method-editing box, the ‘evaluation’ settings box, and the fundamental parameter calibration box showing the settings for Fe respectively. ....	130
Figure 19. The principle of Rayleigh scattering (on the left) compared to Compton scattering (on the right). ....	133
Figure 20. Periodic table of elements. Copyright Dr. Mark J. Winter; <a href="http://www.webelements.com/UniversityofSheffield">www.webelements.com/University of Sheffield</a> . ....	133
Figure 21. Isopachs (contours indicating the thickness) and cross sections of the iron ore deposit at Mugharet al-Warda, from Bender (Bender 1968, 150, figure 144), after van den Boom and Lahloub (van den Boom and Lahloub 1962). ....	147
Figure 22. Haematite ore sample HA 65, sampled by the author from the surface near one of the mineshafts at Mugharet al-Warda.....	148
Figure 23. SR-XRD spectrum of sample HA 65, showing two measurements, one with the beam at a 0 degree angle (in black), the other at a 90 degree angle (in red). Both measurements show a clear pattern that corresponds to haematite (the standard peaks of haematite are shown in blue). Analysis	

by Synchrotron Radiation-XRD, at the Daresbury Synchrotron Radiation Source (SRS), by Dr Manolis Pantos. ....	150
Figure 24. Plan of square A/B7 near the end of excavation, showing the 75 x 75 cm grid in blue, and the location of several larger tuyère segments within that grid in green. Empty grids were either excavated before the drawing was made (e.g. F4), or have not been fully excavated (row D). ....	154
Figure 25. Frontal and lateral view of tuyère IPAB7.161a, showing the molten nozzle of a square section tuyère, fused with the technical ceramic of the furnace wall. Remnants of unvittrified furnace wall are also preserved, both below and above the tuyère. An 'eyelid', formed by molten technical ceramic flowing down and pushed up and forward by the airflow, is visible above the bore. A large 'beard' of molten ceramic material with adhering slag can also be seen. Some three centimetres behind the molten nozzle, one can see the 'rim', a greyish band indicating the extent to which reducing conditions in the furnace affected the ceramic, simultaneously suggesting a downward angle for the tuyère. ....	156
Figure 26. Four 'complete' (i.e. rear-end to molten nozzle) tuyères from Tell Hammeh, showing lengths up to 25 cm, with burnt and molten nozzles, and widened rear ends. The possible angle of insertion of these tuyères in the furnace wall is reflected by the grey/black demarcation of the reducingly fired zone at the nozzle (especially in the second sample from the left). The fragments further show a slight tapering towards the nozzle. ....	157
Figure 27. Reconstruction of the potential full length of a Hammeh tuyère. This image shows 'complete' rear end IPAB7.137 (seen from the top) and small molten nozzle IPAB7.37 (seen from the side). The dashed line indicates the possible tapering from rear to front of the tuyère. ....	158
Figure 28. Square section tuyère F1270 from Tell Deir 'Alla. ....	162
Figure 29. Furnace slags B1 and B2, showing the rusty exterior of the samples, with organic material embedded in the rust (both samples) and a lump of adhering ceramic (sample B1). ....	170
Figure 30. BSE micrograph of furnace slag D1, showing wüstite (egg-shaped, light grey), xenomorphic iron hydroxide (FeOOH, mid grey), and a few inclusions of metallic iron (white). The matrix consists of variations of glass with precipitating laths (dark grey). ....	171
Figure 31. Cross Polarised Light Micrograph of furnace slag B4, image width ca. 1.8 mm, showing massive haematite ore with formations of goethite (indicated by the orange internal reflections). The cracks in the otherwise solid haematite indicate the first stages of breaking up of the ore through roasting. ....	171
Figure 32. Cross Polarised Light Micrographs of furnace slags B3 (left, image width ca. 1.8 mm), showing a fragment of unreduced haematite contained within formations of iron hydroxides (banded structures), and B4 (right, image width ca. 1.8 mm), showing unreduced haematite (blue-grey, on the left) and (possibly postdepositional) iron hydroxides (possibly goethite (FeOOH) (red-brown internal reflection, centre), and lepidocrocite (FeOH) (orange internal reflection, on the right). ....	172
Figure 33. Sample F2, showing a layered structure, with rust and organic material between those layers. ....	174
Figure 34. BSE micrograph of sample F2, showing a glassy matrix, (mid-dark grey), with olivine laths (mid grey), and thick dendritic wüstite in the left bottom corner, and a skin of mostly various iron hydroxides (FeOOH) that has partly separated from the slag. The dark areas are voids, and a small piece of attached charcoal can be seen in the centre right of the picture. ....	174
Figure 35. Tap slags A1 and A2, showing free flowing (tapped) structure of the slag (both samples), as well as 'striation' of the surface (sample A1). ....	176
Figure 36. Tap slag C2, showing a clear flowing structure with multiple runs of slag. The right bottom shows some contact with soil or furnace wall, and may indicate a vertical flowing, presumably down the outside of a furnace shaft. ....	176
Figure 37. BSE micrograph of tap slag A1, showing a glassy matrix (dark grey), with feathery devitrification (mid-grey) and wüstite dendrites (light grey). ....	177
Figure 38. BSE Micrograph of tap slag A1. Showing a glassy matrix (dark-grey), with feathery devitrification (mid-grey), wüstite dendrites (FeO, white), magnetite from oxygen penetration near the surface (light grey), and possible iscorite (Fe <sub>7</sub> SiO <sub>10</sub> , needle-shaped), the black area is the edge of the sample and shows a band of iron hydroxide (FeOOH). ....	177
Figure 39. BSE micrograph of tap slag C1, showing an aggregate of metallic iron (pan-shaped, whitish) in a glassy matrix with olivine and pyroxene laths (dark-mid grey), groups of thin wüstite dendrites (light grey) and some zoned hercynitic magnetite (block-shaped, mid-grey). Some of the hercynite spinels are zoned, with a darker core of more hercynite component and a rim of magnetite. The black areas are pores in the sample. ....	178
Figure 40. BSE micrograph of tap slag C1, showing a tapping band between two flows of slag. The edges of these flows consist predominantly of a glassy matrix (grey) with small formations of fayalitic laths (lighter grey) and some precipitation of thin wüstite dendrites (light grey) where the two flows touch. ....	179

- Figure 41. BSE micrograph of tap slag E2 showing skeletal fayalitic/olivine laths (mid-grey) in a glassy matrix (darker grey), with small dendritic wüstite (light grey). Tiny droplets of probable FeS (lightest grey) are interspersed between the laths..... 179
- Figure 42. The tap slags plotted in the  $\text{CaO (+MgO)} - \text{FeO (+MnO)} - \text{SiO}_2 (+\text{Al}_2\text{O}_3)$  liquidus temperature diagram, indicating their solidification temperature. The linear spread of the samples illustrates that they form a continuum of compositions, ranging between ore like ( $\text{FeO}+\text{MnO}$  corner) and more ceramic like ( $\text{SiO}_2+\text{Al}_2\text{O}_3$  corner). Most samples cluster in a (minimum) temperature area of between 1100 and 1150 °C..... 182
- Figure 43. Samples G1 and H1, showing bottom of black glass 'ceramic' slag with flow patterns and impressions (G1), and black-green flows of 'ceramic' slag with attachment to ceramic material on one side (H1)..... 183
- Figure 44. BSE micrograph of 'ceramic-rich' slag G1, showing an amorphous mass of glass and a thin tapping band of iron oxide or hydroxide (possibly wüstite) flanked by darker conglomerates of glass that is richer in  $\text{Al}_2\text{O}_3$  and  $\text{K}_2\text{O}$  than the matrix. .... 184
- Figure 45. Primary smithing slag F1, showing a concavo-convex shape, soil embedded in the bottom and rust as well as remains of furnace/hearth ceramic on top; primary smithing slag F3, showing a more plano-convex shape, and revealing the internal vesicular structure of the slag..... 186
- Figure 46. BSE micrograph of primary smithing slag F1, showing a calcio-olivine glassy matrix, (mid-dark grey), with solid laths of leucite ( $\text{KAlSi}_2\text{O}_6$ ; dark grey), large 2-phased olivine blocks (mid-grey, and slightly lighter), and precipitations of spinel with hercynitic (Al) and ulvitic ( $\text{TiO}_2$ ) components (whitish). .... 187
- Figure 47. Principal Component Analysis of the Tell Hammeh Smelting System. The graph shows how each of the Hammeh smelting residues forms a relatively clear cluster, whilst the samples as a whole clearly illustrate the continuum of composition. This continuum ranges from being more closely related to the Warda ore, to being more closely related to the tuyère technical ceramic. The loading vectors of the original variables support this interpretation. The graph shows Principal Components 1 and 2. (The scores and loading vector values can be found in appendix 3)..... 193
- Figure 48. Principal Component Analysis of the Tell Hammeh Smelting System. The graph shows a second view (more linear) of how each of the Hammeh smelting residues forms a relatively clear cluster, whilst the samples as a whole clearly illustrate the continuum of composition. This continuum ranges from being more closely related to the Warda ore, to being more closely related to the tuyère technical ceramic. This corresponds with the loading vectors of the original variables. The graph shows Principal Component 1 and 3. (The scores and loading vector values can be found in appendix 3). .... 194
- Figure 49. Mass balances of Mugharet al-Warda ore (sample HA 65), showing the composition of the hypothetical slag resulting from that ore, in comparison with the actual Hammeh slag. The graph clearly shows the large discrepancy in the major oxides  $\text{SiO}_2$ ,  $\text{Al}_2\text{O}_3$ , and  $\text{CaO}$ , as well as in the alkali and earth-alkali oxides. Results by (P)ED-XRF, using the 'slag\_fun' calibration method (April 2005). Values are expressed in wt% and normalised to 100%. .... 206
- Figure 50. Mass balances of Mugharet al-Warda ore (sample HA 66), showing the composition of the hypothetical slag resulting from that ore, in comparison with the actual Hammeh slag. The graph clearly shows the large discrepancy in the major oxides  $\text{SiO}_2$ ,  $\text{Al}_2\text{O}_3$ , and  $\text{CaO}$ , as well as in the alkali and earth-alkali oxides. Results by (P)ED-XRF, using the 'slag\_fun' calibration method (April 2005). Values are expressed in wt% and normalised to 100%. .... 206
- Figure 51. Mass balances of the average composition of Mugharet al-Warda ore (average of samples HA 65 and HA 66), a hypothetical slag based on this average, and the average Hammeh tapped smelting slag. The graph shows the remaining discrepancies between hypothetical and actual slag in the majors  $\text{Al}_2\text{O}_3$  and  $\text{CaO}$ , as well as in the alkali and earth-alkali oxides. Results by (P)ED-XRF, using the 'slag\_fun' calibration method. Values are expressed in wt% and normalised to 100%. .... 207
- Figure 52. Mass balances of Mugharet al-Warda ore (HA 65, HA 66, and the average ore), showing the composition of a hypothetical slag resulting from each ore sample together with a ceramic contribution, in comparison with the actual Hammeh slag. The graph indicates an improved match in most components, with remaining discrepancies in predominantly  $\text{Al}_2\text{O}_3$  and  $\text{CaO}$ . Results by (P)ED-XRF, using the 'slag\_fun' calibration method (April 2005). Values are expressed in wt% and normalised to 100%. .... 211
- Figure 53. Regression line showing the correlation between the actual Hammeh slag compared with the hypothetical slags based on ore HA 65, HA 66, and the average of these two samples respectively. FeO is excluded from these analysis and values are expressed as wt%..... 212
- Figure 54. The average value of the Hammeh tap slags plotted in the  $\text{CaO (+MgO)}-\text{FeO (+MnO)}-\text{SiO}_2 (+\text{Al}_2\text{O}_3)$  liquidus temperature ternary diagram. This composition is compared to the hypothetical ceramic-free slag based on the average of the two ore samples, the average ore, and average ceramic composition. Comparing the actual slag with the ceramic-free slag shows how the ceramic



contribution significantly affects the solidification temperature of the Hammeh slag, lowering it from around or above 1250 °C to around 1100 °C.....	215
Figure 55. Section of SHB slag E/T48 SF. The SHB clearly shows a porous slag core of concavo-convex shape, with rust adhering to the top and soil embedded at the bottom.....	218
Figure 56. Top view of SHB slag E/T48 2824.23, showing a depression at the centre, indicating where the airflow from the tuyère hit the forming slag. The approximately straight side at the bottom of the picture may be the place where the SHB was in contact with the hearth wall, indicating that the tuyère was located on this side of the SHB (Serneels and Perret 2003).....	218
Figure 57. Schematic representation of contributions to the formation of a smithing hearth bottom slag (from Serneels and Perret 2003, 472).....	219
Figure 58. Samples TBS 1 (E/T48 grid K10, unit 2) seen from the top, and TBS 2 (E/T48 grid I15 unit 2) seen from the bottom.....	220
Figure 59. Back Scatter Electron (BSE) micrograph of sample TBS 1, showing the very heterogeneous microstructure of this sample. It consists of a heterogeneous glassy matrix (mid grey and dark grey), incorporating partly fused and thermally cracked quartz grains (dark grey), a large inclusion of iron rich ceramic material (left centre, with cracks), iron hydroxide (around holes), and wüstite (FeO) dendrites (whitish).....	222
Figure 60. Back Scatter Electron (BSE) micrograph of sample TBS 2, showing a kalsilitic ( $\text{KAlSiO}_4$ ) glassy matrix (dark grey), large kirschsteinitic ( $\text{CaFeSiO}_4$ ) laths (mid grey), and precipitation of magnetite crystals (whitish).....	223
Figure 61. Principal Component Analysis of the Tel Beth-Shemesh secondary smithing slags, compared with the Hammeh tap and primary smithing slags. The graph illustrates how the Beth-Shemesh slags form a different group from the Hammeh slag types, and how their variance is more strongly influenced by $\text{K}_2\text{O}$ , $\text{CaO}$ , and $\text{Ba}$ than the Hammeh slags, whose variance is more strongly influenced by $\text{FeO}$ and $\text{MnO}$ for example. The plot uses Principal Component 1 and 3. (The PCA scores and loading vector values can be found in appendix 3).....	224
Figure 62. Regression analysis of dirty versus clean weight of the 40 processed batches.....	226
Figure 63. Distribution of hammerscale and artefacts in Square E/T48 (and surface of E/T49). The bottom of units 1 and 2 are 5 and 15 cm below the surface respectively. The remaining empty grids seen in unit 2 relate to a partially unexcavated intermediate baulk in rows H and I, and those in unit 1 to a few missing bags of hammerscale. The artefacts plotted in the lower right hand plan are from the 2003 season only, and have not been separated into the units excavated. Each dot represents a single artefact (SHB, metal object, or tuyère).....	227
Figure 64. Distribution of hammerscale, presented through Inverse Distance Weighting (IDW2) of the hammerscale distribution in square E/T48 (created in ArcGIS 8.3 using Spatial Analyst). Please note that the plotting spills over into the empty grid row 8/9 for both unit 1 and 2.....	228
Figure 65. One of (smaller) Beth-Shemesh tuyères, registration number 2319, which was excavated during the 2001 season. The tuyère clearly shows the narrow bore and square section, as well as the molten nozzle. This particular tuyère has a smaller cross section (3.5 x 3.5 cm) than the other Beth-Shemesh tuyères (After photograph by Zvi Lederman).....	230
Figure 66. BSE micrograph of sample F2, showing a glassy matrix, (mid-dark grey), with olivinic laths (mid grey), and thick dendritic wüstite in the left bottom corner, and a skin of mostly various iron hydroxides ( $\text{FeOOH}$ ) that has partly separated from the slag. The dark areas are voids, and a small piece of attached charcoal can be seen in the centre right of the picture. ....	266
Figure 67. BSE micrograph of tap slag A1, showing a glassy matrix (dark grey), with feathery devitrification (mid-grey) and wüstite dendrites (light grey).....	267
Figure 68. BSE Micrograph of tap slag A1. Showing a glassy matrix (dark-grey), with feathery devitrification (mid-grey), wüstite dendrites ( $\text{FeO}$ , white), magnetite from oxygen penetration near the surface (light grey), and possible iscorite ( $\text{Fe}_7\text{SiO}_{10}$ , needle-shaped), the black area is the edge of the sample and shows a band of iron hydroxide ( $\text{FeOOH}$ ).....	268
Figure 69. BSE micrograph of tap slag C1, showing a tapping band between two flows of slag. The edges of these flows consist predominantly of a glassy matrix (grey) with small formations of fayalitic laths (lighter grey) and some precipitation of thin wüstite dendrites (light grey) where the two flows touch.....	269
Figure 70. BSE micrograph of tap slag E2 showing skeletal fayalitic/olivine laths (mid-grey) in a glassy matrix (darker grey), with small dendritic wüstite (light grey). Tiny droplets of probable $\text{FeS}$ (lightest grey) are interspersed between the laths.....	270
Figure 71. BSE micrograph of 'ceramic-rich' slag G1, showing an amorphous mass of glass and a thin tapping band of iron oxide or hydroxide (possibly wüstite) flanked by darker conglomerates of glass that is richer in $\text{Al}_2\text{O}_3$ and $\text{K}_2\text{O}$ than the matrix. ....	271
Figure 72. BSE micrograph of primary smithing slag F1, showing a calcio-olivinic glassy matrix, (mid-dark grey), with solid laths of leucite ( $\text{KAlSi}_2\text{O}_6$ ; dark grey), large 2-phased olivinic blocks (mid-grey, and	

slightly lighter), and precipitations of spinel with hercynitic (Al) and ulvitic (TiO <sub>2</sub> ) components (whitish). .....	272
Figure 73. Back Scatter Electron (BSE) micrograph of sample TBS 1, showing the very heterogeneous microstructure of this sample. It consists of a heterogeneous glassy matrix (mid grey and dark grey), incorporating partly fused and thermally cracked quartz grains (dark grey), a large inclusion of iron rich ceramic material (left centre, with cracks), iron hydroxide (around holes), and wüstite (FeO) dendrites (whitish). .....	273
Figure 74. Back Scatter Electron (BSE) micrograph of sample TBS 2, showing a kalsilitic (KAlSiO <sub>4</sub> ) glassy matrix (dark grey), large kirschsteinitic (CaFeSiO <sub>4</sub> ) laths (mid grey), and precipitation of magnetite crystals (whitish). .....	274
Figure 75. PCA plot of the Hammeh System, using PC1 and PC2. ....	276
Figure 76. PCA plot of the Hammeh System, using PC1 and PC3. ....	276
Figure 77. PCA plot of the Beth-Shemesh smithing slags, compared to the Hammeh tap and primary smithing slags, using PC1 and PC3. ....	278

## LIST OF TABLES

Table 1. Provisional classification of the main Hammeh material, based on macroscopic analysis.....	91
Table 2. Results of the AMS Radiocarbon dating of charcoal samples IPAB7.118 and IPAB7.157 .....	93
Table 3. Results of the AMS Radiocarbon dating of three olive stones (short-lived material) from the Beth-Shemesh smithy. AMS analysis by the Institute of Particle Physics, Swiss Federal Institute of Technology, Zurich. Calibration was performed using the CalibETH program (www.ipp.phys.ethz.ch) .....	102
Table 4. Comparison of the measured and known values for volcanic basalts (USGS CRMs) BIR-1, BCR-2, and BHVO-2. Samples were measured at various occasions during the analysis of the Hammeh and Beth-Shemesh slags, and show a high level of consistency in the accuracy and precision of the ESEM analyses. ....	122
Table 5. X-Lab Pro targets and their tube settings. ** Depending on the application (based on Spectro Calibration Manual). ....	131
Table 6. The 33 standards presently used in the 'slag_fun' calibration method on the Spectro X-Lab 2000. ....	136
Table 7. Showing the main and trace elements of which detection by the 'slag_fun' calibration method (April 2005), can be considered quantifiable. Reliability of each element is based on a minimum of 5 CRMs available in the correlation of that element, and a correlation coefficient ( $r$ ) of $>0.95$ . The table further shows the standard deviation ( $d$ ) and the range of actual concentrations covered by the CRMs for each element. (The correlation coefficient, standard deviation, and covered range derive from the calibration screen for each element in the Spectro software).....	141
Table 8. Bulk chemical composition (major elements) of the Swedish reference slag W-25:R, comparing known values (the mean of values obtained through several different analytical techniques) with the average of two analyses of the same reference slag using the 'slag_fun' calibration method ((P)ED-XRF, April 2005). The standard deviation indicate the relative percentage of error by the various analytical techniques (Kresten and Hjärthner-Holdar 2001, 49-50). Values are expressed in wt%, and normalised to 100%. ....	142
Table 9. Bulk chemical composition (trace elements) of the Swedish reference slag W-25:R, comparing known (mean) values with the average of two analyses of the same reference slag using the 'slag_fun' calibration method ((P)ED-XRF, April 2005). The standard deviation indicate the relative percentage of error by the various analytical techniques (Kresten and Hjärthner-Holdar 2001, 49-50). Values are expressed in ppm. ....	143
Table 10. Comparison of methods. Results of the 'slag_fun' method, compared with 'true' values obtained through EPMA, and the linear 'slag' and oxide methods. The comparison is performed on mounted sample HA2002 A7, a mounted Hammeh tap slag. All values are expressed as wt%. ....	144
Table 11. Development of the 'slag' and 'slag_fun' methods over time. Results are shown with the most recent at the top, and are off-set against the results obtained with the 'oxides' method, at the bottom. Test sample HAT 1 is a homogenised pellet of a Hammeh tap slag. All values are expressed as wt%. ....	144
Table 12. Comparison of given values of four CRMs, with the values of the same standards obtained with the 'slag_fun' method. All results have been normalised to remove differences caused by elements not measurable under XRF and Loss on Ignition (L.O.I), and are expressed as wt% Measurements ca. February 2003. ....	144
Table 13. Bulk chemical composition (major elements) of the Mugharet al-Warda ore sampled by the author. Note how these ore samples show a high grade of iron oxide, making them eminently suitable for smelting, but very low in silica, which hinders the formation of a liquid slag. Analysis by (P)ED-XRF (slag_fun calibration method, April 2005). Values are expressed in wt%, and normalised to 100%. ....	149
Table 14. Bulk chemical composition (trace elements) of the Mugharet al-Warda ore sampled by the author. Analysis by (P)ED-XRF (slag_fun calibration method, April 2005). Values are expressed in ppm (parts per million). ....	149
Table 15. Bulk chemical composition (major elements) of the possible discarded 'ore'. Analysis by (P)ED-XRF (slag_fun calibration method, April 2005). Values are expressed in wt%, and normalised to 100%. ....	150
Table 16. Bulk chemical composition (trace elements) of the possible discarded 'ore'. Analysis by (P)ED-XRF (slag_fun calibration method, April 2005). Values are expressed in ppm (parts per million). ....	150
Table 17. Bulk chemical composition (major elements) of the Lisan clay local to Hammeh and two Hammeh tuyères. Analysis by (P)ED-XRF (slag_fun calibration method, April 2005). Values are averaged over two repetitive readings per sample, expressed in wt%, and normalised to 100%. ....	160

Table 18. Bulk chemical composition (trace elements) of the Lisan clay local to Hammeh and two Hammeh tuyères. Analysis by (P)ED-XRF (slag_fun calibration method, April 2005). Values are averaged over two repetitive readings per sample, and expressed in ppm (parts per million).....	160
Table 19. Initial classification of the Hammeh 2000 slag samples, based on macroscopic characteristics, as used during the 2001 sampling. ....	167
Table 20. Final classification of the main slag groups found at Tell Hammeh. ....	169
Table 21. Bulk chemical composition (major elements) of the furnace slags. Note how these samples contain far more iron oxide and far less lime than the tap slags, which brings them closer to the average composition of the Warda ore (see page 147). Analysis by (P)ED-XRF (slag_fun calibration method, April 2005). Values are expressed in wt%, and normalised to 100%. ....	173
Table 22. Bulk chemical composition (trace elements) of the Hammeh furnace slags. Analysis by (P)ED-XRF (slag_fun calibration method, April 2005). Values are expressed in ppm (parts per million). ....	173
Table 23. Bulk chemical composition (major elements) of the furnace bottom slags. Note how these samples are quite similar to the furnace slags. Analysis by (P)ED-XRF (slag_fun calibration method, April 2005). Values are expressed in wt%, and normalised to 100%. ....	175
Table 24. Bulk chemical composition (trace elements) of the Hammeh furnace bottom slag. Analysis by (P)ED-XRF (slag_fun calibration method, April 2005). Values are expressed in ppm (parts per million). ....	175
Table 25. Bulk chemical composition (major elements) of the Hammeh tap slags. Note the progressive leanness from samples A to samples E. The overall tap slags average does not include samples E1 and E3. Analysis by (P)ED-XRF (slag_fun calibration method, April 2005). Values are expressed in wt%, and normalised to 100%. ....	180
Table 26. Bulk chemical composition (trace elements) of the Hammeh tap slags. The overall tap slags average does not include samples E1 and E3. Analysis by (P)ED-XRF (slag_fun calibration method, April 2005). Values are expressed in ppm (parts per million). ....	181
Table 27. Bulk chemical composition (major elements) of the ceramic-rich slags. Note how these samples contain far more silica and lime, and less iron oxide than the tap slags, which brings them closer to the average composition of the local clay and tuyères (see page 159). Analysis by (P)ED-XRF (slag_fun calibration method, April 2005). Values are expressed in wt%, and normalised to 100%. ....	184
Table 28. Bulk chemical composition (trace elements) of the Hammeh ceramic-rich slags. Analysis by (P)ED-XRF (slag_fun calibration method, April 2005). Values are expressed in ppm (parts per million). ....	185
Table 29. Bulk chemical composition (major elements) of the primary smithing slags. Note how these samples are quite similar to the tap slags. Analysis by (P)ED-XRF (slag_fun calibration method, April 2005). Values are expressed in wt%, and normalised to 100%. ....	188
Table 30. Bulk chemical composition (trace elements) of the Hammeh primary smithing slags. Analysis by (P)ED-XRF (slag_fun calibration method, April 2005). Values are expressed in ppm (parts per million). ....	188
Table 31. Comparison between the average trace element compositions of the Warda ore, the various Hammeh slag types, the local clay and Hammeh tuyères, and the Hammeh charcoal. In addition, the trace elements of the Tell Beth-Shemesh secondary smithing slags are shown. Analysis by (P)ED-XRF (slag_fun calibration method, April 2005). Values are expressed in ppm (parts per million), except sulphur, which is expressed in wt%. ....	190
Table 32. Bulk chemical composition (major elements) of Hammeh charcoal. Analysis by (P)ED-XRF (slag_fun calibration method, April 2005). Values are expressed in wt%. The difference to 100% is assumed to be predominantly carbon, undetectable under XRF. A normalised composition of the detected elements is provided as well. ....	199
Table 33. Bulk chemical composition (trace elements) of Hammeh charcoal. Analysis by (P)ED-XRF (slag_fun calibration method, April 2005). Values are expressed in ppm (parts per million). ....	199
Table 34. Mass balances of ore sample HA 65, showing the differences in composition between a hypothetical slag calculated from that ore, and the actual Hammeh slag (average value of the tap slags). Results by (P)ED-XRF, using the 'slag_fun' calibration method (April 2005). Values are expressed in wt% and normalised to 100%. ....	205
Table 35. Mass balances of ore sample HA 66, showing the differences in composition between a hypothetical slag calculated from that ore, and the actual Hammeh slag (average value of the tap slags). Results by (P)ED-XRF, using the 'slag_fun' calibration method (April 2005). Values are expressed in wt% and normalised to 100%. ....	207
Table 36. Mass balances of average composition of Mugharet al-Warda ore (average of samples HA 65 and HA 66), showing the differences in composition between a hypothetical slag calculated from that ore, and the actual Hammeh slag (average value of the tap slags). Results by (P)ED-XRF, using	

the 'slag_fun' calibration method (April 2005). Values are expressed in wt% and normalised to 100%.....	207
Table 37. Mass balances of the three ore samples (HA 65, HA 66, and their average, showing the differences in composition between a hypothetical slag with additions of technical ceramic, and the actual Hammeh slag (average value of the tap slags). Results by (P)ED-XRF, using the 'slag_fun' calibration method (April 2005). Values are expressed in wt% and normalised to 100%. .....	210
Table 38. The remaining discrepancies between the hypothetical slag based on the average of ore samples HA 65 and HA 66 with ceramic contribution, compared to the amount of these samples present in the analysed charcoal from Hammeh. The charcoal values are normalised and all values are expressed in wt%. Analysis by (P)ED-XRF (slag_fun calibration method, April 2005).....	213
Table 39. Bulk chemical composition (major elements) of the Beth-Shemesh secondary smithing slags. Analysis by (P)ED-XRF (slag_fun calibration method, April 2005). Analysis by (P)ED-XRF, normalised to 100% and expressed in wt%.....	221
Table 40. Bulk chemical composition (trace elements) of the Beth-Shemesh secondary smithing slags. Analysis by (P)ED-XRF (slag_fun calibration method, April 2005). Values are expressed in ppm (parts per million), or as bdl (below detection limit). .....	221
Table 41. Bulk chemical analysis (main elements) of the Tell Hammeh and Tel Beth-Shemesh slags, the Warda and discarded Hammeh Ore, Hammeh charcoal, Lisan clay and tuyère ceramic. Sodium is presented here in <i>italics</i> , to indicate that it is not fully quantifiable (see chapter 7). Results of the CRMs ran in parallel with the samples are grouped at the bottom of the table. Analysis by (P)ED-XRF, slag_fun calibration method, at the given date. ....	256
Table 42. Bulk chemical analysis (trace elements) of the Tell Hammeh and Tel Beth-Shemesh slags, the Warda and discarded Hammeh Ore, Hammeh charcoal, Lisan clay and tuyère ceramic. Results of the CRMs ran in parallel with the samples are grouped at the bottom of the table. Analysis by (P)ED-XRF, slag_fun calibration method, at the given date. ....	264
Table 43. SEM-EDS analyses of furnace bottom slag F2. Values are presented as compounds, and are normalised to 100%. .....	266
Table 44. SEM-EDS analyses of tap slag A1. Values are presented as compounds, and are normalised to 100%. .....	267
Table 45. SEM-EDS analyses of tap slag A1. Values are presented as compounds, and are normalised to 100%. .....	268
Table 46. SEM-EDS analyses of tap slag C1. Values are presented as compounds, and are normalised to 100%. .....	269
Table 47. SEM-EDS analyses of tap slag E2. Values are presented as compounds, and are normalised to 100%. .....	270
Table 48. SEM-EDS analyses of ceramic-rich slag G1. Values are presented as compounds, and are normalised to 100%. .....	271
Table 49. SEM-EDS analyses of primary smithing slag F1. Values are presented as compounds, and are normalised to 100%. .....	272
Table 50. SEM-EDS analyses of secondary smithing slag TBS 1. Values are presented as compounds, and are normalised to 100%. .....	273
Table 51. SEM-EDS analyses of secondary smithing slag TBS 2. Values are presented as compounds, and are normalised to 100%. .....	274
Table 52. PCA scores of the Hammeh Smelting System, PC1 – PC4. Scores were calculated with statistical software package SPSS 12. ....	277
Table 53. Loading vector values for the Hammeh Smelting System, PC1 – PC4. Values were calculated with statistical software package SPSS 12. ....	277
Table 54. Table 55. PCA scores of the Hammeh Smelting System, PC1 – PC4. Scores were calculated with statistical software package SPSS 12. ....	278
Table 56. Loading vector values for the Hammeh Smelting System, PC1 – PC4. Values were calculated with statistical software package SPSS 12. ....	279

## ACKNOWLEDGEMENTS

### Affiliations

The excavations at Tell Hammeh (az-Zarqa) are part of the *Deir ‘Alla Regional Project*, a joint undertaking of Leiden University (the Netherlands) and Yarmouk University (Jordan) in conjunction with the Department of Antiquities of Jordan. Early analysis (in 1996 and 1997) of the Hammeh material took place at the Archaeometry laboratory of Yarmouk University, Irbid, Jordan. Export of and destructive analysis on the Hammeh material was kindly granted by the Department of Antiquities of Jordan. The excavations at Tel Beth-Shemesh are a project of Tel Aviv University, Israel. The directors of this project kindly invited me to direct the excavation of the smithy, and granted me permission to export and perform destructive analyses on the material with approval of the Israel Antiquities Authority. Subsequent research on the Hammeh and Beth-Shemesh material was carried out at the Wolfson Archaeological Science Laboratories, Institute of Archaeology, University College London. This was sponsored by a three year grant from BHP Billiton through the Institute for Archaeo-Metallurgical Studies (IAMS).

I am indebted to the Scientific Directors of the *Deir ‘Alla Regional Project*, Dr Zeidan Kafafi (Yarmouk University) and Dr Gerrit van der Kooij (Leiden University), for their support. They enabled me to direct the excavations at Hammeh in 2000, with scientific excavation of the iron production remains as the main aim, and permitted me to select freely from all excavated material. I am grateful to the Department of Antiquities of Jordan, for their kind permission to take this material to the UK for further study. I am equally indebted to the Scientific Directors of the Tel Beth-Shemesh Excavations, Dr Shlomo Bunimovitz and Dr Zvi Lederman (both Tel Aviv University), for inviting me to their site, letting me excavate the smithy with dedicated metallurgical techniques, and allowing me to export and study all their material.

I am furthermore indebted to The Institute of Archaeology, UCL, for housing me and my samples at various locations, and for their financial support towards conferences as well as the <sup>14</sup>C dating of the Hammeh production. Similarly, I would like to thank the Graduate School Conference Fund for their sponsoring of two conference trips. I am very grateful to the Institute for Archaeo-Metallurgical Studies (IAMS) for their support towards the 2002 Jordan Valley Conference I

organised at the British Museum, providing the grant that allowed me to study at UCL, and paying my overhead when excavating in Israel.

## Acknowledgments

The first two people I would like to thank are my two supervisors, Thilo Rehren and Vince Pigott, for their unending support, patience, and encouragement during the course of my PhD research at the Institute of Archaeology.

Gratitude is due to Peter Ditchfield, Kevin Reeves, Simon Groom, Lorna Anguilano, and Mike Charlton, who for their immeasurable contributions, support, and feedback in taming the XRF. Mike Charlton is due additional gratitude for his help with statistics. Sincere thanks are further owed to Eleni Asouti, John Meadows, and Phil Austen, for identification of the Hammeh charcoal, and help in selecting specimens for AMS  $^{14}\text{C}$  dating; Yuval Goren, for identification of the Hammeh and Beth-Shemesh tuyère ceramic; Thérèse Kearns and Beth Harley, for the laborious task of cleaning and weighing the hammerscale; Andy Bevan, for help with GIS.

I would further like to express my gratitude to Eva Kaptijn, Jacqueline Smak Gregoor, Marloes Borsboom, and Hussam Abbas for their excellent digging and cheerfully putting up with an extra form to fill out at Hammeh; Shira Mishlin, Maya Moyal, Keren Oren, and Carlton Winbery for their slow-digging, singing, and endlessly dragging the magnets at Beth-Shemesh. In lieu of all my Jordanian friends, I would like to thank Maher and Abu Shobash, as they in particular taught me how to wield a trowel and to do the dabkah. Eveline van der Steen and Margreet Steiner, thank you for ‘giving’ me Tell Hammeh and the unforgettable experiences at Khirbet Balamah, Jenin.

Of course, little would have been possible without the friendship of my friends at UCL, especially research room B53: Pepi Vacharopoulou, Joanne Rowland, Kevan Edinborough, Marcos Martín-Torres, Ceri Ashley, Aude Mongiatti, Duncan McAndrew, Myrto Georgakopoulou, Petros Prokos, Satoko Tanimoto, Scott Haddow, Shadreck Chirikure, Claire Cohen, Shin’ichi Nishiyama, Sophia Labadi, Anna Stellatou, Borja Legarra, Reuben Grima, and many others. A special thanks to Sarah McCartney, for linguistic fights and too much coffee.

Special thanks to my parents, Ines and Harm, for their encouragement and support. Finally and most importantly, all my love and twinkling thanks go out to Esther, who survived this with me.

# CHAPTER 1: INTRODUCTION

## Introduction

Over the last decades, there has been a discernible increase of interest among archaeologists in the production, working, and use of metals in antiquity. This field of study is often referred to as ‘archaeometallurgy’, a term first coined by Ronald Tylecote and Beno Rothenberg in the early 1970s. Archaeometallurgy can be defined as “the study of archaeological metal processing waste and intentional metal products in order to reconstruct the processes used, to infer the technological skill of the manufacturers, and to derive a record of the human choices, decisions, and influences involved in metals production and use” (Miller and van der Merwe 1994, 33). Archaeometallurgy can also involve the study of materials obtained from experimental or ethnographical reconstructions or observations. The ultimate aim is to reconstruct and understand ancient human behaviour related to metallurgical processes, in order to understand these processes in their archaeological context.

Archaeometallurgy, with its focus on metals (and the materials related to their production and processing), e.g. copper and its alloys, gold, silver, tin, or lead, forms part of the larger body of research where scientific analytical methods are applied to materials excavated in archaeology. Depending on the history or terminological preference of an institution or researcher, this overarching body of research is usually designated with terms like ‘archaeological science’, ‘archaeometry’, or ‘geo-archaeology’.

Considering the nature and aim of archaeometallurgy, it is obvious that both archaeologists and material scientists are active in the field. In the most common set-up, however, these perform separate roles. The archaeologist will conduct fieldwork, which may be specifically geared to the study of metal technology in its cultural context to varying extents, with laboratory analyses then forming one link in the subsequent chain of interpretative activities. The laboratory work is usually outsourced to the material scientist. The systematic analysis of materials, with a separation of the interpretation of materials from the interpretation of the excavation of those materials, is especially present in the study of copper and copper alloys.

This pattern of separate fieldwork and laboratory work carries both advantages and disadvantages. Systematically performing analytical research does ascertain that archaeological materials of a metallurgical nature do receive proper



attention and scientific treatment, which is desirable. However, with the inbuilt separation, such analyses often end up either relegated to an appendix to an archaeological fieldwork report, culminate in a highly specialised scientific publication with a limited, non-archaeological audience, or sometimes both. These appendices or scientific publications often boil down to the same thing: a detailed study of metallurgical debris on a technological and material level, where archaeological context and questions are secondary to the analyses performed or research methodology used, if they are considered at all.

In the Levant, copper metallurgy is represented by large production centres such as Timna in Israel and the Wadi Feinan in Jordan. Both the production sites and copper/bronze artefacts are quite systematically studied archaeometallurgically. The production of iron and the processing remains this leaves behind are, technologically as well as in the nature of the residues involved, quite comparable to those of copper/bronze. Nevertheless, in Near Eastern Archaeology, systematic analysis is far less common with this metal. This is partly related to a significant lack of iron production or working finds in the entire pre-Roman Near East, as discussed in chapter 3, page 67, and furthermore to the relative rarity and poor state of preservation of most iron artefacts from an archaeological context.

In hardly any archaeological subject does the dichotomy between fieldwork and laboratory work appear stronger than in metallurgy, and nowhere as strong as in early iron production, which may have several reasons. Metallurgical finds, particularly when iron is concerned, are less abundant in the archaeological record than, for example, ceramics, which hinders archaeological interpretations concerning metal on issues such as changes over space and time, and innovation and development. Because of their abundance, it is chiefly ceramics that are used to answer such questions, and they are furthermore used for relative dating, usually based on (morphological) typology studies. In quite sharp contrast, the sparser finds of metal (or debris of metal production) are perceived to be less useful in this respect, as well as far more complex and expensive to study and analyse.

The material scientist performing the laboratory work more often than not has a scientific rather than an archaeological background. Much research on ancient technological processes is, therefore, performed with research questions of a purely scientific perspective. However, archaeology itself does not use the information gathered through excavation and laboratory work optimally either. As

argued by the theoretical studies that will be discussed in chapter 2, artefacts, and certainly also the way they are produced, form an inseparable and active part of any culture and its economical and social systems, in prehistory as much as in modern times.

Artefacts and (debris from) a production sequence do not only reflect technological necessities, but also personal and cultural ideas, meanings, feelings, and choices. Explorations of these choices usually takes place in an anthropological context, and are regularly quoted and referred to, but hardly ever translated into archaeological interpretation of excavated material. Simply publishing classificatory and analytical data in tables in an appendix bypasses interpretation of the convoluted role of technology within a society, and more importantly, leaves one of archaeology's main goals, trying to get to the person behind the technology, unexplored.

## Aims and Objectives

### Introduction

During three excavation seasons (1996, 1997, and 2000), extensive remains of an iron production operation, specifically smelting and primary smithing, were excavated at Tell Hammeh (az-Zarqa), Jordan, a relatively small site close to the central Jordan Valley (discussed in chapters 4 and 8). A fourth season of excavation was planned for spring 2003, to revisit and further excavate Hammeh using the intermediate results of the research. However, the fully prepared and planned season had to be cancelled as Iraq was invaded on the proposed first day of excavation. Nevertheless, this cancellation created the opportunity for the author to direct the excavation of the remains of an iron working operation, specifically secondary smithing, at Tel Beth-Shemesh, a larger city on the edge of the then Philistine coastal plain of Israel (discussed in chapters 5 and 9).

Dedicated excavation techniques were developed and applied at both Tell Hammeh and Tel Beth-Shemesh, which aimed at optimal recovery of technological and archaeological information. The recovered materials were studied macroscopically, classified preliminarily, and sampled, based on their external characteristics as observed in the field, and comprehensively analysed using relevant scientific analytical techniques. It was sought to establish the nature of the metal in question and then to identify and reconstruct the *chaîne opératoire* of the technologies excavated at each site, as well as to investigate the similarities and dissimilarities between a smelting and a smithing site, both in

terms of their archaeological context and of the characteristics of their residues. Through this research, it is attempted in this thesis to bridge the usual gap between fieldwork and laboratory work, and interpret the scientific and field data within the framework of both archaeological and anthropological methods and theories on technology.

### **Three Areas of Interest**

The metallurgical materials excavated at Tell Hammeh and Tel Beth-Shemesh have repercussions for several areas of interest for our knowledge about the past. In the first place, they provide a new and comprehensive set of technological (macroscopic, microscopic, and chemical) data about early iron production and its technology. Secondly, the finds at Hammeh and Beth-Shemesh provide a factual contribution to the discussion on origin and history of iron production, an area of intense speculation but little real data. Last but not least, these new finds allow a glimpse into the relations between an emergent technology and the society in which it is embedded. Each of these areas of interest interrelates with the other two and the distinction between them here is merely a way to structure thought and approach.

All three areas of interest are discussed at various points in this thesis. The archaeological context of the finds and the results of the scientific analyses performed on them form the core of the discussion, but it is sought to place this within the wider context of the society in which the Hammeh and Beth-Shemesh metallurgical activities take place. It would after all be pointless to consider any technology as an event operating in a social, economic, cultural, or ideological vacuum.

### **Objectives and Context**

In itself, the study of iron production remains is not unique, but particularly the extensive iron smelting related residues at Tell Hammeh are interesting due to several characteristics. From an archaeological perspective, the Hammeh material is interesting, as it constitutes the earliest known example of iron smelting technology in the Near East. The finds at Hammeh allow for exploration of the role of this technology in the local and regional social, economic, and cultural context of late 2<sup>nd</sup> and early 1<sup>st</sup> millennium BC of the Levant (discussed in chapter 3), which is characterised by a conspicuous lack of comparable iron production related material. This thesis explores issues such as the presence or absence of

activity areas within the iron production area, technological choices and style, the choice of location, and organisation and scale of the production.

From a metallurgical perspective, the Hammeh bloomery smelting slags are quite interesting as they reveal a relatively rare high lime content (ca. 11 wt%) coupled to a low iron oxide content (ca. 52 wt%), when compared to 'regular' bloomery iron slags (see chapter 8). Such lean slags are not unknown in ancient metallurgy, but are usually associated with (early) blast furnace technology. Extensive finds of such early blast furnace slags are known from various medieval iron production contexts in France. These slags (usually referred to as *laitiers*) are relatively similar to the Hammeh material in elemental composition and their highly vitreous matrix. Nevertheless, they are typically richer in lime (up to 20 or 30 %) and lower in iron oxide (less than 30 %) than the Hammeh slags, and clearly relate to a different technological process (Pleiner *et al.* 2002; Mahé-le Carlier *et al.* 1998; Ploquin 1993).

Lime rich slags are much rarer in the bloomery process. One example of lime-rich bloomery slags (up to 20 %) is known from the Sussex area of the Weald in the South of England. Here, the lime content is thought to derive from the ore that is smelted (Paynter 2005; Cleere and Crossley 1995; Worssam and Gibson-Hill 1976). In this light, a specific aim of the analyses of the Hammeh material is to explore the origin of the lime in the Hammeh slags, and to establish the contribution of different materials to the Hammeh smelting system.

Study of the Beth-Shemesh material is performed using the same approach and methodology as the study of the Hammeh material, again to identify the nature of the metal worked, and to reconstruct the *chaîne opératoire* of the smithing technology at the site. Here, the combination of archaeological data with subsequent laboratory analysis allows investigation of specific activities within the metallurgical workshop area, and the examination of issues of technological choices and style, choice of location, and organisation and scale of the production. In order to do so, an excavation technique was developed to recover all relevant metallurgical residues. This allowed a detailed examination of the use of space in the smithy. Furthermore, study of the Beth-Shemesh material in parallel to that of Hammeh creates the opportunity to compare early smelting with early smithing material from the same region, and explore connections or differences between two distinct stages of a technology, both in terms of the archaeological context as well as of the technological residues themselves.

As indicated above, most claims of early (primary) production of iron metal, particularly in the Near East, are based on artefactual evidence rather than slag and furnaces (see chapter 3). For the research presented here, this means an important lack of comparative production material and data, which only makes the study of the Hammeh and Beth-Shemesh material more relevant. It is hoped that, beyond the insight into early iron metallurgy provided by the two case-studies themselves, the integrated archaeological and laboratory approach, the excavation methods applied, the analytical methodology, as well as the archaeometric data presented here can serve as a model for the excavation, interpretation, and comparison of future (and previous) discoveries of iron metallurgy in the Near East.

## CHAPTER 2: THE SOCIAL CONTEXT OF TECHNOLOGY

### Introduction

Technology, whether today or in antiquity, is not a phenomenon that is solely bound to materiality, isolated from other aspects of human life and culture. Technology does not operate simply because it is there, ruled only by the laws of nature. Neither does it always follow the shortest or most logical route towards the intended product nor a path of unstoppable evolutionary progress towards increasing complexity. It is exactly these kinds of assumptions, however, that have long formed the basis of thinking about technology, in what Bryan Pfaffenberger has termed the 'Standard View of Technology'. This view comprises three major paradigms: 'necessity is the mother of invention', 'form follows function and style, and meaning is a surface matter', and 'development is unilinear evolution, from simple to complex' (Pfaffenberger 1992; discussed in detail below).

The 'standard view' is often quite commonsensical, e.g. technology today is certainly more complex than 3000 years ago. Nevertheless, anthropological and archaeological observations in a range of different settings and localities indicate clearly that each of these statements can be falsified, and that technology is not just about material culture and the development of techniques. Technology is but one part of that larger system we term culture or society, and which archaeologists (and anthropologists) try so hard to reconstruct and understand.

Within that larger system of society, technology forms a subsystem that inescapably affects and is affected by other subsystems such as social, political, and economic organisation, ideology, value systems and meaning, or religion, to name but a few. All subsystems together constitute the cultural system of which they are part, and are thus not mutually exclusive. To use the terminology of Bryan Pfaffenberger once more, technology is an inseparable part of a *sociotechnical system* (Pfaffenberger 1992, 493). Acceptance of the fact that technology does not operate in a vacuum but relates to other aspects of society means that archaeological finds related to technology, like those treated in this research, should be examined in the light of that sociotechnical system, to the extent that this is possible.

Over several decades, many definitions of and theories concerning technology have been formulated in different academic disciplines, all reflecting the myriad perspectives with which one can look at technology and its social context, and often bringing their own emphases and terminology to the subject. In looking at

the corpus of theoretical thought on technology, different schools and traditions can be recognised (Killick 2004a; Schiffer 2001; Hamilton 1996, 3-9).

It is beyond the scope of this research to review the entire development and history of all these traditions in detail. This chapter presents a brief summary of two major traditions, analogous to Hamilton's divisions, and the latest theoretical developments. It then focuses on the definitions, concepts, and ethnographic studies concerning technology that are potentially relevant to this research. These concepts and the ethnography all centre on production and together set the stage for the conceptual template that informs the interpretation of the Tell Hammeh and Tel Beth-Shemesh technologies.

## **Traditions in Thinking about Technology**

Until quite recently, the theoretical background of thinking about technology largely evolved in social anthropology, and to a lesser extent in archaeology. Several schools of thought, each with its own leading paradigm(s), core beliefs, and/or application of models existed and still exist. The 'rise and fall' of such schools is characterised by separate and different developments in diverse areas of the world and at different periods in time. Several of the paradigms or beliefs involved have gone in and out of favour over time, many have been reassembled in new approaches, and others have been discarded altogether. All have one thing in common, however, they attempt to understand and explain technological variations and technological change as they are observed in anthropology and archaeology. A brief summary is presented here of two major traditions that each provide much of the groundwork for most current thinking on technology. This is followed by a short overview of recent developments in technology theory.

### **The French-European Tradition**

The French-European tradition originates in a longstanding French tradition of interest in the relation between technology and society (Lemonnier 1989b). Due to language barriers or geographical distance, most Anglo-American scholars remained unaware of this tradition for an extended period, where it has since long informed French and continental European anthropology and archaeology.

The tradition largely goes back to the work of Marcel Mauss. Mauss is often regarded as the founding father of (French) ethnography and cultural anthropology, and is most famous for his '*Essay sur le Don*' (Mauss 1923), a comparative essay in which he explores forms and function of gift-giving and

exchange in 'primitive' societies, an essay that influenced large areas of social anthropology.

In another important article, Mauss discusses the cultural variation that can be observed in gestures and movements of the human body (Mauss 1935). Here he describes how every technique, every operation performed, knowledge of which is acquired and transferred within society through tradition, originates in the energy and use of muscles and nerves. The movements and gestures resulting from this energy form complex systems, i.e. the use of the human body, which in turn affects, and is affected by, its sociological context. Knowledge of gestures and movements in their sociological context is, for example, important when examining how mechanical means are used. The adaptation to tools and related changes in existing gestures or movements can show variations between societies.

His train of thought was extended to the study of the 'technical act', where matter is affected and used in actions that are simultaneously traditional, reasoned, conscious, and social, e.g. to technologies where artefacts are created from raw materials. This involves the use of the human body in movements and gestures that work and shape the raw material in question into an object, or in other words a 'technique'.

Mauss and subsequent (French) theoreticians such as André Leroi-Gourhan focused primarily on 'techniques', knowledge, and actions, in which every movement or 'gesture' of a technique expresses its social nature. All emphasise the importance of the (technological) *process*, which Leroi-Gourhan terms the '*chaîne opératoire*' (Leroi-Gourhan 1957), i.e. linear operational sequences leading from the raw material to the finished product. Leroi-Gourhan further argues that without their cultural context, tools or objects lose their significance (Leroi-Gourhan 1957, 65).

Mauss' and Leroi-Gourhan's ideas on the social context of technological processes were continued in the work of others (Haudricourt 1988; Gille 1978; e.g. Haudricourt 1962), and also found their way into, for example, the highly influential social anthropological work of Lévi-Strauss (Lévi-Strauss 1976, 11). This Franco-European tradition of thinking about technology in its social context culminates in the work of Pierre Lemonnier (Lemonnier 1993b; Lemonnier 1993a; Lemonnier 1992; Lemonnier 1990; Lemonnier 1989b; Lemonnier 1989a; Lemonnier 1986). He argues that technique and technology form a *technology system*, similar to the body movement and gestures system of Mauss. A technology system comprises all aspects of a technology. Not only the raw material acted upon, the



tools and (mechanical) means involved, the gestures and movements that change the material, and the specific knowledge necessary to perform the technology, but also the personal or cultural choices and actions made during the technological act, as well as the final product and its cultural and stylistic characteristics (Lemonnier 1992).

He insists that the study of technology should examine the reciprocal relationship between society and such technological systems, particularly through the reconstruction of the *chaîne opératoire* (Lemonnier 1992; Lemonnier 1990). From the various aspects of the Franco-European tradition, it is especially this system view, the concept of *chaîne opératoire*, and the role of choices in that concept as presented by Lemonnier (which are discussed in more detail below), which are potentially relevant and applicable to the research on the Hammeh and Beth-Shemesh technologies.

### The Anglo-American Tradition

Until about a decade and a half ago, the Anglo-American tradition developed largely separate from the Franco-European tradition. Initially, anthropologists in this tradition looked predominantly at the material aspects of technology, i.e. at tools, raw materials, and the artefacts produced, i.e. the material culture. This material culture remained largely 'deculturalised'; no link was considered with a human or social context, with many strictly classificatory and descriptive studies as a result.

When Anglo-American (social) anthropology later broadened its view beyond the artefact itself, the dominant theoretical paradigm was *linear evolution*: the assumption that technology progresses inevitably towards more complexity. This went hand in hand with *technological determinism*, which assumes that all aspects of a society (religion, art, kinship, and social relations) derive solely from a society's technology and economy. Later, this determinist view was reversed and social anthropology became '*idealist*': which means that ideology, personality, and social arrangements were now seen as what determines and directs cultural change, rather than the state of technology or material factors.

In both the technological determinist and the idealist approaches, the 'technological somnambulists', as Pfaffenberger calls them (Pfaffenberger 1988a, 238), that supported these views detached technology from the broader culture. They maintained that social structure and ideology are independent of technology

and technological change, implying that any level of social complexity could be found at any level of technology (Benedict 1948, 589; Boas 1940, 226-267).

An important exception to these approaches in the Anglophone world was Gordon Childe, in his time one of the most prominent prehistorians in Europe (and director of the Institute of Archaeology, UCL, from 1946 until 1956). His early work revealed a basically *functionalist* appraisal of artefacts, where 'practical' material culture such as tools and weapons spread rapidly between societies, and less functional materials such as ornaments or domestic pottery reflect local taste and thus identify specific cultures (Childe 1929, 248). This was still very much a 'somnambulist' approach.

He soon realised that this functional determinism did not work, when he found that bronze technology in Europe operated within a very different social complexity than the same technology in Mesopotamia (Childe 1944). Childe now started to look at broader social and economic trends, and explained that effects of technologies depend on particular social and economic relations of production in a society. He still considered technological developments as independent variables arising from human intelligence, but whose effects are filtered and altered by cultural patterns (Trigger 1986, 4-5). Later, he observed that technological change occurs in a "social context that could facilitate, hinder or block specific developments", and should be studied in relation to the total cultural system (Trigger 1986, 6).

Childe's later work is a clear forerunner of more modern thought, but his contemporaries did not incorporate his pioneering formulations. Instead, the main anthropological paradigm at that time was *neo-evolutionism*, which to a certain extent meant a return to material and technological determinism, where social systems were determined by technological systems (White 1962; e.g. White 1949, 391).

Other studies at this time explored the repercussions of a new technology or new devices on society and culture, but technological innovation was seen as an independent factor, i.e. a given, which was introduced from outside. This is called a *processualist* view, wherein the relation between technology, material culture, social organisation, and ideology is strictly one-directional: the (independent) emergence of a new technology will change the organisation and ideology of society, but changes in society do not affect technology (Trigger 1989, 292).

In the 1970s and 1980s, Childe's observations were finally taken aboard. It was realised that different cultures can arise from the same environment and technologies, and that cultural traits and technology can diffuse between very diverse cultures. This led to a *post-processualist* approach, which rejects cultural and technological determinism and sees the heart of culture in human relations.

Largely parallel to these developments, an important contribution to thinking on technology comes from historians and sociologists of science and technology. With examination of progress in technological skills as a starting point, historians of technology (Tylecote 1992; Tylecote 1987; Tylecote 1976; Forbes 1964-1972; Singer *et al.* 1954-1958; e.g. Forbes 1950; Forbes 1940-1963) merged their approach with sociologists to deal with interactions of technology and society. This merged approach is termed *contextualism* (see Reber and Smith 1986; Staudenmaier 1985, 144), and focuses on the technical characteristics and constraints of a technology, and their relation to the economical, social, and political contexts of that technology (Killick 2004a, 571; Sillar and Tite 2000; Pétrequin *et al.* 2000; Lemonnier 1993b).

This approach is further widened to include the study of technological characteristics and processes of cultural contact. Some studies document how technological traits transfer to new areas and how they are transformed there (Costin 1998; Hosler 1994; Ehrenreich 1991; Hosler 1988; Wright 1986; Wright 1985; Ehrenreich 1985). Other studies focus on craft specialisation or manufacturing systems (Costin 2001, see below; Costin and Wright 1998; Costin 1998; Costin and Hagstrum 1995; Costin 1991; Levy 1991; Rice 1981), or construct models for social change in relation to technology (Geselowitz 1993; McGovern 1989; Schiffer and Skibo 1987; Kingery 1986).

As David Killick argues in a recent article, the contextualists, largely comprised of 'non-archaeologists' have developed a large range of sophisticated and creative methods to deal with issues of interaction between technology and society (Killick 2004a, 572). There are several variants within contextualism (see Hamilton 1996), but all broadly agree on what Thomas Hughes has termed a 'seamless web' of technology and society (Hughes 1987; Hughes 1986). In such a web, technological progress is not inevitable, nor is the acceptance or success of a technological system determined solely or even largely by efficiency (Dobres and Hoffman 1994, 230). Cultural factors affect and are in turn affected by technological development.

A key development in the Anglo-American tradition is the work by Bryan Pfaffenberger (Pfaffenberger 1992; Lemonnier and Pfaffenberger 1989; Pfaffenberger 1988b). Influenced by the historians and sociologists of technology, as well as the Franco-European tradition discussed earlier, Pfaffenberger developed the idea of a *sociotechnical system*. This expands on Lemonnier's idea of technology systems, and incorporates society-wide organisation and control of joint labour. In a *sociotechnical system*, a wide array of social and non-social actors link together in a seamless web. Similar to the contextualists, Pfaffenberger states that physical objects and culture form a seamless web, in which sociotechnical activities are defined and shaped by society. Society itself is in turn shaped by the sociotechnical system-building resulting from the sociotechnical activities of the various actors involved (Pfaffenberger 1992, 500).

Contrary to the paradigms of the 'standard view' (see the introduction and the further discussion below), it is not (necessarily) pragmatic needs that drive technological innovation or change within society, resulting in ever more complex technologies and products, but the way in which the various actors manage to construct a successful system together.

Using the example of the organisation of irrigation in Sri Lanka, Pfaffenberger shows that several organisational levels act simultaneously to ensure an optimal and effective distribution of water. This involves, for example, the land-workers who dig the irrigation channels, the local authority who partly controls the communal labour, but also religion and a range of rituals. These (socially undisputed) rituals often include components with explicitly stated productive goals, e.g. enhancing the fertility of the earth, that an outside observer would see as 'false', and as serving no 'real' technological purpose. However, where the ritual itself may not factually contribute, its execution ensures the coordination of shared labour and equal distribution of the resources (Pfaffenberger 1992, 501).

All the actors involved are thus *systembuilders*, each performing, coordinating, or facilitating a part of the system as a whole, whether consciously or not. It is the way in which all systembuilders manage and adapt existing resources that makes a sociotechnical system work, and which determines the success of that system and the society in which it is embedded, rather than whether the techniques or tools are superior to others. Pfaffenberger's system view is applicable at several levels, from the system of a technology itself and its relation to the society in which it is embedded to overarching local or regional systems.

In line with the system views and the integration of the two traditions in the last two decades, several concepts were developed that are potentially applicable to the study of archaeological remains of technology. Examples are the concept of *technological style* and *choice* by Heather Lechtman, and that of the organisation of production by Cathy Lynn Costin, which are discussed in more detail below, after a brief review of current developments.

### **Recent Development: Agency and Practice Theory**

A currently widely debated development in thinking about technology is *agency theory*. Within agency theory, scholars including Marcia-Ann Dobres, Christopher Hoffman, and John Robb (Dobres and Robb 2000; Dobres 2000; Dobres and Hoffman 1999; Dobres and Hoffman 1994), attempt to combine the work of Lemonnier, Pfaffenberger, as well as the sociologists of technology with concepts such as technological style (discussed below) into a theoretical framework that is rooted in *practice theory*.

*Practice theory*, a concept derived from social science, is defined as a framework that focuses on individuals' expression and use of shared meanings in personal activity and identity construction, and on how these shared meanings are produced and reproduced through personal action and interaction. It examines (individual) 'agents' that act inside a social environment, and assumes that they often act with an incomplete knowledge of social rules, incomplete knowledge of their situation and with their actions producing unexpected consequences (e.g. see Ortner 1984).

The emphasis of Dobres et al. is on the '*social agency*' of technologies, using a model of scale, dynamic contexts, materiality, and social theory. Dobres and Hoffman believe that a perspective rooted in *practice theory* can be used to understand dynamic social processes involved in technological production. According to them, human agents act strategically, and not according to fixed social rules, but other actors, such as social groups, built and natural environment, traditions, and power relationships may impinge on the individual's actions.

In Marcia-Ann Dobres' opinion, 'standard' procedure in the interpretation of archaeological finds does involve rigorous hypothesis-testing, but this is not applied to the question of agency. Agents are standardized along the lines of a rational choice or 'optimal foraging' model and their technologies are taken to be cultural adaptations to the environment. Variability in artefacts and ways of

production are treated as statistical noise, whereas agency theory takes such variability more seriously: variation shows how particular agents make particular choices or develop a particular practice to solve particular problems related to general questions of gender, society, and cultural identity. This is very much in line with technological choice as formulated by Lemonnier and Heather Lechtman (see the relevant concepts below).

Dobres sees an opposition between practice (technology) and activity (handling an artefact). 'Technology', 'practice', and 'agency' thus become conflated in a systematic way: "People and social collectives are the active agents of prehistory: not stone tools, pots, nor artifact physics; not the environment, efficiency, nor biological capacity; not rationality, functional need, nor practical reason" (Dobres 2000, 132).

Dobres and Hoffman claim that practice theory, which looks at such human agency, social relations, and consequences over time, can provide a link between individual actions and larger scale social transformations (Dobres and Hoffman 1994, 223). Again, as discussed with all theories, when applied to archaeology, it is difficult to see how reasonably testable and empirically compelling scenarios based on practice theory can be constructed from archaeological evidence. Dobres herself acknowledges the methodologically difficult task of 'finding' agents in the archaeological record, a record that often contains only the remains of artefacts (Dobres 2000).

Agency theory as a concept does clearly build on the 'seamless web' and the technology systems of Lemonnier and Pfaffenberger, but at the same time show a strong tendency to focus primarily and heavily on political (power) relations between various agents or agent groups in society, exploring issues of control over resources, knowledge, and production itself.

In my opinion, using concepts from agency theory is made even more difficult by the following factors: it is difficult to determine how different proponents of the concept each define what constitutes an 'agent' (e.g. see Gardner 2004 and the papers therein). The various studies on agency furthermore apparently invent a completely new set of highly theorised terminology to denote known concepts. I would, for example, argue that the concept of an 'agent' might largely equal what Pfaffenberger calls a 'systembuilder'. With David Killick I do agree that much of the current debate about agency and practice theory seems to aim first and

foremost at (post-processual) theorists themselves, and is “largely indigestible by almost everyone else” (Killick 2004a, 572).

## Definitions of Technology

When formulating theories or concepts on technology, it is necessary to define the meaning of the terminology used to formulate those theories. The principal thing to define is, of course, what one understands under the term *technology* itself. Definitions of technology as formulated and used by both anthropologists and archaeologists have a long and varied history, generally as part of the developments in theoretical paradigms discussed in this chapter, and several of those definitions were already mentioned in their corresponding theoretical context. It should be noted that it is the intention to present a review relevant definitions here and not to present a history of the term ‘technology’.

In the first half of the last century, views on technology started out as strictly non-cultural, simply examining the physical manipulation of materials, and the technological knowledge, mental rules, and skills necessary for that manipulation (Schiffer and Skibo 1987, 595). Later, in the 1960s and 1970s, culture enters definitions of technology, and technology is seen to influence social life and carry cultural meaning, or as Lechtman and Steinberg put it: “technologies are the cultural traditions developed in human communities for dealing with the physical and biological environment... They are important not only because they affect social life, but also because they constitute a major body of cultural phenomena in their own right” (Lechtman and Steinberg 1979, 136; after Merrill 1968, 577).

Later, in the 1990s, in what can be termed the ‘anthropology of technology school’, Pierre Lemonnier and Bryan Pfaffenberger postulated their system views, stating that technology not only includes techniques and material culture but also the ‘social coordination of labor’ and the social context and meaning of technological activities. These techniques, material culture, and social coordination together form a *sociotechnical system*, which encompasses the social nature of human technological activity, and consists of the physical world, knowledge, know-how, social organisation, as well as meaning and values (Pfaffenberger 1992, 493, 502). In the view of Lemonnier and Pfaffenberger, a technological system (or sociotechnical system) can ultimately be defined as the entire culture (Hamilton 1996, 3).

Recent theoretical developments such as agency theory try to meld several of these different lines of thought and concepts of system views, technological style

and choice, organisation of production, and the contextualism of the historians and sociologists of technology. That this process of fusion is not yet at an end is clearly witnessed in the ongoing agency debate. In a recent article, David Killick argues that all these concepts can be seen as part of what he terms a *social constructionist* approach (Killick 2004a, 571). However different these concepts may be or seem, contrary to, for example, behavioural (Schiffer 2004 and the references therein) or (non-linear) evolutionary (Kuhn 2004) approaches, they all at least share an absence of core beliefs or paradigm(s), and they all share a 'seamless web' approach.

Although thinking about technology can take place at different organisational, temporal, and spatial levels, as is clear from the overview presented above, the *social constructionist* approach agrees that technology is not an isolated phenomenon, it is an integral part of a system, and fully interactive in culture and society. In other words, technology forms a 'seamless web' with society, where more technological ways exist to perform a given task, and where a choice for one of those ways may be influenced by beliefs, social structure, and earlier choices made in the society being studied (Killick 2004a, 571; Pfaffenberger 1992). Technological change and variation may be ascribed to various and different causes, and seen as related to individuals, agents, evolutionary models or power structures, but no theoretical trend today denies the social context of technology.

Such system views are a clear rejection of what Pfaffenberger refers to as the 'Standard View' of technology (Pfaffenberger 1992). Under this term, he bundles several widespread and seemingly commonsense assumptions about how technology relates to and changes within society. The 'Standard View' comprises three major themes:

- 'Necessity is the mother of invention', which refers to the assumption that all artefacts fulfil a need, and the most 'successful' artefacts are, therefore, those that function most efficient in what they are created for. The technology to create those artefacts will thus evolve progressively towards more efficiency and as a result of the needs of society.
- 'Form follows function and style, and meaning is a surface matter'. As a result of the necessity view, technology and artefacts can have no other meaning than their alleged function, whereby style is a secondary and superficial matter.



- 'Development is unilinear evolution, from simple to complex'. If artefacts have no further principal meaning than their function, and seek to fulfil a need in the most efficient way possible, it automatically follows that developments in artefacts and technological change must evolve towards ever more efficiency and thus complexity.

The 'Standard View' thus clearly concerns itself exclusively with techniques and material culture, ignoring the social context that these may have. However, as stated in the introduction to this chapter, archaeology, anthropology and ethnography all show numerous examples of artefacts where it is not necessity that leads to their production, or artefacts that have no practical function, only a social or ritual one. Similarly, technology is not always or only, determined by efficiency or physical constraints, but often shows signs of conscious human choice for alternative paths towards an intended product.

It is the complementing views of Lemonnier and Pfaffenberger, and how they define the inseparability of technology and the culture in which it is embedded, which primarily inform the theoretical background behind the research on the Hammeh and Beth-Shemesh material. Various elements from other theoretical frameworks are used as well, especially the concepts of technological style and choice, aspects of the organisation of production and the picture of social complexity of technology derived from (African) ethnoarchaeology.

I agree with David Killick that all approaches he labels as *social constructionist* can be seen as variations or syntheses of Lemonnier's and Pfaffenberger's groundwork: sharing a belief that more technologies can lead to the same result, and that choices in technology are influenced by the social and cultural beliefs, structure and choices of the society under study. From these social constructionist views, three concepts relevant to the current research are discussed in more detail here. To these theoretical concepts a brief review of the ethnography of Sub-Saharan iron production has been added, which provides the primary comparative material for the study of pre-industrial ironworking.

## Relevant Concepts

### The Concept of the *Chaîne opératoire*

A concept that forms the basis of most current technological studies is that of the *chaîne opératoire*. The way this concept is used today in the context of studying ancient technology derives from the work of Lemonnier as introduced above in the

Franco-European tradition. When he presents his system view of technology, he argues that technique and technology consist of five elements that make up a complete *technology system*:

- *matter* (the material acted upon),
- *energy* (forces of movement and transformation of that matter),
- *objects* (tools or means of work: e.g. a hammer or factory),
- *gestures* (which ‘move’ the object, these are organised into linear operational sequences, called *chaînes opératoire*),
- *specific knowledge* (know-how: this “is the end result of all perceived possibilities and choices, made on individual or social level, which have shaped that technological action” (Lemonnier 1992, 5)).

His work and his vocabulary follow the approaches of Leroi-Gourhan and Mauss: “without gestures that move it, without matter on which it acts, without the knowledge involved in its use, an artefact is as strange as a fish without water” (Lemonnier 1989a, 156). However, he goes much further, postulating that anthropology of technology is the study of the relationship between society and technological systems, where:

- the reciprocal effects of technological system and social system have to be considered, and
- the more physical aspects of a technical system (matter + energy) have to be considered as well as stylistic traits.

This means that the exact *chaîne opératoire* of a technology has to be studied, in order to allow isolation of what he calls ‘strategic moments’: technological operations that are essential and unalterable if the given result is to be achieved. “Examining the social control of these moments or strategic tasks is a simple and fertile means to bridge the gap between technological phenomena and other social phenomena” (Lemonnier 1986, 155). Or to put it differently, as a change in strategic moments will alter the final result, these aspects of the *chaîne opératoire* relate to social and economic factors such as control over and use of resources or knowledge.

When these ‘strategic moments’ have been defined, studying a *chaîne opératoire* reveals technological variants, i.e. different actions or ways leading to the same result. Such variants “often designate different social realities” (Lemonnier 1986,

155), can represent *social choices* (as opposed to (lack of) knowledge), even within culturally homogeneous societies, and do not have to be material in nature either (Lemonnier 1986, 156-ff).

Lemonnier's work is an intriguing approach to the study of technology. It has certainly informed, if not formed, several of the theoretical concepts discussed in this chapter, particularly through the concepts of *chaîne opératoire* and the distinction between strategic moments and choice in a technology. As Lemonnier himself states very clearly, various components of a technology system will hardly be recoverable in archaeology, and assigning symbolic functions (and Lévi-Strauss 1983; see also Lévi-Strauss 1966) or choices is difficult if not impossible (Lemonnier 1986, 179). Nevertheless, detailed technological analyses of raw materials, tools, and remains of processes, as well as similar technological systems in other aspects of the culture, combined with detailed ethnoarchaeological recording of *chaînes opératoire* will provide more cultural information than classification of a few stylistic traits. The reconstruction of as much of the technological *chaîne opératoire* as possible will help to differentiate between those actions that are 'strategic moments', and those that represent a 'choice' within the technology studied. This then provides possibilities to identify social phenomena of the technology studied that go beyond the physical activities themselves.

### The Concept of Technological Style

Clearly related to Lemonnier's social choice, but developed independently, is the concept of *technological style*. Here, the main idea is that there are different ways of producing the same result, and that a *choice* for a particular technological path may extend beyond a single material or the technological context of that material into the entire technological universe of a particular society. Heather Lechtman, the principal scholar behind this concept, constructed a hierarchy of investigations for the study of technology (Lechtman and Steinberg 1979):

- First, extensive laboratory analysis of both artefacts and processes of manufacture (i.e. the *chaîne opératoire*) are necessary. This helps to identify and distinguish essential operations from variants. Variants result from technologically equivalent, but mechanically different operations (compare the social choice of Lemonnier 1986, 155)

- Then, one should examine the development of a single technology within a single culture area (however defined), and try to define how technological changes correlate with other cultural changes
- Processes of innovation and retention of technologies must be examined (e.g. Pigott 1980, 446), to trace common approaches to materials through the whole culture area and the period in question.

Lechtman maintains that technologies often reflect a common attitude towards materials, and that one can: “elicit.. from the technology information about its own symbolic message, and about cultural codes, values, standards, and rules that underlay the technological performance” (Lechtman 1977, 17). Lechtman’s own work investigates how Inca gold work and textiles both share a preoccupation with integrity or ‘essence’. Specific technologies are used in each to integrate the characteristics that are valued most (colour and design) in the object, as opposed to creating those through a surface application. She relates these shared (or common) technological traits to elements, known or putative, of the Inca value system. Very similar observations are made by Dorothy Hosler in her extensive study of technological style in Mexican metallurgy (Hosler 1994).

Heather Lechtman’s approach is very ambitious, most of her own work and that influenced by her concept of *technological style* confines itself to the study of specific technologies (Childs 1991; Lechtman 1988), sometimes across cultures (Hosler 1994). Only occasionally do people attempt to compare multiple technologies, and even then the focus is usually predominantly on one of them (Friedman 1995).

The concept of *technological style* is not without its problems in archaeology, as many scholars use a ‘fairly passive definition of style’ (Hegmon 1992, 529), and to a certain extent, the concept itself is rather static. As long as one studies technological situations that are static themselves this is no problem, but if the archaeological study concerns cultural and/or technological change, then the concept is more difficult to apply.

In practise, when studying archaeological debris of one technology, trying to define technological choices and style remains very similar to Lemonnier’s distinguishing between choices that represent technological requirements, and those that reflect a social choice by the practitioner. Thus, defining a technological style first relies on a reconstruction of the *chaîne opératoire*. It is in comparing the social choices of one technology with those of other technologies

and other aspects of society that a symbolic content or cultural code may be reconstructed.

The concept of *technological style*, in its search for congruencies between different technologies, may offer interpretations beyond simple speculation. Nevertheless, it shares with Lemonnier's *technological system* that it is difficult to see this fully applied to archaeological remains, resulting in proven relationships between technological system and particular features of social organisation. Still, "Every social theory of material culture should, also, necessarily, explain the specificity of these relationships; why they exist in the given case, *and* try to understand cases when they do *not* exist" (Lemonnier 1989a, 157).

### Organisation of Production

Related to the system views of Lemonnier and Pfaffenberger, the third concept that is relevant for the study of the Tell Hammeh and Tel Beth-Shemesh metallurgy concerns itself with the various ways in which a production system can be organised. It further examines how such organisation is embedded in the social and economic context of the society in which it takes place. In doing so, this concept has a more pragmatic approach to the study of technology than the previous two concepts. It is primarily concerned with the economic and social side of organisation and provides clear definitions and terminology to describe aspects of organisation.

The prime study concerning the organisation of production is the work of Cathy Lynne Costin (Costin 2001; Costin and Wright 1998; Costin and Hagstrum 1995; see also Costin 1991). Costin applies a structured approach to looking at technology, focussing more on pragmatic aspects of production such as specialisation, producer-consumer relations, and technological variation than on symbolic or cultural traits, which certainly does not imply that such aspects are ignored. Equivalent to Lemonnier's *technology system* and Pfaffenberger's *sociotechnical system*, Costin uses the term *craft production* to denote the larger system that comprises all aspects of society affecting and affected by technology, including symbolic and cultural ones.

In her definition, a craft production system consists of artisans, means of production, organisation and social relationships of production, objects, and relations of distribution and consumption (Costin 2001). Costin herself clearly states that a production system will be difficult to recognise in archaeology, and that different interpretations of what is found are often possible. As especially

non material aspects of a system such as interactions, beliefs, and principles (Costin 2001, 278) are invisible in the archaeological record, multiple lines of evidence are necessary to demonstrate a craft production system. Notwithstanding these difficulties, several concepts Costin defines with regard to production and technology do at least provide a framework that can guide the interpretation of remains of a technological activity.

Starting with the producers, a first aspect of production that Costin discusses is *specialisation*. Although production is variable over time, space, and people the core definition of specialisation is “that fewer people make a class of objects than use it”, i.e. a specialist produces more than needed for personal consumption. The level of specialisation will vary based on the size of the production unit, i.e. from household level to workshop level, and on organisation, i.e. as *independent production* (for general consumption) or as *attached production* (where production is by or for elites). Levels or degrees of specialisation further depend on intensity of production, i.e. does it take place occasionally or full-time, and the scale and output of the production. All factors can overlap, e.g. production might be small scale by individuals through small groups in a domestic setting to large production units producing large quantities. It is generally assumed that specialisation involves some manner of compensation for the time spent in production, usually in some form of exchange with other goods from whose production the specialist is more or less ‘freed’. Similar to Lemonnier’s ‘know-how’, Costin further defines *skill* as a defining factor of specialisation, which generally translates to: more complex technology requires more skill, and will therefore be more specialised.

Levels of specialisation and especially possible related compensation are extremely difficult to demonstrate in an archaeological context. For example, a large-scale operation might take place on a seasonal basis. This would mean that the specialist(s) involved is still largely self sufficient with regard to the procurement of other goods, obscuring social organisation or compensation patterns, or even result in an interpretation as small-scale household production.

Moving on to production itself, Costin concludes that a reconstruction of the *chaîne opératoire* is necessary in order to understand the full technological process, to reveal aspects such as task division, labour intensity and investment, training and skill required. By first reconstructing the *chaîne opératoire* from the

residues of production, one can examine five aspects that connect technology to the organisation of production:

- **Technological complexity.** This is often assumed to correspond with organisational complexity, but this is generally based on the perceived complexity of techniques and tools, disregarding the potential complex know-how and skill that may be involved in a technologically 'simple' operation (see Hegmon 1998, 279).
- **Efficiency.** This is the amount of time, energy, and input of raw material per unit of output. It is often assumed that independent production will gear itself more towards efficiency than attached production. This idea can be misleading, and is often based on modern Western economic concepts where efficiency equals time. It also ignores other factors that may define 'efficiency' for the artisan or consumer, such as (social) meaning and relationships. In other words, social or cultural considerations may lead to a technology we perceive as inefficient, but that is very sensible to the artisan(s) involved.
- **Output.** The amount of material produced, signifying both the absolute total of material and the volume per production unit. High output is often equalled to high specialisation, but once more, caution is due, e.g. small quantities do not necessarily correlate to small-scale production, or highly specialised workshops may produce a very low number of labour intensive objects.
- **Control.** Some technologies are often seen as indicators for a high level of (political) organisation, based on how they can be controlled through access to tools, raw materials, or knowledge.
- **Variability.** Variation in production techniques and sequences are often studied (e.g. Lemonnier's social choices, and Lechtman's technological style), and may reflect social aspects of a technology. Variability can be an indicator of individual artisan or group identities, or of distinction between local production versus imported goods. Such interpretations are difficult due to uncertainties regarding scale of the operations and ease of technological transfer, an area that still needs more research. Variability will furthermore often reflect adaptation to what materials or circumstances are present at a given time and place.

Besides the caveats that go with each of the five point outlined above, none of them should be considered to indicate aspects of organisation on its own. It is only after careful examination of each and in combination as multiple lines of evidence that an insight into organisation might be proposed.

The last concept Costin discusses with regard to the organisation of production that is relevant to this research, is the concept of *standardisation*. Homogeneity of artefacts in an assemblage is often seen as evidence of specialised production. The degree of standardisation is then assumed to indicate the level of (elite) control over production. As with the five aspects of technology, many problems exist in this view, e.g. the scale at which one examines the technology in question may lead to a very different interpretation of the level of standardisation. What looks random at a community level may represent a highly specialised operation on a regional level. In addition, elite goods may be produced by specialists, but purposefully not standardised.

In archaeological practise, as Costin clearly states, each single aspect discussed above may be difficult to find, or may at the very least be contentious in its interpretation. Nevertheless, awareness of these concepts can certainly inform and guide interpretation or discussion about the organisation of archaeological remains of production.

## The Ethnography of African Metallurgy

The ethnography of Sub-Saharan iron production is in itself not a theoretical strain or concept. It does however provide a body of data on which the theories and concepts outlined above can be applied. It is relevant to the research presented in this thesis, in that it is the only comparative material of (pre-industrial) bloomery iron smelting and smithing.

Although direct comparison with archaeological materials over continents and over time should be approached with care, these ethnographical observations do provide a glimpse of the techniques, styles, choices, and organisation of production that can never be found in excavation. Because indigenous iron working industries survived for so long in Sub-Saharan Africa (Childs and Herbert 2005; Killick 2004b; Childs and Killick 1993, 325), researchers are also presented with an incredibly full array of cultural practices and value systems surrounding metal production, that have disappeared in the rest of world (Childs 1994). (Veldhuijzen 2002; Veldhuijzen 1998, 23-56) This creates a unique possibility to observe social, cultural, and economic aspects of technology that normally remain



invisible to an archaeologist. In that respect, they provide a tool to create awareness of the complexity of technology that has no equal, especially in the context of iron production technology.

Most of these ethnographic studies are quite recent, and clearly show the cultural complexity in which the technologies are embedded. Different studies have examined various aspects of technology, such as the role of ritual and gender in metal production (Goucher and Herbert 1996; Childs and Killick 1993; Herbert 1988); issues of power and control (Wade 1989); the role of metal in political organisation (Killick 2004b; de Barros 1997; Kusimba 1996; Childs and Killick 1993; de Barros 1986); the social position of smiths (Childs and Killick 1993; Rowlands 1971) and the social meaning of artefacts that are produced (Childs 1991; Wade 1989).

The African ethnographic studies allow examination of the relationship between metallurgical processes and how these are affected by “indigenous theories of natural and social order” (Childs and Killick 1993, 319), and they provide a very strong illustration for the ‘seamless web’ of technology and society. Most ethnographical studies of technology in Sub-Saharan Africa concern a single case study or tend to make synchronous comparisons, and focus less on technological change over time. This is directly related to the fact that most studies observe a technological activity as it happens, and more specifically a technological activity that is on the brink of disappearing completely, preventing repeated visits. In fact, several of the case studies are actually reconstructions, where former smelters re-enact their craft (Killick 2004a, 572).

In archaeological practise, comparison of such relatively modern observations with archaeological finds of different times and locations should be treated with extreme caution. Nevertheless, the African cases clearly show the enormous array of choices available in a *chaîne opératoire*. This ranges from who executes the technology, the choice of location relative to raw materials and consumers, rituals and meaning involved in production, to shape and size of furnaces, yield per operation, or status of the producer and the products in society. These observations thus greatly enrich the conceptual template with which to approach archaeological finds.

## Discussion and Conclusion

As mentioned at several points above, it is can be difficult to apply the various theoretical strains outlined above to actual archaeological finds. This also applies

to the concepts of *chaîne opératoire*, technological style, and organisation of production, and the Sub-Saharan ethnography. Most of the theories and concepts are based on ethnographical or anthropological observations in societies, locations, and/or times that are incomparable to those of the iron smelting and smithing at Hammeh and Beth-Shemesh. Comparison of these theories and concepts with the archaeological and archaeometric data from Hammeh or Beth-Shemesh to reconstruct sociotechnical systems, their participants, or related social and cultural meaning should therefore be approached with extreme caution, as already indicated with the African ethnography.

Furthermore, most studies underlying the theoretical considerations discussed above were performed over several decades, examining multiple dimensions of large geographical areas, using large quantities of different archaeological, ethnographical, as well as material science methods and data. This stands in stark contrast with the quite fragmentary remains of early iron production excavated in just a few seasons at the two sites of Hammeh and Beth-Shemesh, for which also as yet no comparable data exists in the entire Near East. In the case of Hammeh in particular, the excavation seems devoid (but perhaps significantly) of any evidence for a social or economic context, precluding interpretation regarding organisation or embedding of the technology in society.

Another problem is that most theoretical studies primarily focus on artefacts, and their social contexts and meanings, even when a lot of attention is paid (or indicated that it should be paid) to the production sequence or techniques leading to those artefacts. Applying such theoretical models, concepts, and interpretations to a virtually artefact-free case study like Hammeh is at least problematic.

A further problem is caused by the fact that most theories, models and case studies discussed here concern historic or proto-historic 'known' societies, and that it is therefore, as many studies themselves indicate, very unlikely that all aspects of technological systems as they describe them can be extended to, interpreted from, or simply found in the fragmentary record of prehistoric societies that we find in archaeology (see Lemonnier 1986, 179).

Acknowledging the limitations in applying the theories and concepts on technology to actual finds of technology in archaeology does certainly not equal rejecting them. The theories and concepts concerning technology that are discussed here, and in my opinion especially the system views of Lemonnier and Pfaffenberger and

the related concepts of *chaîne opératoire*, technological style, and organisation of production, as well as the ethnographical observations in Sub-Saharan Africa, create a conceptual template for the study of technological finds. With this template in mind, it is possible to approach the debris of iron production at Tell Hammeh and Tel Beth-Shemesh with the aim to go beyond the purely material aspect and try to interpret what these technologies mean in the context of the society of which these processes are an inseparable part.

It follows from most theories and concepts outlined above that the study of the Hammeh and Beth-Shemesh material should start with thorough technological analyses of raw materials and remains of the iron production process found at these sites, in order to reconstruct the individual *chaînes opératoire* of these technologies. Consequently, a first attempt can be made to identify characteristics of these technologies that may relate to the society in which they took place, and as such reveal their meaning in the archaeology of the Levant.

## CHAPTER 3: A BRIEF TECHNOLOGY AND HISTORY OF IRON

### Introduction

When remains of metal production are found in an archaeological excavation, a wide-ranging assemblage of materials is likely to be encountered, comprising, for example, various types of slag, technical ceramics, clay, ash, charcoal, ore, and (although often absent) metal. Such finds raise several questions an archaeologist would want to answer. It needs to be determined what metal was produced or worked, and what stage or stages of the technology to produce or work that metal are represented. Further detailed study of the various materials can reveal more specifics about the technology under study that will enhance the interpretation of both the technology itself and its meaning within the archaeological and ancient cultural context.

Every stage of a metallurgical process will produce its specific assemblage of debris, but these can not easily interpreted through macroscopical and morphological analysis alone. Where the production of iron metal is concerned, as is the case in this research, further (chemical and microstructural) analyses are required to enable distinction between the smelting of ore and the smithing of objects, as both can result in macroscopically highly similar debris (description and methodology of the various analytical techniques are discussed in chapter 6).

The chemistry, mineralogy, and mechanics of either technique all interact and determine the formation, properties, and final composition of the slag that is produced. This means that to accurately identify and interpret slag and furnace or hearth remains, one first needs to understand the technology of iron production as a whole. This chapter therefore first provides a basic description of the pre-industrial direct or 'bloomery' technological process of iron production, as opposed to the modern indirect or 'blast-furnace' process. It will summarise the various stages of iron production technology, from procurement of raw materials to the creation of an iron object in a smithy, and introduce the terminology used in this research.

The objective is a general chemical and technological description of iron smelting and smithing, as background to the research presented in this thesis, but not a comprehensive treatment of all known peculiarities or specialist details. It is nevertheless sought not to oversimplify a process that, as will become clear, is a highly intricate one.

Basic information on iron is followed by a summarised description of pre-industrial ‘bloomery’ iron production technology and a presentation of the different materials, actions, and processes that form the *chaîne opératoire* leading to the creation of an iron object. It should be noted that the *chaîne opératoire* presented here is very broad, and includes all possible technological stages, whereas an actual production site will more likely only show a selection of those stages.

For a long time, most of what was known and surmised about ‘bloomery’ iron smelting and smithing was largely based on laboratory and field experiments (Tylecote and Merkel 1992, 3-20; Tylecote *et al.* 1971, 342-363; Pleiner 1969, 458-486), which were only partly informed by the study of actual archaeological production finds. In recent years, studies of iron production related materials have increased considerably in number (e.g. Joosten 2004). In the context of Near Eastern archaeology, however, evidence for iron production remains extremely scarce, and as a direct consequence, so does knowledge about early iron technology in that region.

The scarcity of actual production finds in the Near East also heavily influences what is known or thought about the historical origin and development of iron technology in this region. After the generic *chaîne opératoire* of ‘bloomery’ iron metallurgy and the relevant technological terminology have been discussed, a brief chronological overview of the history of iron in the region will be presented. This overview reviews the artefactual evidence for use of iron in the Near East and bordering regions, and examines current thinking on how this metal was first developed and how knowledge about iron or the technology itself may have spread over this region. The artefactual evidence and ideas about the ‘coming of iron’ are contrasted with the paucity of actual evidence for iron smelting and smithing in the entire Near East, which underlines the importance of studying the material from Tell Hammeh and Tel Beth-Shemesh.

## **Making Iron Metal; Smelting and Smithing Technology**

Several concise and exhaustive descriptions of iron technology exist, and the overview presented here draws on these sources, including (Joosten 2004; Pleiner 2000; Craddock 1995; Tylecote 1992; Rostoker and Bronson 1990).

## Basic Information on Iron

The element iron, or Fe, from the Latin *ferrum*, is number 26 in the periodic table. It has an atomic weight of 55.847. It has a density of 7.88 g/cm<sup>3</sup>, and its melting point lies around 1535 °C. It is, after silicon and aluminium, the third most common non-gaseous element in the earth's crust, to which weight it is estimated to contribute approximately five percent. It is also the fourth most common of the eight elements that make up 98% of terrestrial rock: O, Si, Al, Fe, Ca, Na, Mg, and K.

Iron rarely occurs in its metallic, 'terrestrial' or 'native', form, due to its chemically reactive nature. Native iron has only been found in exploitable amounts on Disko Island in West-Greenland (Buchwald 2005, 35-37; Buchwald 1992; Coghlan 1977, 1). The only other form of pure, directly forgeable iron has a meteoritic origin and is a little more common (Buchwald 2005, 13-38; Buchwald 1992; Buchwald 1976). Most commonly, iron appears as a chemical compound, an iron mineral, e.g. Fe<sub>2</sub>O<sub>3</sub> or haematite, often in association with varying rates of other, non-ferrous, minerals. A mixture of iron oxide(s) and other minerals is called an 'ore' if and when it contains sufficient iron oxide for economically viable extraction of metallic iron. What constitutes economic viability can and will vary significantly in both time and space, and is culturally determined.

## Summary of Bloomery Iron Smelting and Smithing Technology

Iron production, that is the production of metal from an ore, is an integrated process. This means that it incorporates a logical succession of separate actions and processes, in which the product from one action or operation is the starting material of the next. Ores first need to be procured, which usually involves a more or less complicated form of mining. The complexity and labour intensity of mining will vary from deposit to deposit, and this may play a role in choosing a location for smelting operations. To gain the iron contained in the ore, its mineral structure has to be broken up and unwanted materials (gangue) have to be removed. This may start by what is called mineral dressing, or in other words the upgrading of the ore, through physical operations like comminution (breaking up) or chemical operations such as roasting (heating). To varying degrees, the mining work itself already contributes to the comminution, and pieces of rock that are deemed unsuitable are often discarded at this stage.

Beneficiation and selection of the ore can continue or take place in full at the smelting location. The selected pieces of ore are then charged into a furnace

together with a fuel. In antiquity, the fuel is generally charcoal. The furnace is fired so that a reducing atmosphere is maintained. This operation is called *smelting*. Air supply for the burning fuel is provided by forcing air into the furnace either by using bellows and tuyères (i.e. a hole in the furnace wall or a ceramic tube that both protects the bellow from heat and directs the airflow), or by natural draught, using the chimney effect of the furnace. Natural draught of a furnace may be amplified by (strong or constant) local winds enhancing the chimney effect, and/or the airflow through tuyères. The last is known from the very specifically designed Sri Lankan wind-powered furnaces, where a row of tuyères is aligned in one side of a wide, rectangular furnace structure. This structure, constructed near the top of a hill, uses the airflow from the local wind, the force of which is further enhanced by the pressure differential created by the uphill flow of the air (Tabor *et al.* 2005; Juleff 1998; Juleff 1996).

During smelting, the iron minerals are reduced and broken up by reaction with the carbon monoxide gasses released from the burning fuel. The unwanted chemical compounds, of which silica ( $\text{SiO}_2$ ) is the most important, react with part of the iron oxides from the ore, ceramic material from furnace and/or tuyères, and with the fuel ash to form a liquid slag. It is possible to add extra agents to the furnace, called fluxes, to change parameters of the operations. Addition of lime ( $\text{CaO}$ ), for example, may help to lower the melting temperature of the slag, and may increase the yield of iron metal. There is no evidence to suggest that fluxing was done intentionally in prehistoric iron production, but fluxing effects can also occur as a function of ore or ceramic composition, something the smelters may well have been aware of.

The liquid slag transports the reduced iron, in particles or flakes, downward through the furnace, and simultaneously protecting it from reoxidation by enveloping the metal. The final product of smelting, besides ash and slag, is a *bloom*. This is a rough and often spongy mass of solid iron metal that consists of flakes and nodules that have welded and sintered together, mixed with bits of slag, incompletely reduced ore, unburnt fuel, and parts of furnace ceramic. It is this bloom that gives pre-industrial iron production technology its name of 'the bloomery process'.

Typically, the bloom has to be refined before it can be used to produce artefacts. One way of refining the bloom is by hammering it to smaller pieces and sorting out the iron particles. These metal fragments are heated in an open hearth with a

forced air-supply, until red-hot and soft. They are subsequently hammered to squeeze out remaining slag and to consolidate the fragments into a larger workable size. Alternatively, a more coherent or massive bloom can be consolidated by hammering it when it is still red-hot from the smelting process. The process of consolidation of the bloom, often to a bar or 'billet', is called bloomsmithing. This smithing of a bloom, taking place as part of the first heat (i.e. immediately after a smelt), or following cooling and reheating, forms the *primary smithing* process. Depending on the organisation of the production, all, part of, or no primary smithing may take place at the smelting location.

If primary smithing is not or only partly performed at the location of smelting, the remainder may take place at the location of and prior to the actual shaping of the metal into artefacts. The forging of metal into artefacts is called *smithing*, and to avoid confusion with primary smithing, this can be referred to as *secondary smithing*. The secondary smithing process comprises the heating and hammering of the metal in order to create the desired shape, and involves various techniques, e.g. annealing and quenching, that will influence the properties of the final product. For a clear description of these techniques and resulting properties of iron artefacts see Scott (Scott 1991, 1-10, 31-42).

Secondary smithing is carried out by repeatedly heating the iron in a hearth and hammering it on an anvil. The smithing hearth may vary from a shallow open hole in the ground to a rather large structure, and is operated at high temperatures under mostly oxidising conditions. Almost all remaining smelting slag is now squeezed out of the iron billet, and together with oxidising metal from the billet, ceramic hearth material, and fuel ash will form a characteristic slag at the bottom of the hearth. A generic *chaîne opératoire* incorporating the technological steps as summarised above is presented in Figure 1.

## Ore

Besides iron minerals (iron oxides), an iron ore is composed of non-ferrous components and minerals, also referred to as gangue or impurities. The gangue consists of both major and trace elements. The most common non-ferrous gangue compounds are  $\text{SiO}_2$ ,  $\text{Al}_2\text{O}_3$ ,  $\text{CaO}$ ,  $\text{MnO}_2$ ,  $\text{MgO}$ ,  $\text{K}_2\text{O}$ ,  $\text{P}_2\text{O}_5$ , and  $\text{TiO}_2$  and these are found in varying ratios in most iron ores. The quantities of trace elements like Zn, Ni, As, or Ba will differ in each ore body and may allow the determination of which ore led to which slag or object. Some gangue compounds are beneficial in a



bloomery process, e.g. manganese, others like sulphur are undesirable (Rostoker and Bronson 1990, 45-46).

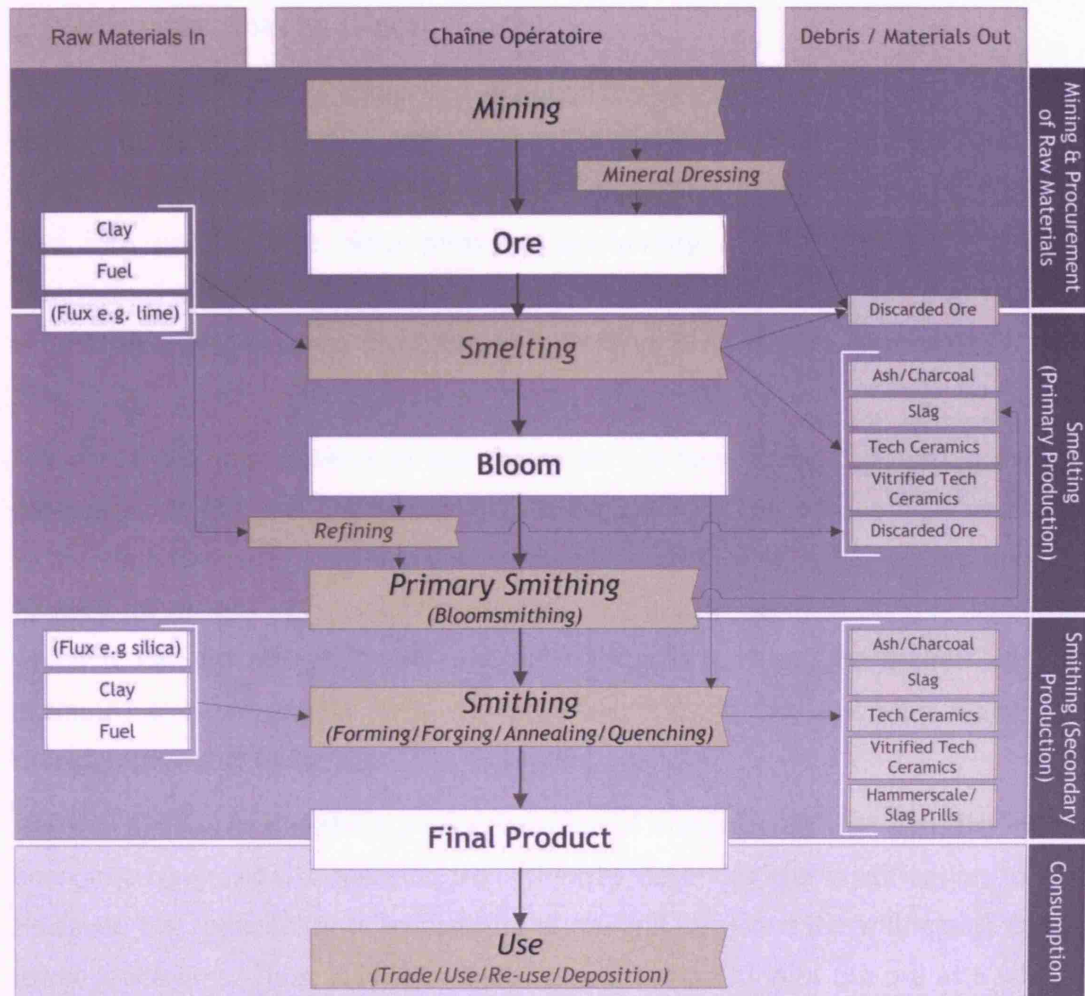


Figure 1. Flow chart of the integrated process of pre-industrial iron production. The chart shows four stages (black labels) of a generic *chaîne opératoire* (central column). Materials entering the process are in the left column, those produced are in the right column. Activities are in italics, materials used and produced in regular case. The chart does not represent processes that move 'upwards' such as repair or reworking of objects.

In many areas of the world, iron ores are quite commonly available, allowing a smelter to choose between ores, or offering the possibility to mix different ores to optimise properties. When no choice is available, due to local geology or issues of control over resources, a smelter will have to use the available ore, and possibly adjust the technological process to its particular properties.

Ores are found in many forms, ranging from sands that have to be sieved or washed, to hard rocks that have to be broken up. Many classifications are possible, but most frequently ores are classified by the nature of the iron mineral. The individual ores are most commonly also named after their (main) iron mineral:

- **Oxides** ( $\text{Fe}_x\text{O}_y$ ): e.g. magnetite ( $\text{Fe}_3\text{O}_4$ ); haematite ( $\text{Fe}_2\text{O}_3$ ); limonite ( $\text{FeO}(\text{OH}) \cdot n\text{H}_2\text{O}$ ).
- **Carbonates**: (mainly) siderite ( $\text{FeCO}_3$ )

Another group of ores is comprised of sulphidic ores (e.g. pyrite,  $\text{FeS}_2$ ) but these are rarely, if ever, used in iron production due to their sulphur content. The distinction between ores used here is relatively arbitrary; for example, it does not take into account the reducibility or availability of the ore. More specific descriptions of ores as well as their respective properties can be found in Tylecote and Rostoker and Bronson (Rostoker and Bronson 1990, 42-47; Tylecote 1987, 47-52).

The classifying iron mineral in question does not have to be the most prevalent component of the ore, but in practice, it typically is. The iron content of an ore forms one important factor in a smelter's appreciation of it. However, not only the 'quality' of an ore determines its 'value', but it also depends on the ease with which it can be obtained and how easy its structure can be broken up. For example, some magnetite ores are extremely rich in iron but very dense and therefore difficult to reduce.

Any iron ore has by definition a concentration of iron minerals that is sufficient for economic conversion to metallic iron (thereby deserving the qualification 'ore'). However, the reducibility or availability of ore will influence the willingness to use lower-grade ores. Thus, it is clear that mineral composition of the ore as a whole, both of the iron mineral and of the gangue, as well as availability of ores must have exerted their influence on the technological paths chosen in (early) iron production.

## Mineral Dressing

To enable the production of iron metal, the chemical structure of the ore has to be broken up. This can only be done by the reduction process, or *smelting*. Some dense or very hard ores such as magnetite and hydrated ores such as limonite are difficult to smelt without prior treatment, and require preparation of the ore or 'mineral dressing'. There are two methods to upgrade ore in preparation for smelting: comminution and roasting.

### Comminution

Comminution is the physical breaking up of the ore into smaller lumps, often with hammer stones. Some comminution of the ore always takes place through the

physical actions involved in mining. This may be followed by more crushing and grinding, further reducing the size of the ore pieces. This allows the removal of visible impurities, and a smaller size of the ore nodules ensures better reduction during the smelt. Too small a size, however, would result in clogging up the furnace rather than promoting reduction.

### **Roasting**

A further step in preparation of ores for smelting is roasting, which involves the heating of ore in an open, oxidising, fire, within a temperature range of 500-800 °C. The ore can be put on piles of wood or in a shallow basin with the wood on top. It is important to allow a maximum access of air, but tuyères or bellows, which are commonly used in smelting, are not usually necessary. This is both because of the relatively low temperature needed for roasting, and because the open structure of the roasting pile, which allows sufficient access of air.

Hydrated ores are roasted in order to remove the water. Carbonate ores are roasted to remove the carbon dioxide and to break up the ore nodules ( $\text{FeCO}_3 \rightarrow \text{FeO} + \text{CO}_2$ ). Dense oxide ore, particularly magnetite, is often hard to reduce and can be roasted too, which will both turn it into haematite ( $4\text{Fe}_3\text{O}_4 + \text{O}_2 \rightarrow 6\text{Fe}_2\text{O}_3$ ), and make it softer due to the internal cracking from the expansion that goes with the reaction. In general, roasting causes ores to break up into smaller bits by the opening up of cracks in the particles, thus ensuring a more effective smelt. It should be noted that the exposure to rising temperatures of ore travelling down in a furnace charge also triggers these roasting effects to varying extents.

### **Smelting**

Smelting is the firing of ore and fuel in a furnace to remove unwanted earthy material (gangue) and reduce iron oxides to produce iron metal. What sets iron apart from other metals, is the fact that the metal remains in the solid state during the bloomery smelting operation.

Several processes take place simultaneously during a smelt, and different areas of the furnace show different actions at the same time. Simplified, the main process is the reduction of ore, by carbon from the fuel, at a sufficient temperature. Furnace gasses, consisting of carbon monoxide (CO; reducing) and carbon dioxide (CO<sub>2</sub> not reducing), result from combustion of fuel (charcoal) near the air-inlets and rise up through the furnace. Rising CO<sub>2</sub> encounters unburnt fuel and is converted into CO, which makes the gasses reducing. At the same time, the ore

travels down and is gradually reduced until it reaches the combustion zone. This happens as the CO meets unreduced ore, when it converts the iron oxides into iron metal by extracting its oxygen, as well as when the ore is exposed to solid carbon (charcoal).

As the ore descends, it goes through various temperature zones, and in each it progressively breaks down and is reduced. At different temperatures (and, therefore, also at different locations in the furnace), different CO-CO<sub>2</sub> ratios occur that influence the efficiency and nature of the reduction taking place. For example, more CO in the process may result in the formation of mild steel (iron metal containing 0.3 - 0.6 % carbon) (see for example Rostoker and Bronson 1990, 98, Fig 9.7).

In the case of haematite (or roasted limonite and siderite ores), the reduction steps follow these lines:

- $3\text{Fe}_2\text{O}_3 + \text{CO} \rightarrow 2\text{Fe}_3\text{O}_4 + \text{CO}_2$
- $2\text{Fe}_3\text{O}_4 + 2\text{CO} \rightarrow 6\text{FeO} + 2\text{CO}_2$
- $6\text{FeO} + 6\text{CO} \rightarrow 6\text{Fe (metal)} + 6\text{CO}_2$

Where the ore is in direct contact with solid carbon, the reduction might follow:

- $6\text{Fe}_2\text{O}_3 + \text{C} \rightarrow 4\text{Fe}_3\text{O}_4 + \text{CO}_2$
- $4\text{Fe}_3\text{O}_4 + 2\text{C} \rightarrow 12\text{FeO} + 2\text{CO}_2$
- $12\text{FeO} + 6\text{C} \rightarrow 12\text{Fe (metal)} + 6\text{CO}_2$

Changes in the nature of the charge, e.g. fuel to ore ratio, size and type of fuel and ore, and the characteristics of the airflow influence several factors of the smelting process such as the furnace temperature, which in turn influences characteristics of both the smelting process and of the metal produced. In theory, smelters can manipulate the CO-CO<sub>2</sub> ratio in the furnace to influence the final product. Below 1% of CO<sub>2</sub> gasses in the furnace, i.e. highly reducing circumstances, results in cast iron (which does liquefy during smelting, and therefore requires temperatures of ca. 1250-1350 °C), between 1 and 3% results in steel, and above 3% results in bloom iron. In practice, the result will be a very heterogeneous bloom with differing carbon contents. The nature of the bloom, in particular its carbon content, influences the subsequent treatment of the iron (Scott 1991, 31-42; Rostoker and Bronson 1990, 121-152; Tylecote 1987, 243-290; on properties of iron metal, see Reed-Hill 1973).

At the same time, the unwanted minerals (gangue) have to be removed. To do this a slag has to form by reaction of some of the iron oxide with the unwanted minerals, predominantly quartz, according to the reaction:



Theoretically, this means that all slag should consist of only two components, FeO and SiO<sub>2</sub>, appearing together in the form of the iron silicate fayalite (Fe<sub>2</sub>SiO<sub>4</sub>), whilst all remaining ('free') iron oxide will be reduced to iron metal, or remain in the slag as wüstite. However, depending on their presence, reducibility, and chemical nature other gangue minerals and trace elements from the ore as well as components from the technical ceramics and fuel ash enter the slag. Because of the large number of factors influencing the overall process, the system is hard to keep under complete control, and the resulting slag is generally less lean (i.e. low in iron oxide) than the system might theoretically allow, and may show varying amounts of free iron oxide.

The nature of the gangue, technical ceramics, and fuel ash all exert influence on the melting temperature of a slag, and thus on the necessary operating temperature of the furnace. The operating temperature typically lies at least somewhere between 1100 and 1200 °C. However, not all furnaces operate at the temperatures where all slag is fully liquid. The final composition of slag depends on furnace operating temperature(s), atmosphere (redox conditions and pressure of the airflow), and whether or not it is run off, 'tapped', from the furnace.

The clay used in construction of the furnace and/or tuyères is subjected to the same high furnace temperatures. Depending on its exposure to sufficient heat and on the refractoriness of the material, it may melt, eventually resulting in molten *technical ceramic*, and/or partly dissolve in the slag. The ceramic material, when absorbed, may even help the formation of slag by lowering its melting point or its viscosity. The same applies to the ashes formed by the burnt fuel.

To help the formation of slag, smelters may add a fluxing agent or 'flux'. An extra ingredient, for example lime (CaO), can be added to the furnace charge to help lower the melting temperature or improve viscosity of the slag, similar to the possible contribution of the technical ceramic. In general, the intentional application of fluxes is presumed common in copper production, but evidence is rare in pre-modern or bloomery iron smelting. On the subject of fluxes, see (Rostoker and Bronson 1990, 83-85; and Tylecote 1987, 107-108). The technical ceramic from tuyères and (lining of) the furnace wall (with varying degrees of

refractoriness) may act as a flux. Iron ores, which are themselves often used as a flux for copper smelting, are often 'self-fluxing' (See Rostoker and Bronson 1990, 57-60 on refractories; Tylecote 1987, 291-300, 310-321, on slag and its properties).

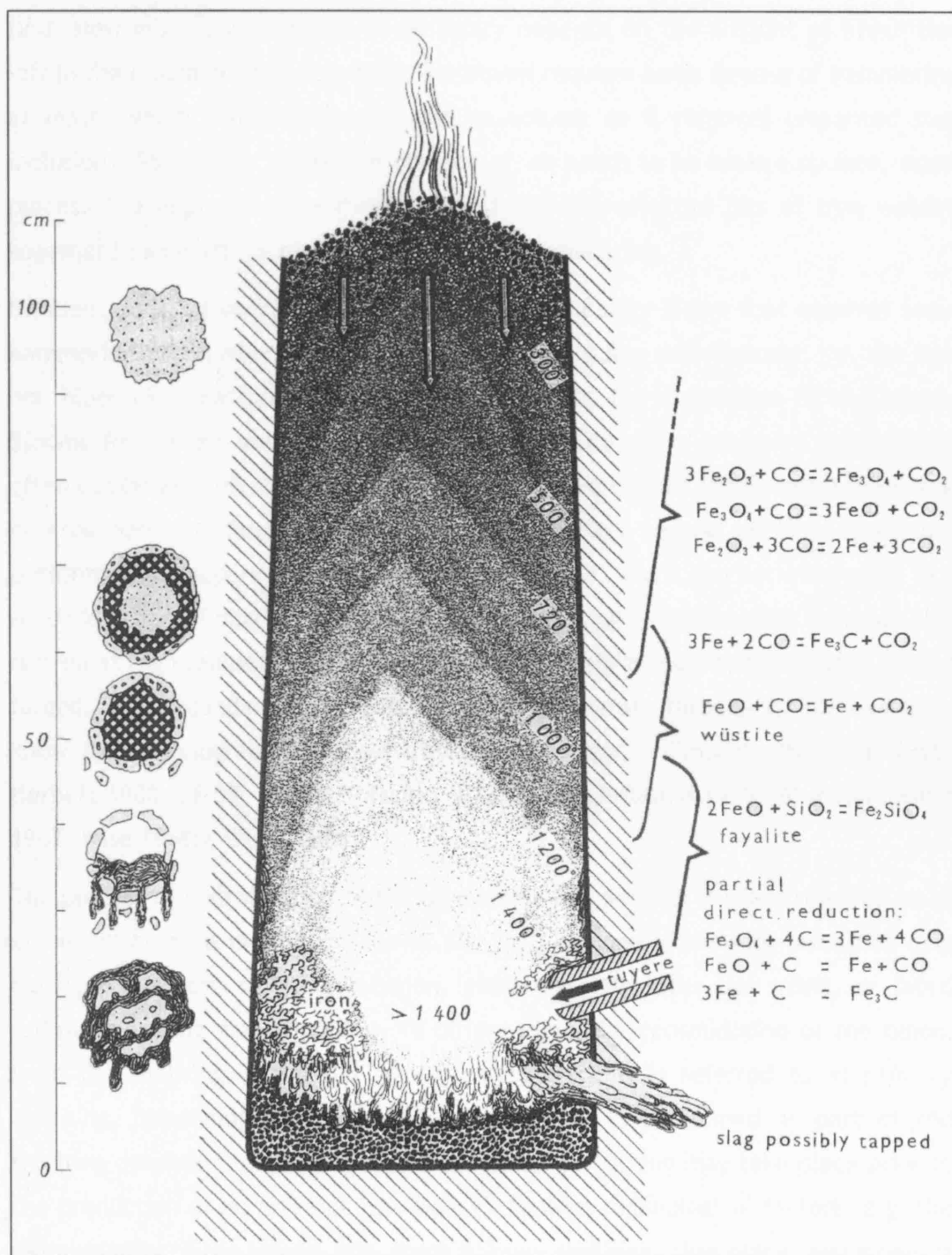


Figure 2. Theoretical model of a bloomery iron shaft furnace. The drawing shows various stages of the smelting process. The physical breaking up of the ore, the formation of slag, and the transportation of metal particles by the slag are schematically shown on the left. Ranges of furnace temperatures, the formation of an iron bloom near tuyère level, the deposition of slag at the bottom of the furnace as well potential tapping of the slag, and melting of furnace wall and/or tuyère ceramic are indicated in the furnace itself. The chemical reactions taking place at the various locations and temperature zones of the furnace are indicated on the right (from Pleiner 2000, 134, Fig. 33).

## Primary Smithing

The iron metal, or bloom, produced during smelting is typically not solid enough to be directly forged into finished products. The bloom needs to be consolidated first. How much consolidation is necessary depends on the amount of impurities left in the bloom during the smelt. The bloom requires some degree of hammering at least, which considerably reduces its volume as it removes unwanted slag inclusions. Sometimes the bloom consists of, or needs to be broken up into, small pieces. The impurities are then removed and the selected bits of iron welded together in a hearth by repeated heating and hammering.

Efficient smelting operations can achieve a high quality bloom that requires some hammering, often when still hot, to expel adhering slag and charcoal; i.e. the red-hot bloom is consolidated immediately following the conclusion of the smelt. Blooms from more average operations will require more extensive hammering, often combined with reheating. Some operations result in a highly unconsolidated, heterogeneous bloom, which might be subjected to a second smelting operation, performed in a separate, typically smaller, furnace, which can be referred to as a secondary or 'refining' furnace. The broken up bloom together with iron rich slag is fired at high temperature producing slag and a higher quality bloom that can be forged. This secondary refining stage using a separate furnace is, for example, known from ethnographical observations of the Fipa in Tanzania (Barndon 1996; Herbert 1988, 58-59; Wembah-Rashid 1973; Wembah-Rashid 1969; Wembah-Rashid 1967; Wise 1958b; Wise 1958a).

The process of consolidation of the bloom to a bar or billet is often referred to as *bloomsmithing*. As mentioned above, all, part, or none of the bloomsmithing may take place at the smelting location, either directly after the smelt, or later, following cooling and reheating. To differentiate the consolidation of the bloom from the smithing of a billet to (an) artefact(s), it is referred to as *primary smithing*. Depending on how much consolidation is performed as part of the smelting operation, no, additional, or all primary smithing may take place prior to the production of an artefact (see below). Besides technological factors, e.g. the initial quality of the bloom, how much primary smithing takes place, and where it takes place will relate to cultural choices and/or economic organisation of the iron production. This may depend, for example, on whether the smelter and the smith are different persons, whether they are part of a larger economic

organisational structure, or on whether the smelting and (secondary) smithing operations actually take place at different locations.

### Secondary Smithing

Smithing, also often referred to as ‘forging’ or (as opposed to primary smithing) as *secondary smithing*, is the operation where the consolidated billet is shaped into a finished product. Secondary smithing is carried out by repeatedly heating the iron in a hearth and hammering it on an anvil. The hearth may take the shape of a shallow open hole in the ground to a rather large structure and is operated at temperatures of ca. 1200 °C, which is necessary to render the slag that remains incorporated in the consolidated bloom fluid.

Almost all slag that remained from smelting is squeezed out of the iron, analogous to the squeezing of a sponge. Nevertheless, small inclusions of slag almost always remain, which may help identifying the source of the metal. These inclusions (often referred to as ‘slag stringers’) can theoretically resemble either the original smelting slag, or acquire characteristics typical of a smithing slag. The composition of the slag inclusions in ancient iron potentially can be linked to the composition of known slag and/or ore. So far, however, this kind of provenancing suffers from both a lack of comparative material and a reluctance to sacrifice surviving iron artefacts. Moreover, it is hindered by a restricted number of variables that can be studied, as well as potentially large degrees of internal variation within a single object (Buchwald and Wivel 1998).

The pores in the iron that result from the removal of the remaining original slag are closed and their surfaces welded together. Unlike the squeezing of a sponge, however, iron undergoes a plastic deformation, which means that the pores stay closed and the metal forms a solid mass that can be shaped into an object, using various techniques. For detailed information on smithing techniques and the resulting properties of the produced iron object, (Rostoker and Bronson 1990, 1-8; see Tylecote 1987, 243-290).

Part of the original smelting slag that drains out during smithing ends up in the bottom of the forging hearth and fuses with iron oxide from the forged metal and ceramic material from the hearth and/or tuyère. The resulting smithing slag usually differs from smelting slag in that it is magnetic to varying degrees. This is caused by a combination of factors. Part of the free iron oxide in the smelting slag that drips into the hearths, will reoxidise from wüstite (FeO) to magnetite (Fe<sub>3</sub>O<sub>4</sub>) on its exposure to oxygen. More magnetite is contributed to the formation of



smithing slag by the *hammerscale*, the platy, reoxidised, crusty surface of the metal being worked, part of which also drops into the hearth. A further addition to the formation of a secondary smithing slag comes from slag created by the use of a flux, for example from the sprinkling of sand onto the heated metal to bind with the reoxidised surface and run it off. This fluxing is often performed in order to create a clean surface for the next session of hammering, and to retain or improve welding capacity.

A secondary smithing slag is most commonly typified by a concavo-convex or plano-convex shape in section, the shape of which is a function of both the shape of the hearth and the slag's position in that structure. These slags can also reveal a pushed-up ridge of slag, situated opposite to where the airflow stoking up the hearth hit the surface of the slag during its formation. Angle and force of the airflow further influence horizontal roundness or ellipsicity of the smithing slag. Each smithing slag probably represents one session of smithing, which may range from a single episode of smithing to one cycle or one working day. Larger smithing slags can occur as well, which then often show a layered structure, caused by partial fusion of material from successive smithing cycles (see the detailed discourse on the various morphological and formation characteristics of smithing slag in Serneels and Perret 2003; see chapter 9 for further discussion on secondary smithing in the context of Tel Beth-Shemesh). More smelting slag is expelled, and hammerscale scattered, at the location of the anvil where the hammering causes most of the expulsion of liquid slag, and breaks up the oxidised crust of the metal billet.

## The Early History of Iron Metal in the Near East

### Introduction

The origin and early history of iron is a widely debated and discussed topic. Several studies exist that outline general ideas, regions and locations, and the problematic nature of reconstructing the innovation or spread of knowledge about this new technology due to the scarceness of iron artefacts and iron production evidence (see the discussions in Pleiner 2000, 7-22; Waldbaum 1999; Wertime and Muhly 1980; Curtis *et al.* 1979). As with the description of iron technology above, this presentation of data does not seek to emulate or replace those detailed studies. The objective of this description is to serve as historical background information for the Tell Hammeh and Beth-Shemesh materials.

The overview presented here first examines the chronology of the appearance and subsequent development of iron metal in the Near East, as witnessed by artefactual evidence. This is followed by a brief review of the most common theories and ideas about the origin and diffusion of knowledge of ironworking, ideas that largely rest on that artefactual evidence. The artefactual evidence and the related ideas are contrasted with the significantly scarce evidence for actual production in the region.

### **The Chronology of Iron Artefacts**

The oldest iron artefacts that have tentatively been identified as being the result of intentional smelting date somewhere before 2000 BC, thus predating the first archaeological evidence of that technological process by about a thousand years. One should, however, be aware that terms like ‘oldest’ or ‘first’, often used in the context of metallurgical discoveries, generally refer to the archaeological data available in the public domain, and not to the actual first appearance of such a metallurgy, and is therefore subject to change following re-evaluation of the archaeological evidence, and/or new discoveries (Waldbaum 1999; Waldbaum 1980). Any attempt to create a tentative chronology of manufacture and use of iron metal must take this large chronological discrepancy between excavated artefacts and excavated production finds into account.

One issue concerning the earliest iron artefacts has to be mentioned here. It is thought that many of the oldest iron artefacts are made of meteoritic iron, and it is not always easy to distinguish them from iron that was deliberately smelted from ore. Since meteorites are generally (but not always) rich in nickel (Ni) and smelted iron is not, testing for nickel usually provides the distinction between them, but this is not foolproof (Buchwald 2001; Buchwald 1992; Buchwald and Mosdal 1985; Buchwald 1976). The extensive corrosion effects of most iron artefacts may easily lead to false identification. In addition, many of the oldest artefacts have not been analysed at all, leaving all questions and options about their manufacture open (Pleiner 2000, 7-8).

The chronology presented here is largely based on Jane Waldbaum’s exhaustive overviews of archaeological evidence related to iron (Waldbaum 1999; Waldbaum 1989; Waldbaum 1980; Waldbaum 1978). The periods and the corresponding dates used in this chronology are partially based on her divisions, here and there adjusted to common practice in the archaeology of the Near East. It is clear that divisions between a Stone, Bronze and Iron Age, based on the presumed prime

artefact material in that period, were later changed by different (predominantly historical) factors, leading to (sub-)divisions that are unrelated to the stone or metal of the period. The term Early Iron Age (or Iron Age I, 1200/1150-1000 BC) refers to that period in Near Eastern history when utilitarian iron artefacts first appeared and slowly started to replace copper (alloys) as the prime utilitarian metal. The term Full Iron Age (or Iron Age II, 1000 BC to 586 BC) refers to the period when iron artefacts become far more numerous (between 1000 and 800 BC) and iron apparently became the primary utilitarian metal (after 800 BC), with corresponding influence on all social and economic structures in society (see Wertime and Muhly 1980, xiii-xix). Specific years demarcating the start or end of a period such as 586 BC refer to historic or archaeological 'key events' (in 586 BC the destruction of the temple in Jerusalem) rather than abrupt and total changes in the cultural, ethnic, or metal-related fabric of society in the Near East.

In Waldbaum's definition of the term 'Full Iron Age' as the period when iron metal sees a sharp rise in quantity in the archaeological record, this period starts at different times in different regions. Evidence so far points at a start somewhere around the 10<sup>th</sup> century BC in the Near East, 9<sup>th</sup> century BC in Mesopotamia, 8<sup>th</sup> century in the Aegean and somewhat later in Europe and farther to the east and west (Pleiner 2000, 7-22; Waldbaum 1999; Craddock 1995; Tylecote 1992; Tylecote 1987; Échard 1983; Pigott 1983; Tylecote 1976). However, the chronology presented below can only presume to be a snapshot of a moment in time, as new material is found constantly, and other finds may be re-dated, re-examined, or even discredited.

### ***Before 3000 BC***

The oldest known iron artefact in the world is a four-sided instrument, which is dated to approximately 5000 BC. It was found in grave A at the site of Samarra in northern Iraq. Only thirteen other iron objects predate 3000 BC, all found on three sites in the Middle East. Three small balls were found in a habitation level at Tepe Sialk in northern Iran, dated at 4600-4100 BC, nine beads were found in graves at El Gerzeh in Egypt, dated to 3500-3100 BC, and a roughly contemporary ring was found in a grave at Armant, also in Egypt.

### ***The Early Bronze Age (ca. 3000-2000 BC)***

From this period, a few more iron fragments have been excavated, mostly in Anatolia, Mesopotamia, and Egypt. Most of these pieces appear to be made of meteoritic iron, and vary from mere lumps of rust to recognisable artefacts such

as daggers or pins. It is at the end of this period that the first smelted iron artefacts appear in the archaeological record.

### ***The Middle Bronze Age (ca. 2000-1600 BC)***

Only a handful of iron artefacts is reported from the Middle Bronze Age, mainly from Anatolia, one from Crete and two from Cyprus. From this period stems the first literary information on iron. In texts from the Old Assyrian trading colony of Kültepe in central Anatolia, dated ca. 1900-1800 BC, iron is referred to as a very expensive commodity, worth more than gold and used for decoration and luxury items. Iron is also mentioned in texts from the Old Hittite Kingdom, Alalakh, and Mari. Apparently, iron is (still) a rare and precious material.

The artefacts and texts together suggest that the first iron was produced in eastern Anatolia from the late third millennium BC onward, and that production was limited and the quality of the artefacts uncertain. This situation seemingly continues into the Late Bronze Age (Yalçın 1998). It is suggested that some of the smelted iron from this period and the Late Bronze Age may be the accidental result of lead and silver smelting or copper smelting, since haematite ore was often used as a flux in those operations (Wertime and Muhly 1980, 7-9). However, none of these early iron artefacts appears to have elevated base metal levels, as one would expect to be the case were this hypothesis true.

### ***The Late Bronze Age (ca. 1600-1150 BC)***

It is especially during the Late Bronze Age that one can see a considerable increase in excavated evidence of the use of iron. More objects are found over a wider geographic area. This area ranges from Mesopotamia to Greece and includes the Levant, Anatolia, Egypt, and the islands of the eastern Mediterranean. The range of objects now also includes a few utilitarian applications, like tools and weapons, but the bulk comes from funerary contexts. A possible first artefact in the Levant may be a small, corroded blade from a grave at Pella, Jordan, dated around 1500 BC (Smith *et al.* 1984, 234-236), but as the excavators indicate, it was found under problematic stratigraphical circumstances, at the disturbed end of a grave. However, several of the analysed LBA iron objects were apparently made of meteoritic iron, and there is little evidence up to this point in time for intentional smelting of iron ore.

***The Early Iron Age / Iron Age I (ca. 1150-1000 BC)***

It is only around 1200 or 1150 BC, at the beginning of what was therefore called the Iron Age, that one finds the first indications that iron is changing from a luxury material (Pleiner 2000, 10-11) to a widely used metal that will eventually take priority over the use of bronze. A shift in preference towards the use of iron first becomes apparent in the artefact category of knives, where advantageous properties of iron are most apparent (amongst other things sharper edges, less bending).

James Muhly has suggested that, based on the archaeological record up to that point, iron technology may well have developed in the Levant, spreading from there via Cyprus to the Aegean (Muhly 1980, 51). Anthony Snodgrass discussed the possible relation of the increase in iron metal from 1200 BC onward in the light of the advent of the Philistines, as earlier proposed by Ernest Wright, one of the excavators of Tel Beth-Shemesh (Wright 1939). Snodgrass further states that several of the Levantine sites where iron metal is found in larger numbers, e.g. Lachish and Tell Jemmeh in Palestine, or Hama in Syria, have connections to Cyprus and the Aegean, but it remains unclear in which direction influences are travelling (Snodgrass 1980, 356-357).

In the archaeology of the Levant, the transition from Iron Age I to II is usually put around 1000 BC. From about 1000 BC onward, judging by the range and frequency of attested iron artefacts, the quantity and quality of iron work increases and iron starts to replace bronze as the prime, everyday material for tools, agricultural implements, and weapons. Some have argued that this may be caused by a disruption of the copper or tin trade, which prompts the need for another metal (see Snodgrass 1980, 357). In my opinion, it is probably more because of improving techniques in smelting and especially the smithing of iron (Craddock and Hughes 1992, 258; Snodgrass 1980, 338). It is likely a combination of these and similar factors, combined with the relatively ubiquitous nature of iron ores when compared to copper and tin, which led to the rise in use of iron.

***The Full Iron Age / Iron Age II (ca. 1000-586 BC)***

The Full Iron Age can be considered to start when iron constitutes the majority of metal weapons, tools et cetera, or in other words, when iron became the main utilitarian metal. This could be related to the development of new techniques for the treatment of iron during secondary smithing, like annealing, quenching, and carburisation. An impressive find illustrating the quantities of iron produced in this

period is the discovery of 160 tons of iron in a store house of Sargon II (722 - 705 BC) in Dur Sharrukin ("Sargon's fort") at Khorsabad in present day Iraq. This is a large collection of artefacts that includes forged blooms and a wide variety of tools and weapons (Craddock 1995, 258; Loud 1936). This material, which dates to the late 8<sup>th</sup> century BC, certainly underlines the important role the Assyrian empire plays in the innovation and use of iron, as discussed below.

A further argument that favours a relation between the increase in use of iron with improving techniques is formed by a group of iron artefacts, dating to ca. 900 BC, excavated at Taanach (Stech-Wheeler *et al.* 1981). Based on the metallurgical examination of these artefacts, the authors suggest that the smiths that created them were able to produce carburized iron, a material that can be considered to have qualities that surpass those of bronze. The authors further suggest that the fragmentary nature of the political situation in the region at the end of the 10<sup>th</sup> and beginning of the 9<sup>th</sup> century BC provided a socio-economic climate in which local industries could develop, exploiting local raw materials, and that the production of iron must have been one of those industries (see also chapter 4).

## **Ideas on the Origin and Spread of Iron Technology in the Near East**

### ***Introduction***

Not much is certain about the origin and early history of iron production. Most ideas and proposals derive from allusions to iron in written sources and the presence and distribution of iron artefacts as reviewed above. Several theories have been proposed, sometimes mutually exclusive, on who invented what where and why, how knowledge moved from one region to the next, and who controlled the 'secret' advantage of this technology. One thing most of these ideas have in common is that they indicate various locations around the eastern side of the Mediterranean as the possible 'birthplace' of iron (Pleiner 2000, 7-8). Most commonly, the smelting of iron is supposed to have been 'invented' in (eastern) Anatolia, with the start of real production taking place in the Levant, probably as a by-product of established copper smelting (Pleiner 2000, 13-14, but see the nature of evidence in his Fig. 4, 21). The idea that iron started as a by-product of existing copper smelting was largely based on copper-rich iron artefacts found at Timna in the Wadi Araba. This idea has since been refuted by re-examination of the artefacts (Merkel and Barrett 2000).

### **Anatolia**

The fact that most of the earliest iron artefacts were found in Anatolia, in the context of the Hittite Empire and several mentions of iron in Hittite texts, brought about the idea that it was here that iron smelting had been invented, and subsequently kept as a secret (Siegelová 2005; see Yalçin 1998, for a discussion of the texts and the artefacts; Košak 1986; Siegelová 1984; Košak 1982), which was seemingly borne out by the lack of finds elsewhere. Although this is not necessarily an invalid argument, many more objects have since been found in various regions. This goes hand in hand with increased cases of actual analysis of those objects, leading to a re-examination of the 'old' ideas (see the remarks by Snodgrass 1980, 357). The artefactual evidence in Anatolia sums up to a handful of objects dating to the early second millennium BC (Yalçin 1998), after which quantities drop significantly, and from ca. 1200 BC onward, iron objects become most common in the Levant (Waldbaum 1999). Although the idea of a Hittite monopoly on iron technology is not in any way sustained by archaeological evidence, the number of references to iron in Hittite texts does seem to indicate a well established knowledge, and use, of iron metal in Anatolia as early as the second millennium BC (Muhly 1980, 50-51).

### **Cyprus/Greece**

Susan Sherratt has postulated the idea that iron metallurgy in the Levant derives from Cyprus, and that the Cypriot iron metallurgy has its origin in Greece or the wider Aegean (but compare the opinion of James Muhly as discussed above. Muhly 1980, 51). Metal specialists, possibly already familiar with iron, coming from the Aegean, supposedly settled on Cyprus in the 12<sup>th</sup> and 11<sup>th</sup> century BC where they introduced or developed iron technology within the context of the extensive copper-metallurgical and related socio-economic structures already present there. Then the metal and its technology purportedly spread from there, amongst other places back to Greece itself (Sherratt 1994). However, it should be stressed, as Susan Sherratt does herself acknowledge, that these ideas rest on the presence of iron artefacts, in this case particularly 12<sup>th</sup> and 11<sup>th</sup> century BC Aegean weapons and tools from funerary contexts. Notwithstanding this caveat, metallurgy was certainly well known on Cyprus, and intensive contact between Cyprus and both Anatolia and the Levant is also widely attested, so a Cypriot role in development or spreading of iron technology can not be discounted (Muhly *et al.* 1982; Muhly and Maddin 1981).

## Assyria

Similar to the ideas about iron in Anatolia discussed above, the assumed role of the Assyrians in the development and spread of early iron technology rests predominantly on a relatively low number of artefacts and several mentions of iron in texts (Curtis *et al.* 1979, and the references therein; Pleiner and Bjorkman 1974). Production evidence, as in Anatolia, is absent. The textual evidence suggest that iron working was established at least in the 13<sup>th</sup> century BC, and that iron was well known in the context of the royal palace of the 11<sup>th</sup> century BC (Curtis *et al.* 1979, 369). However, especially the larger cities of the Assyrian empire such as Nineveh and Assur have yielded very few iron objects, and what has been found is often difficult to assign to an exact date.

Wider use of iron by the Assyrians seems to start in the 9<sup>th</sup> century BC, with iron supposedly exceeding bronze as the prime utilitarian metal only in the 8<sup>th</sup> or 7<sup>th</sup> century BC. Again, these assumptions are based on literary sources rather than archaeological evidence. As mentioned above, larger quantities of iron are only attested from the late 8<sup>th</sup> century BC, with the find of 160 tons of iron in a store house at Khorsabad, in present day Iraq. This large collection of artefacts that includes forged blooms and a wide variety of tools and weapons, does at least indicate the important role the Assyrian empire plays in the use of iron (Craddock 1995, 258) at this time. There are also indications that the Assyrians, before their actual occupation of the southern Levant in the late 8<sup>th</sup> century (during the military campaigns of Tiglat Pileser III (ca. 730 BC), Shalmaneser V and Sargon II (ca. 720 BC) and Sennacherib (ca. 700 BC)), had contact with or exerted an influence over the Levant (Bienkowski 2000). Knowledge of iron may well have been part of that contact.

## Iran

The geographical position of western Iran forms a crossroads of contact between Central and South Asia with the Caucasus, Anatolia, Mesopotamia, and the Levant. Iron ores are abundant in the region, which makes this area potentially highly interesting in the context of the spread of early knowledge of iron (Pigott 1989b; Pigott 1989a; Pigott *et al.* 1982a; Pigott 1980; Pigott 1977). However, early iron artefacts that pre-date the 12<sup>th</sup> century BC are very rare. The artefactual evidence does indicate more extensive use of iron in the region at the end of the second and beginning of the first millennium BC, when iron metal started to



surpass bronze as the main metal (Pigott 1980, 417-418). As elsewhere, evidence for production of metal remains absent thus far.

### **Levant**

The occurrences of iron in the Levant have been mentioned in several contexts above. Whereas iron objects are very rare in the second millennium BC, their number increases considerably from 1200 BC onward (Waldbaum 1999; Muhly 1980). Several ideas on how the knowledge of iron develops or arrives in the Levant have been discussed previously. Very often, it is assumed that knowledge of iron must have spread from its birthplace in Anatolia or the Caucasus (see discussion on the Caucasus below) to the Levant, either directly within the Hittite empire, or via Aegean influence through Cyprus, or as a monopoly held by the Philistines. All ideas about early iron in the Levant thus far are based, as elsewhere, on only a small body of artefactual evidence, and none of the ideas seems certain or conclusive.

It is interesting to see that, in contrast to the absence of production evidence at the supposed 'birthplace' of iron, Anatolia, as well as in the context of those groups that are supposed to be the main early producers of the metal, i.e. the Hittites and the Assyrians, it is in the Levant that we do find some of the earliest (known) examples of actual production (see below). In the light of these production finds, it is furthermore interesting to examine the common idea of a Philistine monopoly on iron technology. This idea derives from just a single textual reference: in the bible, in I Samuel 13: 19-21, it reads "Now there was no smith found throughout all the land of Israel: for the Philistines said, Lest the Hebrews make [them] swords or spears; But all the Israelites went down to the Philistines, to sharpen every man his share, and his coulter, and his axe, and his mattock; Yet they had a file for the mattocks, and for the coulters, and for the forks, and for the axes, and to sharpen the goads". This is usually interpreted as indicating a Philistine monopoly on iron technology. However, little archaeological evidence supports such a monopoly. The 9<sup>th</sup> century BC smithy excavated at Tel Beth-Shemesh, discussed later in this thesis (see chapter 5), rather seems to falsify the idea. The city of Beth-Shemesh, which is situated on the border of the Philistine coastal area, is certainly not a Philistine site itself (Bunimovitz and Lederman 2003).

## **Discussion**

What is currently known about the early history of iron in the Near East, as reconstructed through the indirect evidence of artefacts, remains very fragmentary, and this state of affairs continues well into the Roman era. In light of this very poor state of current knowledge, each newly discovered early iron artefact, and even more so any find of actual iron smelting or smithing, will provide key data towards an enhanced understanding of early developments, especially in the assumed 'birthplace' of iron, the Near East. Current ideas about the origin of iron technology, as discussed above, will probably change significantly along with new discoveries. In my opinion, even with the significant lack of production evidence in most of the Near East, the artefactual and textual evidence does seem to indicate that (some of the) earliest iron technology did evolve in (north-eastern) Anatolia, and perhaps spread from there. Nevertheless, it cannot be ruled out that the spread of knowledge followed very different paths from what we now assume.

## **Evidence for Iron Production in the Near East and Mediterranean World**

When examining what is presently known about actual production, particularly the remains of smelting operations, the amount of evidence is very different from that of artefacts. Whereas (possibly) smelted iron artefacts appear in quite early contexts in the Near East (see the discussion above), evidence for smithing and especially smelting is almost if not completely absent from most periods. In 1978, Jane Waldbaum stated that "no direct evidence for mining, smelting or forging of iron is yet available for the Early Iron Age" (Waldbaum 1978, 65, referring to the wider Near East). This statement was supported by Paul Craddock in 1995 (Craddock 1995, 259). Today the picture has certainly changed, with several claims for production and (mostly) working remains, but these are still not many (Pleiner 2000, 7-8). The few cases where direct evidence for iron production has been discovered are reviewed here.

The thus far earliest known evidence for smelting activity in the Levant is that of Tell Hammeh in Jordan, which is the main subject of this thesis. Smelting operations there apparently started in ca. 930 BC. The only other location where evidence of iron smelting has been excavated is a group of sites in the Black Sea Coast region (ancient Colchis) in modern-day Georgia (Khakutaishvili 2001; Khakutaishvili 2001; Khakutaishvili 1976). Until recently, the operations in the Colchis were dated to begin around 1100 BC (Pleiner 2000, 36-37, 58). However,

recent re-examination of the radiocarbon dates and stratigraphy, as well as renewed excavation work, seems to point to a starting date of ca. the late 11<sup>th</sup> to 8<sup>th</sup> century BC, i.e. roughly or partly contemporary with Tell Hammeh in Jordan (Jens Nieling, personal communication). In addition to this re-evaluation of the dating, the interpretation of these structures as belonging to iron smelting is currently put in doubt. Recent examination of slags from some of the Caucasian slag-pit furnaces showed the presence of copper sulphide prills as well as matte (i.e. a mixture of copper metal with its sulphides, produced by smelting the sulphide ores), indicating a relation to copper smelting rather than iron (Jens Nieling, personal communication).

In contrast, documented remains of iron smelting from other regions are generally younger. Possible smelting remains that are among the earliest in Europe have recently been reported from both Sweden and Greece, dating back to the 8<sup>th</sup> century BC (Stenvik 2003, 126; Hjärthner-Holdar and Risberg 2003, 84; but see discussion in Pleiner 2000, 30-32). If correctly dated, these finds raise interesting questions with respect to the spread of iron technology, the direction(s) this may have taken, and/or whether independent invention can be considered.

Until recently, the same opinion was held with regard to Sub-Saharan Africa. Here, iron smelting remains were known from near Agadez in Niger, which possibly date back to the 5<sup>th</sup> century BC. However, these and several other cases are widely disputed with regard to actual dating (Miller and van der Merwe 1994; Gordon and Killick 1993; Childs and Killick 1993; Kense 1985; Calvocoressi and David 1979, 10; see Posnansky and McIntosh 1976, 184). However, recent discoveries and re-evaluation of some of the known sites have changed the chronological picture in Sub-Saharan Africa considerably. Several sites in different parts of the Sub-Saharan continent are now dated to earlier times than previously assumed, some as far back as 1000 BC, although many of the older dates are characterised by both stratigraphical and radiocarbon problems. An extensive overview of the current state of knowledge about early (Sub-Saharan) African iron metallurgy, and debates about dating of these finds, are presented by David Killick (Killick 2004b). He also discussed the widespread debate about the origins of iron technology on the African continent, again concerning directions of knowledge transfer versus independent invention (see also Pleiner 2000, 18; and Veldhuijzen 1998, 23-56).

When examining documented production evidence in the Near East, one claim for early smelting stands out. According to Harold Liebowitz, furnace-like structures were found at Tel Yin'am in northern Israel, surrounded by some iron slag and ochre ore. These remains were dated by associated pottery to the 13<sup>th</sup> century BC (Liebowitz and Folk 1984; Liebowitz 1983; Liebowitz 1981, 82-84; Liebowitz and Folk 1980). Beno Rothenberg, however, visited the site immediately after excavation and had some of the 'slag' and 'ore' analysed. On this basis, he found the identification of furnaces, slags, and ore to be unfounded as the presumed slag contains less than 5 wt% iron oxide, which is too low for proper bloomery iron smelting slag (Rothenberg 1983, 69-70). More recently, Vincent Pigott re-examined the evidence and suggested a far more likely interpretation of the site as a possible production site for red ochre pigments, by heating ochreous bog ores taken from a local swamp (Pigott 2003).

It is from the Iron Age II (1000-586 BC) onward that some, still rather sparse, occurrences of iron production have been reported in the Near East. A few slags were found in a room on Tell Afis in Syria, apparently dated to the middle of the 8<sup>th</sup> century BC (Ingo *et al.* 1992b; Ingo *et al.* 1992a; Ingo and Scoppio 1992). Their context, apart from the remark that they were "found ... on the floor of a building of Iron Age II" (Ingo *et al.* 1992b, 285-286) remains unknown for now, but it seems likely that there is no further production context, and even from the analyses performed determination of the processing stage remains unclear.

Recently more cases, mostly of smithing slag, have been reported. One such example is a handful of samples of varying nature including some slags, but again without a production context, from Tell Siukh Fawqani, Syria (Luciani *et al.* 2003). These samples are probably related to smithing activity, and date to the 7<sup>th</sup> century BC. Other cases include 7<sup>th</sup> century BC smithing hearth bottom slags excavated at Tell Ahmar (Til Barsip) in Syria in 2004 (John Russell and Elizabeth Hendricks, personal communication; the identification as smithing was done by the author, and is based on morphology). At Tel Hamid in Israel, 7<sup>th</sup> century BC but as yet unassigned slag and tuyères were excavated (Samuel Wolff, personal communication; these are to be studied by the author at UCL at a later date, see also chapter 8 on tuyères in the Near East, page 161-ff). A further recent discovery is the smithy at Tel Beth-Shemesh, partially excavated in 2001, and excavated by the author in cooperation with UCL in 2003. The hearth structures, hammerscale, slag prills, and concavo-convex smithing slags excavated there date to the 9<sup>th</sup>

century BC, and comprise the second major subject of this thesis (see chapters 5 and 9).

More secondary smithing slag has been excavated at Tell es-Sa<sup>c</sup>idiyeh, Jordan, again from the 7<sup>th</sup> century BC (Mascelloni 2004). The site is relatively close to Tell Hammeh, and it is envisaged to compare these smithing slags to the smelting and smithing remains from Tell Hammeh and Tel Beth-Shemesh at a later date. Other iron metallurgical finds have been reported from sites such as Tel Dan, Hazor, and Tel Masos, all in Israel, but no data on these finds is available in the public domain, so nature, dating and interpretation remain questionable. One article describes the archaeometallurgical analysis of some 75 kilograms of slag from Tel Dor. Unfortunately, the article is in Hebrew, but the author, Nimrod Shay, identifies these slags as related to secondary smithing, and belonging to the Persian period (ca. 586-332 BC).

Another location where evidence for secondary smithing has been attested is at Tel esh-Shari'a (also known as Tel Sera) in the northern Negev, Israel, where an Assyrian smithy dating to the late 7<sup>th</sup> century BC was found in the citadel (Rothenberg and Tylecote 1991, see also chapter 8). Besides a hearth structure with two tuyères, four pieces of magnetic slag were found here, as well as hammerscale, an iron spike, and a completely corroded piece of iron metal. From the presence of a few slags away from the hearth context, the authors suggest that other metallurgical installations existed nearby, and that the smith reused tuyères from those installations in the construction of this hearth.

Recent reports describe the excavation of industrial-scale iron smithing activity on the outskirts of Phoenician Carthage, dating to the 7<sup>th</sup> and 6<sup>th</sup> century BC (after 675 BC). Excavator Roald Docter and metallurgist Hans Koens interpret the excavated area as a large scale smithing operation at the edge of the city, represented by numerous small hearths, slag, tuyères, and a thick deposit of hammerscale. In connection with every hearth, they found large quantities of crushed Murex shell, possibly debris from royal purple pigment production (from the hypobranchial gland of Murex molluscs) elsewhere on the site. This led them to propose the intentional use of the lime-rich shells as a flux, which would serve to free the consolidated metal from impurities such as sulphur. Little analytical data has been published so far, so this suggestion is difficult to evaluate. An extensive report about the finds and the subsequent metallurgical analyses is expected in the final publication (Docter in press; Docter *et al.* 2003, 44-46; the

discussion of the tuyères and slags by Hans Koens is found on page 60-65; Docter 2002).

In the 1980s, it was reported that debris from iron production activity had been excavated at the site of Kamid el-Loz in Lebanon, ca. 60 km southeast of Beirut. The authors describe how a few small fragments of iron metal (e.g. a ring and a needle point) were found in a workshop area between the North gate and a temple, in the context of the LBA palaces (Frisch *et al.* 1985, 77-78). The authors then speculate that the presence of these iron objects in the same context as slags and lumps of haematite ore lumps (whilst haematite formations are not locally available) might mean that the iron was produced in this workshop area. An argument they present as supporting this interpretation is the fact that some of the haematite ore lumps were found in the vicinity of a furnace structure. The authors further mention the recovery of small pieces of slag, green, grey green, and black in colour, and bubbly in appearance from the same area. They add that, in the field, they classified all material that was neither haematite nor finished product as slag.

Although it is difficult to follow their exact argumentation and simultaneously evaluate their interpretation of the actual material, as all is presented at various locations within the report, a close examination of the evidence seems to raise strong doubts about an interpretation of any of the material as belonging to iron metallurgy. From an archaeological perspective, the excavators' assertion that the ore, slags, and metal artefacts are largely found in secondary context (Frisch *et al.* 1985, 77) makes the proposed relation between the various materials doubtful. More specifically, the authors mention that the iron objects stem from a foundation trench of a wall, and the mortar between two mudbricks respectively (Frisch *et al.* 1985, 96). Lastly, on examination of the chemical and microscopical analysis of the very low number of very small (0.5 - 2 cm<sup>3</sup>) fragments of slag, all presented data shows significant presence of copper sulphide in all the samples (Frisch *et al.* 1985, 107; 134-146; 161; 178-180; and especially the elemental compositions and micro-photographs presented in tables 49, ff in the appendix). The authors propose that their discoveries represent an early attempt of iron smelting, which is based on the same technology (process and furnace) as in contemporary bronze production. However, the authors further speculate about a virtually slag-free process, where the tiny amount of slag that is produced would end up as stringers in the metal artefacts produced. In my opinion, the Kamid el-Loz material shows no link to iron metallurgy besides the presence of a few LBA

iron artefacts, and a, however tentative, interpretation as experimental iron smelting on the site is certainly not substantiated by the available archaeometric data.

## Summary

What is currently known about the early history of iron in the Near East can only be described as fragmentary. Most of what we know and think about the innovation and spread of the knowledge of iron production technology is reconstructed through the indirect evidence of artefacts. Even there, early evidence is scarce, and may reflect the density of excavation as much as an actual prehistoric situation. In light of this very poor state of current knowledge, each newly discovered early iron artefact provides key data towards an enhanced understanding of early developments in what is assumed to be the 'birthplace' of iron, the Near East. Current ideas about the origin of iron technology, as discussed above, will likely change significantly along with new discoveries. In my opinion, even with the significant lack of production evidence in most of the Near East, the artefactual and textual evidence does seem to indicate that (some of the) earliest iron technology did evolve in (north-eastern) Anatolia, and perhaps spread from there. Nevertheless, it cannot be ruled out that the spread of knowledge followed very different paths from what we now assume.

Direct evidence for production, particularly smelting, remains extremely rare. Using all available (archaeological, artefactual, and textual) evidence, the production of utilitarian iron metal on some scale appears to start around 1200 BC, and the number of iron artefacts seems to rise rapidly from the 9<sup>th</sup> century BC onward. It is certainly possible that various trade and/or military contacts played a role in the dissemination of the technology of iron over the region and perhaps beyond, but without more primary production evidence, firm conclusions remain extremely difficult. Evidence for secondary smithing, such as at Beth-Shemesh and several reported finds of (probable) secondary smithing slags at a handful of sites in the Levant and Syria, dating from the 9<sup>th</sup> to the 7<sup>th</sup> and 6<sup>th</sup> centuries BC, seems to confirm the impression that manufacture and use of iron is fully integrated in the socio-economic fabric of the region.

In the above picture, the finds at Tell Hammeh, with furnace structures, large quantities of different types of slags, large amounts of tuyères, and an haematite iron ore deposit nearby, allow new insight in part of that elusive history of iron in the Near East, historically, technologically, as well as socio-economic. As will be

discussed in the following chapters, the Hammeh smelting material (see chapters 4 and 8), as well as the Beth-Shemesh secondary smithing material (see chapters 5 and 9) reveal various stages of the technological *chaîne opératoire* of an early, but well-established and relatively large scale iron production, both primary and secondary. They further allow the examination of issues such as technological choices and style in those processes (see chapter 2). In addition to this technological information, both assemblages and their archaeological context provide socio-economic information about organisational and social context of the operations such as the use of raw materials, and choice of location for each technique.



## CHAPTER 4: THE ARCHAEOLOGY OF TELL HAMMEH

### Introduction

Excavations in 1996, 1997 and 2000 at Tell Hammeh (az-Zarqa), Jordan, the last season directed by the author, uncovered extensive remains of iron smelting and primary smithing operations that date back to ca. 930 BC. The assemblage of tuyères, charcoal, and large quantities of various types of slag that was found at Hammeh is the earliest example of primary iron production known in the Near East thus far. All material was found in clear stratigraphic context, and within what is evidently an area used strictly for metallurgy at that moment of the site's occupational history.

Apart from their local and regional significance (see page 95), the finds at Tell Hammeh are significant for at least four reasons: their age, their quantity and variety, their geographical location, and their elemental composition. With production starting around 930 BC, and ending no later than 750 BC, the finds are chronologically early when compared to the remarkably few other archaeological finds of regular iron production activity in south-west Asia. In comparison, the vast majority of 'early' iron smelting in Europe is Imperial Roman in age; very few smelting sites anywhere predate 500 BC, as described in chapter 3 (Pleiner 2000, 7-8,13; Waldbaum 1999).

The finds at Hammeh are furthermore characterised by their quantity: a total of more than 700 kg of slag and some 350 tuyère segments were excavated during the three seasons. The bulk of that material was excavated from a single 5 x 5 metre square (A/B7; see Figure 6), and the whole assemblage from an area that forms between 5 and 10 percent of the estimated original total production area. Even more striking is the wide range and variety of the assemblage: tapped and furnace slags, furnace bottom and primary smithing slags, 'intermediate' ceramic-rich slags consisting of technical ceramics 'mixing' with slag, technical ceramics (e.g. tuyère nozzles (usually molten), mid-pieces, and rear ends), olive wood charcoal, and the bottom of furnace structure(s).

The Hammeh material is also quite remarkable in a geographical sense, as it is probably the only known early first millennium BC evidence of iron production activities across south-west Asia. The aforementioned finds of younger or similar age are mostly located in Israel, northern Syria, or Anatolia (see chapter 3), and can in general be attributed to secondary smithing activity rather than primary production. The only other sites with significant remains of what may be primary

production of iron metal are those in the Colchis region in Transcaucasian Georgia, but it is hard to imagine any direct contact between Georgia and Jordan when considering both the geographical and socio-economic separation between the two. Furthermore, doubt has been cast on the relation of these sites to iron production very recently (see chapter 3).

Finally, the Hammeh slags are materially different from most other documented early iron production slag. On the macroscopic level alone, they are noticeably glassier, indicating a different elemental composition. Bulk chemical analysis, using the calibration method described in Chapter 7: Development of 'Slag fun', an Analytical (P)ED-XRF Method for Iron-Rich Materials, confirms the peculiar elemental composition of the Hammeh slag, which clearly sets it apart when compared to 'common' bloomery slag (e.g. Kronz 1998, 224; see chapter 8). With a high lime and low iron oxide content, it resembles slag that results from a technological process that was not in use until at least two millennia later, i.e. the early blast furnace process (Pleiner 2000, 251-252, 255-256), even though the Hammeh slags are the result of a regular bloomery smelting operation. This different elemental composition is a function of the ore used in the process and a contribution to the slag from the technical ceramics, as will be discussed in chapter 8. Both archaeologically and metallurgically, the Hammeh material provides a rare example of early iron production in the Near East, and the analysis of this material contributes to our current understanding of the early technological developments that form the 'coming of iron' (Pleiner 2000; Craddock 1995; Tylecote 1992; Wertime and Muhly 1980).

## The Location of Tell Hammeh

Tell Hammeh (az-Zarqa) is a relatively small site, located at the point where the Wadi Zarqa opens into the central Jordan Valley. Although at present quite diminished in flow by an upstream dam, the river Zarqa forms one of the major tributaries of the river Jordan. The site is close to several of the larger tells that dominate this part of the Jordan Valley; approximately 2.5 kilometres to the north-west is Tell Deir 'Alla, 2.5 kilometres to the north of Deir 'Alla lies Tell Mazar and 6 kilometres further north is Tell es-Sa'idiyeh (Figure 3).

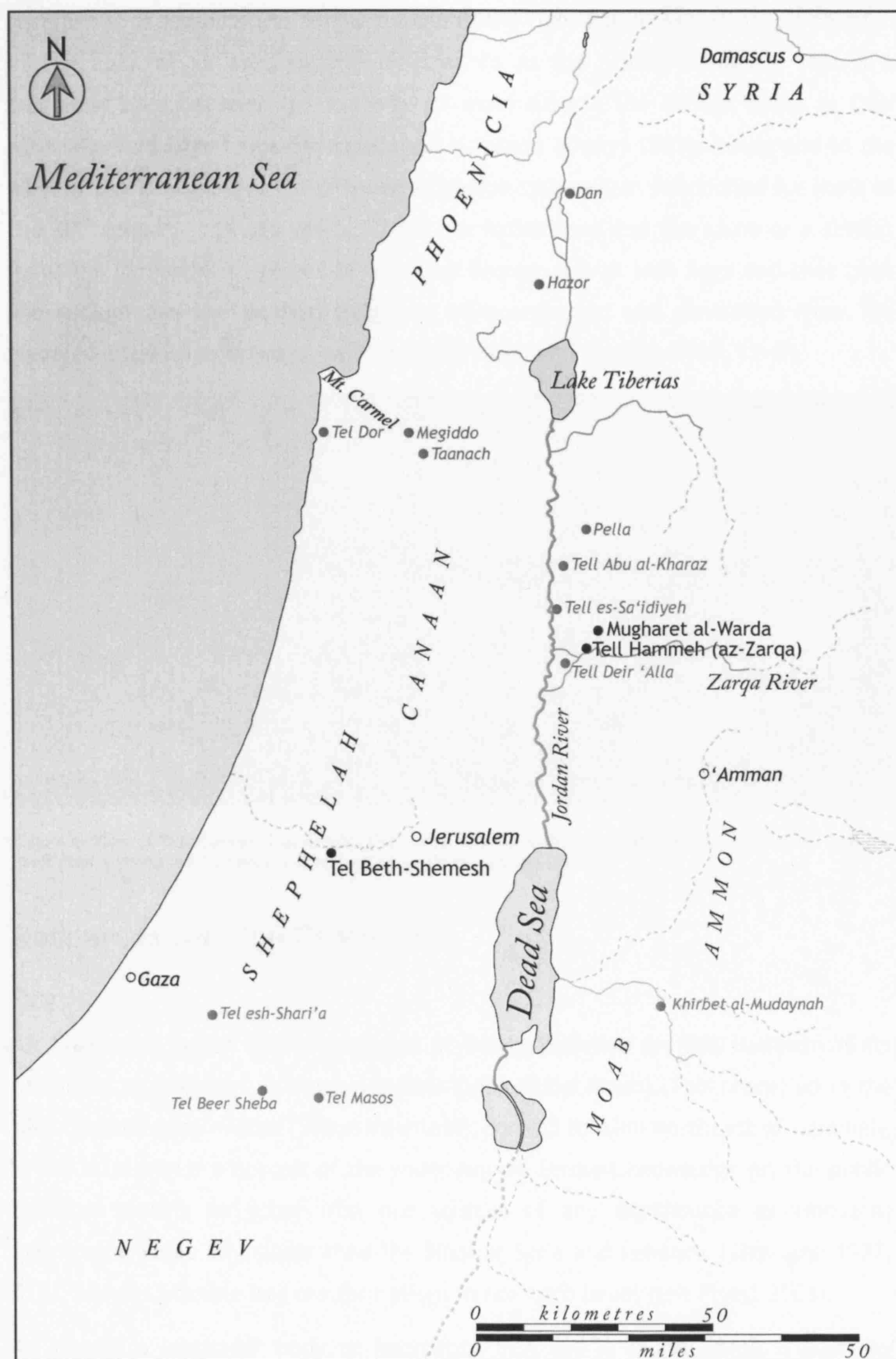


Figure 3. Map of the southern Levant, indicating the location of Tell Hammeh (az-Zarqa) and several of the major sites in the Jordan Valley.

Hammeh is situated on the northern bank of the river Zarqa, in a strategic position at the apex of an area usually referred to as the 'Zarqa-triangle'. This is a triangular area between the north-south main road in the Jordan Valley at Deir ʿAlla, the East-Ghor irrigation canal, and Hammeh (Khoury 1981). Inside and to the west of this triangle lies a traditional irrigation system that functioned for most of the 20<sup>th</sup> century until the 1960s. There are indications that the same or a similar irrigation system was present here in the Bronze and/or Iron Ages and that both the ancient and the modern irrigation were organised and controlled from Tell Hammeh (Tarawneh in press, 14-ff; van der Kooij and Ibrahim 1989, 12-ff).



Figure 4. View of Tell Hammeh, seen from the south. The Zarqa River is visible in the foreground. The tell itself clearly shows the bulldozer cut around its southern and eastern side.

## Resources for Iron Production

### Ore

An important factor in the presence of iron production on Tell Hammeh is its proximity to Mugharet al-Warda (English: Cave of the Roses). This place, up in the hills towards Jebel ʿAjlun (ʿAjlun Mountain), some 3 to 4 km northeast of Hammeh, is the main iron ore deposit of the wider region. Present knowledge (in the public domain) reveals no other iron ore sources of any significance or (modern) economical value any closer than the Sinai or Syria and Lebanon (Zitzmann 1977, 219), besides possible bog ore formations in northern Israel (see Pigott 2003).

At Warda, a lenticular body of haematite iron ore is found which is partially exposed to the surface (see chapter 8, page 147-ff). Several horizontal mine shafts have been reported at the site, first in the notes of the Deutsche Palestina Verein surveys by G. Schumacher (as discussed in Steuernagel 1925), later by

Robert Coughenour, who dates these mining works to the Roman or Byzantine period. Coughenour further reports excavation of furnaces and slag from iron metallurgy adjacent to the mine shafts, but no further data, archaeological or archaeometric, is available about the nature of this production (Coughenour 1989; Coughenour 1976). Others have proposed a medieval date for the mining and smelting activities (Bender 1968, 150, and references therein). Further discussion on the chemical and mineralogical characterisation of this ore as well as its role in the Hammeh iron production is given in chapter 8. It is important to note that, as opposed to the metallurgical activity mentioned by Coughenour, the metalworkers at Hammeh did not choose the ore site as their location for smelting. It is not unreasonable to assume that they had unhindered access to this vital resource, and chose their location based on other considerations, such as the availability of water or clay, or proximity to the site that instigated or controlled production.

## Clay

A second crucial resource in any (pre-industrial) iron production process is clay, which mixed with water and possibly temper, provides the building material for furnaces and/or tuyères. At Hammeh, clay and clay-rich soils are abundant. Most of the Jordan Valley is covered in a Late Pleistocene lacustrine deposit, generally referred to as the 'Lisan marls' after its composition and the prehistoric Lisan Lake (Maandag and Macksoud 1969, 5-6; Reifenberg and Whittles 1947). On the valley plateau and at the edges of the Jordan Rift Valley (Ghor), as well as in tributary wadis (including the foothills and wadi-fan of the Zarqa river), these marls are in turn covered and/or mixed with calcareous fluvial-colluvial deposits (Landmann *et al.* 2002; Stein *et al.* 1997; Begin *et al.* 1974; Maandag and Macksoud 1969, 14-15, 20-21, 24). These 'Ghor-Lisan' soils are generally of a light and laminated nature, with a clay content that varies from approximately 10 to 20 %. Occasional outcrops of marly clays occur. The soils are further characterised by a high concentration of calcium, often as calcium carbonate, varying between 25 and 50 % (Maandag and Macksoud 1969, 20, 25-29).

Around Tell Hammeh, the soil has a moderately fine texture and consists of clay loams. Close to the site a large outcrop of clay occurs, situated just outside the village of Dubaib, which is still in use by the local population today (Maandag and Macksoud 1969, 20-21). It is not unlikely that this outcrop, or one very similar, was used as the source for the construction material in prehistoric times as well. It is a fact that most historical and even modern-day structures in the region, and on Tell

Hammeh itself, are built using the clays from these Lisan soils. The tuyères and furnace structure(s) of the Hammeh iron production apparently form no exception (see below). A sample was taken from this local outcrop of clay at Dubaib, and used to help assess the role of technical ceramic in the Hammeh process (see chapter 8, page 201-ff). The technical ceramics (i.e. the tuyères and probably the furnace wall) appear to be made from the locally available material, with some organic material and occasionally small stones as temper.

## Fuel

The next major factor in the production of metal is fuel. Fuel plays a significant role in the smelting process, as it reduces iron oxide in the ore by reaction with the carbon monoxide gasses it releases on combustion, and works as a solid reduction agent when in direct contact. In general, charcoal would be most suited for this function (as opposed to feeding wood into the furnace), and it is supposed to be the main fuel of ancient bloomeries (Pleiner 2000, 115-ff).

A large number of charcoal fragments found together with the Hammeh metallurgical debris was examined by Dr Eleni Asouti, and all were identified as short-lived olive wood (*Olea europaea*) (Eleni Asouti, Institute of Archaeology, UCL, personal communication). Two pieces of charcoal were carefully selected to be used in AMS <sup>14</sup>C dating of the Hammeh iron smelting operations, and the identification as olive was confirmed a second time by John Meadows and Phil Austen during this selection (John Meadows and Phil Austen, Institute of Archaeology, UCL, personal communication). All pieces were of significantly small diameter, which suggest that most if not all the charcoal used at Hammeh derives from young branches or twigs, not large pieces of older wood (see also chapter 8, page 197).

The growing and domestic use of olive trees (both the fruits and the wood) are clearly attested in the archaeological record, and olive trees were certainly present and used in the Jordan Valley area during the Bronze and Iron Ages. Olive trees are very slow to grow, but deliver a substantial and constant supply of olives when mature. These can be used as fruits, to make oil, or even as fodder for livestock. In the present-day Near East and elsewhere, olives form a highly valued commodity, and the trees are almost never wilfully felled. It is difficult to assume a different attitude towards olive trees in the Levantine Iron Age. It thus also seems unlikely to assume a felling of olive trees on any substantial scale, even to stoke the furnace for another desired product. Considering this, and noticing the

consistently small size of the Hammeh charcoal specimens, leads to the interpretation that the fuel used in the Hammeh production could very well be charcoal made from the olive wood that results from the annual or bi-annual pruning of nearby orchards.

### **Water**

The river Zarqa, which skirts around the southern edge of the tell, must have provided the essential resource of water in relation to metal production carried out at Hammeh. Sulphur-rich thermal springs emanate from the banks of the Zarqa right next to the site (Blanckenhorn 1912, 320; Merrill 1881, 193) giving it its present day name of hammeh or hamma (plural: hammam), which means hot spring in Arabic. Water is essential in mixing clays to construct furnace wall and tuyère ceramics or to repair cracks in a furnace during a smelt.

### **Wind**

A hot wind blows through the Wadi Zarqa from the eastern desert (hence its Arabic name: 'Sharqiya', 'from the east') most of the year. Hammeh's location near the mouth of the Zarqa Valley puts it directly in the path of this wind. Especially the eastern side of the tell, where most of the iron production appears to have taken place, is affected, and the strong and almost permanent prevailing wind may have played a role in augmenting a natural draught or chimney effect in iron production furnaces. At Tell Hammeh, any such effect from the wind is in addition to the use of forced draught by bellows, and does not form the sole air-supply for the furnace as, for example, seen with the exclusively wind-driven furnaces in Sri Lanka (Tabor *et al.* 2005; see Juleff 1998; Juleff 1996).

## **Excavation history**

### **The 1994 Survey**

The first time Tell Hammeh was investigated archaeologically was in 1994, when the site was surveyed by Eveline van der Steen and several Leiden University students as part of a wider regional study. Her survey tried to identify (remains of) sites in the central Jordan Valley and surrounding foothills, and more specifically, to establish which of those sites featured material from the transition from the Late Bronze to the Early Iron Age. As a result of this survey, Hammeh was earmarked as a potentially interesting multi-period site (van der Steen 2003, 164-190).

Earlier surveys of the region had already noted the possible importance of Hammeh in several periods, notably the Late Iron Age, which is also one of the main occupation periods of Deir ʿAlla (Glueck 1951; Glueck 1935; Glueck 1933). The strategic location of the site, and the periods that were assumed present on the site from the survey results, made Tell Hammeh into an interesting prospect for excavation. Hammeh is furthermore of interest to biblical scholars, who often identify the site with Penu'el (or Pnuel, or Pniel), the location where Jacob fought with an angel and was crippled before crossing the river Jabbok (the present day Zarqa river) (Genesis 31, vs 21-32, Zwickel 1996, and personal communication).

### **The 1996 Rescue Excavation**

In early 1996, the owner of the land on which Hammeh lies used a bulldozer to level some of the sloping slides of the tell, in order to gain more arable land. Large areas of the southern and eastern side were thus removed (see Figure 5), which left a vertical bulldozer-cut that is almost three metres high in places. With Hammeh now at risk from imminent destruction as well as the erosion prone nature of the vertical cut, members of the Department of Antiquities and the Deir ʿAlla Regional Project team inspected the site. It was considered both necessary and opportune to combine the 1996 Deir ʿAlla season with a rescue excavation at Tell Hammeh. The aim was to clean and study the bulldozer-cut, and dig a few test trenches westward from that cut.

This trial excavation was conducted from November 3 until December 5 1996, supervised by Eveline J. van der Steen. The bulldozer-cut presented a large section that only needed cleaning to gain a first impression of the occupational history of Hammeh. However, severe winds (as described above in 'resources') hampered the work and only part of the cut could be cleaned. The 1996 season resulted in sections A and B, which are 10 metres long when taken together, and are situated along the central eastern side of the Tell.

Cleaning these sections revealed evidence for the existence at Tell Hammeh of, from the top down: Iron Age II and I layers, Late Bronze Age, and Chalcolithic layers. No Early Bronze Age material has been found thus far. Later, two trenches were cut into the section, one three metres wide (square I, into section B), one four metres wide (square II, which borders to section A). Again, because of the severe Sharqiya winds, work was hardly possible in the squares, and only the Iron Age layers could be excavated. The location of the sections and squares of the 1996 season are indicated on Figure 5.



In these layers, a small mud-brick wall was found, running north to south through both squares. A mix of slag, ash, and charcoal was at that time thought to be lying against this wall in square I. A small amount of these remains of metal production was sampled, but the locus (I-109) was not completely excavated. The sampled material was inventoried by the author at the Deir ʿAlla station in December 1996, and analysed by the author at the Archaeometry Laboratory of Yarmouk University, between December 23, 1996 and February 8, 1997. Of the eleven samples that were examined at that time, at least one was positively identified as a slag from bloomery smelting of iron. This was based on its outer appearance, a free-flowing tapped structure, and microscopic inspection, where the sample revealed a glassy matrix with fayalitic laths and free iron oxide in the form of wüstite (see also al-Amri 1998, who was a team member during the 1996 and 1997 seasons on behalf of the Department of Antiquities; Veldhuijzen 1998).

### **The 1997 Rescue Excavation**

A second rescue season took place just a few months later, from February 18 until March 31, 1997, primarily to continue the work of the 1996 season. Eveline J. van der Steen again directed the excavation. Work on the bulldozer-cut was continued, and sections were created to the south (sections C and D) and to the north (sections E and F) of the area that was cleaned in 1996. The north-western sections, E and F, revealed remains of structures that were at that time assumed to be possible iron smelting furnaces. In section D, Chalcolithic and Early Bronze Age material was found.

Excavation was continued in the two trenches from 1996; squares I and II. In these trenches, virgin soil was reached in square II. Only a little Chalcolithic or Early Bronze Age material was found, but there were heavy layers of Late Bronze Age material. There appears to have been a continuous occupation from the Late Bronze into the Early Iron Age here. Some stone walls were found from this period, but the excavated area was too small to establish any definite structures. The layer of slag and ash that was found in square I in 1996 was further exposed and found to extend to square II, where it was disturbed by large structures of later phases (van der Steen 2003, 149; fig 9-1).

In square I, the remainder of the iron production debris was excavated. It contained large amounts of slags, ash, charcoal, and molten and vitrified technical ceramics. Within the layer, two potential furnace structures were found; one of them located in and under the southern section of the square, and therefore not

excavated completely, the other at the northern side of the square. The latter is more a high concentration of fragments of molten technical ceramic and slags than a recognisable structure. The southern structure was apparently round, built up of clay, and filled with ash, charcoal, various slags, and molten technical ceramic. A few fragments of tuyères were also found in the debris layer.

Finally, in order to collect more information on the iron industry a new trench was opened, square IV, integrating one of the potential furnace structures that were seen in section E. This very large structure with an internal diameter of around two metres was almost entirely excavated. It was made of heavily burnt mud-bricks and filled with ash, apparent slag, and burnt brick fragments. An ashy layer surrounded the structure, and it was resting on a layer of heavily burnt material, possibly incorporating an older furnace. The location of the new sections and squares of the 1997 season are indicated on Figure 5.

Doubt about the identification of this structure as related to iron production led to renewed excavation of this structure in the 2000 season. The last remaining mud-brick parts were examined as well as remnants of what had been identified as slag. This would-be slag turned out to be light and foamy remains of molten ceramic material. Notwithstanding the obvious presence of high temperature operations in relation to this structure, no connection with any aspect of iron production processes can be assumed. Two smaller but similar structures were identified in section F, but again, no link to metallurgy can be assumed for these. Lack of indications for other possible uses of these structures leaves identification of their actual function open to debate. The tuyère fragments that were excavated here must relate to the chronologically and stratigraphically younger layer of smelting debris that was excavated in bordering square A/H9 during the 2000 season.

## **The 2000 Season**

### **Aims of the 2000 Season**

The presence and importance of the large quantities of iron production related material resulted in a shift in the research questions and excavation goals. From identifying the different periods present at the site (1996, bulldozer-cut) and exploring the transition from Late Bronze to Iron Age (1997, square I and II mainly), the research aims now transferred fully to investigation of the iron production remains. The third season took place from April 4 until May 30 2000

under the direction of the author, again as part of the joint Leiden University, Yarmouk University Deir ʿAlla Project.

Several squares and two trenches were planned for this season, in order to thoroughly inspect the eastern side of the tell (see Figure 5). Of the second planned trench, only B/A5 could be excavated due to lack of time. The aim of the projected squares and trenches was on the one hand to recover as much information and material from the iron production area as possible, which area was considered to concentrate on the eastern side of Hammeh. On the other hand they aimed to investigate the spatial spread and extent, volume, and possibly the social context of the production. The results from the previous two seasons did influence the location of some of the squares, especially A/H9, where clarification was sought for the assumed furnace structure(s) there.

### **Excavation Method: Laying out a Grid and Squares**

With work aiming specifically at clarifying the previous discoveries related to iron production, a far more extensive excavation of the tell was planned for the 2000 season. A formal grid was now applied to the site analogous to the system at Deir ʿAlla, dividing the tell into four main areas (A-D), with each area consisting of 5 x 5 metre squares (see Figure 5). The squares are numbered alphabetically along the north-south axis and numerically along the east-west axis of the grid, with both numberings ascending from the central point of the tell outwards. Baulks 50 cm wide were left standing on the northern and western side of each square.

Two squares were opened adjacent to the main previous find spots of square I and II (squares A/B6 and A/B7), a third next to the assumed furnace structure(s) of square IV (A/H9). Furthermore, two trenches of 1 x 4.5 m were projected to try and track the distribution of the material within the south-eastern quarter of the site, and to try and identify possible different uses of space within this part of the tell. In the end, only trench 1 (A/D5 to A/D8) was excavated as planned, of trench 2 only one 1 x 4.5 m part was opened (B/A5). Two additional 1.5 x 4 m trench parts (A/C7 and A/D7; the last connects at a right angle to trench 1) were opened near the end of the season to connect trench 1 to the main production area (square A/B7). These two were excavated until the slag deposit was reached there.

Several reasons existed for focussing the excavation work on the central- and south-eastern side of the tell. The first is very simple: not all parts of the tell are readily available for excavation. Most of the northern part is occupied by a

complex of a 1950s mud-brick house with auxiliary buildings, whilst a historical stone structure with its related significantly higher ground levels makes excavation down to the iron production layers difficult and too time-consuming for a single season in the central and western parts of the tell.

Additionally, small surveys of the tell surface and surroundings by the author in 1998 and 2000 showed a scattering of slag concentrated on the eastern half of the site, and an almost complete absence of slag on the western half of the tell. Metallurgical activity on the western side, however, can not be excluded completely, as the mound slopes down quite steeply here, which may have influenced the retainment of material, and thereby the survey results. Low numbers of slag fragment were found in the northern part, in between and in front of the mud-brick structures. It is not clear whether these pieces should be interpreted as *in situ* or as the result of (ancient or modern) terrain modification.

The bulk of iron production related material was excavated from square A/B7, where the deposit proved to be of very loose consistency. This considerably hampered proper stratigraphic excavation. For example, only the vertical sections of A/B7 slowly revealed the complex layering of the iron production debris during, and largely only after, excavation. This layering is interpreted as a possible indication of seasonal activity, very likely taking place over an extended period. It was impossible to establish the exact nature of each individual layer. Apart from actual layers of technological activity, some may represent a levelling of terrain and/or structures after or just prior to a new smelt, others may be the result of weathering of the remains between seasonal operations. In order to separate the possibly present but invisible stratigraphy, a grid system of 75 x 75 cm was devised (shown in Figure 6). These 'mini-squares' were termed 'grids' and subsequently excavated in 5 cm deep spits that were called 'units'.

### Collection and Registration in the Field

During the 2000 season, it was attempted to register all iron production related material in the field. All square supervisors used a special form (the Iron Production or 'IP'-sheet) in addition to the regular registration of the excavation. The form registers several macroscopical features for the different materials involved (based on the finds of 1996 and 1997). It also provides all finds with a unique IP-number. As the excavation progressed, however, the number of finds started to increase at such a rate that piece by piece registration quickly became untenable. First the slag, and later also the tuyères, came to be collected by the

bag, and detailed description of the features per sample made way for more generic bag-content indicators.

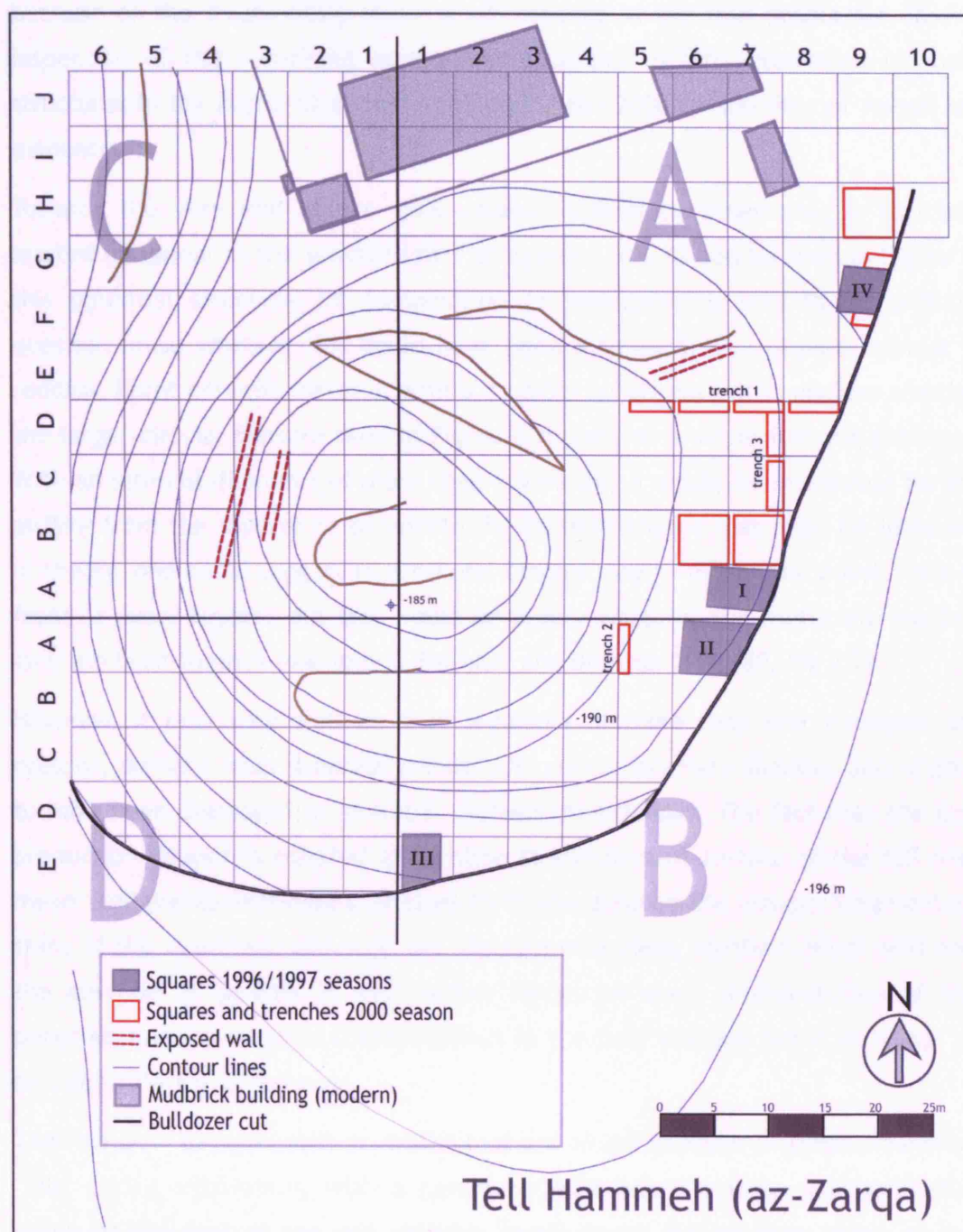


Figure 5. Plan of Tell Hammeh, showing the 1996 and 1997 squares in grey, and the 2000 squares in red (based on the survey of the Tell by Muwafaq Bataineh, Yarmouk University)

### The Furnace Structures

During the excavation in 2000, one of the great hopes was to discover an undisputed furnace structure. From the two earlier seasons possible crushed furnace remains were reported, in corners of square I, as well as in the bulldozer-

cut sections E and F, but later inspection of these reports did not lead anywhere. Field drawings, for example, do not show these possible structures, probably because of the fragmentary state of all remains in the iron production layers. Inspection of the remaining sections or attempts to find extensions of these structures in the adjacent square A/B7 during the 2000 season did not reveal any evidence.

Towards the very end of the 2000 season, something resembling a structure started to appear in the southern half of square A/B7. As can be seen in Figure 6, this potential structure (or combination of structures) is very large, and the question arose whether this could have been a furnace. The remains consist of reddish, burnt ceramic material with a crumbly consistency. It is unclear whether the larger circular feature seen in Figure 6 represents a single furnace structure. With an internal diameter of more than 1.5 metre, it would be impossible for the airflow from the tuyères to penetrate the massive charge that must be involved. In theory, one could suggest that several blooms may form simultaneously; one in front of every tuyère, but this would be a very wasteful and inefficient method (see the blast furnace example in Rostoker and Bronson 1990, 80, Fig 7.7).

However, it may very well be that segments of more than one structure are present, perhaps from separate smelts. All remains are very shallow, and appear to have been destroyed or levelled, perhaps intentionally. The fact that the iron production deposit is situated quite close to the present surface of the tell may mean that postdepositional processes have exacerbated the already fragmentary state of the materials. Although the absence of a clear, vitrified, inner wall and the absence of tuyères *in situ* further hinder an exact interpretation of the potential furnace(s), several observations in the field strongly argue in favour of an interpretation as furnaces.

The rounded 'furnace wall' or 'walls' that are shown in Figure 6 could clearly be 'felt' during excavation, with a perceived hard baked bottom, and upturning ridges at the foot of the red, crumbly 'wall' parts. Furthermore, most of the charcoal and ash was contained within these structure(s), as were many of the tuyères. A new season of excavations, especially in squares A/C7 and A/D7 (trench 3), is likely to supply more evidence to enhance the furnace interpretation. This season was planned for the spring of 2003, but had to be postponed due to the invasion of Iraq. It is now hoped that renewed excavations can be held in spring 2006.



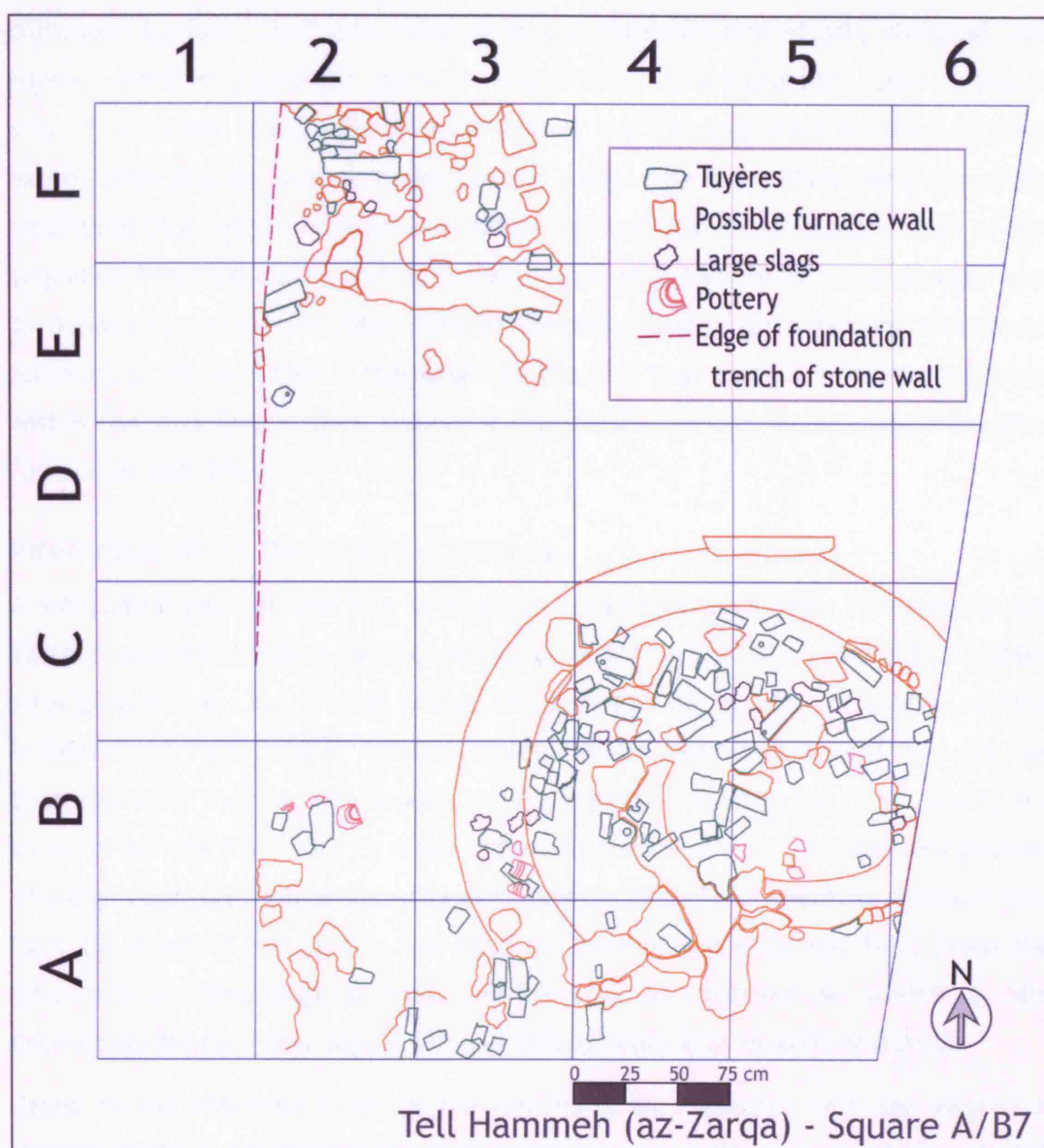


Figure 6. Plan of square A/B7 near the end of excavation, showing tuyère fragments in green, possible furnace wall material in orange, larger slag pieces in black, scarce pottery in pink, and the 75 x 75 cm grid in blue. Empty grids were either excavated before the drawing was made (e.g. F4), or have not been fully excavated (row D).

No features or structures were found thus far that relate to any other activity related to the smelting *chaîne opératoire*. No (primary) smithing hearth, (separate) ore roasting, or charcoal production areas were identified. The absence of such features, structures, or areas does not imply that such activities or activity areas did not exist on Hammeh. This is, for example, evident from the presence of primary smithing slags (see chapter 8, page 186) among the metallurgical debris, clearly indicating that primary smithing did take place at Hammeh.

In my opinion, and with due caution, it is reasonable to interpret the structures excavated in square A/B7 as the remains of more than one -albeit heavily

damaged- furnace structures. Judging by the concentration of ash, charcoal, and tuyères within the confines of these structures, they are probably more or less *in situ*. It is further reasonable to assume that the furnaces were levelled to some extent after use, possibly to make way for a new structure. What remained of the structures that were excavated in 2000, does not allow the identification of any sequence between them, and it further seems as if they were subsequently used to deposit remains from later runs performed in other (thus far not recovered) furnace(s). This last idea is supported by the fact that there are far more tuyères within the structure(s) then would be expected to belong to one single smelting furnace or operation.

### Interpretation of the 2000 Excavation

A substantial part of the iron production area must have been removed on the eastern side of the site by the bulldozer activity. The iron production related stratigraphy can be traced along large stretches of the resulting vertical bulldozer-cut face, and it radiates at least 20-25 metres westward into the tell from there. At the cut, the deposit is clearly present both to the north and to the south of square A/B7, but is often disturbed there by later (occupation) phases. The high concentration of material at squares A/B7 to A/D7 seems to indicate that here (or more to the east in the removed part of the tell) may have been the epicentre of (smelting) activity. Tell-inwards, as observed in trench 1, the production debris slowly tapers off, but still appears in both A/D5 and B/A5.

Based on the elevation levels of the remaining tell, together with the westward stretch of the production layer, it is estimated that half or more of the original production area may have been removed. Approximately 5 to 10 % of that projected production area has now been excavated, and even that area only in part. So far, this has yielded roughly 700 kg of slag material and more than 350 tuyère fragments, mainly from square A/B7.

As far as Tell Hammeh has been excavated to this date, there is, significantly, no indication of contemporaneous occupation, habitation, or other non-metallurgical use of the site. This seems to suggest that, from ca. 950 to 800 BC (see chronological framework below), Hammeh may have been used exclusively for smelting iron. An interesting concept by itself, it both feeds and hinders interpretation of the local socio-economic context and organisation of the iron production. No indicators pointing towards outside control or connections with neighbouring sites have been found. For example, the very limited amount of



pottery found within the iron production deposit shows no immediately identifiable links to the contemporaneous assemblage at neighbouring sites (Eveline van der Steen and Gerrit van der Kooij, personal communication). Further study on the pottery from Hammeh, including the periods immediately prior to and after the metallurgical deposit, is scheduled to take place at Leiden University in the near future. Nevertheless, it can be assumed that the operations at Hammeh were associated with, if not coordinated from, another location nearby.

### **The 2001 Sampling Season**

A provisional classification of the material was first drawn up in 1997, based on macroscopic analysis of the Hammeh material excavated up to that moment. External features such as shape, colour, density, tapping (flowing) evidence, size, weight, and magnetism of that material were studied and recorded. Based on these parameters, tentative types and sub-types were determined.

This initial classification was further amended during study of the 2000 material and helped to organise the subsequent sampling. In the field, all material excavated was kept and stored. In spring 2001, all the excavated material was restudied and where necessary reclassified during a dedicated sampling season. Now, additional information was recorded on the season 2000 IP-sheets, and a database was designed to digitise this information.

All remains were spread out on 2 x 4 m makeshift tables, and studied per IP-number. The ratio of estimated volume of the main slag types (black-grey, rusty, and cakes) was recorded. Next, the tuyères were studied and recorded in very much the same way, recording colour, state of preservation, which segment of the original tuyère (nozzle, mid-piece, or rear end) was retained, presence of vitrification/molten material, and measurements of both the piece itself and its bore.

Based on this macroscopic examination of the 2000 material, a few changes were made to the initial classification. One was the possible re-interpretation of two magnetic and rusty slag sub-types as partly reduced ores, the other is a refinement of the tuyère types, necessitated by the large amount of new tuyères excavated, and the information this revealed. The resulting provisional classification of the Hammeh material is shown below in Table 1.

I-Slag				II-Furnace remains		III-Ore		IV-Tuyères		
A-Magnetic		B-Non-Magnetic		A-Molten	B-Non-Molten	A-Tell Hammeh		B- Warda	A-Vitrified	B-Non Vitrified
1-Strong	2-Weaker	1-High Density	2-Low Density			1- Partly reduced?	2-Discarded			
a-Black / grey flow	a-No rust	a-Black / grey flow	a-Black glass	a-Grey Porous	a-Red + lining?	a-Rusty =IA1b and IA2b?	a-Discarded or Weathered	Haematite	a-Nozzle	a-Nozzle
b-Rusty =IIIA1a?	b-Rusty =IIIA1a?	b-Slag-cakes	b- Green glassy	b- Green glassy	b-Grey / White				b-Side	b-Rear
			c-Slag/ rust mix	c-Mid-stage					c-Whole	c-Middle
									d-Slag attached	d-Slag attached

Table 1. Provisional classification of the main Hammeh material, based on macroscopic analysis.

This time up to ten samples were selected for each (sub)type, with the intention of bringing this down to five during the actual research. The selection procedure followed a basic form of ‘adaptive sampling’ (Orton 2000, 16; 34), where the samples were taken in equal quantities for each assumed artefact (sub)type. This allocates each type equal importance within the total assemblage, regardless of actual quantity differences between (sub)types, allowing for modifications to the sampling after more data is obtained. The adjusted classification and related sampling are interwoven parts of the structured approach to the instrumental analysis of metallurgical material. The classification serves to sort the large mass of finds into types, based on their external appearance, i.e. getting a first impression of the different material present. It is sub-divided according to properties such as density, magnetism, shape, colour, and porosity. The macroscopic analysis in this case both defines and refines the initial working classification of the samples. Subsequent analysis of the various materials showed that many of the groups and sub-groups defined in the field and already adjusted in 2001 can be considered superfluous, and these were subsequently dropped from the research (see chapter 8).

## Chronological Framework

### Periods Present on Tell Hammeh

Several periods have been attested at the site. From bedrock upward, remains of Chalcolithic (ca. 4500-3000 BC) and Early Bronze Age (ca. 3000-2000 BC) occupation were found, followed by more substantial layers of Late Bronze Age (ca. 1600-1150 BC) material. The Late Bronze Age appears to continue into Iron Age I (ca. 1150-1000 BC) without interruption (van der Steen 2003).

Although speculative, it seems as if Hammeh was continuously settled through the Late Bronze Age and Iron Age I up to the moment when iron production started. All domestic structures (in the excavated areas at least) then cease to exist, and are covered by a continuous layer of iron production debris. It is as yet unclear whether the site was abandoned before or in relation to the subsequent metallurgical activities, but stratigraphically no interruption or abandonment was observed. It should be noted that excavation in square A/B7, which had provided most of the data concerning the iron production had to be stopped before excavation reached below the slag-layer. Therefore, further excavation that extends below the iron production phase in this square is necessary to establish the exact nature and date of this transition. Production of iron then appears to have taken place for a considerable period, perhaps as a seasonal activity, starting somewhere before 900 BC.

It does appear that very soon or immediately after iron production ceased, settlement of the site resumed, without observable abandonment. Extensive pavements and large domestic structures immediately overlay and often cut through the preceding industrial layers in all excavated squares and trenches. Most significant is the large stone wall at the baulk between A/B7 and A/B6. The foundation trench of this wall (seen as the dotted line in Figure 6), which is part of a large building that extends into square A/B6 and A/A6 (square I), cuts cleanly through the slag deposit. Only two or three pieces of slag were found inside this building, likely as debris from the foundation trench. The floor levels of this building reach below the lowest point of the slag deposit.

Based on examination of the extensive pottery finds from the phase that follows the iron production debris, it is assumed that the iron production activities must have ended no later than 750 BC (Gerrit van der Kooij, personal communication). This late Iron Age II phase seems to form the last extensive occupation of Tell Hammeh, with the exception of a large stone structure near the apex of the tell, which is provisionally assigned to early Islamic or Medieval times (see Figure 5 on page 86).

### **Dating the Iron Production**

As mentioned above, two samples of olive wood charcoal were taken from within the metallurgical material (samples IPAB7.157 and IPAB7.118) and sent out for accelerator mass spectrometry (AMS) radiocarbon dating at Beta Analytic, Miami,

Florida. The AMS dating was performed with  $^{13}\text{C}$ - $^{12}\text{C}$  correction and using the INTCAL 98 calibration database (Stuiver and van der Plicht 1998; Stuiver *et al.* 1998).

Sample Data	Measured Radiocarbon Age	$^{13}\text{C}/^{12}\text{C}$ Ratio	Conventional Radiocarbon Age (*)
<b>Beta 192343 / SAMPLE: IPAB7.118</b> <b>ANALYSIS: AMS</b> <b>MATERIAL/PRETREATMENT: (charred material): acid/alkali/acid</b>	2760 +/- 40 BP	-22.5 ‰	2800 +/- 40 BP
2 SIGMA CALIBRATION (95% probability): Cal BC 1030 - 840 (Cal BP 2980 - 2790) 1 Sigma Calibration (68% probability): Cal BC 1000 - 900 (Cal BP 2940 - 2850) Intercept at Cal BC 930 (Cal BP 2880)			
<b>Beta 192342 / SAMPLE: IPAB7.157</b> <b>ANALYSIS: AMS</b> <b>MATERIAL/PRETREATMENT: (charred material): acid/alkali/acid</b>	2730 +/- 40 BP	-22.3 ‰	2770 +/- 40 BP
2 SIGMA CALIBRATION (95% probability): Cal BC 1000 - 820 (Cal BP 2950 - 2780) 1 Sigma Calibration (68% probability): Cal BC 940 - 850 (Cal BP 2890 - 2780) Intercept at Cal BC 910 (Cal BP 2860)			

Table 2. Results of the AMS Radiocarbon dating of charcoal samples IPAB7.118 and IPAB7.157

The results of the two  $^{14}\text{C}$  AMS analyses show an intercept at 930 and 910 Cal BC ( $\pm 40$  years) respectively, indicating a date range of (1 sigma calibrated) ca. 1000 to 900 and 940 to 850 Cal BC. The results of the radiocarbon dating are given in Table 2. The two samples in question derive from the lower part of the slag deposit, the first just outside, and the second from within the furnace structure(s) in the southeast corner of A/B7.

It should be pointed out that these dates should not be considered as all explaining and fixed. Several caveats apply (see van Strydonck *et al.* 1999). An important caveat is that more samples should be analysed to counter possible measurement errors, sample contamination, and the sampling of 'old wood'; especially this last factor is often a case for chronological reconsiderations (see for example Posnansky and McIntosh 1976). More  $^{14}\text{C}$  analyses would furthermore allow a more balanced view of what part of the possible date range is most likely the actual one. Other caveats concern widely known and discussed issues with accuracy and precision in relation to certain periods in time. In that respect the Hammeh dates fall in a period that is hotly debated throughout the Near East, and is well known for difficult dates.

Another important factor is that within the samples recovered during excavation, not one of the examined specimens shows any remains of bark or bark edge, generally required to be certain about the lifespan of the wood in question. However, it is significant to observe that all metallurgy-related charcoal is very small (less than 1 cm in diameter), and seems to represent young branches and

twigs rather than cores of larger and older wood. In the opinion of John Meadows and Phil Austen, who assisted in the selection of the samples for  $^{14}\text{C}$  dating, the selected pieces have an extremely high likelihood to be short-lived material. This means that they are reasonably well suited for dating, even without proper bark edge.

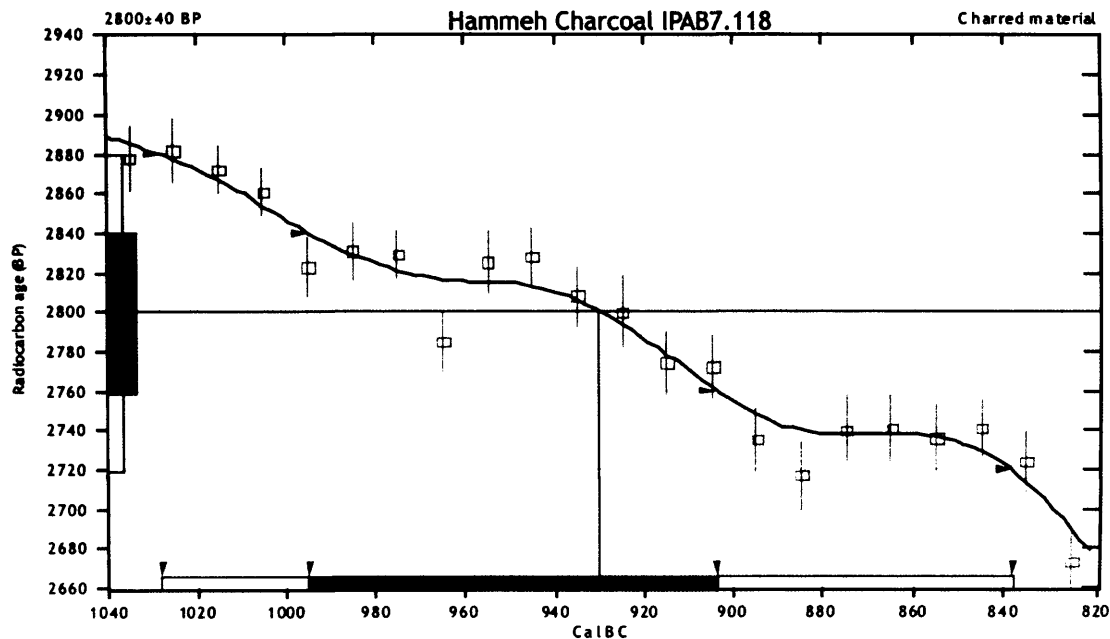


Figure 7. AMS  $^{14}\text{C}$  calibration curve for sample IPAB7.118 (source: Beta Analytical)

As can be seen in the graphic representations of the two dates against the calibration curve, the intercepts of both samples lie on a slope, i.e. a very precisely dateable area of that curve, rather than on a plateau, where error margins increase exponentially. With the caveats in mind, the Hammeh  $^{14}\text{C}$  dates can be seen as a very good indicator to a *datum post quem* for the iron production to be active. Although the start of metallurgical activity at Hammeh may actually lie at an earlier time, in which scenario the  $^{14}\text{C}$  dates from the charcoal indicate a time when the production is already active. However, this is not possible to ascertain from the archaeological context, and the  $^{14}\text{C}$  dates should therefore be treated as an approximate starting point of the iron production at Hammeh.

The scant pottery finds within the iron production stratigraphy would also seem to point to a deposition of the material during the early part of the Iron Age II (ca. 1000-586 BC). Two 'conflicting' types of pottery seem to stem from around 1000/950 and 750 BC respectively (Eveline van der Steen and Gerrit van der Kooij, personal communication). The older pottery type (among others cream coloured ware with orange-red circular decoration) may be a contamination of the record

from earlier layers, possibly unearthed during levelling, preparation, or other modification of the production area.

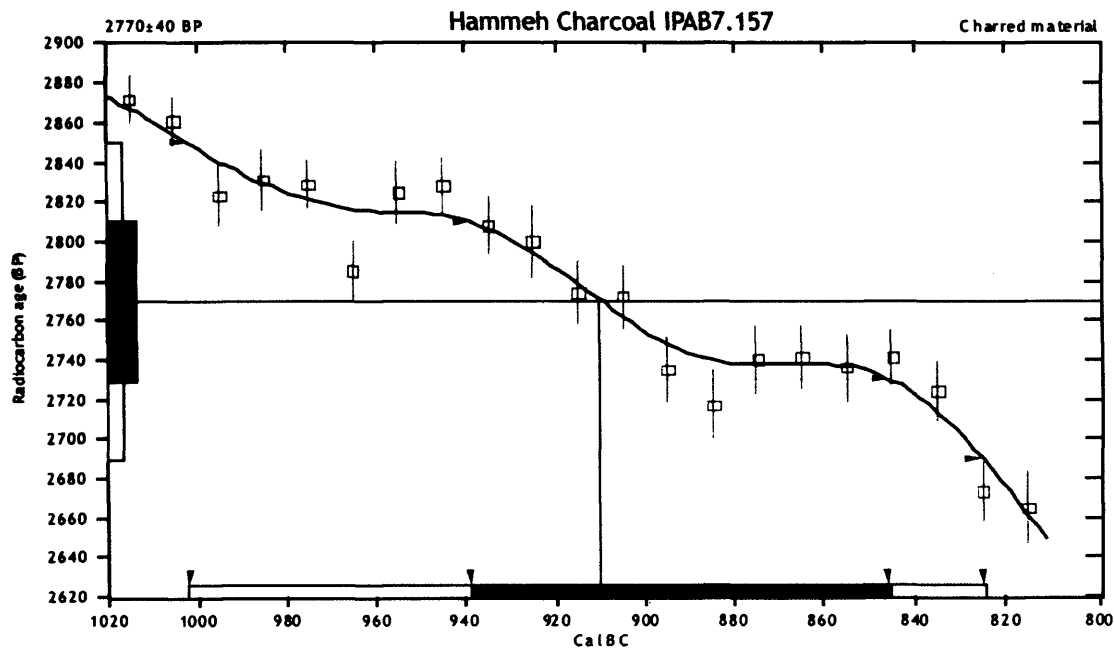


Figure 8. AMS  $^{14}\text{C}$  Calibration curve for sample IPAB7.157 (source: Beta Analytical)

As discussed above, the stratigraphy of the iron production debris, with several layers within the single phase, suggests seasonality of production, wherein the older pottery may stem from the earliest production layers. As described above, a micro-stratigraphic system of excavation was devised to attempt to separate this possible seasonality during excavation (see page 84). The pottery excavated at Hammeh was registered with the grids and units from this system added to the regular stratigraphical data of Area, Square and Locus. Future examination of the pottery (at Leiden University) will have to ascertain whether the two types present do separate between the units excavated, with the older type belonging to the earliest iron production debris, and the younger pottery to the last debris.

### The Socio-Economic Context of the Iron Production

To interpret the archaeological significance of the iron production at Hammeh, it is important to examine it in the social and economic context of the Jordan Valley in the Iron Age. The periods preceding the production activities at Hammeh, the Late Bronze Age (ca. 1600-1150 BC) and the Iron Age I (ca. 1150-1000 BC), are characterised by a collapse of the major powers in the region, both the Egyptian Kingdom and the Hittite Empire. In this part of the Levant this is reflected, for example, in a low number of foreign artefacts in Transjordan (McGovern 1986, 338). The absence of these outside forces, both in terms of actual presence and of

their socio-political or economic influence, possibly causes, or at least coincides with, the partial collapse of the Late Bronze Age city-system in this part of the Levant (LaBianca and Younker 1998, 402; McGovern 1986, 335-344).

Simultaneously, there are extensive movements of Aegean peoples around the Mediterranean, with the Philistine 'section' of these so-called 'Sea Peoples' settling along the coast of Palestine during the transition of the Late Bronze Age to the Iron Age I (Waldbaum 1999; Muhly 1980). It is interesting to note that the iron production at Hammeh, with a starting date of around 930 Cal BC, takes place at a time just when the supposedly principal groups in the innovation, development, and spread of knowledge about iron technology are virtually absent from the region (see chapter 3).

In the context of this waning outside influence, there is little evidence in the Levant for a cultural break between the Late Bronze Age and the Iron Age I, as many previously existing cities and settlements continue to exist (LaBianca and Younker 1998, 406; McGovern 1986, 339-340; Muhly 1980). The exact socio-economic situation in the transition from Late Bronze Age to the Iron Age, and in the Iron Age I and II, is widely debated in terms of the nature of the (indigenous) population in various parts of the Levant, the role and influence of other groups such as the Philistines, and the formation and nature of more decentralised local states (Finkelstein 2003; Joffe 2002; Finkelstein 1999; LaBianca and Younker 1998; Finkelstein 1998; McGovern 1986, 335-344; Dornemann 1983, 4; 22-24; 25-29). These local states may have been tribal kingdoms (LaBianca and Younker 1998), tribal states (Younker 1997) or segmentary states (Routledge 2004; Routledge 2000).

Notwithstanding the different opinions among the various proposed scenarios for state formation and movements of peoples in this part of the Levant, there is a degree of consensus that various indigenous groups in the region established an 'independent' existence after the collapse of the Egyptian and Hittite influences. This resulted in more or less structured local territorial states, perhaps with tribal backgrounds or affiliations at their basis, which are characterised by a regionally largely homogeneous (material) culture (see also LaBianca and Younker 1998; van der Kooij and Ibrahim 1989, 17; and McGovern 1986, 339-340).

Where the Jordan Valley and Hammeh are concerned, the archaeological evidence for either such a continuation or a possible influx of other groups is rather sketchy, although, as mentioned above, an unbroken transition from the Late Bronze Age to

the Iron Age I is also proposed for Tell Hammeh (van der Steen 2003, 157-158). Besides the assumed continued presence of indigenous people in the Jordan Valley, there are indications that there may also be movements of people coming from the east, moving into and settling in the Zarqa Valley and nearby Jordan Valley during the Iron Age I as well (van der Steen 2003, 91-93, and the references therein; McGovern 1986, 339-340; Franken 1969).

Reconstructing the socio-economic context of the iron production at Tell Hammeh itself remains difficult. This is primarily a result of the archaeological context on the site itself, where little or no material culture is present besides the ubiquitous iron production debris. Although the regional and local circumstances at the time when iron was produced at Hammeh remain unclear thus far, a picture does emerge of local (indigenous) people performing the metallurgical activities, perhaps instigated from one of the settlements in the Jordan Valley. The excavations revealed no evidence of outside (foreign) control over either the applied techniques or resources, but the apparent absence of habitation at Hammeh does suggest a strictly metallurgical use of the site in this phase. This in turn suggests that the metalworkers came from elsewhere, probably a nearby site such as Tell Deir ʿAlla or Tell es-Saʿidiyeh. The local nature of the iron smelting activities seems borne out by the choice of location for the metallurgy, where the relative distance from the ore suggests that access to that vital resource was unhindered. Another indicator for the local nature of the metallurgical activities is found in the tuyère design, which is identical to tuyères from other periods, both earlier and later, in the surrounding region (see chapter 8, on the tuyères at Tell Abu al-Kharaz and Tell Deir ʿAlla), which may reflect a local, diachronous, metallurgical tradition.

## Summary and Interpretations

The 2000 season at Tell Hammeh was planned using the hypothesis that the site was an iron production site, with predominantly smelting activity. Examination of the material from the two earlier seasons had not given any indication for (but also not necessarily excluded) the possibility of secondary smithing at the site. The new season, therefore, aimed to test this interpretation of primary production, both by excavating a larger area of specifically the iron production phase to examine the use of space and the layout of the activities, and to excavate a larger quantity of material to allow determination of the nature of the technology through analytical techniques (see chapter 8).



Three new squares were excavated next to areas that had shown high concentrations of iron metallurgy related debris (squares A/B6 and A/B7, near former squares I and II; square A/H9 next to former square IV). Furthermore, initially two, later three trenches were opened to trace the extent of the iron production area. Trench 2, running north to south (square B/A5), could not be completed during the season, and only one section of it was excavated. Trench 3 was opened at a later stage, to connect the large quantities of material found in A/B7 to trench 1.

The 'slag-layer' at Hammeh is one stratigraphic phase of production debris, consisting of multiple internal sub-layers. As noted before, the material in this phase ranges from ash and charcoal, through molten technical ceramics, including ca. 350 fragments of square-section (block) tuyères, to smelting and primary smithing slag and furnace structures. The assemblage is virtually without iron artefacts, and there are no indications for the presence of copper, bronze, or copper related metallurgy.

Most of the iron production related material was excavated in square A/B7. Proper stratigraphic excavation of this square was hindered by the very loose consistency of the deposit, which prompted the use of a grid system of 75 x 75 cm. The grids were excavated in 5 cm deep units, to allow post excavation determination of a possible stratigraphical sequence. Based on the metallurgical material, no such differences are attested. Future study of the pottery, which was separated according to the same grids and units, may show whether a temporal sequence between the units can be defined.

In my opinion, the layered structure of the iron smelting debris originates in a seasonality of the smelting activities, taking place over an extended period. Each of the layers may represent an actual smelt or smelting season, levelling of terrain or removal of debris between smelts, or weathering of the remains between two seasons of operations. The seasonality of the operations is underlined by the identification of all charcoal as short-lived olive wood, which suggests that the fuel for the furnace(s) derived from the (seasonal) pruning of olive trees. This possible relation between smelting activity and the maintenance of olive trees further suggests a local or regional level of organisation of the iron production (see chapter 2).

No specific activity areas could be discerned within the 'slag-layer', with the exception of the furnace structure(s) that were observed in A/B7 (see Figure 6). As

discussed above, it is difficult to draw any firm conclusions with regard to these structures, as no clear *in situ* molten or vitrified parts were found. This might have enabled a firmer reconstruction of inner and possibly outer diameters. Nevertheless, several observations were made during the excavation of the square, such as the distinct concentration of ash within ridges of thermally affected ceramic material, a concentration of tuyères and slag material within those ridges, and finally a distinct feel (literal) of bottom and edges. These observations do, in my opinion, support an interpretation of these features as (in all probability several) furnace structures in their original location, albeit in a heavily disturbed state.

A large part of the original total iron production area was removed together with the eastern part of the tell. Based on the concentration of material in square A/B7, trench 3 and trench 1, in combination with the survey plan of the tell, it is estimated that between 5 and 10 percent of the original production area has been excavated so far. Considering the large quantity of slags (700 kilograms) and tuyères (ca. 350 separate fragments) excavated from what is a fraction of the original smelting area, it is clear that Hammeh produced far more iron than necessary for the consumption of a single settlement.

The excavations show no indication of occupation, habitation, or other non-metallurgical use of the site at the same time that iron was smelted there. This apparently exclusive use of the site for seasonal metallurgical activity, together with the large quantities of slags and tuyères and absence of iron artefacts, strongly suggests an interpretation of the site as a local or regional production centre (see the calculations of the yield of iron metal in chapter 8). It seems reasonable to assume that the production at Hammeh, which clearly extends beyond the consumption needs of a single settlement, is instigated or controlled from one of the larger settlements in the nearby region, such as Tell Deir ‘Alla or Tell es-Sa‘idiyeh.

The absence of secondary smithing or finished artefacts at Hammeh suggests that only the primary production of iron metal took place at Hammeh, and that a more or less consolidated bloom or billet was subsequently transported or traded. The choice of Hammeh as the location for metallurgical activity seems to reflect primary production as well. The site is ideally located near all resources for production, but less optimally for supplying the metal to ‘consumers’. This is in contrast to Tel Beth-Shemesh, where the metallurgical activities (secondary

smithing) take place within the ‘industrial quarter’ of a large settlement, i.e. directly at the ‘consumer’ (see chapters 5 and 9).

Secondary smithing of the metal to create finished artefacts in all probability took place elsewhere. Different scenarios are possible for such a set-up, as attested by several ethnographical studies of iron production (see chapter 2). As will be discussed in chapter 5 and 9, the smithy at Tel Beth-Shemesh may be metallurgically related to the smelting at Hammeh (as indicated through identical tuyère design as well as clay). It is tempting to speculate that such a relation means that the Hammeh smelters themselves may have travelled around after their seasonal smelting, smithing their metal to artefacts at various sites in the region. Alternatively, the smelters at Hammeh, or the site(s) coordinating the smelting, traded or distributed their metal to other settlements in the region, where local smiths produced the desired artefacts.

## CHAPTER 5: THE ARCHAEOLOGY OF TEL BETH-SHEMESH

### The Location of Tel Beth-Shemesh

Tel Beth-Shemesh is located in the north-eastern Shephelah (lowlands) of Israel, approximately 20 km west of Jerusalem, and 75 km southwest of Tell Hammeh. It lies on the south side of the upper Soreq Valley, at what once formed the border area between the Philistine territory of the lower Shephelah and coastal plain, and the Judean Hill Country.

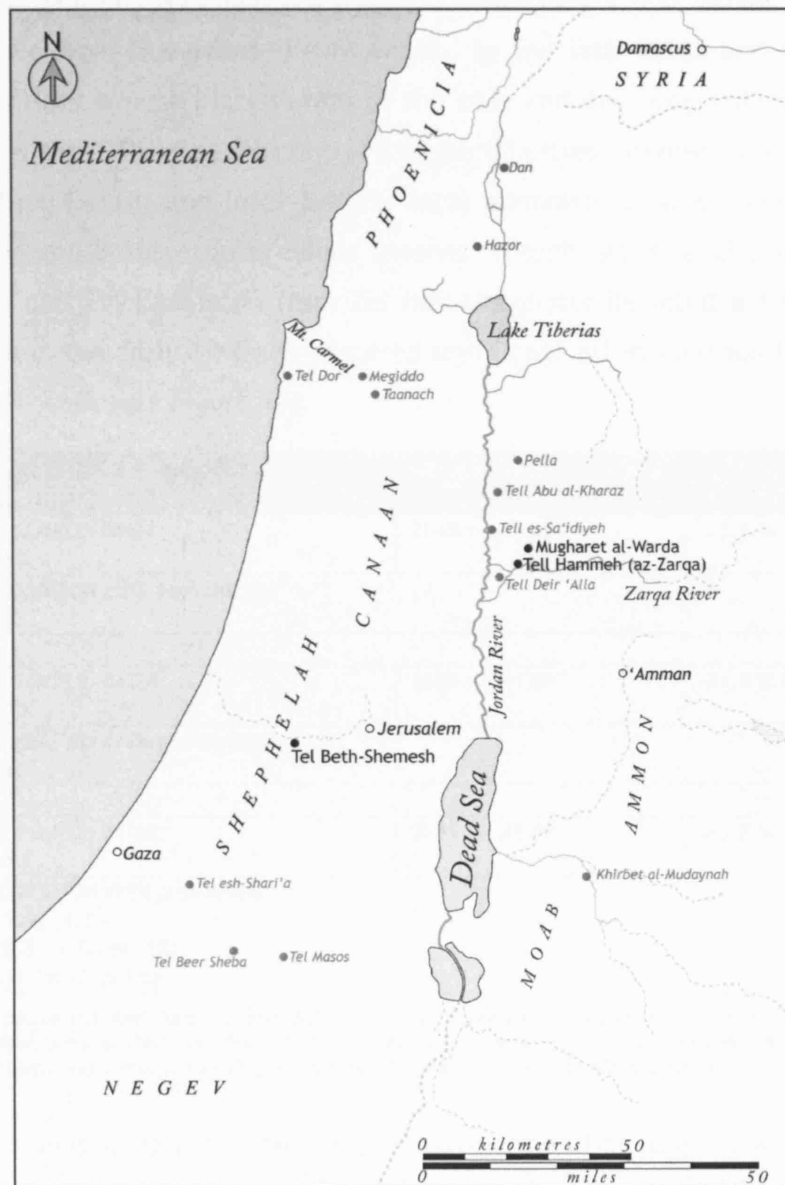


Figure 9. Map of the Southern Levant, showing the location of Beth-Shemesh.

Tel Beth-Shemesh is also strategically positioned to guard one of the main routes that leads into the Judean Hill Country and to Jerusalem. It is close to the town of

Zorah, which lies directly across the Soreq Valley on the northern side and is famously known as the birthplace of Samson. The Soreq itself is a broad, fertile, and well-watered valley that is very suitable for agriculture.

## The Excavation History of Tel Beth-Shemesh

Excavation of Tel Beth-Shemesh was conducted in the course of three major expeditions. The first two excavations were held in 1911 and 1912 by Palestine Exploration Fund archaeologist Duncan MacKenzie (MacKenzie 1914). A second series of excavations was directed by Elihu Grant (Grant and Wright 1939), from Haverford College, Haverford, Pennsylvania, in the late 1920s and early 1930s. Both expeditions exposed large areas of the site, and dug deep trenches reaching down to bedrock. Because of contractual peculiarities between the excavations and the, first Turkish and later British, local administrators, excavated soil was habitually dumped into the previous seasons' trench. As a result, when Shlomo Bunimovitz and Zvi Lederman from Tel Aviv University initiated a third series of excavations in the early 1990s, it required significant effort to trace the extent of the previous work (see Figure 10).

Sample Data	Measured Radiocarbon Age	$^{13}\text{C}/^{12}\text{C}$ Ratio
ETH-30461 / SAMPLE: B4121 ANALYSIS: AMS	2645 +/- 45 BP	-23.1 ‰
2 SIGMA CALIBRATION (95% probability): Cal BC 899-765		
ETH-30462 / SAMPLE: B4126 ANALYSIS: AMS	2660 +/- 45 BP	-21.4 ‰
2 SIGMA CALIBRATION (95% probability): Cal BC 904-787		
ETH-30463 / SAMPLE: B4128 ANALYSIS: AMS	2825 +/- 45 BP	-18.5 ‰
2 SIGMA CALIBRATION (95% probability): Cal BC 1126-1095 (4.9%) Cal BC 1094-895 Cal BC (90.1%) Cal BC 877-842 Cal BC (5.1 %)		

Table 3. Results of the AMS Radiocarbon dating of three olive stones (short-lived material) from the Beth-Shemesh smeltery. AMS analysis by the Institute of Particle Physics, Swiss Federal Institute of Technology, Zurich. Calibration was performed using the CalibETH program ([www.lpp.phys.ethz.ch](http://www.lpp.phys.ethz.ch))

In the 2001 season, the directors of this third expedition started work in Area E (Figure 10). This is a narrow area in the southwestern part of the site that has remained unexcavated in between a 1912 MacKenzie trench and a 1930 Grant trench. According to the records from the earlier two expeditions, large public buildings stood on either side of this area. In between these buildings, several phases of industrial and commercial activity were now revealed. In 2001, after

excavating several phases of these activities, evidence for metallurgical activity, dating to the 9<sup>th</sup> century BC (see Table 3), began to appear in square E/T48 (Figure 13).

After partial excavation of this material work was halted. The considerable quantities of 'rusty lumps', tentatively identified as (smithing) slag, and remains of iron metal artefacts prompted the directors to approach Professor Thilo Rehren and the author at the Institute of Archaeology, UCL, for consultation.


The figure is a plan of the archaeological site of Tel Beth-Shemesh. It shows various excavation areas: MacKenzie (1911-1912) in light grey, Grant (1928-1933) in dark grey, and Tel Aviv University (grey and black). A specific location for an iron workshop is indicated. The drawing is credited to S. Bunimovitz and Z. Lederman.

Figure 10. Plan of Tel Beth-Shemesh, showing the areas excavated by MacKenzie (1911-1912), Grant (1928-1933), and Tel Aviv University (grey and black), indicating the location of the iron workshop. Drawing by S. Bunimovitz and Z. Lederman.

After a meeting and assessment of some of the excavated material, it was agreed to cooperate in further excavation of the potential smithy. As a result, the author travelled to Beth-Shemesh in July 2003, and directed excavation of the metallurgical remains with a specific metallurgical approach. The results of that season and the subsequent analyses of the material are discussed in this thesis, and provide a comparison between primary (Hammeh) and secondary (Beth-Shemesh) iron production material.

## Excavating the Beth-Shemesh Smithy

Finds of metal production processes are scarce across the whole of the Near East, and especially so when looking at iron. In Israel, excavation density is among the highest of the entire region, and even there one only finds sporadic mention of evidence for iron production. No relevant archaeometric data is (yet) available from any of the rare sites where some stage of iron metallurgy is suspected. It also should be realised that production remains, if found at all, are usually excavated within the framework of a 'regular' archaeological project. Without research questions related to metallurgy as such, and unprepared for the particularities of a metal production site, much relevant information is usually not recovered.

The excavation of Tell Hammeh in 2000 (see Chapter 4) did have a specific metallurgical research aim, but even with all the specialised preparation (e.g. registration and description sheets), methods for properly excavating an iron production centre were developed and refined on the spot. Lack of previous experience with what could be encountered stratigraphically as well as some of the material that potentially can be recovered may have resulted in incomplete recording of some data. With this experience in mind, and much better versed in the range of potential metallurgical debris, excavation of the smithy at Beth-Shemesh was approached not only with specific archaeometallurgical questions, but with specific and pre-developed excavation techniques as well.



Figure 11. Possible iron billet found in square E/T49. Exact stratigraphic relation to the smithy unclear.

During the excavation, an attempt was made to see whether the presumed smithy extended further southwards into previously unexcavated terrain. The resulting square, E/T49, however, turned out to be heavily disturbed. Although the layers of metallurgical material do extend from E/T48 into E/T49, apparent

levelling of the slope of the tel in a later phase abruptly cuts off those layers about half a metre south of the baulk that separates the two squares. One interesting

find was made in E/T49, however. Slightly higher than the smithy layers, but stratigraphically very difficult to assess, a large (heavily corroded) iron bar was found, which may represent a possible billet from the smithy (shown in Figure 11). Subsequent X-Ray Radiography did not reveal any preserved metallic iron in this artefact.

## **Aim of the Metallurgical Excavation Approach**

Using a metallurgical style of excavation, the aim of the excavation of square E/T48 in 2003 was to determine the nature, lay-out, and use of space in what was assumed to be a secondary smithing workshop. With advice from the English Heritage 'Archaeometallurgy' brochure (Jones 2001) and the experiences at Hammeh as a guide, dedicated excavation techniques were developed to excavate the smithy with identification of the process and reconstruction of the lay-out and use of space in mind, and to recover as much metallurgical information as possible from the remains.

## **The Metallurgical Excavation Techniques**

The techniques applied at Beth-Shemesh were tested, refined, and adapted in the field. Before actual digging work started, a grid system of 25 x 25 cm was devised and laid out over square E/T48 (see Figure 13). The southern half of E/T48 was least excavated in the 2001 season, and the surface here was first examined. This was done by dragging a magnet over each of the 25 x 25 cm mini-squares of this grid to retrieve all magnetic material (Figure 12).

In the northern part of E/T48, which was more extensively excavated in 2001, the grids were bundled and studied as 50 x 50 cm areas. The northern part of E/T49, which is stratigraphically connected to the smithy in E/T48, was also scanned for magnetic material in 50 x 50 cm units, but revealed only minor quantities of magnetic material.

The magnets were held inside small sealable sample bags, to facilitate removal of the magnetic material being collected. Lifting the magnet within the bag creates sufficient distance between the magnetic field and the material collected on the outside, so the latter drops down into a receptacle. At Beth-Shemesh, Styrofoam bowls were used to collect the material, which was then transferred to plastic sample bags. These bags were labelled with the regular excavation data: area, square, locus, bucket, date and name, followed by the metallurgical grid data: grid number and unit. Here, grid indicates the horizontal location, e.g. H15, and



unit refers to the arbitrary vertical spits of 5 cm that were subsequently excavated. The term *unit* was used rather than *spits*, to avoid confusion with the terminology of the common excavation technique of ‘digging in spits’ and also to reflect the different scale at which this digging took place.



Figure 12. Meitar Lederman dragging a magnet above the surface of a grid in E/T48 to recover hammerscale.

For the surface scanning, it was decided that an arbitrary two minutes per grid should suffice, especially since the surface could be presumed to be quite contaminated or at least disturbed after two years of exposure to the elements. It was found that retrieval of magnetic material decreased significantly after a minute and a half. To a certain extent, the work on the surface was used to build up necessary experience on which to base the subsequent magnet work in freshly excavated layers. When actual excavation of the grid started, in units of (at first) 5 cm, the soil from each grid was put in a separate bucket with a separate label. The contents of each bucket were then spread out on a large plastic sheet. A magnet was subsequently dragged just over or lightly touching the soil for a minute and a half. The soil was then jumbled up by hand, and a second round of dragging, again for a minute and a half, was performed.

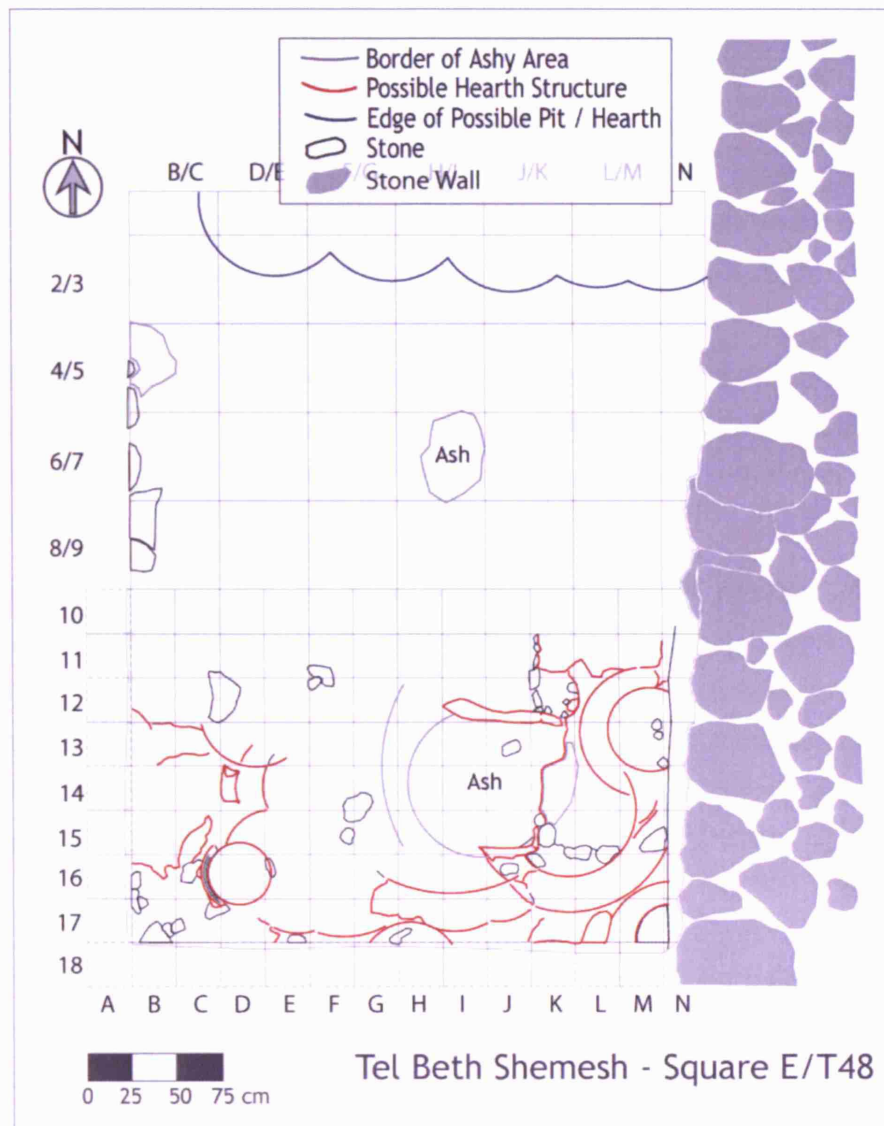


Figure 13. Plan of square E/T48, showing the grid system in light blue, various partial potential hearth structures in dark red, stone wall in grey and concentrations of ash bordered within grey. The blue border in the north of the square indicates a row of pits, or potentially a sequence of hearth structures that was excavated in the 2001 season.

Several times, tests were performed to see if additional or continued dragging would recover more magnetic material. This turned out not to be the case, proving the two times 1.5 minutes approach very efficient. The aim of the grid based magnet work was to create a very detailed mapping of the distribution of magnetic material such as hammerscale and hammer spheres (slag prills) that are commonly associated with secondary smithing work. Mapping their distribution allows interpretation of the use of space within the presumed smithy, and potentially the identification of the hearth location(s) or the position of an anvil. Processing, geophysical mapping, and interpretation of the hammerscale are discussed in Chapter 9.

During excavation of the second unit, several features started to appear (see). The archaeological necessity of recording the stratigraphy, led to the abandonment of the strict 5 cm depth of the units, and it was decided to excavate unit 2 to a depth of 10 cm, and to leave the features intact until future excavation. No metallurgical function can be assigned to these features, as they show no vitrification or other possible indicators for their use. Several of them, nevertheless, contain quantities of ash. Further possible indicators for a relation to metallurgy are that all features do contain hammerscale, and the fact that two ridges (in I12-J12, and in J15, see Figure 13) appear to contain a large ash lens between them. This last factor, although speculative, might indicate a possible hearth location.

The relation between the different features themselves remains difficult to interpret as well. It is not clear whether these round features were dug into a floor of the smithy, or are actually structures, built upon such a floor. It seems clear that most features/structures do form a sequence, as they clearly intersect each other, but it could not be resolved in what order this sequence developed, or whether any of the features co-existed at the same time.

## **The Metallurgical Assemblage at Beth-Shemesh**

A first factor helping the determination of the nature of the Beth-Shemesh activity is the assemblage of metallurgical remains. At Beth-Shemesh, the assemblage is quite different from the varied one encountered at Tell Hammeh (see chapter 4). Most significantly, there is only one type of slag present, with a typical concavo-convex 'cake' shape. This type of slag is also often referred to as a PCB (plano-convex bottom, a term that does not imply process origin, but rather a shape) or SHB (smithing hearth bottom, where process origin is assumed, but shape left open). At Beth-Shemesh, the presumption that we were dealing with a smithy, which was strongly supported by the experiences in the field, led us to use the term SHB.

A second group of finds consists of tuyères. Very interestingly, the Beth-Shemesh tuyères are virtually identical to the Tell Hammeh tuyères in all macroscopic aspects, from size, colour, feel, and temper to the most important: shape. Far less abundant here than at Hammeh, the Beth-Shemesh tuyères are also all square and measure approximately 5 x 5 cm in section, with a bore of approximately 10 mm in diameter. All tuyères are fractured a few centimetres behind their vitrified nozzle, and no rear ends are preserved. Therefore, neither an estimate of their

potential original length can be made, nor can it be determined whether any tapering of the shape from one end to the other may have been present. The remaining finds consist of a few fragments of molten/vitrified hearth material (but not *in-situ*), a range of possible hearth structures (see Figure 13), several iron and a few copper (alloy) artefacts, and the aforementioned hammerscale recovered by the magnet dragging methods.

## Summary

The excavation of square E/T48 started with the assumption that we were working on the remains of a workshop producing iron artefacts from previously smelted metal for consumption at Beth-Shemesh, i.e. a secondary smithing operation. The approach to excavation of E/T48, therefore, was to ensure that if this interpretation would be challenged by the excavation results or subsequent laboratory analysis, a reassessment would be possible. Besides its function in recording the distribution of magnetic material, the subdivision of the square into a 25 x 25 cm grid aimed to allow this.

The nature of the metallurgical assemblage as well as the finds made during excavation rather strengthen the interpretation of E/T48 as a smithy. This is indicated by the presence of large quantities of hammerscale, the absence of a variation in slag types, and the presence of a potential hearth (see chapter 9). Several other factors came to light during the excavation. As will be discussed in chapter 9, the striking resemblance of the Beth-Shemesh and Hammeh tuyères prompted comparative petrographic analysis of the clay used in their construction. This analysis is currently being finalised by Yuval Goren at Tel Aviv University, who reports that both sets of tuyères are made from the same clay. He further suggests that this very likely to be the clay local to Hammeh as it is very different from any of the clays that can be found near Beth-Shemesh (Yuval Goren, personal communication). This idea poses wide ranging questions with regard to who is doing the smelting and smithing, possible cultural, social, and economic relations between the two operations, as well as possibly issues of technological choice in the design of the tuyères.

The fact that a few copper (alloy) objects (all arrow heads) were found in close contact with the production remains that are strictly related to iron raises an interesting but highly speculative question: were the smiths at Beth-Shemesh copying previously existing shapes in a new metal? It is at least very likely that repair work on more than one metal was being performed in the same workshop

where iron objects were being forged. In comparison to Tell Hammeh, the operations at Beth-Shemesh are distinctly smaller. The smithy seems to confine itself to square E/T48 and its immediate surroundings, and contain a (relatively) limited number of slags. This seems to indicate a workshop dedicated to the production (and perhaps repair) of iron artefacts for local consumption, rather than a regional supply centre.

## CHAPTER 6: ANALYTICAL METHODS AND METHODOLOGY

### Introduction

The initial study of iron production involves the description and interpretation of the remains from an archaeological perspective. This obviously starts with excavation, and then macroscopic description of both the site and the material. It ranges from topics such as dating and establishing distribution patterns, to examining the socio-economic context of the production both on the site and within the wider region. The archaeological perspective further aims to define the meaning of the material in the larger historical picture of the development of technology.

Another area of study concerns the extraction of technological information and reconstruction of the production process from a metallurgical perspective. This begins with the selection of relevant samples, and these are subsequently studied using several techniques that range from macroscopical analysis of the material, to chemical (bulk and phase) and mineralogical analyses. The analytical techniques used in the course of this thesis are described in this chapter.

It is important that the archaeological and metallurgical areas of study both complement and overlap each other in several areas of research. Results from one area inform and feed the other, and an answer found in one can lead to a new question in the other. To put it in stronger wording, both areas of study are largely interdependent and should not occur separately, i.e. the two should be considered as one. It is this desirable merger between ‘the field’ and ‘the lab’ that is generally referred to with the terms *archaeometallurgy* and *archaeometry*.

This chapter describes the analytical techniques as performed in the Wolfson Archaeological Science Laboratories at the Institute of Archaeology, UCL. For most of the techniques described here, alternative methods do exist. Which method or technique is chosen depends on three factors. The first is access to equipment and consumables. Any researcher is limited by the availability of analytical equipment, either in one’s own laboratory or through (commercial) contacts. The second is suitability of a choice in the light of the research questions. The third factor is the wish to make resulting data fit in with existing and current work elsewhere, in order to make it easily comparable. The same three factors apply to the choices of sample preparation and presentation of results.

## Sample Selection and Preparation

Sample selection and preparation have a profound influence on the precision and accuracy of subsequent analyses. Therefore, sampling and preparation procedures are discussed as a separate subject here. Where necessary, additional specifics are discussed under the relevant techniques.

### Sample Selection

During the excavation of both Tell Hammeh and Tel Beth-Shemesh, all material that was considered to be related to metallurgy was kept. The Hammeh material, with its wide variety of materials (different slag types, tuyères, charcoal, discarded ore) and large quantities, was later studied and described in detail in the Deir 'Alla dighouse. Based on macroscopic classification and information gained by initial analyses at the Archaeometry Laboratory of Yarmouk University, Jordan, samples were selected from this material (see also chapter 4). A minimum of five specimens was taken from each group and subgroup that was assumed to be represented in the material at that time (Table 1, page 91 and discussion in chapter 8: Table 19, page 167 and Table 20, page 169), and this selection was sent to the Institute of Archaeology, UCL for subsequent research. The selection procedure followed a basic form of 'adaptive sampling' (Orton 2000, 16; 34), where the samples were taken in equal quantities for each assumed artefact (sub)type. This allocates each type equal importance within the total assemblage, regardless of actual quantity differences between (sub)types, allowing for modifications to the sampling after more data is obtained. These relative quantities between (sub)types were recorded separately. Because of the large total amount of material as well as the lack of weighing equipment, they were established by visual quantification, i.e. the author estimated the proportion of each (sub) group within the total assemblage.

The Beth-Shemesh slag consists of only a single type, whilst the total quantities of all materials (slag, hammerscale, and tuyères) from that excavation are lower than at Tell Hammeh. The Beth-Shemesh material (with the exception of the tuyères) was therefore shipped to the Institute of Archaeology, UCL, in its entirety. Five specimens were taken from the collection of slag, as these macroscopically constitute a single group, and prepared and examined like all other samples. The second important group of material recovered from Beth-Shemesh is the magnetic debris recovered from the excavated soil and collected in separate bags for each grid and unit (see chapter 5). These batches of material consist of predominantly

hammerscale and low amounts of slag prills. This material was treated and studied as described in chapter 5 and chapter 9, but was not subjected to further microscopic or chemical analyses.

## **Sample Preparation**

### ***Introduction***

It has been attempted to prepare and analyse each sample ‘as found’, i.e. without drastically changing the state in which the sample was excavated through manual or chemical cleaning. Adhering material that was considered to be (post-depositional) ‘dirt’ was removed using a dry brush, sometimes combined with mild washing with water, and where necessary by using an ultrasonic bath (with the sample submerged in alcohol). Whenever adhering or embedded material seemed to stem from the formation stage of the artefact, it was left in place where possible. This is done to try and preserve potential information contained in, for example, corrosion products. An exception to this rule is the preparation of samples for XRF analysis (see below), where, for example, the aforementioned corrosion products may severely distort the analysis.

The utmost care was taken to prevent contamination of samples during preparation at any stage. The careful cleaning of samples before and after each step of treatment, again using water, alcohol, or ultrasonic cleaning where appropriate, is an important factor in this prevention of sample contamination. Another important factor involves strict control over laboratory conditions during, and storage conditions after, preparation of the samples. Monitoring these conditions aims to minimise transfers of materials between samples, or contamination by airborne materials such as lab dust or debris from other preparation tools in the vicinity. As a result, procedures, location of equipment, and use of materials are adjusted where necessary. As with the analytical techniques themselves, there is generally more than one option of preparation available for each analysis. Which choices were made and why is given with the description of the related analytical technique.

### ***Cutting***

The samples were cut using a tile cutter with a diamond-coated abrasive blade. The location of the cut was determined per sample, and aimed at revealing as many internal area(s) of a sample as possible. Cutting sought to create a surface that includes everything from the centre to the outer regions of a sample, and



where applicable contains features like 'skin', tapping bands, flow strings, or embedded materials.

### **Mounting**

When cut, the samples were mounted in epoxy resin (a thermosetting polymer, characterised by low shrinkage, good adhesion, mechanical strength and chemical stability), using 30 mm diameter casting cups. A (laser-printed) label showing site name, sample number, initials, and year of preparation was mounted with the samples. Samples with more than minimal porosity on the to-be-polished surface were "surface-filled". As the term implies, this involves adding fresh epoxy resin to the surface. Filling of the porosity takes place by replacing any air inside the sample using a vacuum chamber. However, the resin has a tendency to 'boil', thus increasing thermosetting when under vacuum. A procedure with short repetitions of vacuum therefore is best. The chamber is pumped to vacuum for approximately 3 minutes, and then air is let back in. This lets the resin cool, lose its foaminess, and revert to a clear liquid. The pumping to vacuum is repeated five or six times, until no or very little air is seen to escape from the sample.

After hardening, a hole was drilled in each block, adjacent to the sample. The hole allows for insertion of a reference standard when, for example, using the SEM. Additionally, the bottom of the sample block was cut off, level to the surface, to create a uniform height of approximately 1 cm for all samples. This last feature facilitates the use of samples in (electron) microscopy, as it eliminates the need for extensive refocusing. It also provides a relatively level sample surface that is easier to examine in optical microscopy.

### **Grinding and Polishing**

The surface of the mounted samples was subsequently ground, using sandpapers of progressively finer grit, starting at P120 (grit particle size 127  $\mu\text{m}$ ), then progressing through P320 (46.2  $\mu\text{m}$ ), P600 (25.8  $\mu\text{m}$ ), and occasionally P1200 (15.3  $\mu\text{m}$ ). Experience showed that skipping the first, coarser, stage(s), i.e. P120 and P320, reduced the presence of scratches at completion considerably. Which grade to start with, what pressure to apply, and how long to maintain each grinding step, will differ from material to material, and even from sample to sample. Balancing these factors to create an even surface is very much a matter of judgement, motor skills, and experience. The same factors apply in the next step, polishing.

After grinding, samples should have a straight surface without any angled planes, and should be devoid of (large) scratches. Like grinding, the finer surface treatment of polishing goes in steps of progressively finer grades of diamond pastes, which are applied to polishing cloths. For each new step, a different cloth is used and samples are carefully cleaned to prevent transfer of coarse material from one grade to the next. Again, personal preference and experience dictate the exact procedure followed, e.g. hand polishing on rotating plates can be replaced by machine polishing at various stages. Using machine polishing allows up to three samples to be polished simultaneously, at a fixed pressure setting. Generic procedures have been developed in the lab for different materials for each step. These serve as guidelines to get optimal polishing results, and are constantly fine-tuned. The automatic polishing machine used is a Struers Labopol-5, with a LaboForce-3 head.

Polishing is performed using diamond pastes, starting at particle size 30  $\mu\text{m}$ , and progresses through 6  $\mu\text{m}$ , 3  $\mu\text{m}$ , to finally 1  $\mu\text{m}$ . If required, samples can be polished down to  $\frac{1}{4}$   $\mu\text{m}$ . Comparison with the grit size of the P600 grinding papers shows that the 30  $\mu\text{m}$  paste is slightly coarser, thus seemingly forming a step backwards. Nevertheless, the P600 (and P1200) paper, which helps to reduce scratches, still leaves a less smooth surface than the coarser 30  $\mu\text{m}$  diamond paste and water-based lubricant. This is possibly due to the mechanical differences between grinding on paper and polishing with a paste.

In between each polishing stage, samples were cleaned using alcohol in an ultrasonic bath, and dried in hot air. After completion, the samples were stored in a dry and dust-free environment such as a cabinet with silica-gel, to prevent oxidation and other contamination of the surface. The polished surface does have a 'shelf-life', and may require occasional repolishing.

### ***Milling***

In preparation for XRF and XRD analyses, a second piece of a sample was cut off, preferably adjacent to the cut from the part that was mounted in resin. The piece should ideally weigh around 10 grams minimum, to allow for loss of material through drying and transfer between equipment, thus ascertaining the availability of 8 grams for the production of pellets for XRF (see below). Since the aim of the XRF and XRD analyses is a precise characterisation of the material, any embedded or adhering material is now removed entirely. A fast rotating metal brush was tried first, but manually 'skinning' the sample on the tile-cutting blade proved to be the

most efficient and fastest method to achieve this. It should be noted that with rusty pieces of slag, severe cleaning of the surface proved useless, as often the interiors were found to be rather identical in make-up. Brief application of a hard hand brush was found to be sufficient here.

After removal of the adhering material, the samples were crushed by hammering a metal piston encased in a metal cylinder onto the sample. The resulting fragments were then milled to a grain size of approximately 50  $\mu\text{m}$ , using a tungsten carbide swing mill (a Fritsch 'Pulverisette 7' planetary micro mill) with counterweight. Two set-ups were used in the preparation of samples for this thesis, one using a steel vial and the second using a tungsten carbide vial. Both set-ups use tungsten carbide balls. Tests show that when using the tungsten carbide vial to mill, some contamination of the powdered sample does occur, i.e. 20-40 parts per million (ppm) of tungsten oxide ( $\text{WO}_3$ ), as well as a slight enrichment in cobalt (Co). When using the stainless-steel vial, there is no discernible  $\text{WO}_3$  contamination, but still a slight rise in Co (Mike Charlton, personal communication). In either case, measurements for  $\text{WO}_3$  are routinely ignored, and Co is not used because of the analytical difficulties with this element in ED-XRF.

### ***Pelletising***

The milled powder is dried for a minimum of 16 hours at 105 °C to remove moisture. For measurement by XRF (see below), 8 grams of powder were then mixed with 0.9 gram of industrial wax. The wax is carefully and intensively stirred through the powder, and provides a binder for the subsequent pressing. As the wax tends to form small lumps, great care should be applied to the mixing. The more homogeneous the final mix of powder and wax, the more accurate the measurements will be (see chapter 7). The mixture is then heaped into a 32 mm diameter aluminium holder. This aluminium backing provides extra durability, a writable surface, and protection from contamination through handling, as well as easing the pressing procedure. The holder and sample are placed inside a circular holder with piston; these are placed inside the pelletiser. All is then pressed into a homogeneous pellet using 15 tonnes of pressure for 2.5 minutes.

### **Macroscopic analysis**

Most external characteristics of the untreated samples were recorded and described. This description was based on the methodologies set out by Bachmann (Bachmann 1982) and Sperl (Sperl 1980), and covers features such as size, shape,

weight, flow pattern and (if recognisable) its direction, layering, crystallinity, and fabric. Colour, shine, porosity, as well as inclusions and corrosion products, and general state of corrosion were recorded from both the surface and a fresh break (where applicable). Density was determined by submersion of entire samples in water, and measuring the volume of displaced water in relation to the weight of the sample in air. The presence and strength of magnetism was checked using a hand magnet. This was done preferably by moving the magnet upwards towards a suspended sample, so one does not confuse the weight of the magnet itself with the magnetic attraction. This way, a more than sufficient accuracy is achieved (Joosten 2004, 34).

## **Mineralogical Analysis**

### **Optical Microscopy**

The mounted and polished samples were studied using optical microscopy in order to determine mineralogical composition, degree of homogeneity, shapes and sizes of crystals, as well as any possible features revealing characteristics of the production process or formation history of the material. Since many constituents of slag and ore are opaque, only a metallurgical microscope with reflected polarised light was used. In optical microscopy, different phases have a characteristic opacity and reflectivity, resulting in different (faint) colour shades and overall brightness or darkness when viewed in reflected light.

Because of this generally opaque nature of many slag components, it was decided not to prepare thin sections for study by petrographic microscope. This would involve the use of linear polarised (transmitted) light, and analyses the state of polarisation after interaction with the sample. Using thin sections would also have meant an extra preparation stage for all samples, and creating special adapters to enable use of the thin sections in the electron microscopes.

### **X-Ray Diffraction (XRD)**

X-Ray Diffraction is primarily a qualitative method, used to identify mineral phases that cannot be defined microscopically, by determining the nature of crystalline components and structures. A small quantity of milled sample is dried for 16 hours at 105 °C, and subsequently spread out over a glass stage. The stage and its holder are inserted in the diffractometer, and the sample is irradiated by X-Rays.

The X-Ray tube rotates around the sample over the course of several hours, on a circular path spanning 180 degrees. The diffracted X-Ray intensities are recorded and plotted against the diffraction angle (or reflected angle) multiplied by two. The plotted pattern of peaks is compared to the distances between diffraction planes of the atoms within the crystals.

According to the mathematical calculation called *Bragg's Law* ( $n \lambda = 2d \sin \theta$ ; Figure 14), this distance (expressed as  $d$ ) is fixed and characteristic for each crystal, just like the wavelength (expressed as  $\lambda$ ) of an incident X-Ray is fixed, resulting in a unique X-Ray diffraction pattern for each phase. This means that each mineral phase present can be identified by its pattern.

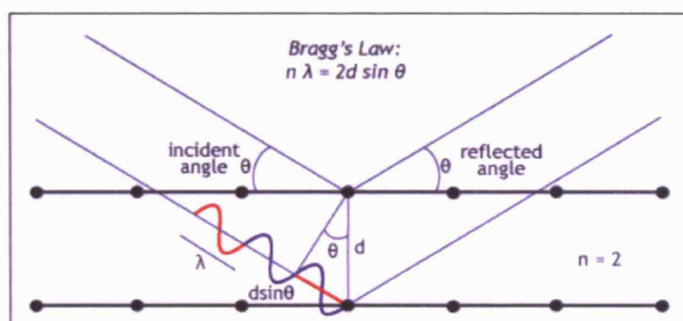


Figure 14. Shows the principle of Bragg's Law, where incident beam angle equals the diffracted beam angle. Image after MATTER (MATTER 2000)

As each plotted peak has to be matched with a corresponding known atom-distance pattern, the presence of a large number of peaks can make this process quite cumbersome.

Most modern machines have software attached that facilitate this search

by providing a searchable database (see below), but this database is not (yet) present in the machine used for this study.

XRD was used to characterise the ore samples from Mugharet al Warda and the slag samples from Tell Hammeh. The XRD machine used is a Siemens D5000, and is located at the Department of Chemistry, UCL. With the ore samples, results were limited. Due to incompatibility of the X-Ray tube with the nature of the analysed samples, analysis over an extended time period gave only a faint pattern of peaks above a massive background. Still, this did allow determination of at least the main composite minerals in the ore. The Hammeh slag samples, however, consistently produced no readings. This must be due to the particularly glassy nature of the material. As the slag proved too non-crystalline to produce any readable peaks, further XRD analysis was abandoned.

One ore sample was later examined again using Synchrotron Radiation XRD (SR-XRD) at the Daresbury Synchrotron Radiation Source (SRS), by Dr Manolis Pantos. In SR-XRD, the tube is not rotated over the sample in an arc, but the beam is

directed at the sample at a fixed angle. Depending on the results, repeat analyses at differing angles can be performed to clarify or confirm the measured pattern. The Warda ore sample was measured twice. A primary measurement was performed with the tube at a 0 degree angle, and a second confirmation analysis was performed at a 90 degree angle. Both these measurements lasted for 60 seconds. Both measurements with the SR-XRD clearly identified the dominant mineral of the ore. Identification of the possible presence of other mineral phases (by matching their pattern against a mineral database) is currently being carried out (see also chapter 8).

### **Back Scatter Electron Imaging (BSE)**

Scanning Electron Microscopy (SEM, see below) can provide imaging in different ways. This is done by scanning the surface of a sample with a focussed probe beam (a beam of high energy electrons, typically 10 - 20 kV (kilo Volt) in energy) to obtain spatial localisation. Electrons of varying energies are emitted from the surface in the region where the beam is incident. These electrons include backscattered primary electrons and Auger electrons, but the vast majority will be secondary electrons. It can create a direct image of the topographical nature of the surface of a sample from all the emitted secondary electrons (called Secondary Electron Imaging (SEI)). A detector records the secondary electron current; this current is 'plotted' against the probe position on the surface, producing a topographic image of the sample surface. The contrast of secondary electron images depends mainly on the topography of the sample surface. With polished sample surfaces, therefore, this is not an ideal imaging method.

Another way to create an image is through Back Scatter Electron imaging (BSE). After incident electrons are scattered within the specimen some of them are backscattered while keeping a relatively high energy and are emitted again from the specimen surface. These electrons are called backscattered electrons. The contrast of the backscattered electron image depends less on the topography of the specimen surface and mostly on the mean atomic number of the substances that constitute the specimen, providing a compositional image.

A large part of the imaging work on the samples in this thesis was performed on the Philips XL 30 ESEM. The quality of the BSE imaging on the ESEM proved equal to that obtained through optical microscopy. Since this allowed for simultaneous spot chemical analysis (see below) and imaging of the phases observed, this method was generally preferred. The same mounted and polished samples that

were used in optical microscopy were studied using the ESEM, after they were coated with a thin layer of carbon, using an Edwards Auto 306 carbon coater. The carbon coating improves conductivity and thereby prevents charging of the sample by the incident electron beam.

## Chemical analysis

### X-Ray Fluorescence Spectrometry (XRF)

Quantitative bulk chemical analysis of the samples was performed by (Polarising) Energy Dispersive X-Ray Fluorescence Spectrometry ((P)ED-XRF) on homogeneous pellets. In order to gain accurate results from the iron-rich samples from Hammeh and Beth-Shemesh, a specific mathematical procedure for calibration (called a 'method') was developed on the Institute of Archaeology's Spectro X-Lab Pro 2000 machine. Development and application of this method, as well as the principles of XRF and (P)ED-XRF, and additional details about sample preparation for XRF are discussed in chapter 7.

Certified Reference Materials were run alongside the analysed samples, to monitor the quality of the results. The accuracy of results (i.e. the degree of conformity of a measured or calculated value to its actual or specified value) in XRF (using the 'slag\_fun' calibration method, see chapter 7) is better than 5 percent relative for major elements and traces, as seen in the repeated measurement of standards BHVO-2 (volcanic basalt) and BCS-381 (industrial slag). The number of samples under study here does not allow a full and statistically proper estimate of the precision (i.e. reproducibility of the calibrated values by the same technique), but all measurements are very consistent, and never vary more than a few percent relative for major elements and traces. Which elements are considered accurate and why, is discussed in detail with the development of the 'slag\_fun' calibration method in chapter 7. All measured values for the two standards are presented in Appendix 1, together with the full chemical analyses of all samples discussed in this thesis.

### Scanning Electron Microscope- Energy Dispersive Spectrometry (SEM-EDS)

Analysis of matrix and phase composition of the mounted and carbon-coated samples was executed using a Scanning Electron Microscope (SEM). The model used for this thesis is a Philips XL 30 ESEM (Environmental Scanning Electron Microscope) with Energy Dispersive Spectrometry (EDS) and Wavelength Dispersive



Spectrometry (WDS) capability. For the study of the Hammeh and Beth-Shemesh metallurgical samples, the ESEM is used as a 'conventional' SEM (Scanning Electron Microscope) at a high vacuum. The attainable spatial and analytical resolution of the technique is limited by the minimum spot size that can be obtained with the incident electron beam, and ultimately by the scattering of this beam as it interacts with the substrate. Depending on the material analysed and the kV setting, a resolution of  $\sim 1 - 5 \mu\text{m}$  is achievable, as well as an imaging resolution as fine as or better than 5 nm. This is more than adequate for most archaeometallurgical studies.

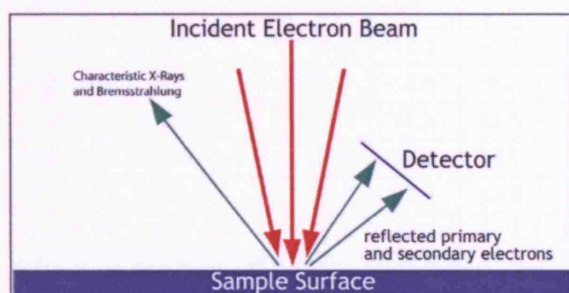


Figure 15. Schematic view of the incident electron beam and reflected primary and secondary electrons in a Scanning Electron Microscope (SEM).

When electrons interact with a sample surface, characteristic X-Rays are produced, which are directly related to the chemical composition of the material. Using the attached ED or WD spectrometers, the elemental composition of materials can be obtained. A relative accuracy of  $\sim 1 \%$  can be obtained using WDS,

whilst slightly lower precision and accuracy (1-10 % relative) may be obtained through EDS. All chemical characterisation of matrix and phases present in the Hammeh and Beth-Shemesh material was performed using SEM-EDS, as its precision and accuracy are sufficient for this purpose. Furthermore, the better precision of WDS has to be set off against the disadvantage that a single WDS measurement lasts up to more than one hour, as only a single spectrometer is available at this instrument.

Performance of the SEM-EDS was monitored by repeated calibration against a standard of pure cobalt at set intervals before and between measurements. The accuracy of the results was further monitored by occasional and repeated measurement of three Certified Reference Materials (CRMs). Parallel to the Hammeh and Beth-Shemesh slag, three basalt CRMs from the United States Geological Survey (USGS), in the form of homogenised glass, were used: BHVO-2 (Hawaiian Volcanic Observatory basalt; this standard in pelletised form was also used in the (P)ED-XRF calibrations), BIR-1 (Icelandic basalt), and BCR-2 (Colombia River basalt). These glasses have a composition that is relatively comparable to that of iron production slag, containing a similar array and content of chemical components. Comparison of the repeated measurements of these glasses with



their known values shows that both accuracy and precision lies below 10 percent relative (Table 4).

Glass Standards by SEM-EDS	SiO <sub>2</sub>	Al <sub>2</sub> O <sub>3</sub>	FeO	TiO <sub>2</sub>	MnO	CaO	MgO	Na <sub>2</sub> O	K <sub>2</sub> O	P <sub>2</sub> O <sub>5</sub>
<b>BIR-1</b>										
January 15, 2004	50.2	14.1	11.2	0.9	n.d.	13.4	8.7	1.6	n.d.	n.d.
February 2, 2004	49.5	13.6	11.4	1.0	n.d.	13.8	9.2	1.5	n.d.	n.d.
February 10, 2004	48.7	14.4	11.1	1.3	n.d.	14.1	9.0	1.5	n.d.	n.d.
February 26, 2004	49.2	14.5	10.9	1.1	n.d.	13.8	8.9	1.6	n.d.	n.d.
March 15, 2005	49.1	14.7	11.1	0.9	n.d.	13.8	8.5	1.8	n.d.	n.d.
March 15, 2005	49.7	14.4	10.8	1.1	n.d.	13.7	8.9	1.4	n.d.	n.d.
Certified Values	48.0	15.5	11.3	1.0	0.2	13.3	9.7	1.8	0	0
<b>BCR-2</b>										
January 15, 2004	56.1	12.5	13.7	2.8	n.d.	7.0	3.3	2.7	1.9	n.d.
February 2, 2004	56.7	12.8	13.0	2.8	n.d.	7.3	3.1	2.7	1.7	n.d.
February 10, 2004	56.7	12.2	13.5	2.5	n.d.	7.0	3.7	2.6	1.8	n.d.
February 26, 2004	56.0	12.8	13.8	2.5	n.d.	7.1	3.2	2.8	1.8	n.d.
March 15, 2005	56.7	12.9	13.4	2.3	n.d.	7.0	3.1	2.5	2.1	n.d.
March 15, 2005	56.4	12.1	14.1	2.6	n.d.	7.5	3.5	2.1	1.8	n.d.
Certified Values	54.1	13.5	13.8	2.3	0.2	7.1	3.6	3.2	1.8	0.4
<b>BHVO-2</b>										
January 15, 2004	51.3	12.6	12.5	3.1	n.d.	11.7	6.6	1.8	0.4	n.d.
February 2, 2004	51.6	12.6	12.3	3.1	n.d.	11.2	6.6	2.1	0.5	n.d.
February 10, 2004	52.0	12.4	12.0	3.1	n.d.	11.5	6.7	1.9	0.6	n.d.
February 26, 2004	51.4	12.6	12.5	3.4	n.d.	11.2	6.7	1.7	0.5	n.d.
March 15, 2005	51.5	12.3	12.3	3.0	n.d.	12.0	6.6	1.8	0.5	n.d.
March 15, 2005	51.2	12.2	12.2	3.1	n.d.	12.2	7.0	1.8	0.4	n.d.
Certified Values	49.9	13.5	12.3	2.7	0.1	11.4	7.2	2.2	0.5	0.3

Table 4. Comparison of the measured and known values for volcanic basalts (USGS CRMs) BIR-1, BCR-2, and BHVO-2. Samples were measured at various occasions during the analysis of the Hammeh and Beth-Shemesh slags, and show a high level of consistency in the accuracy and precision of the ESEM analyses.

### Electron Probe Micro Analysis (EPMA)

In the context of the XRF method development (which is described in chapter 7), the elemental distribution within a sample was studied by Electron Probe Micro Analysis (EPMA), using a Jeol JXA 8600 Superprobe with WDS. As in SEM, a beam of high energy electrons is focussed on the surface of a sample. The resulting characteristic X-Rays are then analysed for their wavelengths. The measured intensities are then compared against a (set of) standards and converted to concentrations.

Important factors in EPMA are the very small beam diameter and a very high spatial resolution, allowing quantitative analysis of extremely small areas. In this study, EPMA was used to provide a comparative set of data from the same sample that was used during the development of the XRF method. Several areas of 300 x

300  $\mu\text{m}$  were analysed for a range of elements by WDS-EPMA, averaged and compared to the concentrations as calculated by (P)ED-XRF (see chapter 7).

## Statistical Analysis

### Principal Component Analysis (PCA)

The macroscopical, microscopical, and chemical analytical techniques described above each generate data, which are subsequently used in the characterisation and interpretation of the various materials studied in this thesis (see chapter 8 and 9). The statistical tool of Principal Component Analysis (PCA) is applied to the (chemical composition) data derived from the XRF analyses, in order to test the functional relationships between the different types of materials, e.g. ore, technical ceramics, and slags, as well as among the slags. It is furthermore used to examine the differences and similarities between the (smelting and primary smithing) slag from Tell Hammeh and the (smithing) slag from Beth-Shemesh.

PCA performs a linear transformation of a dataset. It creates a new coordinate system(s) for that dataset (in this case the chemical composition of materials) in such a way that the greatest variance by any projection of the dataset comes to lie on the first axis (called the first principal component), the second greatest variance on the second axis (called the second principal component), and so on. This means that it reduces the original dataset to a lower number of variables based on the covariance (inter-correlation) between the original values. The more closely related the original values are, the better the summary of the data in new variables will be. In other words, PCA is a technique that can be used to simplify a dataset, reducing any number of variables into fewer main variables. Through this low number of variables, the correlation between data from a multi-dimensional dataset can be displayed in a series of two-dimensional views. The mathematics involved in PCA are too complex to discuss here, but a concise explanation of the method and its application in archaeology can be found in Stephen Shennan (Shennan 1997, 265-305).

This simplification of a dataset and the subsequent plotting of a two-dimensional graph can be useful in the study of slag, as it will show clusters that relate to correlation within the original dataset. For example, in a PCA graph that plots the correlation of chemical compositions of slags, samples that are closely related to ore (and to each other), will form a cluster near the loading vectors (which express the magnitude of influence of the original variables on the Principal

Components) of the principal chemical components of the ore, e.g. FeO or MnO. Samples that are more closely related to technical ceramics (and to each other) will form a cluster near the vectors of the principal chemical components of those ceramics, e.g. CaO or Al<sub>2</sub>O<sub>3</sub>. Samples that have an origin in both ore and technical ceramics, e.g. tap slags, should then plot somewhere between the previous two, closer to one or the other depending on their composition. In this way, differences between various slag groups such as tap slags, furnace slags, or secondary smithing slags should become visible. The statistical tool of PCA is applied in chapter 8 and chapter 9, to test and explore the identification of slag types that is based on the analytical techniques described above.

## CHAPTER 7: DEVELOPMENT OF 'SLAG\_FUN', AN ANALYTICAL (P)ED-XRF METHOD FOR IRON-RICH MATERIALS

### Introduction

The first step in the scientific study of slag often is bulk chemical analysis. After the slags have been described, tentatively interpreted, and allocated to various parts of a production process, according to their external appearance, the information of its bulk composition is the first tool to confirm or deny these interpretations (Kronz 1998; Bachmann 1982, 8; Sperl 1980, 63). Identical looking slags may have very different chemical compositions, possibly indicating different origins or processes. A good example is the difference between copper and iron smelting slag, which can often only be determined by measuring the minute copper content of the slag. Other chemical elements or ratios between elements can help to determine the nature of the production process. For example, the ratio between iron and lime can indicate whether a slag derives from a bloomery or a blast furnace, or may indicate the accidental or purposeful use of fluxes (Morton and Wingrove 1972; Morton and Wingrove 1969).

Bulk chemical analysis is also necessary to assist the interpretation of microscopic examination of mineral phases within samples, and can be used to assess the need for, and nature of, further scientific analysis (Kronz 1998, 44-59). Different techniques exist to perform bulk chemical analysis. Only the one in use at the Institute of Archaeology, UCL: X-Ray Fluorescence Spectrometry (XRF) is discussed in this chapter.

### X-Ray Fluorescence Spectrometry (ED-XRF and WD-XRF)

A very commonly used technique of bulk chemical analysis is X-Ray Fluorescence Spectrometry, of which there are two kinds: energy dispersive (ED-XRF) and wavelength dispersive (WD-XRF). The main difference between EDS and WDS occurs at the last stage of energy determination. WDS identifies the wavelengths of the X-Rays emitted from the sample by diffraction on specific crystals, which results in a much higher spectral resolution and better peak to background ratio, and therefore lower detection limits than EDS. The enhanced resolution of the sequential energy lines by WDS, as opposed to measuring the entire spectrum in parallel as in EDS, avoids difficulties associated with overlapping element peaks (van Grieken and Markowicz 2002, 100-104). A disadvantage associated with the

higher resolution of WDS is the very long time it takes to perform a measurement. A single WDS measurement can last up to several hours, whereas an EDS measurement takes place in 10 to 20 minutes. The exact amount of time depends on the particular settings of the applied calibration procedure, i.e. the number of targets and the measuring time for each target (see pages 129 and 131).

Both XRF techniques can reach detection limits of a few tens of parts per million (ppm), depending on the nature and preparation of the sample, as well as the particulars of the XRF instrument used. Each requires the measurement of standards of known composition, against which the results of an unknown sample are compared. At the Institute of Archaeology, UCL, the available XRF technique is polarising ED-XRF ((P)ED-XRF), on a Spectro X-Lab Pro 2000 machine.

## **Polarising Energy Dispersive X-Ray Fluorescence ((P)ED-XRF)**

In (P)ED-XRF, an X-Ray beam is directed at the surface of the sample under study. The interaction of this beam with the sample generates secondary (fluorescent) X-Rays. Each chemical element produces characteristic secondary X-Rays with different energies. These 'dispersed' energies are detected and displayed as a spectrum, where intensity is set against energy. The resulting peaks shown in the spectrum indicate two things: the position of the peak indicates what element is present, and the peak height identifies how much of that element is present.

The primary X-Ray beam can be aimed directly at the sample, but is generally directed at a so-called 'secondary target' first. The primary beam is unpolarised, i.e. the photons are directed, but their amplitude has no preferred orientation. This causes extensive scattering effects on the sample, which in turn generates significant background noise in the detection. The primary purpose of some of the secondary targets therefore is to polarise the primary beam, so only waves with parallel amplitude orientation will hit the sample (Figure 16). In this way the peak to background ratio is considerably enhanced, bringing the detection limits of EDS closer to the level of WDS.

Some secondary targets are furthermore applied in the measurement of specific effects that occur during analysis of a sample, which measurements are used in the subsequent calibration of the raw X-Ray count (Compton targets, see Table 5; see discussion on the Molybdenum target on page 132). Other secondary targets are used because of their mirroring properties, i.e. direct reflection of the

incident beam by the surface of the target, as in a mirror (Bragg targets, see Table 5; see discussion about the HOPG target on page 133).

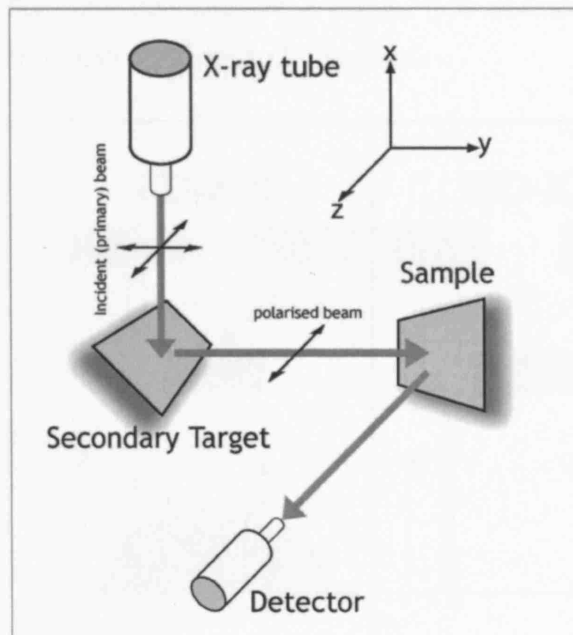


Figure 16. The principle of polarisation (P)ED-XRF, showing the orientation of secondary target and sample in relation to the beam.

A further purpose of a secondary target is to limit the range of wavelengths hitting the sample. The nature of the secondary target determines which range of wavelengths from the primary beam is directed towards the sample. The energy range of these wavelengths corresponds with a certain range of elements, which are selectively excited by the incident beam. The selection of secondary targets is thus directly related to the elements one wants to analyse for (Table 5).

ED-XRF theoretically can reach a detection limit of a few ppm, but, depending on sample matrix, trace element concentrations (i.e. those present at levels below about 1000 ppm, or 0.1 percent) are generally difficult to ascertain or judge for accuracy, since they tend to 'disappear' within the background noise (van Grieken and Markowicz 2002, 104). As described above, using secondary targets to enhance the peak to background ratio can improve detection limits significantly (Figure 11 shows schematically the effect of background reduction by (P)ED-XRF compared to ED-XRF and WD-XRF).

An advantage of the ED-XRF technique, especially for archaeologists, is the possibility of studying complete artefacts, i.e. performing a non-destructive analysis of the surface of an object. (P)ED-XRF is well suited for determination of alloy compositions of metal objects, or analysis of non-metallic materials such as ceramics and glass. A limitation of the technique is that only the surface of a sample, to a maximum depth of ca. 1 mm, is actually analysed. This may lead to confusing or misleading results if the surface differs from the bulk composition of its body, as when corroded, painted, or otherwise covered. Problems also occur when a surface is rough, striated, or heterogeneous. This can often be (partially) avoided by scraping or cleaning and polishing the surface prior to analysis or by using different means of sample preparation (see below). As the surface of an

artefact is often not of ideal quality for analysis, and may differ from the body of the artefact, performing non-destructive analysis provides only qualitative data. For fully quantitative analysis, it is necessary to prepare a homogeneous sample from the material to be studied.

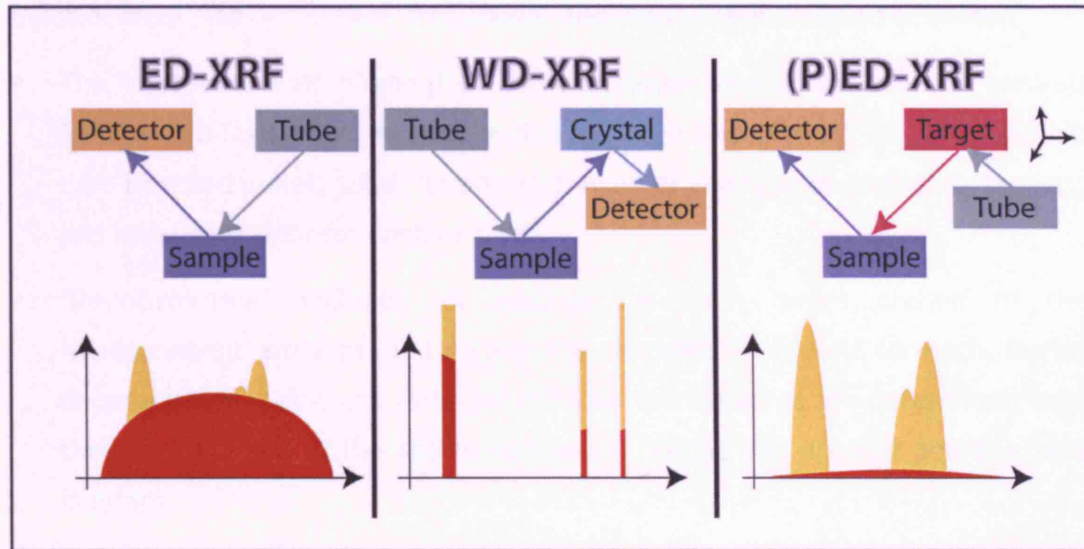


Figure 17. The effect of background noise reduction by (P)ED-XRF, compared to (standard) ED-XRF and WD-XRF (after Schramm undated b, 10, figure 7).

With slag and related materials, a destructive approach for suitable sample preparation is not an issue, and quantitative data can be obtained. To prepare a homogeneous sample, ideal for XRF analysis, (part of) a sample is crushed to a powder of homogeneous grain size, preferably around 50  $\mu\text{m}$ . From this powder, a pellet is produced by thoroughly mixing the sample with a small amount of industrial wax, which serves as a binder, and then pressing it in a pellet-press for a fixed amount of time at a certain pressure (see chapter 6). It is paramount that the utmost care is taken in preparation of the pellets, since precision and quality of sample preparation have a considerable influence on the accuracy of the XRF measurements (van Grieken and Markowicz 2002, 933-944; Buhrke *et al.* 1998).

A further advantage of the ED-XRF technique is that it provides (quantitative) results in a relatively short time. Depending on the set-up of the calibration method, i.e. the number of secondary targets selected, and the measurement time for each of those targets, almost all elements (from sodium to uranium) present in a sample can be measured and quantified within a period of 10 to 15 minutes.

## The Spectro X-Lab Pro 2000 (P)ED-XRF calibration methods

The Spectro X-Lab Pro 2000 (P)ED-XRF obtains the counts for each element from the detector and submits this data to a calibration process. The combination of measurement, deconvolution, evaluation, and data-output is called a *method*:

- The 'measurement' element of the calibration method includes all settings for the XRF instrument proper, such as voltage and current, vacuum, sample type (pressed pellet, solid, liquid, etc), number and type of secondary targets, and measuring time for each of them.
- 'Deconvolution' includes all settings for each target chosen in the 'measurement' settings, and defines the elements of interest for each. During deconvolution, net count rates for the selected elements are determined from the size and slope of the appropriate peaks, taking into account possible peak overlaps.
- 'Evaluation' includes all settings pertaining to what is generally termed calibration. This involves the selection of a calibration model such as linear, fundamental parameters etc. During evaluation, the correlation between net count rates and actual concentrations are determined. Part of the calibration model uses the differences between known and measured values of known *standards*, ideally certified reference materials (CRMs).
- 'Data-output' includes all settings that define the format in which the data is presented after analysis, such as in oxides or elements, in percentage or ppm.

Optimisation of a method for particular materials and/or elements is achieved by changing the settings of each of the first three parts of the method, until the best fit is achieved between given and found concentrations of the CRMs (Figure 18 shows the X-Lab Pro software; first the 'slag\_fun' method (see page 131) screen, showing the CRMs, in the background, then the method-editing box, the 'evaluation' settings box, and finally the fundamental parameter calibration box showing the settings for Fe).

The X-Lab Pro comes with a range of pre-set methods; each is designed for a generic group of sample types (oxides, alloys), uses three targets, and provides initial screening analyses only (Spectro Analytical Instruments undated). None of these methods, however, is specifically aimed at, or accurate with, iron-rich materials such as slag. The main reason for this inaccuracy lies in the matrix



compositions of different types of materials. Different matrices have considerable and specific effects on the analysis through differential scattering, and these so-called 'matrix effects' can only be resolved by applying specific settings for specific materials.

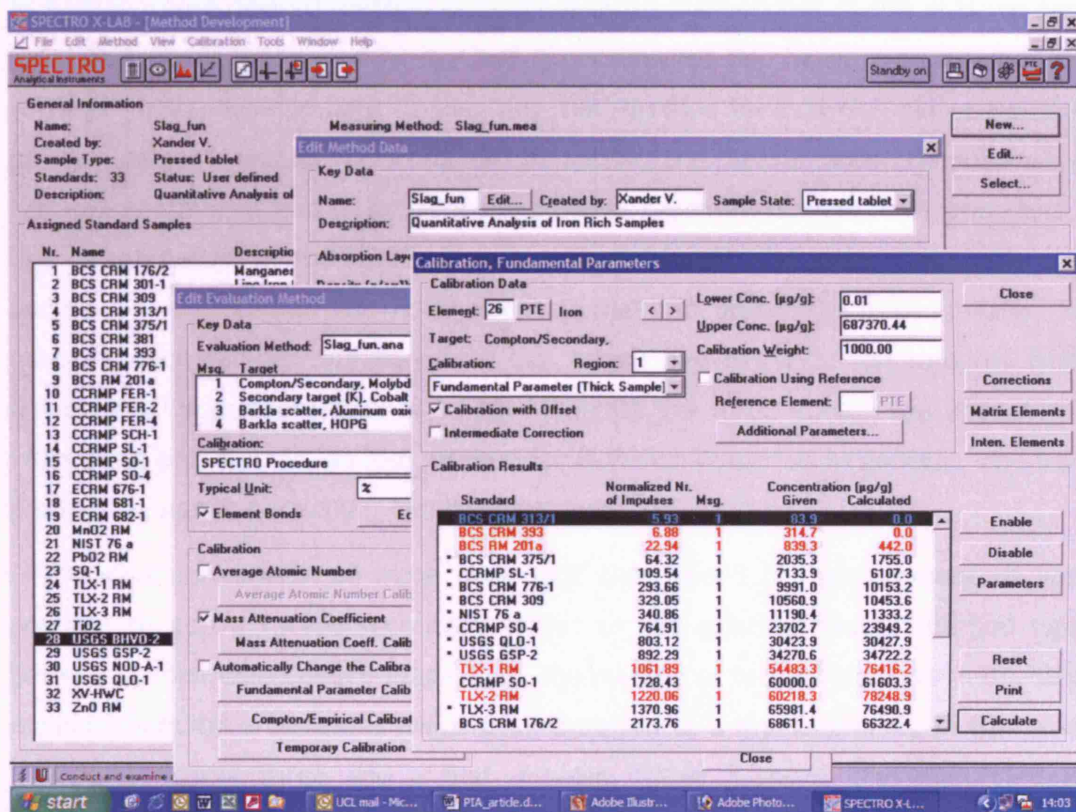


Figure 18. X-Lab Pro method development. Showing the 'Slag\_fun' development screen with the CRMs in the background. The cascading boxes show the method-editing box, the 'evaluation' settings box, and the fundamental parameter calibration box showing the settings for Fe respectively.

A particularly difficult matrix is presented by slags, where an unusually high iron content caused several problems in calibration. The pre-set Spectro calibration method called 'oxides' (which was used as the basis for the development of the 'slag\_fun' calibration method described below), aims at pelletised samples that consist mainly of element oxides, and would, therefore, be the logical choice when analysing an oxide-rich material such as slags. In samples with medium (5-15%) to high (over 20%) concentrations of iron oxide(s), however, the matrix effects of the iron tend to both swamp and absorb the counts of the lighter elements. Within the Hammeh and Beth-Shemesh material, the vast majority of samples consists of at least 40% iron oxide(s), explaining the need for a new and specific calibration method for iron-rich materials.

## Design and Development of the 'Slag\_fun' method

### Measurement Settings

Development of a new method is initiated most easily by copying an existing one, as similar to the desired method as possible. From the settings of this existing and functioning calibration, a new method is constructed by changing and/or adding settings. In the development of the 'slag\_fun' method for iron-rich materials, the pre-set 'oxides' method was used. Before setting the measurement conditions for this new method, it had to be determined what parameters were most important. Due to the nature of the research on the Hammeh material, detection limits and accuracy were deemed far more essential than the amount of time it takes to measure each sample. Furthermore, the nature and origin of the samples (slag from metal production) defines which elements are to be considered important. With these parameters, an XRF method for iron-rich materials in general, and iron production slag in particular, can be developed.

With accuracy considered more important than speed of measurement, it was possible to add a fourth secondary target to the existing 'oxide' method (see below). As mentioned above (page 126), the number of targets and their individual measurement time increases the overall duration of a measurement, in this case by approximately three and a half minutes. Table 5 shows the eight targets available in the Spectro X-Lab Pro 2000 and their corresponding measurement settings.

Target	Type of Targets	Typical Peak Time [μs]	Energy Range [KeV]	Tube Voltage [kV]	Elements (K: K-Series) (L: L-Series)	Notes
Mo	Compton/Secondary	4, 8, 13	25	35 ... 45**	K: 24-39 L: 72-92	
Pd	Compton/Secondary	4, 8, 13	25	40 ... 50**	K: 26-42 L: 72-92	Alternative Compton target
Al <sub>2</sub> O <sub>3</sub>	Polarisation (Barkla Scatter)	4, 8	50	50 ... 55**	K: 40-60 L: 90-92	
B <sub>4</sub> C	Polarisation (Barkla Scatter)	8, 13	25	38 ... 48**	K: 22-42 L: 55-92	For low Z matrix, Alternative Compton target
Co	Secondary	8, 13	12.5	30 ... 35**	K: 19-25 L: 47-62	Useful in Fe/Co-Matrix
Ti	Secondary	8, 13	12.5	25	K: 11-20 L: 37-51	
Al	Secondary	13	12.5	15	K: 9-12	Na, Mg in fused beads
HOPG	Bragg-Polarisation	8, 13	12.5	10 ... 25**	K: 9-30	The higher the tube voltage, the more Fe intensity

Table 5. X-Lab Pro targets and their tube settings. \*\* Depending on the application (based on Spectro Calibration Manual).

The column titled 'elements' shows which range of elements (see the periodic table in Figure 20) is excited by each individual target, both K lines (primary electron orbit) and/or L lines (secondary electron orbit). All pre-set Spectro methods, including 'oxides', use three targets, which Spectro considers sufficient for general screening needs: Compton/Secondary Molybdenum, Barkla Scatter Aluminium Oxide, and Barkla Scatter HOPG.

Since the aim was to develop a method for the analysis of iron-rich samples, it was decided to select a fourth target, which counters measurement problems related to medium to very high iron oxide contents. As mentioned above, the matrix effects (i.e. absorption of both the primary and emitted radiation by the elements present in addition to those of interest) of iron upon lighter elements are problematic. Within an iron-rich sample, the secondary X-Rays of elements lighter than iron are either absorbed or distorted. Therefore, Cobalt (Co) was selected as an additional target, since this secondary target specifically excites all elements up to but not including iron (van Grieken and Markowicz 2002, 627-628).

Every method should start with a (non-polarising) 'Compton' type target, which provides information about various types of radiation scattering, most importantly Compton and Rayleigh scattering. Compton scattering, also known as incoherent scattering, occurs when the incident X-Ray photon transfers part of its energy onto an electron from an atom within the sample, and an X-Ray photon is scattered from the atom in the process. The scattered X-Ray photon is of lower energy and therefore a longer wavelength than the incident photon. Compton scattering mainly occurs from low atomic number specimens.

Rayleigh scattering, also known as coherent scattering, occurs when the incident X-Ray photon interacts with the whole atom so that the photon is scattered with no change in internal energy to the scattering atom, nor to the X-Ray photon. In Rayleigh scattering, X-Ray photons of shorter wavelengths have an increased relative chance to be scattered (Figure 19).

The proportion of Compton to Rayleigh scattering therefore carries information on both the X-Ray photon energy of the beam and the atomic number of the sample. With a known beam energy, this enables determination of the average atomic number of the sample (van Grieken and Markowicz 2002, 21-26, on Compton and Rayleigh scatter: 603-610). Since the scattering is matrix dependant, the software uses the information from a 'Compton' target on scattering effects and their relations for matrix correction of the results obtained with the targets that follow.

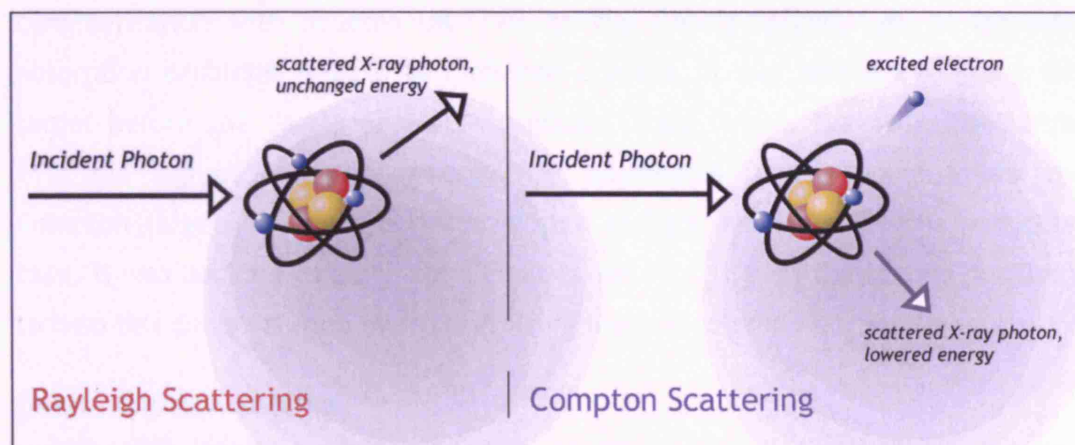


Figure 19. The principle of Rayleigh scattering (on the left) compared to Compton scattering (on the right).

In the same vein, the HOPG (i.e. Highly Ordered Pyrolytic Graphite) target should end the measurement. The high reflectivity of the surface of the HOPG target (i.e. mirroring effect) permits a very wide range of angles of the incident beam. As a result, a large range of energies is covered by this target, which assists in the deconvolution of intensities measured by the preceding targets, particularly those of lighter elements (Schramm 1998, 7-10, on HOPG targets 11-21; Schramm undated b; Schramm undated a). This target, therefore, was kept at the end and moved to position four.

1 hydrogen 1 H 1.00784(7)	2 helium 4 He 4.0026032(5)	3 lithium 7 Li 6.941(2)	4 beryllium 9 Be 9.0121831(3)	5 boron 10 B 10.811(7)	6 carbon 12 C 12.010778(1)	7 nitrogen 14 N 14.00643(4)	8 oxygen 16 O 15.999(4)	9 fluorine 18 F 18.9984032(3)	10 neon 20 Ne 20.1797(6)	11 sodium 23 Na 22.9897692(2)	12 magnesium 24 Mg 24.3050(6)	13 aluminum 27 Al 26.9815385(3)	14 silicon 28 Si 28.0855(3)	15 phosphorus 31 P 30.9737619(5)	16 sulfur 32 S 32.06(6)	17 chlorine 35 Cl 35.453(2)	18 argon 39 Ar 39.948(1)	19 potassium 39 K 39.0983(1)	20 calcium 40 Ca 40.078(4)	21 scandium 44 Sc 44.955910(9)	22 titanium 47 Ti 47.867(1)	23 vanadium 50 V 50.9415(1)	24 chromium 52 Cr 51.9961(6)	25 manganese 54 Mn 54.938045(9)	26 iron 56 Fe 55.845(2)	27 cobalt 58 Co 58.933200(9)	28 nickel 58 Ni 58.6934(2)	29 copper 63 Cu 63.546(3)	30 zinc 65 Zn 65.409(4)	31 gallium 69 Ga 69.723(1)	32 germanium 72 Ge 72.64(1)	33 arsenic 74 As 74.9216(2)	34 selenium 78 Se 78.96(3)	35 bromine 79 Br 79.904(1)	36 krypton 83 Kr 83.799(8)	37 rubidium 85 Rb 85.4678(3)	38 strontium 87 Sr 87.62(1)	39 yttrium 88 Y 88.90585(2)	40 zirconium 90 Zr 91.224(2)	41 niobium 92 Nb 92.90638(2)	42 molybdenum 94 Mo 94.941(1)	43 technetium 98 Tc 98.9062(1)	44 ruthenium 100 Ru 101.07(2)	45 rhodium 102 Rh 102.90550(2)	46 palladium 106 Pd 105.921(1)	47 silver 107 Ag 107.8682(2)	48 cadmium 112 Cd 112.411(3)	49 indium 114 In 114.818(3)	50 tin 118 Sn 118.710(7)	51 antimony 120 Sb 120.904(3)	52 tellurium 127 Te 127.603(3)	53 iodine 126 I 126.90447(3)	54 xenon 131 Xe 131.29(6)	55 cesium 132 Cs 132.90545(2)	56 barium 137 Ba 137.327(7)	57-70 * lanthanoids	71 thulium 168 Tm 168.934(2)	72 ytterbium 173 Yb 173.054(7)	73 lutetium 175 Lu 174.967(1)	74 hafnium 178 Hf 178.49(2)	75 tantalum 180 Ta 180.9479(1)	76 tungsten 183 W 183.84(1)	77 rhenium 186 Re 186.207(1)	78 osmium 190 Os 190.23(3)	79 iridium 192 Ir 192.222(3)	80 platinum 195 Pt 195.075(2)	81 gold 197 Au 196.96655(2)	82 mercury 200 Hg 200.59(2)	83 thallium 204 Tl 204.383(3)	84 lead 207 Pb 207.976(2)	85 bismuth 208 Bi 208.98039(2)	86 polonium 209 Po [209]	87 astatine 210 At [210]	88 radon 222 Rn [222]	89-102 ** actinoids	103 thorium 232 Th 232.0377(2)	104 protactinium 231 Pa 231.03688(2)	105 uranium 238 U 238.02891(3)	106 neptunium 237 Np 237.04817(3)	107 plutonium 244 Pu 244.0642(8)	108 americium 243 Am 243.06137(1)	109 curium 247 Cm 247.0763(7)	110 berkelium 247 Bk 247.06715(7)	111 californium 251 Cf 251.07887(8)	112 einsteinium 252 Es 252.083(2)	113 fermium 257 Fm 257.10(5)	114 mendelevium 258 Md 258.10(8)	115 nobelium 259 No 259.10(9)	116 lawrencium 260 Lr 260.10(10)	117 tennessine 289 Ts [289]	118 oganesson 289 Og [289]	119 bohrium 264 Bh [264]	120 hassium 265 Hs [265]	121 meitnerium 266 Mt [266]	122 darmstadtium 269 Ds [269]	123 roentgenium 272 Rg [272]	124 copernicium 285 Cn [285]	125 nihonium 286 Nh [286]	126 flerovium 289 Fl [289]	127 tennessine 291 Ts [291]	128 oganesson 294 Og [294]	129 bohrium 294 Bh [294]	130 hassium 297 Hs [297]	131 meitnerium 298 Mt [298]	132 darmstadtium 301 Ds [301]	133 roentgenium 303 Rg [303]	134 copernicium 309 Cn [309]	135 nihonium 310 Nh [310]	136 flerovium 311 Fl [311]	137 tennessine 315 Ts [315]	138 oganesson 316 Og [316]	139 bohrium 317 Bh [317]	140 hassium 318 Hs [318]	141 meitnerium 320 Mt [320]	142 darmstadtium 321 Ds [321]	143 roentgenium 324 Rg [324]	144 copernicium 325 Cn [325]	145 nihonium 326 Nh [326]	146 flerovium 327 Fl [327]	147 tennessine 329 Ts [329]	148 oganesson 331 Og [331]	149 bohrium 332 Bh [332]	150 hassium 333 Hs [333]	151 meitnerium 335 Mt [335]	152 darmstadtium 337 Ds [337]	153 roentgenium 339 Rg [339]	154 copernicium 341 Cn [341]	155 nihonium 343 Nh [343]	156 flerovium 345 Fl [345]	157 tennessine 348 Ts [348]	158 oganesson 350 Og [350]	159 bohrium 351 Bh [351]	160 hassium 353 Hs [353]	161 meitnerium 355 Mt [355]	162 darmstadtium 357 Ds [357]	163 roentgenium 359 Rg [359]	164 copernicium 361 Cn [361]	165 nihonium 363 Nh [363]	166 fler
---------------------------------------	--	-------------------------------------	---	------------------------------------	--	---	-------------------------------------	---	--------------------------------------	---	---	---	---	--	-------------------------------------	---	--------------------------------------	--	--	--	---	---	--	---	-------------------------------------	--	--	---------------------------------------	-------------------------------------	--	---	---	--	--	--	--	---	---	--	--	---	--	---	--	--	--	--	---	--------------------------------------	---	--	--	---------------------------------------	---	---	---------------------------	--	--	---	---	--	---	--	--	--	---	---	---	---	---------------------------------------	--	--------------------------------------	--------------------------------------	-----------------------------------	---------------------------	--	--	--	---	--	---	---	---	---	---	--	--	---	--	---	--	--------------------------------------	--------------------------------------	---	---	--	--	---------------------------------------	--	---	--	--------------------------------------	--------------------------------------	---	---	--	--	---------------------------------------	--	---	--	--------------------------------------	--------------------------------------	---	---	--	--	---------------------------------------	--	---	--	--------------------------------------	--------------------------------------	---	---	--	--	---------------------------------------	--	---	--	--------------------------------------	--------------------------------------	---	---	--	--	---------------------------------------	-------------

Figure 20. Periodic table of elements. Copyright Dr. Mark J. Winter; [www.webelements.com/University of Sheffield](http://www.webelements.com/University%20of%20Sheffield).

The Co target was added on the second position; a choice based on the Spectro Calibration Manual (Spectro Analytical Instruments undated) as well as personal



communication with Spectro UK. Due to the Cobalt target's use in resolving absorption problems related to high iron content, it was decided to place this target before the Barkla Scatter Aluminium Oxide target. Normally, the target with the highest excitation energy (i.e. Aluminium Oxide) should follow the Compton target, to improve deconvolution of light elements. In this particular case, it was decided to place the Cobalt target first (i.e. in the second position), to help this deconvolution by first resolving the iron related matrix effects.

### **Deconvolution Settings**

Moving the original second and third target to the third and fourth positions effectively removed their original deconvolution settings from the software. As well as defining new settings for the Cobalt target, those of the Aluminium Oxide and HOPG had to be reprogrammed. The new target, Cobalt, was programmed to measure the concentrations of elements 19 to 25, potassium to manganese (see Figure 20). The deconvolution sub-settings (settings for intensity and stripping elements, electron line to measure from, deconvolution strategy, and background, deconvolution, and normalisation regions) were set as they were for these elements in the Aluminium Oxide target. In this last target, elements 19 to 25 are now only measured for intensity, i.e. for internal use by the calibration software, but not to determine their actual concentration (an explanation of the various measurement, line, region, and strategy settings, which are related to the particular XRF machine used, is given in the Spectro Calibration Manual (Spectro Analytical Instruments undated)).

### **Evaluation Settings**

In XRF, the count rate of elements is influenced by the sample matrix. To determine and correct the relation between the measured net count rates and the given values of standard CRMs, an evaluation procedure is employed. These procedures can be divided into two basic principles. The first is an empirical calculation model. Here, the relation between net count and given values is calculated linearly, and all matrix effects are corrected using real measured standards. The second principle is based on fundamental parameters. Here, inter-element effects are calculated based on physical relations. This implies that fewer actual standards are necessary but the demands on each standard are much higher. The complete composition of the standard has to be known (the software tolerates a margin of 2.5% either way of 100%), including elements not measurable

by XRF, such as oxygen or carbon, to allow theoretical calculation of all inter-element effects.

At the beginning, a method named 'slag' was developed using the "Lucas-Tooth, Price" empirical calibration method, to test settings and effectiveness. This calibration is a mathematical model in which the X-Ray fluorescent radiation of the measured element is corrected with the effect coefficients of the compounds present in the sample (Lucas-Tooth and Pyne 1964). The calculated correlation between net count and given values of the standards used in the 'slag' method is represented on or near a line in a graph. This graph shows concentration horizontally and energy vertically, for one element at a time. On measuring an unknown sample, each element count is compared to this line and evaluated accordingly.

When this method was up and running, the maximum level of refinement was quickly reached, which still left considerable error margins for certain elements. The same method was therefore rebuilt with the same measurement and deconvolution settings, but now using an adjustable combination of empirical and fundamental parameter models. The new 'slag' method using fundamental parameters method was therefore renamed 'slag\_fun'.

## **Certified Reference Materials (CRMs)**

In theory, software running an XRF instrument could calibrate raw net counts to actual percentages using theoretically based calculations of inter-element effects. This would imply, however, that the samples analysed have to be known completely. When measuring unknown samples, this knowledge is not available, so the net count and the calibrations performed on them have to be compared to known samples and their values.

A range of samples with known compositions, as similar as possible to the expected element composition(s) and matrix (matrices) of the unknowns to be analysed, is chosen. Since fundamental parameter analysis also needs the values of elements not measurable on an XRF such as those originating from organic material, one generally uses Certified Reference Materials (CRMs or 'standards'), which are fully characterised for their composition.

### **Selection and Preparation**

For the further development of the 'slag\_fun' method, a range of CRMs was selected that was deemed relevant to iron-rich materials. First, related materials,

where one could expect a similar matrix and composition, such as iron ore or slag, were selected. Then standards were selected that were similar in matrix, representing major compounds of iron production related samples, such as lime, manganese, silica and alumina.

Name	Description	Reason(s) for Selection
BCS-CRM 176/2	Manganese Ore	Mn content (Al, Fe)
BCS-CRM 301-1	Lincolnshire Iron Ore	Iron Ore matrix and composition, Ca content
BCS-CRM 309	Sillimanite	Si, Al content
BCS-CRM 313/1	High Purity Silica	Si content
BCS-CRM 375/1	Soda Feldspar	Na content
BCS-CRM 381	Basic Slag	Slag matrix and composition
BCS-CRM 393	Limestone	Ca content
BCS-CRM 776-1	Firebrick	Al, Si, K content: furnace wall elements
BCS-RM 201a	Nepheline Syenite	Na, Al, Si, K content
CCRMP FER-1	Magnetite/Quartz iron formation	Generic Iron standard
CCRMP FER-2	Magnetite/Quartz/Amphibole Iron Ore	Generic Iron standard
CCRMP FER-4	Cherty Magnetite/Chloritic tuff iron formation	Generic Iron standard
CCRMP SCH-1	Schist/Mica Iron Ore	Iron Ore matrix and composition
CCRMP SL-1	Blast Furnace Slag	Industrial Slag composition and matrix
CCRMP SO-1	Champlain Sea Clay	Clay matrix and composition
CCRMP SO-4	Chemozemic Soil	Si, Al, Na, K composition
ECRM 676-1	Iron Ore sinter	Iron Ore matrix, Si, Al
ECRM 681-1	Iron Ore	Iron Ore matrix and composition
ECRM 682-1	Iron Ore	Iron Ore matrix and composition
MnO <sub>2</sub> RM	Manganese dioxide laboratory standard	Mn content
NIST 76a	Burnt Refractory	Ceramic matrix and composition (furnace wall)
PbO <sub>2</sub> RM	Lead dioxide laboratory standard	Pb content
SQ-1	Spectro Quartz Disc	Company calibration standard
TiO <sub>2</sub> RM	Titanium dioxide laboratory standard	Ti content
TLX-1 RM (own standard)	PbO 15%/ZnO 6% in USGS BHVO-2 matrix	Laboratory mix of CRM with laboratory standards; Pb, Zn, Mg, Ca, Fe content
TLX-2 RM (own standard)	PbO 10%/ZnO 4% in USGS BHVO-2 matrix	Laboratory mix of CRM with laboratory standards; Pb, Zn, Mg, Ca, Fe content
TLX-3 RM (own standard)	PbO 5%/ZnO 2% in USGS BHVO-2 matrix	Laboratory mix of CRM with laboratory standards; Pb, Zn, Mg, Ca, Fe content
USGS BHVO-2	Basalt Hawaiian Volcanic	Slag-like glassy matrix and composition
USGS GSP-2	Silver Plume Granodiorite	Slag-like glassy matrix and composition
USGS NOD-A1	Manganese Nodule	Mn content
USGS QLO-1	Quartz Latite	Si content, matrix
XV-HWC	Hoechst Wax	Dilution material (C+H)
ZnO RM	Zinc Oxide laboratory standard	Zn content

Table 6. The 33 standards presently used in the 'slag\_fun' calibration method on the Spectro X-Lab 2000.

Finally, a few standards were selected to ameliorate the calibration of elements that are not well covered by the other standards. A further range of standards was created for the same purpose, i.e. the 'TLX' standards (the acronym refers to the names of the three people involved in their development) were prepared by adding analytical grade metal oxides to selected CRMs, primarily to enhance the

calibration of Pb and Zn. The standards currently used in the 'slag\_fun' method are shown in Table 6, with the principal reason(s) for their selection.

After selection, the CRMs have to be prepared for measurement in the XRF instrument. This is done in a way that is analogous to the preparation of unknown samples. In fact, the preparation should be as identical as possible, to create comparable sample matrices. The standards come as powders, which are first dried for a minimum of 16 hours at 105 °C. This is to ensure that the standard will have the same structure and condition as when it was tested by the referencing laboratories. Next, the dried powders are mixed with a quantity of industrial wax.

The mixture should be as homogeneous as possible to prevent heterogeneous areas or differing matrix effects. In the 'slag\_fun' method, a sample composition was chosen with 8 grams of sample diluted with 0.9 grams of wax. Different amounts and different ratios are also possible (e.g. 4 grams mixed with 0.9 grams of wax), but the 8 gram pellets were considered easier to make and more durable. The mixture is then pressed to a 32 mm diameter pellet at 15 tonnes for 2.5 minutes.

It should be noted that a higher dilution ratio leads to a decrease of matrix effects, but simultaneously has a negative influence on the peak-background ratio and therefore the accuracy of results. Several experiments have been carried out to establish the 'ideal' dilution factor for iron-rich samples. Noticeable changes in the matrix effects, however, only appear at very low amounts of sample, and this is very difficult to achieve. As the dilution factor becomes better in terms of measurement behaviour (i.e. less sample and more wax resulting in less matrix effects), the actual production of a homogeneous mix of sample and wax becomes virtually impossible, as the wax tends to clot together. As a result, it was decided to continue with the 8/0.9 ratio described above.

In the area of the physical preparation of samples, the procedure shifted from pressing plain pellets to using aluminium cups in early 2004. Using these cups allows (if desired) for the use of smaller amounts of sample (at the same dilution ratio), makes samples longer lasting, protects contamination of pellets from handling, and provides a clean surface at the back for labelling. Incidentally, the actual pressing of the pellets becomes easier as well, with less breakage and shattering during production as a result.



## Installing the Standards

The prepared standards can now be used in the method. First, they are measured, one by one, using the new method. This results in net counts for the standard, with a theoretical calibration. These results are copied from the measurement data, and pasted into the standards list. Then, the known values of the standard have to be entered against the calculated values, including the percentages of elements that are either not measurable under XRF or are below the detection limit. Now, the method with its new standard has to be recalculated by the software, which results in newly calculated values. Then the next standards can be measured, installed, and provided with their certified values one by one.

Although the most important (major) elements to be analysed in iron-rich materials are now well covered by the standards in the 'slag\_fun' method, development is ongoing. One area of development is the implementation of additional CRMs to cover varying percentages of elements such as potassium, titanium, calcium, manganese, and magnesium. Another is the ongoing refinement of the current calibration settings per element.

## Testing and Application of the 'Slag\_fun' method

Notwithstanding ongoing development, the method in its present form functions very well, producing more accurate results on iron-rich samples than any other X-Lab Pro method. This is demonstrated in Table 10 (page 144), where repeated analyses (i.e. the sample was newly measured and the results calibrated with the adjusted method each time) of a black-grey tapped smelting slag, HA2002 A7, with 'slag\_fun' are set against results of the same sample analysed using a different analytical technique: Wavelength Dispersive Electron Probe Micro Analysis (EPMA), on the JEOL 8600 Microprobe at the Institute of Archaeology. Table 10 also shows results from the linear 'slag' and the original 'oxide' methods to indicate how measurements of this control sample with the 'slag\_fun' method improved in comparison.

HA 2002 A7 is a relatively homogeneous tapped iron smelting slag with a glassy matrix, mounted in resin as a polished block, rather than a pressed pellet. It has a composition that is assumed typical of much of the Hammeh material. The microprobe analysis was performed by analysing nine (one line of five and one line of four) areas of approximately 300  $\mu\text{m}$  x 300  $\mu\text{m}$ . Each area was measured at an interval of approximately 300  $\mu\text{m}$ , resulting in one line of about 1.8 x 0.3 mm and

a second line of 1.2 x 0.3 mm, continuing in the same direction but 0.8 mm to the side of the first. The lines are separated by approximately 1.7 mm. From these nine measurements (calibrated against four CRMs), the average value for each element was calculated.

From the similarity between the XRF and EPMA results, it could be argued that all samples might be analysed by solely using the microprobe. It should be stressed, however, that the strength of the microprobe lies in providing point analysis (i.e. to establish the composition of mineral phases), providing results for a maximum of 18-20 major elements per measurement. The high number of measurements required, combined with the considerable time each measurement takes (over 15 minutes each), and the restricted number of elements (trace elements are not detected) that can be determined in one measurement make the microprobe highly unwieldy and inappropriate for bulk analysis.

A re-evaluation of HA 2002 A7 that reflects the current state of the method was performed as well. However, this recent analysis cannot be directly compared to the measurements performed during the development of the method. This is due in part to the replacement of the detector of the X-Lab Pro in June 2003, which makes the re-evaluation of raw counts obtained with the previous detector unreliable), as well as a peculiar software problem that was only discovered and solved after these measurements were taken. This problem relates to a hidden and uncontrollable 'normalisation' function that particularly affects analyses of mounted samples and whole artefacts due to their inherent heterogeneity and related matrix effects, and which has been removed since. A new analysis of HA 2002 A7 (i.e. measurement and calibration) produced results that are quite similar to the re-evaluated one, but is equally incompatible with the measurements during development due to subsequent alterations in the state of the sample itself. The 2005 values presented here should therefore not be seen as an indicator of improvement or deterioration of the method in any way. In this context, it should be noted that all CRMs in the 'slag\_fun' method were re-measured and re-calibrated after the change of detector.

Table 11 shows stages of the development of the 'slag' and later the 'slag\_fun' methods, compared to the original 'oxide' method. This is shown through repeated analyses of test sample HAT 1; a homogeneous pressed pellet made from a black-grey tapped bloomery smelting slag similar to HA 2002 A7. Although the recorded stages might be considered arbitrary, it should be noted that these

analyses were each performed after major adjustments to the calibration settings. As with HA 2002 A7, a measurement reflecting the most recent state of the method is added to the overview, which for this sample is fully compatible with the previous measurements. The analyses clearly illustrate significant improvement of the method over time, particularly once the fundamental parameters were included (although it should be noted that the 'true' composition of the sample is unknown and, therefore, the judgement of improvement an opinion). Lighter elements such as magnesium, aluminium, and silicon have improved, as has the sum of the measured elements. Sodium, the lightest element measurable under XRF, remains problematic, which may be the combined result of its peak lying at the very edge of the spectrum measured by XRF, and absorbing matrix effects of magnesium and iron K-lines. The measured quantities for sodium are therefore routinely ignored in the chemical analyses elsewhere in this thesis.

Table 12 shows how measurements of four CRMs with the 'slag\_fun' method compare to the given values of these standards after development of the method had been mostly completed, ca. February 2003. To compensate for carbonate and other materials present in some of the CRMs, which are not measurable under XRF, the results have been normalised to 100 percent. This table shows that the results obtained with the 'slag\_fun' method are accurate and can be used in quantitative analyses. Table 10, Table 11, and Table 12 also reveal a few remaining problems that are still being addressed. These problems occur mainly at low element concentrations (<2%), with Al and Mg, and low to medium concentrations (<10%) of Al. This is very likely due to the matrix and intensity effects, not fully resolved thus far, between Si and Al, and between Al and Mg. It is to be expected that the addition of more CRMs that contain these elements in the relevant percentage ranges will help to resolve these problems. Nevertheless, as shown in Table 7, the reliability of all three elements is currently very high, and measured values for these elements are considered quantitative.

In the development of 'slag\_fun', the focus was primarily on the major elements. CRMs, of which only a limited number was available, were selected on the basis of their major element composition in combination with as high a level of matrix compatibility to iron-rich (slag) samples as possible. The presence of trace elements in the CRMs was not specifically monitored during their installation, nor during the various adjustments to the calibration settings as described above. Nevertheless, the current state of 'slag\_fun' (April 2005) does allow the quantification of not only 12 major elements, but also of 9 trace elements, which

are both listed in Table 7. Where these trace elements are presented in this thesis, all values are rounded to the nearest 10 ppm, and the nearest 5 ppm if the values for an element lie below 50 ppm. Values that fall below the range indicated in Table 7 are presented as below detection limit (bdl).

	r	d (%)	range (in % or ppm)	
Major elements				
Si	0.988	0.0187	1.781	46.637
Al	0.996	0.0083	0.203	37.340
Fe	0.989	0.0412	0.031	68.737
Ti	1.000	0.0046	0.005	59.940
Mn	1.000	0.0017	320 ppm	18.500
Ca	0.999	0.0059	0.029	39.594
Mg	0.978	0.0038	0.240	7.399
K	0.998	0.0010	0.004	4.466
P	0.999	0.0074	0.027	6.851
S	0.979	0.0009	0.040	1.260
V	0.993	0.0002	0.005	0.527
Cr	0.999	0.0000	47 ppm	0.226
Trace elements				
Ni	1.000	662 ppm	17 ppm	0.636
Cu	0.998	0.0000	0.000	0.110
Zn	0.998	480 ppm	0.003	0.350
Rb	0.998	0.0000	0.001	245 ppm
Sr	1.000	0.0000	58 ppm	0.364
Y	0.952	2 ppm	15 ppm	28 ppm
Zr	0.996	0.0000	0.001	550 ppm
Ba	0.975	0.0003	0.005	0.300
Pb	0.994	7115 ppm	4 ppm	12.774

Table 7. Showing the main and trace elements of which detection by the 'slag\_fun' calibration method (April 2005), can be considered quantifiable. Reliability of each element is based on a minimum of 5 CRMs available in the correlation of that element, and a correlation coefficient (r) of >0.95. The table further shows the standard deviation (d) and the range of actual concentrations covered by the CRMs for each element. (The correlation coefficient, standard deviation, and covered range derive from the calibration screen for each element in the Spectro software).

The reliability of quantification is determined by both the number of CRMs that is used for each individual element, which should be five or higher, and the correlation coefficient (Table 7; this data is provided in the calibration screen for each element in the Spectro software). This last value (expressed as r) indicates how well the measured and calibrated value is likely to reflect the actual amount of that element. Only elements with a correlation coefficient higher than 0.95 are considered in the use of analyses by 'slag\_fun' in this thesis.

To further enhance the reliability of (P)ED-XRF bulk chemical analysis using the 'slag\_fun' calibration method, each individual sample from Tell Hammeh and Tel Beth-Shemesh discussed in this thesis was measured three times, and the average of those three repeat runs is used as the composition of a sample. The full

chemical analyses of all repeat runs of all samples and the CRMs that were analysed in parallel can be found in appendix 1. As mentioned before (see chapter 6), the number of analysed samples is too low for proper determination, but the high similarity between the repeated measurements indicates a high precision (i.e. repeatability) of the results.

The chemical analyses presented in Appendix 1 also include  $V_2O_5$ ,  $Cr_2O_3$ , and  $Na_2O$ , elements that are disregarded in the text and calculations. Although, the measured concentrations of these elements appear to be generally correct, they are nevertheless disregarded. Vanadium and chromium are disregarded as most results are below the detection limit, and, therefore, have no comparative function. As mentioned above, sodium is also disregarded. It should be noted that the fact that sodium is routinely ignored slightly increases the normalised values of all other elements. This is important, for example, when considering the average iron oxide content of the Hammeh tap slags, which is calculated as 52.52 wt% (see chapter 8). However, if the disregarded elements were to be counted (e.g. the presence of sodium at concentrations of ca. 0.3 to 1 wt% is confirmed both by the SEM-EDS analyses and the microprobe investigation of HA 2002 A7), the actual iron oxide average of the Hammeh tap slags is closer to 50 wt%.

A further test of the reliability of the slag\_fun method was performed by analysis of Swedish reference slag W-25:R. This sample has been analysed by various analytical techniques at different laboratories (e.g. wet chemical, atomic absorption, induced coupled plasma spectroscopy and XRF) to create a relevant reference material for the study of ancient (bloomery) slags (Kresten and Hjärthner-Holdar 2001). Its matrix and composition are therefore ideally suited for analysis with the 'slag\_fun' calibration method.

Swedish reference slag W-25:R	SiO <sub>2</sub>	Al <sub>2</sub> O <sub>3</sub>	FeO	TiO <sub>2</sub>	MnO	CaO	MgO	K <sub>2</sub> O	P <sub>2</sub> O <sub>5</sub>	S
Actual (mean)	26.0	7.49	59.9	0.34	3.16	1.49	0.40	1.07	0.12	0.04
Standard deviation (% rel.)	2	9	7	11	9	12	19	6	43	11
Slag_fun values	24.6	7.68	61.7	0.22	2.75	1.44	0.26	1.09	0.15	0.08

Table 8. Bulk chemical composition (major elements) of the Swedish reference slag W-25:R, comparing known values (the mean of values obtained through several different analytical techniques) with the average of two analyses of the same reference slag using the 'slag\_fun' calibration method ((P)ED-XRF, April 2005). The standard deviation indicate the relative percentage of error by the various analytical techniques (Kresten and Hjärthner-Holdar 2001, 49-50). Values are expressed in wt%, and normalised to 100%.

The analyses shown in Table 8 and Table 9 indicate how analysis of W-25:R by the 'slag\_fun' method compares to the (mean of) results derived through other analytical techniques. Especially when considering the standard deviation (in

percent relative) of these analyses, it is clear that 'slag\_fun' performs at least as well as the other techniques used to determine the composition of this sample.

Swedish reference slag W-25:R	Ni	Cu	Zn	Rb	Sr	Y	Zr	Ba	Pb
Actual (mean)	70	29	48	nd	94	95	92	806	nd
Standard deviation (% rel.)	91	79	59	na	3	8	9	13	na
Slag_fun values	bdl	25	35	bdl	90	130	140	1000	bdl

**Table 9.** Bulk chemical composition (trace elements) of the Swedish reference slag W-25:R, comparing known (mean) values with the average of two analyses of the same reference slag using the 'slag\_fun' calibration method ((P)ED-XRF, April 2005). The standard deviation indicate the relative percentage of error by the various analytical techniques (Kresten and Hjärthner-Holdar 2001, 49-50). Values are expressed in ppm.

## Conclusions

Table 10, Table 11, and Table 12 all show that the 'slag\_fun' method improved significantly over time, and now provides an accurate and valid tool for bulk chemical analysis of iron-rich materials. The fact that 'slag\_fun' can achieve quantitative analysis of a wide range of major and trace elements is demonstrated in Table 7, Table 8, Table 9, and Table 12. The calibration settings for the measurement of certain elements may still be adjusted further, and most importantly, the number of standards and specifically the percentage ranges they cover for elements should be enlarged as much as possible. This will improve the method even further, providing quantitative analysis of an even wider range of elements, but the method as it stands today is by far the most reliable and accurate for iron-rich oxidic samples currently available on the Institute of Archaeology X-Lab Pro 2000.

It outperforms, as intended, all pre-set Spectro calibration methods where iron-rich samples are concerned. Surprisingly, it is more accurate than more recent 'slag\_fun' derived methods, such as 'slag\_cu', a customised version of 'slag\_fun' for copper-rich slag, which has specific copper and bronze CRMs added to the calibration. The exact reason for this better performance is difficult to determine, but a likely reason lies in the fact that adjusting the settings in the quite idiosyncratic Spectro software is an extremely intuitive undertaking that requires large amounts of time.

Sample	Date analysed	Method / Technique	SiO <sub>2</sub>	Al <sub>2</sub> O <sub>3</sub>	FeO	TiO <sub>2</sub>	MnO	CaO	MgO	Na <sub>2</sub> O	K <sub>2</sub> O	P <sub>2</sub> O <sub>5</sub>	S	Sum
HA2002 A7	08/2002	EPMA	23.30	5.17	53.35	0.25	1.37	12.03	2.59	0.30	0.46	1.54	0.34	100.80
HA2002 A7	01/2003	Slag_fun	21.58	4.11	55.84	0.35	1.16	11.52	2.46	n.d.	0.71	1.63	0.18	99.54
HA2002 A7	01/2003	Oxides	30.80	6.49	87.44	0.52	2.05	14.88	3.84	n.d.	1.17	2.24	0.13	149.56
HA2002 A7	08/2002	Slag	17.38	3.26	49.56	0.31	2.08	6.34	1.84	n.d.	0.66	1.09	0.27	82.80

Table 10. Comparison of methods. Results of the 'slag\_fun' method, compared with 'true' values obtained through EPMA, and the linear 'slag' and oxide methods. The comparison is performed on mounted sample HA2002 A7, a mounted Hammeh tap slag. All values are expressed as wt%.

Sample	Date analysed	Method	SiO <sub>2</sub>	Al <sub>2</sub> O <sub>3</sub>	FeO	TiO <sub>2</sub>	MnO	CaO	MgO	Na <sub>2</sub> O	K <sub>2</sub> O	P <sub>2</sub> O <sub>5</sub>	S	Sum
HAT 1	10/04/2005	Slag_fun	24.93	4.77	48.57	0.32	1.01	14.08	1.75	0.63	0.88	0.92	0.25	98.10
HAT 1	03/01/2003	Slag_fun	25.85	4.26	51.63	0.40	1.04	17.63	1.99	n.d.	0.90	0.96	0.26	104.92
HAT 1	11/09/2002	Slag_fun	24.94	4.79	46.57	0.37	0.95	14.40	2.52	0.37	0.89	0.97	0.28	97.05
HAT 1	09/09/2002	Slag_fun	23.28	3.45	39.25	0.23	1.74	9.66	0.74	n.d.	0.93	0.81	0.26	80.35
HAT 1	09/09/2002	Slag	9.49	1.83	28.10	2.37	0.61	53.62	1.77	n.d.	2.52	0.24	0.07	100.62
HAT 1	07/06/2002	Slag	14.07	3.48	40.37	0.11	0.72	10.37	1.49	n.d.	0.70	0.54	0.21	72.06
HAT 1	05/03/2002	Slag	9.53	1.84	27.23	2.30	0.59	51.72	0.80	n.d.	2.33	0.29	0.07	96.70
HAT 1	02/05/2002	Oxides	21.58	3.52	46.92	0.37	1.13	14.87	1.07	n.d.	0.82	1.10	0.10	91.48

Table 11. Development of the 'slag' and 'slag\_fun' methods over time. Results are shown with the most recent at the top, and are off-set against the results obtained with the 'oxides' method, at the bottom. Test sample HAT 1 is a homogenised pellet of a Hammeh tap slag. All values are expressed as wt%.

Sample	Sample Type	Method / Given	SiO <sub>2</sub>	Al <sub>2</sub> O <sub>3</sub>	FeO	TiO <sub>2</sub>	MnO	CaO	MgO	Na <sub>2</sub> O	K <sub>2</sub> O	P <sub>2</sub> O <sub>5</sub>	S	Sum
BCS-CRM 381	Basic Slag	Slag_fun	9.88	0.11	17.53	0.33	3.31	49.86	0.06	0.76	0.03	17.91	0.23	100
		Given	9.15	0.70	17.82	0.36	3.29	51.05	1.07	n.d.	n.d.	16.36	0.20	100
BCS-CRM 301-1	Lincolnshire Iron Ore	Slag_fun	10.93	5.65	44.92	0.23	1.75	31.87	2.66	0.06	0.46	1.20	0.27	100
		Given	10.62	6.12	44.04	0.23	1.79	32.44	2.48	0.10	0.46	1.15	0.57	100
CCRMP SL-1	Blast Furnace Slag	Slag_fun	36.00	8.72	0.92	0.39	0.87	36.77	14.42	0.09	0.59	0.01	1.22	100
		Given	35.93	9.68	0.93	0.38	0.87	37.69	12.34	0.39	0.51	0.02	1.27	100
BHVO-2	Basalt CRM	Slag_fun	50.17	14.91	11.09	2.59	0.14	10.96	7.02	2.29	0.50	0.30	0.03	100
		Given	50.41	13.64	11.19	2.76	0.13	11.52	7.31	2.24	0.53	0.27	n.d.	100

Table 12. Comparison of given values of four CRMs, with the values of the same standards obtained with the 'slag\_fun' method. All results have been normalised to remove differences caused by elements not measurable under XRF and Loss on Ignition (L.O.I.), and are expressed as wt% Measurements ca. February 2003.

During the development of 'slag\_fun', more and more was understood about Spectro-specific terminology, allowing for a more software independent and scientifically proper approach, but this has apparently not resulted in better performance. A peculiar example of this phenomenon is that, rather than adjusting the selection of CRMs per element by looking at the relevant calibration curve, repeated trial and error sequences with different combinations of CRMs often give a better result for that element.

Primarily, 'slag\_fun' was developed to create a necessary tool for the archaeometric study of the Hammeh and Beth-Shemesh material, in providing an accurate and quantified bulk chemical analysis of these iron-rich materials (see chapters 8 and 9). However, since its initial development it has also benefited several other research projects involving iron-rich slag at the Institute of Archaeology, UCL, including iron production slag from Nigeria (Ige and Rehren 2003), Wales (Stanway 2003), Jordan (Mascelloni 2004), Uganda (Humphris 2004), and Zimbabwe (Chirikure and Rehren 2004; Chirikure 2002), as well as lead slag from Greece (Anguilano 2002).

The creation of 'slag\_fun', and particularly the surmounting of software idiosyncrasies during that process, also resulted in a 'manual' for method building. Based on the 'slag\_fun' method, and using this manual, several additional methods have been developed (or are in the process of being developed) for the calibration of ceramic materials (cer\_v2a), copper-rich materials (slag\_cu, mentioned above), and lead-rich materials (slag\_pb, this last method is a continuation of the work of Lorna Anguilano in 2002 (Anguilano 2002)).



## CHAPTER 8: ANALYSIS OF THE HAMMEH MATERIAL

### Introduction

The archaeometallurgical finds from Tell Hammeh comprise a variety of materials, ranging from slag through technical ceramics and charcoal to ore. These materials form the debris from a metallurgical process, and it is this process that is examined in this chapter. Based on the circumstances observed during the excavation (see chapter 4), the working hypothesis for this examination was that the Hammeh materials represent an iron smelting and primary smithing operation based on the exploitation of a local ore source at Mugharet al-Warda, as opposed to, say, copper smelting or secondary smithing of iron.

Presented first is a characterisation of the different Hammeh materials, through macroscopic, microscopic, and chemical analyses. This characterisation is used to confirm that iron was the metal produced at Hammeh. Subsequently, the nature of the technological stages (i.e. smelting, primary smithing, or smithing) involved in the production of that metal is determined, and the *chaîne opératoire* of the metallurgical process at Hammeh is reconstructed.

This chapter also explores the relations between the various materials discussed, starting with the suitability of the Warda ore for smelting and its relation to the Hammeh operations and slag composition. It is demonstrated how, as concluded from the examination of the ore-slag relation, the technical ceramics, especially the tuyères, played an important and substantial role in the slag formation and operating conditions of the Hammeh smelting process, and the nature of that role is discussed.

Based on the reconstructed technological processes, it is assessed what the finds at Hammeh mean archaeologically, e.g. in terms of scale of the operations, social and economic organisation, impact on the environment, or use of resources. The reconstruction of the *chaîne opératoire* further allows the identification of potential choices in the technological process that have no technological requirement, but must be related to social or cultural considerations (see chapter 2).

## The Mugharet al-Warda Ore

### Location and Previous Study of the Ore Source

One of the few iron ore deposits in the Levant, and the main iron ore site in a range of several hundreds of kilometres, is located just a few kilometres from Hammeh, up in the 'Ajlun hills. This ore source, Mugharet al-Warda, was studied extensively in the 1960s and again in the 1980s to establish the economic value of the deposit for potential modern exploitation. This took place in the early 1960s as part of the German Geological Mission in Jordan, a cooperation of the Jordanian government (National Resources Authority) together with the German Federal Institute of Geoscience and Natural Resources (Bundesanstalt für Bodenforschung und Rohstoffe) in Hannover (van den Boom and Lahloub 1962). Unfortunately, their analyses remain classified, and, therefore, little chemical or mineralogical detail is available beyond the description of the deposit by Friedrich Bender, which is largely based on these analyses (Bender 1968, 149-151).

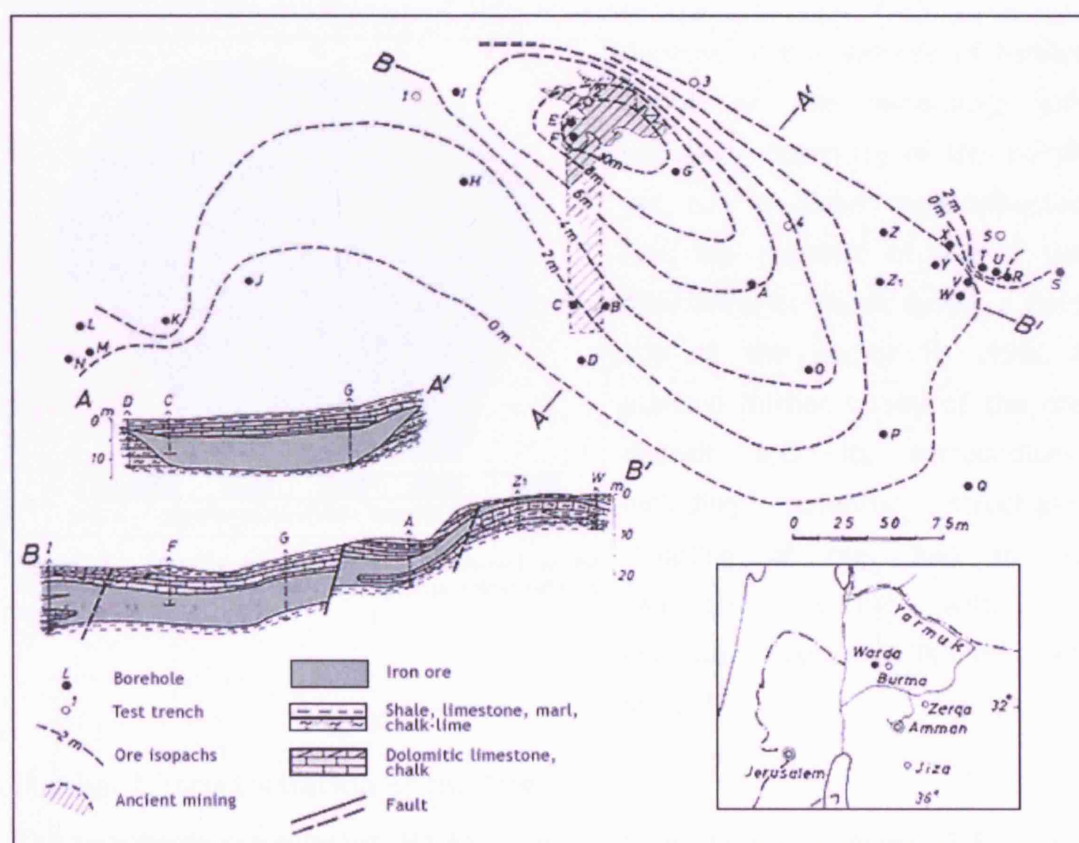


Figure 21. Isopachs (contours indicating the thickness) and cross sections of the iron ore deposit at Mugharet al-Warda, from Bender (Bender 1968, 150, figure 144), after van den Boom and Lahloub (van den Boom and Lahloub 1962).

Bender describes the Warda deposit as a lenticular body of massive haematite ore, with predominantly haematite ( $\text{Fe}_2\text{O}_3$ ) mineral. The ore body measures ca. 300 by 200 metres and reaches a maximum thickness of almost 10 metres. It is exposed and accessible at the surface in a few locations (see Figure 21). The geological mission made 15 boreholes, from which 205 samples were analysed. According to Bender, the iron oxide content of these probes ranged from 43 to 80.5 %  $\text{Fe}_2\text{O}_3$ , with an average of 67.9 % (Bender 1968, 151). No quantities of gangue components such as  $\text{SiO}_2$  or  $\text{CaO}$  were reported.

Bender states the mineralogical components of the Warda ore as primarily haematite, some limonite, and lesser amounts of calcite, quartz, and chalcedony. These last minerals diminish in quantity in the main ore body. Sulphides were not attested. Levels of lime in the ore are higher near the edges of the ore lens, where ranges of mineralization are found that range from haematite ore through more lime-rich mixtures to pure lime, which relate to the lime-rich deposits (seen in Figure 21) in which the ore body is embedded (Bender 1968, 151).

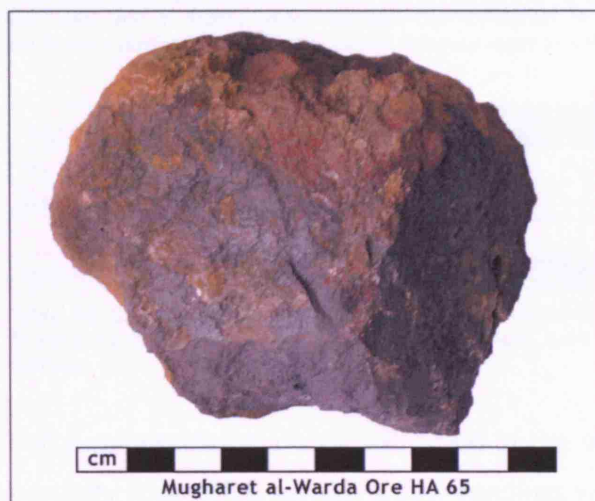


Figure 22. Haematite ore sample HA 65, sampled by the author from the surface near one of the mineshafts at Mugharet al-Warda.

Because of the absence of further details on the mineralogy and especially chemistry of the Warda ore, two specimens were collected near the entrance of one of the mineshafts at Warda during a field trip of the author in 1998. A planned further survey of the ore deposit and its surroundings, including potential structured sampling of ore, had to be cancelled together with the excavation season at Tell Hammeh in 2003.

### Further Characterisation of the Ore

The two Warda ore samples, HA 65 (Figure 22) and HA 66, are dense ( $3.8 \text{ g/cm}^3$ ) pieces of dark-blueish rock, and HA 65 shows some areas that are red in colour. On cutting or grinding, the dark stone turns into bright bordeaux-red coloured powder. Judging by the way this powder stains everything it comes into contact with, the ore could be a very good source for pigments as well. Microscopical

examination of the ore reveals a clear haematitic structure. The (macroscopically) red area of sample HA 65 appears to be more silicate-rich than the dark-blue part.

Both samples show a bulk chemistry that is very suitable for the production of iron, as both contain a high level of iron oxide (ca. 86 and 93 wt% respectively, when normalised and expressed as FeO; Table 13). Differences in composition between the two samples likely reflect variations within the ore body similar to those described by Bender. The main difference is in the lime content. Where the first sample (HA 65) contains approximately 8.4 wt% lime, the second sample (HA 66) contains only 0.27 wt%. This difference is relevant when the relation of the Warda ore to the Hammeh slag is discussed on page 201.

Warda ore samples	SiO <sub>2</sub>	Al <sub>2</sub> O <sub>3</sub>	FeO	TiO <sub>2</sub>	MnO	CaO	MgO	K <sub>2</sub> O	P <sub>2</sub> O <sub>5</sub>	S
HA 65	4.45	0.00	86.5	0.01	0.03	8.45	0.16	0.00	0.06	0.38
HA 66	5.27	0.35	93.3	0.09	0.06	0.27	0.17	0.01	0.26	0.18
average	4.86	0.17	89.9	0.05	0.05	4.36	0.17	0.01	0.16	0.28

Table 13. Bulk chemical composition (major elements) of the Mugharet al-Warda ore sampled by the author. Note how these ore samples show a high grade of iron oxide, making them eminently suitable for smelting, but very low in silica, which hinders the formation of a liquid slag. Analysis by (P)ED-XRF (slag\_fun calibration method, April 2005). Values are expressed in wt%, and normalised to 100%.

Warda ore samples	Ni	Cu	Zn	Rb	Sr	Y	Zr	Ba	Pb
HA 65	bdl	bdl	70	bdl	bdl	bdl	bdl	bdl	bdl
HA 66	bdl	25	60	bdl	bdl	25	70	bdl	bdl
average	bdl	25	65	bdl	bdl	25	70	bdl	bdl

Table 14. Bulk chemical composition (trace elements) of the Mugharet al-Warda ore sampled by the author. Analysis by (P)ED-XRF (slag\_fun calibration method, April 2005). Values are expressed in ppm (parts per million).

Initial mineralogical characterisation of the ore samples using XRD at UCL was only partially successful, as only a few readings were recovered (see chapter 6). These readings matched with haematite (Fe<sub>2</sub>O<sub>3</sub>) and calcite (CaCO<sub>3</sub>) in HA 65, and haematite in HA 66. In April 2005, the kind offer of Dr Manolis Pantos to re-examine the ore samples using Synchrotron Radiation XRD (SR-XRD) at the Daresbury Synchrotron Radiation Source (SRS) resulted in a new examination of sample HA 65. This clearly identified the dominant presence of haematite. The identification of the possible presence of other minerals is currently being undertaken. The clear pattern of haematite, derived from two measurements, one at a zero degree angle and one at a 90 degree angle, is shown in Figure 23.



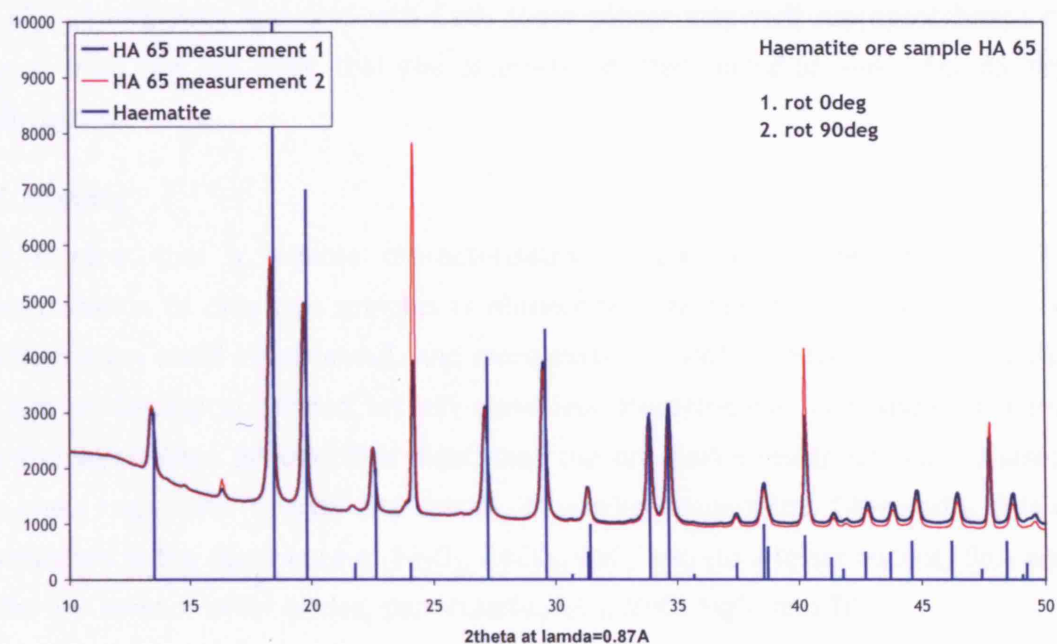


Figure 23. SR-XRD spectrum of sample HA 65, showing two measurements, one with the beam at a 0 degree angle (in black), the other at a 90 degree angle (in red). Both measurements show a clear pattern that corresponds to haematite (the standard peaks of haematite are shown in blue). Analysis by Synchrotron Radiation-XRD, at the Daresbury Synchrotron Radiation Source (SRS), by Dr Manolis Pantos.

### Discarded Ore

On Tell Hammeh itself, a few pieces of stone were excavated from the iron production phase that look similar to the Warda ore, especially in their dark-blue and red colouring, which in the field were tentatively identified as discarded ore. The sample taken from these pieces, HA 64, is far less solid than the two Warda ore samples HA 65 and 66. It is dark-blue to grey and dark red in colour and is relatively crystalline in nature. Microscopically it shows large quartz grains embedded in layers of iron hydroxides.

Discarded 'ore'	SiO <sub>2</sub>	Al <sub>2</sub> O <sub>3</sub>	FeO	TiO <sub>2</sub>	MnO	CaO	MgO	K <sub>2</sub> O	P <sub>2</sub> O <sub>5</sub>	S
HA 64	68.7	1.8	28.1	0.16	0.01	0.15	0	0.25	0	0.29

Table 15. Bulk chemical composition (major elements) of the possible discarded 'ore'. Analysis by (P)ED-XRF (slag\_fun calibration method, April 2005). Values are expressed in wt%, and normalised to 100%.

Discarded 'ore'	Ni	Cu	Zn	Rb	Sr	Y	Zr	Ba	Pb
HA 64	bdl	10	70	bdl	25	bdl	210	bdl	bdl

Table 16. Bulk chemical composition (trace elements) of the possible discarded 'ore'. Analysis by (P)ED-XRF (slag\_fun calibration method, April 2005). Values are expressed in ppm (parts per million).

Chemically, it has a similar composition to the ore samples (Table 15), although the measured iron oxide (28 wt%) content is too low to be smelted to iron, and thus to allow the term 'ore'. Judging by the overall composition of ca. 68 wt%

SiO<sub>2</sub>, 28 wt% FeO, and 0.15 wt% CaO, these pieces may well represent lumps of rock from the ore body that the smelters deemed unusable and subsequently discarded.

## Summary

It is clear that a reliable characterisation of the Warda ore based on the examination of only two samples is illusionary. However, no further samples or information could be obtained, and more extensive details from the work by the German Geological Mission remain classified. Nevertheless, combined with the information from Bender, it is clear that the ore comprises three main phases, namely haematite, quartz, and calcite, in varying proportions. Chemically, this is reflected in the dominance of Fe<sub>2</sub>O<sub>3</sub>, CaCO<sub>3</sub>/CaO, and (to a lesser extent) SiO<sub>2</sub> and the low level of other oxides, particularly Al<sub>2</sub>O<sub>3</sub>, MnO, MgO, and TiO<sub>2</sub>.

The average iron oxide content of the Warda ore quoted by Bender (67.9 % Fe<sub>2</sub>O<sub>3</sub>) is not necessarily indicative of what the ancient smelters used. This number is based on modern (1960s) views of what constitutes an exploitable ore, and thus likely includes low grade samples that may very well have been considered unsuitable in other times and circumstances. The analyses from the 1960s also likely include samples from parts of the ore body that were not accessible in ancient times.

The absence of other iron ore sources in the wider region makes it almost certain that Warda was the source for Hammeh production. The two samples clearly do represent two points on a range of possible Warda compositions, but it is not known where on that range these points fall. Therefore, it cannot be fully determined from the currently available data how representative the two samples are for the Warda ore as a whole. If one, both, or the average of the samples is representative of the ore body exposed today, this does not necessarily mean that that composition is equal to the ore as mined or collected in antiquity by the Hammeh metalworkers.

Nevertheless, the chemical composition of the ore is relevant when the relation to the Hammeh smelting operations is discussed (see page 201), and lacking more extensive data at this moment in time, the chemical analysis of samples HA 65 and HA 66 will have to suffice. In this context, it should be noted that in early 2005 ca. 20 pieces of Warda ore were sampled and subsequently analysed by Yosha Abd el Salam al-Amri and Andreas Hauptmann, from the German Mining Museum in Bochum. The initial results of these samples, which were collected both on the

surface and from one of the mineshafts, show a range of compositions that is very similar to that shown by HA 65 and HA 66 (Yosha al-Amri, personal communication, June 2005).

When considering their iron oxide content composition, or even at the lower average iron oxide value given by Bender, the ore at Warda is certainly sufficiently rich to smelt using the bloomery process. The low silica content of the Warda ore in combination with the presence of lime, however, would make the formation of (sufficient quantities of) a liquid slag, and thus the successful reduction of iron oxide to metal, difficult. This suggests that a contribution to the smelting process from other materials than the ore is required, as has been discussed, for example, for the silica-poor Phalaborwa ore of South Africa (Miller *et al.* 2001-2002; van der Merwe and Scully 1971).

## The Tuyères

### Introduction

A large number of tuyères was excavated at Tell Hammeh. Their macroscopic and chemical characteristics and their role in the Hammeh smelting technology are described in detail below. As has been mentioned earlier (see chapter 4), an important characteristic of these tuyères is their design. All Hammeh tuyères are square in cross-section, of a relatively uniform size, and have a narrow bore of 1 cm in diameter. Most of the few known tuyères in Levantine metallurgy are related to copper or bronze metallurgy and are round in section with a larger bore than the Hammeh ones (e.g. Rothenberg 1990, 6, 29-42, 50-54). Only a few square section tuyères are known from the region, and these are presented after discussing the various design and construction features of the Hammeh tuyères.

### Quantities and Scale of Operation

More than 350 fragments of tuyères were excavated at Hammeh during the 2000 season, in addition to ca. 20 fragments from the earlier two seasons. Most of these fragments are molten and/or vitrified at the nozzle, i.e. the part that entered into the furnace, and are broken off at the other end. A smaller number of fragments represent the rear end, i.e. the part that protruded outside the furnace, and where bellows may have been attached. A third group of fragments is formed by what were then termed mid-pieces, i.e. pieces that are broken off on either side. Only very few fragments show an apparently non-molten nozzle, and these are generally very small (around 3 x 3 cm in section). Only four tuyères were

‘complete’, i.e. they extend from a rear end to a molten nozzle. These different fragments are discussed in more detail below.

During the laying out of all the tuyère samples in 2001, it was examined whether any of these fragments might have formed part of the same tuyères. As all fragments from the same grid and unit were stored together, possible relations between neighbouring fragments were easily checked. Because of the sheer numbers, it was impossible to try every possible combination across all grids and units, but all the likely candidates for a fit (based on their observed shape, colour, size, and texture) were tested. Besides a few broken specimen that were found during excavation, i.e. a single tuyère broken in two or more pieces, not a single fit could be made, neither within each individual grid nor across grids. Furthermore, none of the broken surfaces of the tuyères shows indications for (postdepositional) wear or damage that might obscure possible fits. These observations indicate that almost every excavated fragment probably represents a single tuyère.

The vast majority of the tuyères was recovered from a single 5 x 5 metre square (A/B7, where over 200 fragments were found), i.e. only a fraction of the potential original production area (see chapter 4). Since no tuyères were found that were recognisably *in situ*, it cannot be established how many tuyères were used simultaneously in a single Hammeh smelting furnace. Based on the sacrificial nature of the tuyères (see discussion on page 208, ff), it may be assumed that several may have been used in one furnace for one smelt, and furthermore that they were only used once. Even if one assumes that 10 tuyères would be used in a single smelt, the material from A/B7 alone would then already represent up to 20 separate smelts, and the total material more than 30 separate smelting runs. Based on the number of tuyères and the related considerations outlined here, it is clear that the Hammeh smelting operations must have taken place at a considerable scale.

### Sampling of the Tuyères

All tuyères were retained after excavation, analogous to the slag. In the early stages of digging, each tuyère segment that was found was awarded a separate IP number. As the excavation progressed, however, the quantity of tuyère fragments encountered rose sharply. These high numbers of fragments and the time-pressure these caused, necessitated group sampling of the tuyères. The spatial distribution of all (groups of) tuyères within square A/B7 was recorded using the grid system;



with all tuyère fragments from a single grid and unit labelled with the same IP-number (Figure 24 shows many of the larger (but not all) of the tuyères fragments excavated in square A/B7).

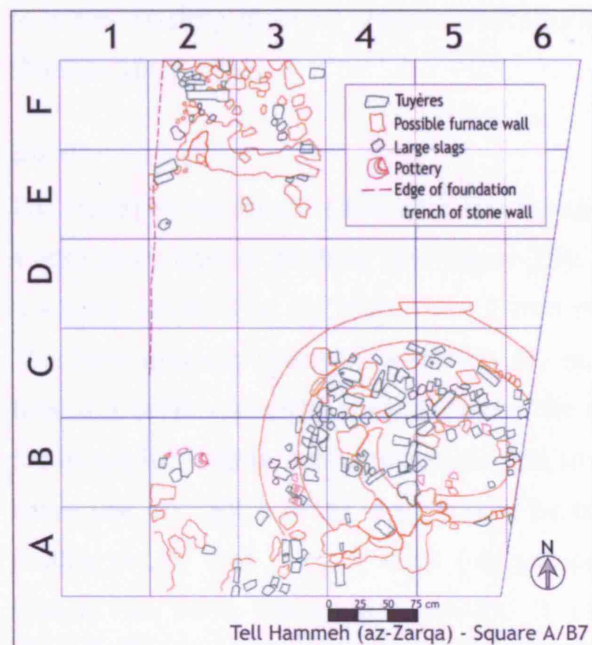


Figure 24. Plan of square A/B7 near the end of excavation, showing the 75 x 75 cm grid in blue, and the location of several larger tuyère segments within that grid in green. Empty grids were either excavated before the drawing was made (e.g. F4), or have not been fully excavated (row D).

During the 2001 season, all tuyères were carefully laid out and arranged on two 2 x 4 m tables. Several tuyères were sketched or drawn, all were measured, and their macroscopic features were recorded. Because of the very low variability in size and shape (see below) that was observed, it was decided to perform a random sampling from each of the three classified segments (nozzle, mid-piece, and rear-end). These randomly selected samples were sent to UCL for subsequent study and analyses, and have been used for, for example, chemical analysis

(see page 160) and petrographic comparison with the tuyères found at Tel Beth-Shemesh (see chapter 9).

### Shape

The most distinct physical characteristic of the Hammeh tuyères is the aforementioned square cross section, which measures 5.1 x 5.1 cm on average (based on the measurements of front and central ends of fragments that retain their full circumference). Tuyères of such a shape are sometimes referred to as *block tuyères*, a shape mainly known from the La Tène and later Romano-Barbaric periods (from 450 BC onward), particularly in central and eastern Europe (Pleiner 2000, 208-212, and Figure 57). Most of these *block tuyères* are of larger size than the Hammeh tuyères (e.g. the specimens shown by Pleiner measure ca. 10 x 10 cm or more), many tend to be rectangular rather than square in shape, and they often have two bores rather than the single one seen at Hammeh. Almost all of the few known tuyères in the Middle East have a circular or semi-circular (“D-shaped”) cross section (see also page 161). No straightforward technological

reason can be identified for a square section. Differential distribution of heat in a square section shape would increase the chance of the tuyères cracking during use, and in terms of production, they involve more labour and material. As will be discussed below, the distinct square section of the Hammeh tuyères may well link to a pre-existing local or regional metallurgical tradition or technological choice (Pleiner 2000, 196).

## Bore

The Hammeh tuyères, in line with the European examples mentioned above, have a very small bore or air hole (see Figure 25). Throughout the length of the tuyères, the bore never diverges more than 2 mm from the average diameter of 10 mm. The bore appears made by insertion of, or, more probable, construction of the tuyère around a straight stick or reed. The use of a stick or reed, as opposed to, for example, fingers (which would be too short), or rope (which would most likely leave less straight a hole) is suggested by the complete straightness of the bore. Pulling out of that reed or stick (my personal opinion favours a reed) after the tuyère has been constructed around it rather than pushing it through after construction of a solid block, is suggested by the fine and smooth and uninterrupted surface, and the fine lines in the inner surface of the bore. The pushing through of a reed or stick would most likely cause harder fragment of clay or stone in the tuyère material to gauge deeper stripes or disrupt the smooth surface of the bore. The narrowness of the bore further strongly indicates that the tuyères were constructed for use with bellows, since a natural draught furnace would require far wider air inlets, typically over 20 or 30 mm in diameter (Pleiner 2000, 141).

In those samples that represent the rear end of the tuyères, i.e. the end that extends outside the furnace, the bore has been widened, here apparently with a finger, to a depth of up to ca. 5 cm (approximately two digits of a finger) and a diameter of ca. 30 mm. The use of fingers rather than an instrument is suggested by the rather uneven shape of these widened bores. Another possibility, that the larger bore at the rear would be the result of cutting out some of the clay is contradicted by the absence of cutting marks, as well as the fact that the widening of the bore also leads to a widening of the tuyère as a whole, which suggest displacement of material rather than removal. The result is a larger tuyère cross section at the rear, often ca. around 8 x 6 cm, with most tuyères

predominantly widened to the lateral sides. It is assumed that this widened bore accommodated the nozzle of bellows.

### Angle

The narrow borehole makes the tuyères very susceptible to blocking by slag and molten ceramic. To resolve this, tuyères are often placed with their nozzle slightly sloping down. It is reasonable to assume that this was done at Hammeh as well, since a reducingly fired zone at the tuyère nozzles, marking the part that protruded through the furnace wall into the furnace chamber, indicates a downward inclination of ca. 15-20°. The end of this reducing zone is often marked by a grey 'rim' that runs at an angle to the body of the tuyère. This angle is further observed in the sloping of the face of most molten nozzles. Both can be seen in Figure 25; here the lateral view of the tuyère is presented with the nozzle rotated until its molten face and the grey 'rim' are approximately vertical, indicating a downward angle (relative to the furnace wall) of the tuyère body of ca. 17°.



Figure 25. Frontal and lateral view of tuyère IPAB7.161a, showing the molten nozzle of a square section tuyère, fused with the technical ceramic of the furnace wall. Remnants of unvitified furnace wall are also preserved, both below and above the tuyère. An 'eyelid', formed by molten technical ceramic flowing down and pushed up and forward by the airflow, is visible above the bore. A large 'beard' of molten ceramic material with adhering slag can also be seen. Some three centimetres behind the molten nozzle, one can see the 'rim', a greyish band indicating the extent to which reducing conditions in the furnace affected the ceramic, simultaneously suggesting a downward angle for the tuyère.

### Length

Four of the tuyères excavated so far seem to be 'complete', meaning that they range from a rear end with widened bore (where the bellow was inserted), to a

vitrified nozzle (where the tuyère was exposed to severe heat inside the furnace, which can be seen in Figure 25 and Figure 26). These four samples measure up to 25 cm in length, and ca. 5 x 5 cm in section at their front (Figure 26). No definite conclusions can be drawn about the original full length of these tuyères, as their vitrification, whilst indicating clearly that the tuyères were used, simultaneously hinders a reconstruction of their original measurements. However, a few smaller nozzles occur among the total assemblage of tuyère segments, which are ca. 3 x 3 cm (up to 4 x 4 cm) in section, mostly unmolten and therefore presumably unused. These tiny nozzle ends, when compared to the measurements of the four 'complete' tuyères, further suggest a longer size for the original unused tuyères (see Figure 27). The 'complete' tuyères themselves show a tapering towards the nozzles, again suggestive of a longer original length.

Figure 26. Four 'complete' (i.e. rear-end to molten nozzle) tuyères from Tell Hammeh, showing lengths up to 25 cm, with burnt and molten nozzles, and widened rear ends. The possible angle of insertion of these tuyères in the furnace wall is reflected by the grey/black demarcation of the reducingly fired zone at the nozzle (especially in the second sample from the left). The fragments further show a slight tapering towards the nozzle.

An attempt to quantify these visual impressions fully failed initially. The various fragments of tuyère (in the field classified into 'nozzle', 'mid-piece', and 'rear-end' segments) show no statistically significant tapering between their frontal and lateral ends, when measuring and comparing the surface area at each end. There are several possible causes for the failure to quantify the potential tapering within each segment. It is very likely, for example, that differential survival of the pieces, both in terms of unequal melting and of postdepositional processes, distorts the picture. It can therefore not be known exactly from what part of the



original complete tuyère an excavated segment originates, e.g. a fragment classified as a mid-piece may have broken off close to the (molten) nozzle end, but equally well close to the rear-end.

It is not unreasonable to assume that more intensely heated and molten segments survive better, whereas the less affected rear end of a tuyère more easily dissolves in the surrounding soil, further enhancing differential survival, which seems to be borne out by the relatively low number of rear ends recovered at Hammeh. Potentially, inaccuracy of field measurements, e.g. recording slightly different values as identical, may further skew the data. Another reason why the three defined tuyère segments do not reveal measurable tapering within themselves, may be that the original complete tuyères featured both straight and tapering segments, from which the tapering parts were not recovered in the excavation. The latter is possible if the tapering segment would be nearest to the nozzle, in which case it will have melted off in most cases. A last possibility, although this is highly unlikely in my opinion, is that there may have been two different types of tuyères present at Hammeh, where the smaller 3 x 3 cm fragments might belong to that second, perhaps smaller or narrower, type of tuyère.

Figure 27. Reconstruction of the potential full length of a Hammeh tuyère. This image shows 'complete' rear end IPAB7.137 (seen from the top) and small molten nozzle IPAB7.37 (seen from the side). The dashed line indicates the possible tapering from rear to front of the tuyère.

When comparing the average surfaces of the frontal ends from segment type to segment type, however, a progressively larger surface is measured, which does strongly support the idea of tapering. In this comparison of surface area, the lateral end of the rear end segments was not taken into account, as the larger size at this end is clearly related to the finger widening of the bore there (see page 155). The average measurements for the three classified segment types (nozzle, mid-piece, and rear end) rise from 24 cm<sup>2</sup> at the front of the nozzle, through 28 cm<sup>2</sup> at the front of the mid-pieces, to 33 cm<sup>2</sup> at the front of the rear ends. This strongly supports an overall tapered shape of the tuyères, as well as the idea that

their original length must have been noticeably longer than the maximum length preserved. Until a complete and unused tuyère is recovered, it will remain difficult to reconstruct the actual total length, and thus to calculate exactly how much ceramic material each tuyère may have contributed to the smelting process. That the Hammeh tuyères contributed a considerable amount of material, however, is without doubt (see page 201, ff).

### **Standardisation**

Another important feature, related to the quantity of tuyères, is their apparent standardisation in shape and size. Hardly any variation of size seems to occur, besides the aforementioned tapering of the shape towards the nozzle, the widening of the bore at the outside end, and potentially some shrinkage and expansion effects due to the heat exposure during use. There are furthermore no indications for the use of a mould of any kind, e.g. marks indicating the edge of the mould, ridges of clay material extending beyond such an edge, or flattened, smeared, or compressed areas on a side surface. Such marks are very frequently observed in the ubiquitous mud-bricks of the region, which were, and are to this day, most often made in moulds. This is not to say that the Hammeh tuyères cannot have been produced in a mould, but if they were, subsequent treatment of the tuyères, perhaps in reshaping to create the tapering, must have eradicated the traces of that mould.

The high degree of uniformity within the large quantity of tuyères certainly seems to indicate regular or even mass production, as opposed to just an ‘experimental stage’ of metallurgy. The degree of standardisation of the Hammeh tuyère production may well be related to concepts of efficiency (Costin 2001, 289-291) and control and organisation (Costin 2001, 301-303) of the smelting operations at Hammeh (see also chapter 3, page 38-ff).

### **Melting of the Ceramic**

The tuyère nozzles clearly show that the ceramic has molten off with considerable loss of material, and are sometimes in direct contact with slag. Just above the front opening of the bore, the vitrified ceramic often forms a slightly protruding and overhanging ‘eyelid’, where softened ceramic and/or slag material flowing down was pushed up and forward by the air blast. Similarly, one side of the tuyères often shows a (often small, usually broken off) extension or ‘beard’ of vitrified ceramic and/or slag pointing downwards beyond the tuyère proper. This beard, similar to the ‘eyelid’, is the result of ceramic material melting off from

the tuyère nozzle (and furnace wall), and flowing downwards. Both features help to identify which side of the tuyère was top or bottom. Most of the melting effects described here can be seen in Figure 25.

### Chemical Composition of the Tuyères and the Local Clay

As described above, the tuyères probably contributed considerable amounts of ceramic material to the smelting process at Hammeh. To enable the examination of that contribution and its potential influence on the parameters of the smelting process, samples were taken from two different tuyère fragments and measured by (P)ED-XRF, to establish their chemical composition. One sample (HAC 2) was taken from the reduced zone at the nozzle end of a tuyère, just behind the vitrified face, the other sample (HAC3) was taken from the body of a tuyère fragment, behind the reduced zone. It was further sought to establish the relation between the ceramic material of the tuyères and the local clay. For this purpose, a clay sample (HAC 1), taken from an outcrop of the local Lisan clay near Hammeh at the village of Dubaib (see chapter 4) was also analysed.

Clay and tuyères	SiO <sub>2</sub>	Al <sub>2</sub> O <sub>3</sub>	FeO	TiO <sub>2</sub>	MnO	CaO	MgO	K <sub>2</sub> O	P <sub>2</sub> O <sub>5</sub>	S
HAC 1 (local clay)	54.8	17.7	6.39	1.22	0.09	12.4	4.03	2.89	0.15	0.28
HAC 2 (tuyère nozzle)	61.8	9.1	3.41	0.74	0.06	20.2	1.8	2.49	0.29	0.12
HAC 3 (tuyère body)	55.1	12.6	4.55	0.91	0.05	19.8	3.05	3.12	0.21	0.6
average	57.2	13.2	4.78	0.96	0.07	17.5	2.96	2.84	0.22	0.33

Table 17. Bulk chemical composition (major elements) of the Lisan clay local to Hammeh and two Hammeh tuyères. Analysis by (P)ED-XRF (slag\_fun calibration method, April 2005). Values are averaged over two repetitive readings per sample, expressed in wt%, and normalised to 100%.

Clay and tuyères	Ni	Cu	Zn	Rb	Sr	Y	Zr	Ba	Pb
HAC 1 (local clay)	60	30	110	80	230	30	340	160	5
HAC 2 (tuyère nozzle)	35	20	70	40	330	25	450	160	5
HAC 3 (tuyère body)	40	20	80	60	270	25	440	190	5
average	45	23	87	60	277	27	410	170	5

Table 18. Bulk chemical composition (trace elements) of the Lisan clay local to Hammeh and two Hammeh tuyères. Analysis by (P)ED-XRF (slag\_fun calibration method, April 2005). Values are averaged over two repetitive readings per sample, and expressed in ppm (parts per million).

Chemically, the local clay and the Hammeh tuyères match quite well, both in the major elements (Table 17) and in the trace elements (Table 18). This is consistent with the fact that most structures and ceramic objects in this region, such as mudbricks for houses, both in antiquity and today, are made from this local clay. The small discrepancies between the three individual samples probably reflect (expected) differences between batches of clay used in the tuyère construction,

as well as between the clay used in antiquity and that sampled near Dubaib. Postdepositional processes (for example, the prolonged proximity of the tuyères to ash and charcoal as well as the lime-rich surrounding soil) may also have influenced the exact composition of each sample. It is exactly to both incorporate and balance out these discrepancies that the average values from the three samples together are used in the calculations concerning the contribution of technical ceramic to the slag formation discussed below.

### Other Square Section Tuyères in the Near East

The oldest square section tuyère known from the region was found during the 1998 excavation season at Tell Abu al-Kharaz, a large multi-period site only a few kilometres to the north of Hammeh in the Jordan Valley. This tuyère dates to ca. 1600 BC, thereby predating the Hammeh tuyères by more than 600 years, and is related to bronze (re)working, according to Peter Fisher, the director of the excavations. The fragment constitutes the rear end (outside a furnace or hearth) of a tuyère, and is very similar in size, shape, and bore to (that part of) the tuyères found at Hammeh (Peter Fischer, personal communication).

In 2003, more square section tuyères dating to the 9<sup>th</sup> century BC, were found during the excavation of the smithy at Beth-Shemesh, which are almost identical in design to the Hammeh tuyères (for further discussion on these artefacts, see page 108).

A single square section tuyère (actually slightly rectangular) from an Assyrian smithy was excavated in the citadel of Tel esh-Shari'a, a site in the northern Negev, Israel. This tuyère dates to the late 7<sup>th</sup> or early 6<sup>th</sup> century BC, and is relatively similar to the Hammeh tuyères in design (Rothenberg and Tylecote 1991). It measures 3 x 4 cm in diameter, has a 1 cm diameter bore, and interestingly it was found *in situ* together with a tuyère of round section, otherwise similar in measurements. According to Rothenberg and Tylecote, both tuyères were in secondary use, and made of the same clay used in the construction of the hearth.

In spring 2004, two more square section tuyères were discovered during the Leiden University excavations on Tell Deir 'Alla, 2.5 km to the west of Hammeh. These date to the 6<sup>th</sup> century BC, and are virtually indistinguishable in size and shape from the Hammeh tuyères (Figure 28). They were not found in a production context, and can as such not be assigned to a specific metal or process (Gerrit van der Kooij, personal communication), but their resemblance to the Hammeh



tuyères does show that tuyères of a square section design are still used long after the Hammeh production ceased.

The author performed an initial inspection in November 2004 of material found during the 1996 excavation season at Tel Hamid, Israel. This site is located in the coastal plain, a few kilometres from Tel Beth-Shemesh. The material has not yet been analysed, but is very likely related to iron metallurgy, probably smithing. This material,

comprising slags (concavo-convex cakes) and tuyère fragments, dates approximately to the 6<sup>th</sup> century BC (Samuel R. Wolff, personal communication). In interesting contrast to the tuyères mentioned above, the Hamid tuyères are round in section.

Square and rectangular section tuyères, some quite resembling the Hammeh ones, furthermore appear in Phoenician contexts, both in late 6<sup>th</sup> century Carthage (Docter *et al.* 2003, 60-65; here the tuyères are rectangular and have two parallel bores) and in 900-700 BC Phoenician-contact contexts in the Huelva province in Southern Spain (González de Canales Cerisola *et al.* 2004). In this light, it is interesting to note that in 6<sup>th</sup> century Deir 'Alla there is archaeological evidence for Phoenician contact (Gerrit van der Kooij, personal communication). However, this observation is not intended to suggest that a square shape is in any way necessarily related to Phoenician contact. The archaeological context of the tuyères and iron production at Hammeh certainly offers no indications for any such contact, and the presence of the square section shape in several periods and in the context of different metals rather suggests a local origin and tradition of the shape.

### Summary and Discussion

The first observation concerning the abundant Hammeh tuyères is the fact that they are very uniform, and quite intricately crafted, suggesting a high level of standardisation that may reflect on concepts of efficiency or control and organisation. This standardisation simultaneously points towards a well-established and probably large-scale production of the tuyères. The second observation regarding the tuyères is their square section. There is no metallurgical requirement for such a square shape, but equally, there seems to be no

detrimental effect from this shape on the operation of the tuyères in the Hammeh process, e.g. since the Hammeh tuyères simply melt off, which is reflected in their molten nozzles, cracks from differential heat distribution can hardly be a factor.

In terms of manufacture, they must represent a larger work effort than a round shape, as the square shape can obviously not be easily created by rolling. Creation of that shape in a mould would still be more labour intensive, judging by the making of modern-day mudbricks in moulds. This raises the question why the Hammeh smelters chose this particular design. On a practical level, the square shape may relate to easier fitting in a furnace structure constructed of, for example, (mud)bricks, or may serve to ensure that they do not roll away during their production or the construction of the furnace. It may also relate to considerations of ease of stacking for storage or even transport.

It is tempting to suggest that the square shape of the Hammeh tuyères may represent an example of *technological style* (see chapter 2), and may even relate to local metallurgical traditions. The 1600 BC bronze related tuyère from Tell Abu al-Kharaz shows at least that the square section shape existed locally prior to the Hammeh smelting operations, and in the context of a different metal. The presence of identically shaped square section tuyères in the Tel Beth-Shemesh smithy shows that the design is also not restricted to just one stage of the iron production process, further strengthening the idea that the square shape may be a local tradition. The presence of the identically shaped tuyères on Tell Deir ‘Alla, now in the 6<sup>th</sup> century BC, shows that the design did not disappear with the iron smelting activities at Hammeh, another argument suggesting a local tradition.

Looking at the Hammeh tuyères in the context of technology, several observations can be made as well. From the spatial distribution of the Hammeh tuyères in the excavation, no specific pattern emerges. There is a strong impression that most tuyères are in a secondary or even tertiary position, rather than in their original location within a furnace structure. A few tuyères seem to form a circular pattern, suggestive of a furnace ground plan with multiple tuyères (see NW corner of square A/B7, Figure 24), but none of these can be identified as being *in situ* either. In that respect, the tuyères do not provide much information with regard to a possible reconstruction of a furnace structure.

However, a further observation is that the very small diameter of the bore, combined with the widening of that bore at the rear end, makes the use of

bellows in the air supply of the Hammeh process almost certain, although no remnants of any such implement has been recovered (or recognised) at Hammeh. Additionally, the fact that some tuyère fragments show remains of furnace wall attached to them, both below and above the tuyère proper, clearly indicates that some form of shaft or superstructure must have been present in the Hammeh process. Lastly, the large number of tuyères with heavily molten nozzles, especially when considering their suggested longer original length, suggests that considerable amounts of ceramic material may have been molten off, which then contributed to the composition and formation of the slag. The potentially important role of the technical ceramics in the Hammeh smelting process will be discussed below.

## The Slag

### Introduction

Analysis of the different Hammeh slags seeks to answer a range of questions. The first question is whether these slags belong to the metallurgy of iron, as opposed to that of copper or other metals. The next question treated here is the identification of what stage (or stages) of the iron production process, e.g. smelting, primary smithing, or secondary smithing, is (are) represented in the Hammeh material, in order to confirm or deny the field interpretation and working hypothesis of the Hammeh technology as predominantly smelting. It can be quite difficult to distinguish between smelting, primary smithing, and secondary smithing slags, and interpretation by macroscopic features such as morphology or colour alone is not sufficient (e.g. McDonnell 1983). Although the presence of tapped slags provides a first and important indicator suggesting smelting activity at Hammeh, this needs to be confirmed by analysis of their microstructure and chemical composition. Other varieties of slags are far less morphologically indicative of their origin or place in the production process, and largely depend on chemical and microstructural analyses to allow an interpretation.

The third aim of analysing the slags is to reconstruct the *chaîne opératoire* of the activity or activities that have been identified, for as far as the recovered material will allow. This is especially desirable, as little is known about early iron technology as a whole, and in the Near East in particular (see chapter 3). The macroscopic features, microstructure, and chemical composition form a characterisation of the various materials, and this aids the reconstruction of the

technology under study. From this characterisation, several issues concerning the technology can be addressed, e.g. operating temperature, efficiency of (parts of) the process, and yield of metal.

The characterisation of the different types of slags is presented below. It must be stressed, as will become clear in the discussion of the samples, that any classification into types is an artificial subdivision of materials that actually represent a continuum, within types as well as across types.

### **Quantities and Scale of Operation**

Substantial quantities of slag were recovered during excavation at Hammeh, especially during the 2000 season. Due to lack of equipment capable of handling these quantities, they could not be weighed exactly. The numbers quoted here are thus no more than extrapolations and informed estimates, but are assumed reasonably accurate. The exact amount of iron production related material excavated during the first two seasons is difficult to determine, since molten ceramic material from square IV was sampled as well. As became clear in the 2000 season, this material was mistakenly assigned to iron production (see chapter 4). A rough estimate (10 large bags at 20-30 kilograms each, subtracting the unrelated material from square IV) puts this at around 200 kilograms.

During the third field season in 2000, ca. 500 kilograms of slag (including a small quantity of discarded 'ore' that was counted together with the slag) were excavated, bringing the total weight of slag recovered at Hammeh from all three seasons to around 700 kilograms. The bulk of this material derives from square A/B7, but considerable quantities were also recovered from all other squares and trench-parts. In the last trench opened (trench 3, A/C7 and A/D7), the excavation only (quite literally) scratched the very surface of the slag deposit, but quite high quantities of slag were sampled here. In combination with the estimated depth of the deposit (based on the north-section of A/B7 and south-section of A/D7 in trench 1), it safely can be assumed that a multiple of the presently excavated quantity of slag remains to be found.

More difficult to estimate is how much production material may have disappeared altogether, both in antiquity itself and because of the bulldozer activity in the 1990s (see chapter 4). It is quite possible that debris from a production sequence was (partially) cleared away by the ancient smelters to prepare for a new run. Such clearing away may range from levelling of the immediate smelting area to more elaborate removal of debris and depositing it elsewhere. This may take

place on the tell, close to the tell, or even at some distance away from the tell. The occurrence of slag deposited in heaps at varying distances around a production area is well attested in European examples such as Baratti Beach, Populonia, Italy (see Pleiner 2000, 38, 39). If such removal of debris to a location outside the tell took place at Hammeh, the intensive agriculture surrounding the site today has most likely removed any trace. Two brief surveys (walking the fields immediately surrounding Hammeh), in late 1998 and preceding the excavation in 2000, produced not a single piece of slag from a radius of 750 metres around the tell. Based on the estimated size of the original tell, it is further assumed that at least half the original production area is no longer there. Both factors are important to keep in mind when looking at the possible yield of metal and scale of the operations.

The ca. 700 kilograms were excavated in just a few squares and trench-parts, which when taken together form no more than five to 10 percent of the estimated original production area. Extrapolating the quantities of slag excavated thus far to the original production area, using the estimated yield of iron metal per unit of ore, shows that more than 10 tons of iron metal may have been produced on the site, in a period of less than 200 years. As shown on page 210, 100 kg of average Mugharet al-Warda ore produces 57.5 kg of slag and ca. 47 kg of iron metal, which means that the excavated 700 kg of slag corresponds to ca. 570 kg of iron metal. At the most cautious estimate, if one assumes that 10 percent of the original total production area has been excavated thus far, this translates to a total production of metal of ca. 5.7 tons. However, if one assumes that only 5 percent of that area has been excavated thus far, which in my opinion is closer to the truth, the present quantity of slag extrapolates to almost 11.5 tons of iron metal. Such quantities show that the smelting activities at Hammeh were a well-established and large-scale operation, as opposed to an early attempt or experimentation with a new technology. From the fact that the metalworkers at Hammeh were able to perform and sustain such a large-scale operation over a considerable period of time one can conclude that they must have had full access to (and control over) the resources necessary in the process, particularly the ore.

### **Classification and Sampling**

Looking at the outer characteristics of the Hammeh slag, a plethora of different types seems to be represented. The slags range from dense, dark black-grey and relatively shiny slags with a clear flow structure, via similar but more string-

shaped and less shiny black-grey slags, through less dense, black and greenish black glass-like ceramic-rich slags, to amorphous rusty lumps. In addition, there is a small range of solid (as well as layered) slag in the shape of 'cakes'. Based on the assemblage of material excavated during the 1996 and 1997 seasons, a working classification of the slag was developed, which was adjusted during the 2000 season. This original working classification is shown in Table 1) and was subsequently further refined during the study and selection of samples in 2001.

Slag			
Magnetic		Non-Magnetic	
Strong	Weak	High Density	Low Density
Group A: Black/grey flow (tapped structure)	Group C: Black/grey flow (tapped, stringy structure)	Group E: Black/grey flow (tapped structure, glassy)	Group G: Black glassy (flowing structure)
Group B: Rusty lumps (with a slag core)	Group D: Rusty lumps (with a slag core)	Group F: Slag-cakes (concavo-convex and layered)	Group H: Green glassy (flowing structure)

Table 19. Initial classification of the Hammeh 2000 slag samples, based on macroscopic characteristics, as used during the 2001 sampling.

The initial classification of the material was structured along those macroscopic features that were easily observed in the field, and which were considered diagnostic, such as shape, colour, density, and magnetism (see chapter 6). These considerations are based on the 'manuals' of Hans-Gert Bachmann (Bachmann 1982) and Gerhard Sperl (Sperl 1980). Classification based on external appearance is common practise in the study of metallurgical production finds, simultaneously providing the first stage of such research, as well as a framework to structure subsequent analyses (e.g. Chirikure and Rehren 2004, 140-142). During the 2001 sampling, five samples were selected from each of the macroscopically defined groups and subgroups, which are shown in Table 19.

The subsequent laboratory analyses of the various slags made it clear that several of the macroscopically separated groups and subgroups must now be considered superfluous. Some of the assumed diagnostic differences turned out not to be related to a different origin within the process, but rather to slight variations in the slags' solidification history.

The most important example of superfluous division is the separation that was originally made between magnetic (groups A), weaker magnetic (groups C) and non-magnetic (group E) tap slags. This division was made in view of the fact that magnetism is potentially an important distinguishing factor between primary

(smelting and smithing) and secondary (smithing) slag. Free iron oxide in smelting slag tends to be in the form of wüstite ( $\text{FeO}$ , non-magnetic) only, whilst the more oxidising circumstances during smithing will let this free iron oxide revert to magnetite ( $\text{Fe}_3\text{O}_4$ , which is magnetic). As it turned out, many of the magnetic tap slags (group A) showed formations of magnetite in the 'skin' of the slag, resulting from contact with the outside air (oxygen) before and during solidification, and the rapid cooling resulting from that contact. Below their surface, however, these slags are all but impossible to differentiate from their weaker magnetic (group C) and non-magnetic counterparts (group E), and all tap slags are now treated as one group.

Two further ideas arose whilst excavating and were captured in the separation into different groups during sampling. The first idea that came up during the field season was that a proportion of the rusty slag lumps (the less magnetic group D) might represent ore in an incomplete stage of reduction, i.e. a semi-reduced furnace charge from above the reaction zone of a bloomery furnace, as described by the late Dietrich Horstmann (Thilo Rehren, personal communication). Others (assigned to the more magnetic group B), might have been either in direct contact with or even been part of the bloom. The adhering rust of these samples would be the result from re-oxidation of iron metal from that bloom. This almost-bloom material is often referred to as so-called 'gromp' or 'crown material', i.e. corroded furnace material that is rich in metallic iron, and contains inclusions of slag and charcoal (Chirikure and Rehren 2004, 142). However, the subsequent analysis of these samples revealed no significant difference between the various rusty lumps, other than that some of them are more magnetic (group B) and others less or not at all (group D), as will be discussed below. Groups B and D, therefore, which together represent a range of ore in various stages of reduction, are also treated as a single group.

The second idea that came up during excavation was that all slag types represent a sliding scale or continuum of 'stages' between proper metallurgical slag (i.e. predominantly resulting from the reduction of ore) and proper technical ceramics (i.e. predominantly resulting from the melting off of furnace wall or lining and tuyères). Several of these latter 'slags' strongly resemble the colour and density of the molten and sometimes vitrified ceramic seen on the nozzles of many tuyères. To cover these more 'ceramic-rich' stages of slag, groups G (more slag-like) and H (more ceramic-like) were sampled, representing this continuum. The subsequent study of these two groups did confirm their ceramic origin as well as

the supposed continuum of compositions between more ceramic-rich and more iron oxide rich. However, this observed continuum simultaneously stresses the close relation between these samples, rather than revealing significant differences between the two groups. Therefore, groups G and H are also treated as a single type.

Further changes in the initial classification had to be made with regard to group F, the concavo-convex slag-cakes, which were found, as discussed below, to result from primary smithing activity. During the laboratory analyses it became clear that one sample from this group was incorrectly interpreted as a primary smithing slag. This specimen represents an important and different type of slag, and a new type was therefore created in the classification: *furnace bottom slag*. The reassessment of the initial classification groups as well as the creation of a new group, based on the considerations outlined above, has resulted in a new and hopefully final classification of the Hammeh slag material. This new classification, which is shown in Table 20, will guide the further description of analyses presented in the rest of this chapter.

Hammeh Slag Types				
Tap slag	Furnace Slag	Furnace Bottom Slag	Primary Smithing Slag	Ceramic-rich Slag
Black/grey flow, dense with a tapping structure and varying degrees of magnetism (former groups A, C, and E)	Rusty lumps with a slag core (former groups B and D)	Slag-cake, with a layered structure	Slag-cakes, with a concavo-convex shape (former group F)	Black and green glassy, not very dense, with flowing structure (former groups G and H)

Table 20. Final classification of the main slag groups found at Tell Hammeh.

Besides the various slag groups discussed above, and based on the material excavated in the 1996 and 1997 seasons, the original working classification also contained a group called ‘furnace material’. These samples were at that time assumed to represent non-molten and unvitified remnants of furnace wall, i.e. technical ceramics. As it turned out, all material constituting this group was excavated from square IV, which was found to be unrelated to the iron production activities during the 2000 season. No further material was recovered in 2000 or during the sampling in 2001 that could be assigned to this group, and the group, therefore, was excluded from the subsequent research. Nevertheless, both the ceramic-rich slags (former groups G and H), with an origin in technical ceramics, and the tuyères as such do represent the furnace structure (or tuyère) material.



## Analysis of the Slag Groups

### *Furnace Slags (Incompletely Reduced Ore)*

The furnace slags make up about 30 percent of all slag at Hammeh. This type consists of rusty lumps of heterogeneous slag material and partly or hardly reduced haematite ore, covered in and penetrated by large quantities of rust (Figure 29). Some of the rust may have formed or changed postdepositional, and preserves organic material. Some of this organic material may be fragments of charcoal from the charge, but this is unclear. The density of these slags is similar to that of the tap slag (up to  $4 \text{ g/cm}^3$ ).

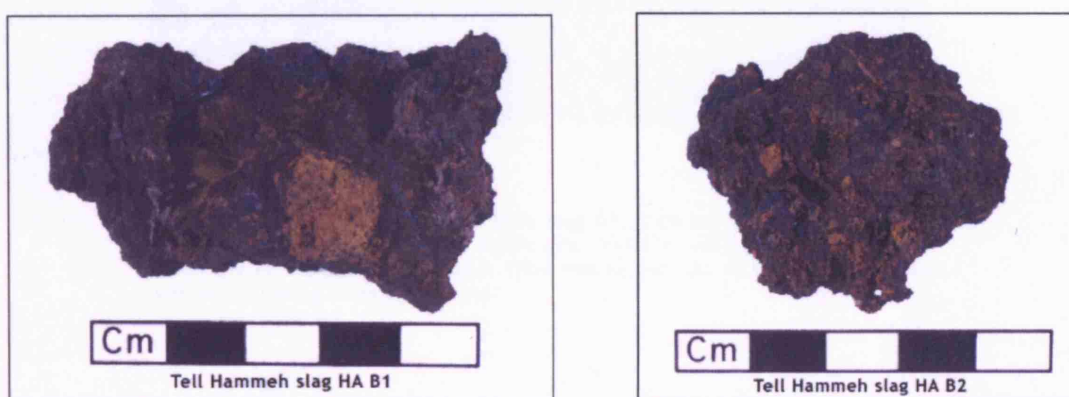


Figure 29. Furnace slags B1 and B2, showing the rusty exterior of the samples, with organic material embedded in the rust (both samples) and a lump of adhering ceramic (sample B1).

The microstructure of these samples varies widely. Some samples show areas of uncorroded slag material (glassy matrix with wüstite dendrites), surrounded by corrosion products such as goethite and maghemite ( $\gamma\text{-Fe}_2\text{O}_3$ ). Others contain almost completely unreduced ore or areas of ore in the process of reduction. With the first set of furnace slags, large quantities of wüstite dominate the microscopic view. Occasionally iron metal appears, still in the same shape as wüstite, and in some places, iron hydroxide ( $\text{FeOOH}$ ) replaces the metal. These hydroxides, like the metal, are xenomorphic, i.e. they retain the shape of the original material (Figure 30).

Taken together, these phases indicate a stage of the smelting operation where raw material is in the process of being reduced (as opposed to, for example, iron metal burning off during secondary smithing). Besides the metallic inclusions, there are also tiny droplets of iron sulphide ( $\text{FeS}$ ) interspersed between the olivine laths. It is possible to identify these samples as an incompletely reduced ore, or 'furnace slag'.

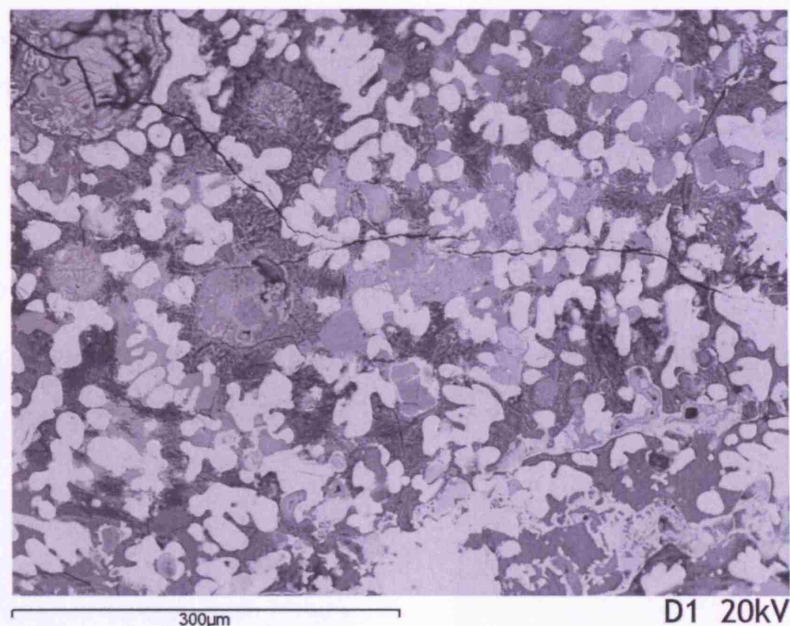


Figure 30. BSE micrograph of furnace slag D1, showing wüstite (egg-shaped, light grey), xenomorphic iron hydroxide (FeOOH, mid grey), and a few inclusions of metallic iron (white). The matrix consists of variations of glass with precipitating laths (dark grey).

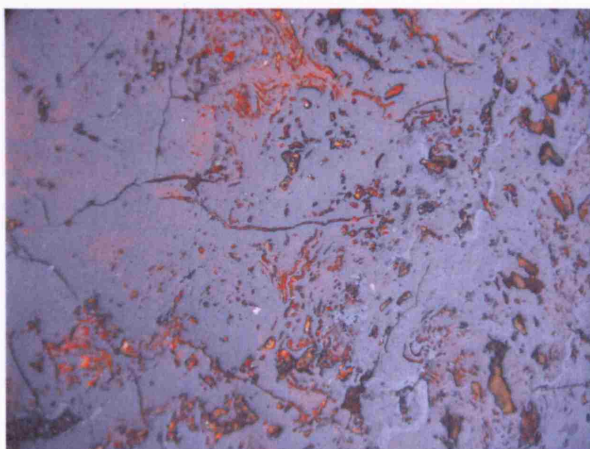


Figure 31. Cross Polarised Light Micrograph of furnace slag B4, image width ca. 1.8 mm, showing massive haematite ore with formations of goethite (indicated by the orange internal reflections). The cracks in the otherwise solid haematite indicate the first stages of breaking up of the ore through roasting.

In the second group of furnace slags, a relationship with the ore is unmistakable, as indicated by the presence of unreduced haematite ore (Figure 31), and areas of partially reduced ore (Figure 32). In some areas, the haematite is turning into wüstite, a further indication that these samples represent varying stages of reduction in progress. In some areas of some of these samples, partially dissolved quartz can be observed as well as fayalitic laths.

The haematite seen in Figure 31 shows cracks in the otherwise massive ore, indicating roasting effects, in this case the initial stage of breaking up of the ore structure. Breaking the ore into smaller bits through roasting takes place at temperatures between 500 and 800 °C (see chapter 3, page 52). This sample (B4),



in combination with the more reduced and slag-forming samples that indicate higher temperatures, clearly shows that the Hammeh process must have featured several temperature zones, and suggests that roasting took place as part of the smelting process proper, rather than in a separate process preceding the smelt. The iron hydroxides observed in these samples (see Figure 31 and Figure 32) are probably related to postdepositional processes, similar to the heavy oxidation of the surface of these samples.

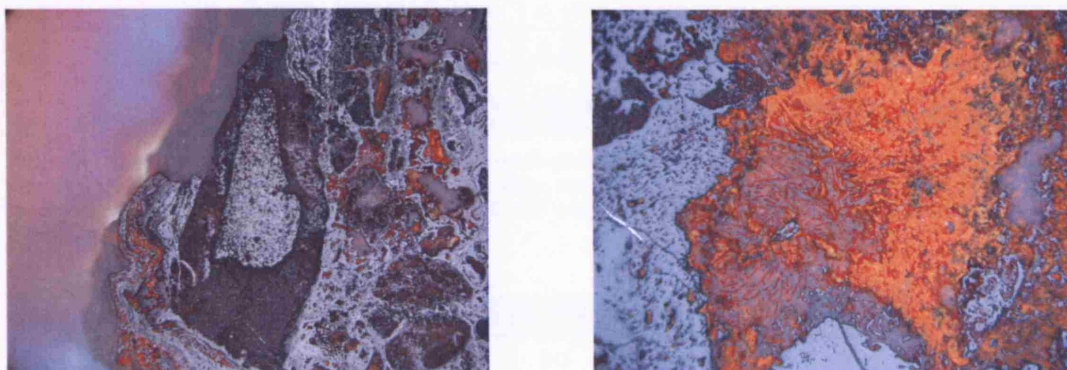


Figure 32. Cross Polarised Light Micrographs of furnace slags B3 (left, image width ca. 1.8 mm), showing a fragment of unreduced haematite contained within formations of iron hydroxides (banded structures), and B4 (right, image width ca. 1.8 mm), showing unreduced haematite (blue-grey, on the left) and (possibly postdepositional) iron hydroxides (possibly goethite ( $\text{FeOOH}$ ) (red-brown internal reflection, centre), and lepidocrosite ( $\text{FeOH}$ ) (orange internal reflection, on the right).

This leads to the suggestion that the variability in reduction stage shown within this group of samples reflects various temperature gradients of pieces of ore moving down the furnace and being reduced progressively, in many instances forming liquid slag, but still needing to lose more iron. It is clear that several non-equilibrium processes are taking place simultaneously, possibly at different locations (and thus temperatures) in the furnace. The presence of such temperature gradients in turn suggests the presence of a superstructure on the furnace.

Chemically, these samples show more variation in their individual bulk composition than the tap slags (see below, page 175), and are characterised by a much lower  $\text{CaO}$  content (average 4.2 wt%), as well as a higher percentage of iron oxide (between 47 to 75 wt%, 70.5 wt% on average; Table 21). Such a composition further underlines an interpretation of these samples being close to the ore. The trace elements of these samples also reflect a relation to the ore (Table 22; see also Table 31 and the discussion on page 190) but simultaneously, through the presence of strontium for example, they indicate a furnace origin of these slag, indicating contact between the charged ore, the fuel, and ceramic material.

Furnace slags	SiO <sub>2</sub>	Al <sub>2</sub> O <sub>3</sub>	FeO	TiO <sub>2</sub>	MnO	CaO	MgO	K <sub>2</sub> O	P <sub>2</sub> O <sub>5</sub>	S
B1	12.4	2.57	76.3	0.18	0.96	4.69	0.87	0.76	0.99	0.28
B2	15.9	4.94	72.4	0.34	0.34	1.89	0.41	1.42	1.88	0.47
B3	14.8	4.04	71.5	0.24	1.22	3.77	0.77	0.95	1.95	0.84
B4	10.9	0.88	85.6	0.08	0.05	1.15	0.21	0.47	0.1	0.51
B5	22.4	4.98	56.0	0.32	1.13	9.57	1.45	1.69	1.69	0.72
D1	18.4	5.41	67.1	0.3	0.87	3.54	0.73	1.24	1.19	1.25
D2	15.7	4.57	72.0	0.27	0.54	3.16	0.78	0.89	1.32	0.8
D3	20.2	3.95	67.8	0.27	0.25	3.84	0.7	1.26	1.22	0.51
D4	18.8	1.98	72.9	0.17	0.24	3.02	0.69	0.61	1.18	0.39
D5	15.4	4.32	66.7	0.22	1.55	7.88	1.12	0.8	1.54	0.45
average	16.5	3.76	70.8	0.24	0.72	4.25	0.77	1.01	1.3	0.62

Table 21. Bulk chemical composition (major elements) of the furnace slags. Note how these samples contain far more iron oxide and far less lime than the tap slags, which brings them closer to the average composition of the Warda ore (see page 147). Analysis by (P)ED-XRF (slag\_fun calibration method, April 2005). Values are expressed in wt%, and normalised to 100%.

Furnace slags	Ni	Cu	Zn	Rb	Sr	Y	Zr	Ba	Pb
B1	bdl	40	50	bdl	570	90	200	80	bdl
B2	bdl	20	160	bdl	460	80	130	bdl	bdl
B3	bdl	20	60	bdl	530	90	150	60	bdl
B4	bdl	50	70	bdl	530	90	170	50	bdl
B5	bdl	5	70	bdl	750	80	130	130	bdl
D1	bdl	50	70	bdl	240	60	110	25	bdl
D2	bdl	40	70	bdl	290	80	120	10	bdl
D3	bdl	50	35	bdl	430	50	160	60	bdl
D4	20	80	25	bdl	200	20	120	bdl	bdl
D5	bdl	70	40	bdl	500	80	110	90	bdl
average	20	43	65	bdl	450	72	140	63	bdl

Table 22. Bulk chemical composition (trace elements) of the Hammeh furnace slags. Analysis by (P)ED-XRF (slag\_fun calibration method, April 2005). Values are expressed in ppm (parts per million).

The chemical variation between individual samples, in line with the microstructure, reflects different stages of reduction, related to location and/or temperature. It is very likely that the magnetism of some of these samples, discussed before (page 166), is strongly influenced by the extensive corrosion rather than representative of any part of the formation history of these specimens.

### Furnace Bottom Slag

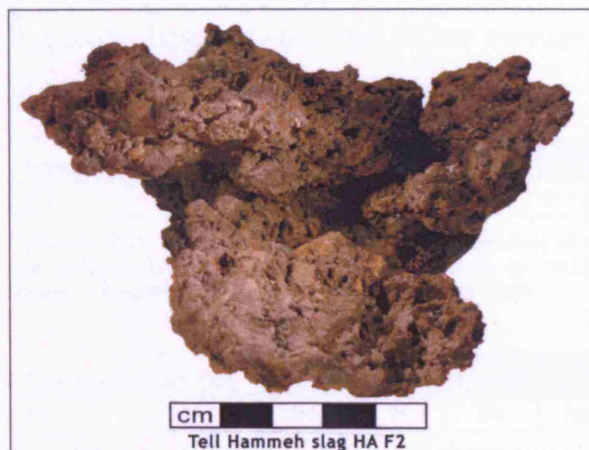


Figure 33. Sample F2, showing a layered structure, with rust and organic material between those layers.

One multilayered sample (F2) resembles the primary smithing slag (discussed below, see page 186), but turns out to be quite different from those samples. Macroscopically, the slag is characterised by a very smooth surface skin that separates from the main slag mass, unlikely to be the result of (primary) smithing, where the surface cools too rapidly for any

separation to occur. The sample has a multi-layered structure that is probably caused by the slag forming in the midst of other material such as charcoal.

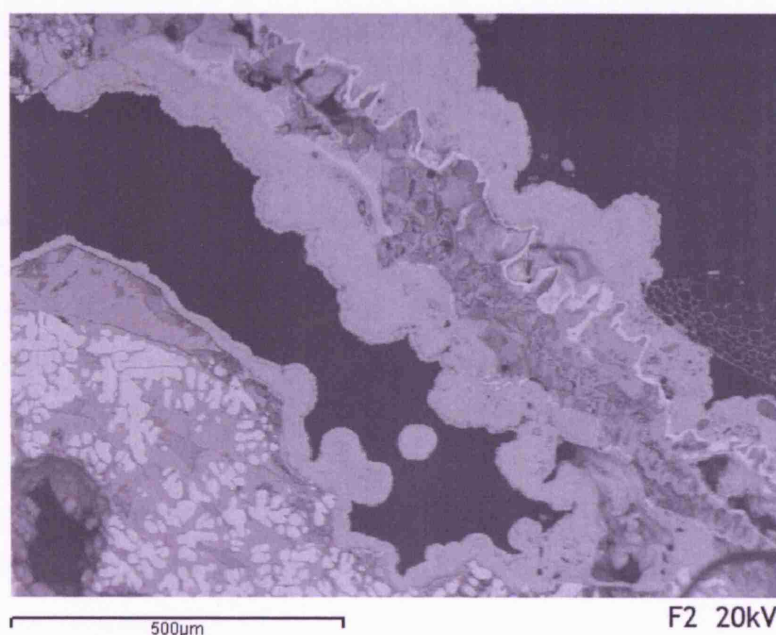


Figure 34. BSE micrograph of sample F2, showing a glassy matrix, (mid-dark grey), with olivine laths (mid grey), and thick dendritic wüstite in the left bottom corner, and a skin of mostly various iron hydroxides (FeOOH) that has partly separated from the slag. The dark areas are voids, and a small piece of attached charcoal can be seen in the centre right of the picture.

Microscopically, this specimen is very rich in unreacted iron oxide, all in the form of wüstite. Only near the skin are bands of magnetite found, some of which seems to be related to haematite. The very dominant and solid wüstite is not the result of reoxidising metal, as no xenomorph shapes are present indicating a reversal of state.



Chemically, this is one of the richest samples in terms of iron oxide with a content of around 70 wt%, analogous to the furnace slags discussed above. Its lime content lies somewhere between that of the average Warda ore (discussed above) and that of the tap slags (discussed below).

Furnace bottom slag	SiO <sub>2</sub>	Al <sub>2</sub> O <sub>3</sub>	FeO	TiO <sub>2</sub>	MnO	CaO	MgO	K <sub>2</sub> O	P <sub>2</sub> O <sub>5</sub>	S
F 2	17.6	2.18	69.6	0.13	0.06	8.10	0.99	1.06	0.21	0.06

Table 23. Bulk chemical composition (major elements) of the furnace bottom slags. Note how these samples are quite similar to the furnace slags. Analysis by (P)ED-XRF (slag\_fun calibration method, April 2005). Values are expressed in wt%, and normalised to 100%.

Furnace bottom slag	Ni	Cu	Zn	Rb	Sr	Y	Zr	Ba	Pb
F2	bdl	20	15	bdl	250	bdl	110	bdl	bdl

Table 24. Bulk chemical composition (trace elements) of the Hammeh furnace bottom slag. Analysis by (P)ED-XRF (slag\_fun calibration method, April 2005). Values are expressed in ppm (parts per million).

It is, therefore, possible to suggest a relation with the furnace slags, and through them with the ore charged to the furnace, perhaps showing the same incomplete reduction of ore characteristics, but with a slightly larger proportion of absorbed ceramic material. It is therefore appropriate to identify this slag as a smelting furnace bottom slag.

### Tap Slags

The Hammeh tap slags are the most common type of slag excavated at Hammeh and make up ca. 60 percent of the total. They are dense (between approximately 3 and 4 g/cm<sup>3</sup>) and black-grey in colour. All show clear flowing patterns that are consistent with being tapped from a furnace structure. The surface of the samples is mostly smooth, with clear runs of slag, sometimes showing 'striation', i.e. a wrinkling of the slag surface into narrow bands as it cools whilst the still fluid core continues to flow (Figure 35, Figure 36). This wrinkling is particularly indicative of tapping, as slower cooling rates inside a furnace prevent this effect from appearing.

Magnetism in these samples ranges from strong, through weak to absent, and where present, the level of magnetism often varies between different areas of the individual samples. The macroscopic features of these slags are quite homogeneous, and all clearly support an interpretation as tapped smelting slag.

In their microscopic constitution, however, the individual tap slags are often less homogeneous. They predominantly show two phases (Figure 37). The first is a glassy matrix with feathery olivine structures (related to fayalite, Fe<sub>2</sub>SiO<sub>4</sub>, but with differing Mg, Mn, and Ca ratios replacing the Fe) precipitating during cooling.

The second phase consists of free iron oxide precipitating from the melt in the form of wüstite ( $\text{FeO}$ ) dendrites. Their fine-grained nature indicates a rapid cooling of the slag.

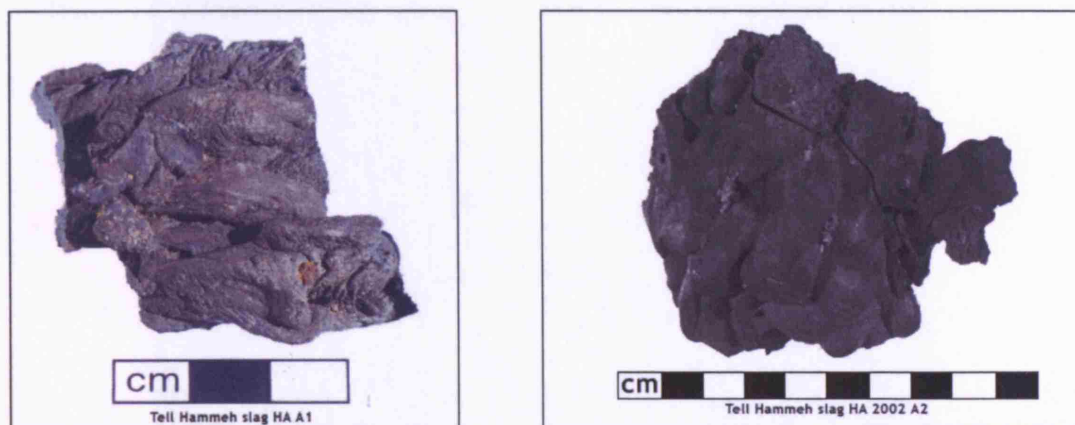


Figure 35. Tap slags A1 and A2, showing free flowing (tapped) structure of the slag (both samples), as well as 'striation' of the surface (sample A1).



Figure 36. Tap slag C2, showing a clear flowing structure with multiple runs of slag. The right bottom shows some contact with soil or furnace wall, and may indicate a vertical flowing, presumably down the outside of a furnace shaft.

Near the surface of the more magnetic samples within this type, crystallisations of magnetite are seen, which result from oxygen penetration on contact with the open air after tapping. Several samples also show a needle-shaped phase (Figure 38), possibly iscorite, an iron silicate ( $\text{Fe}_7\text{SiO}_{10}$ ).

The formation of iscorite often relates to slightly more oxidising conditions than present with the formation of pure fayalite or wüstite, but less than with magnetite. This relation is borne out by the presence of iscorite near the magnetite formations at the surface of the samples.

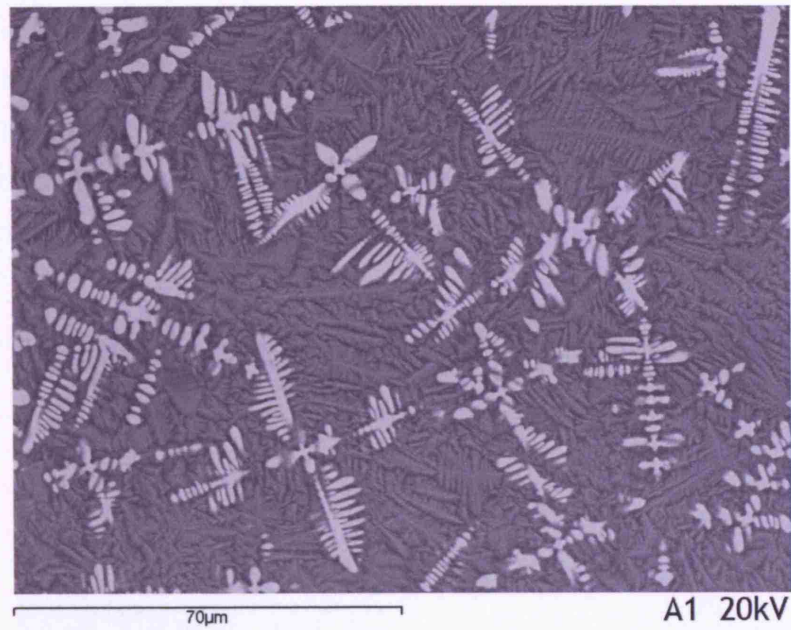


Figure 37. BSE micrograph of tap slag A1, showing a glassy matrix (dark grey), with feathery devitrification (mid-grey) and wüstite dendrites (light grey).

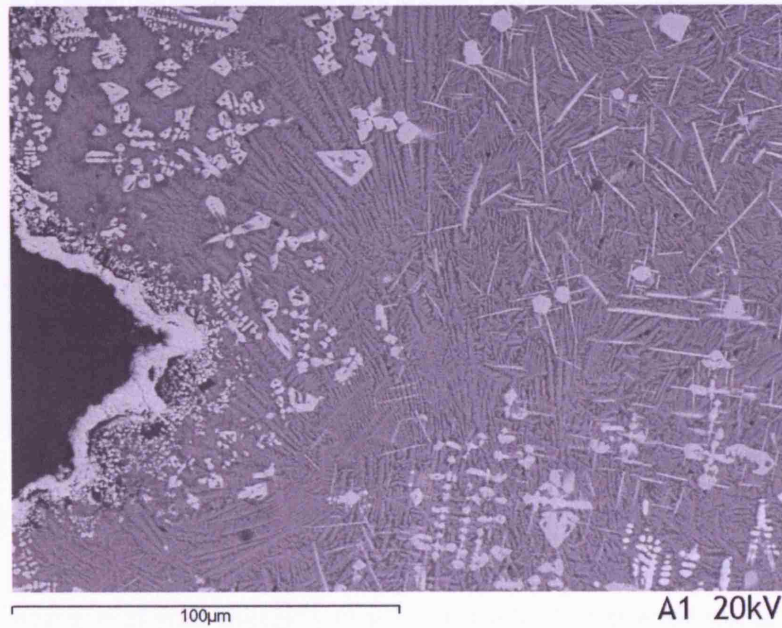


Figure 38. BSE Micrograph of tap slag A1. Showing a glassy matrix (dark-grey), with feathery devitrification (mid-grey), wüstite dendrites (FeO, white), magnetite from oxygen penetration near the surface (light grey), and possible iscorite (Fe<sub>7</sub>SiO<sub>10</sub>, needle-shaped), the black area is the edge of the sample and shows a band of iron hydroxide (FeOOH).



Hercynite ( $\text{FeAl}_2\text{O}_4$ ) or hercynitic spinels also occur occasionally, but less than might be expected given the alumina content of these slags. SEM-EDS analyses indicate that part of the alumina is retained within the glassy matrix (see appendix 2). The presence of hercynite most likely relates to the absorption of technical ceramic material into the slag, rather than from the Warda ore, which is low in both silica and alumina (Table 13).

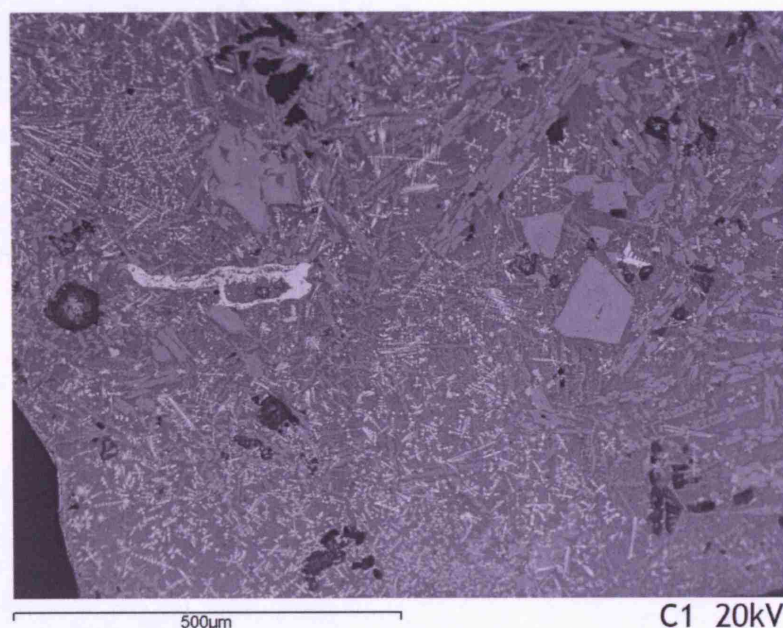


Figure 39. BSE micrograph of tap slag C1, showing an aggregate of metallic iron (pan-shaped, whitish) in a glassy matrix with olivine and pyroxene laths (dark-mid grey), groups of thin wüstite dendrites (light grey) and some zoned hercynitic magnetite (block-shaped, mid-grey). Some of the hercynite spinels are zoned, with a darker core of more hercynite component and a rim of magnetite. The black areas are pores in the sample.

Less magnetic samples show slightly larger quantities of second generation wüstite in a glassy matrix with fayalitic or pyroxene ( $(\text{Ca,Mg,Fe})_2\text{Si}_2\text{O}_6$ ) laths. The small size of the wüstite is indicative of rapid cooling, which together with the presence of 'tapping bands' confirms the macroscopic identification of tapping. Some of the wüstite in these samples is in the process of transforming to metallic iron, and an occasional particle of iron metal is observed, as well as tiny droplets (Figure 39). Occasionally larger amounts of hercynite can be found as well.

The non-magnetic samples within the tap slag overall reveal a more homogeneous fayalitic matrix, with occasional clusters of second generation wüstite (Figure 41). They are very lean and glassy at the edges, with very thin tapping bands (Figure 40), all pointing at rapid cooling of a material that is likely rich in absorbed vitrified ceramic and quartz.

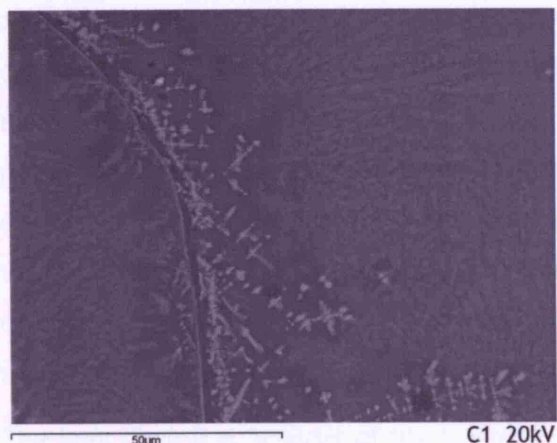


Figure 40. BSE micrograph of tap slag C1, showing a tapping band between two flows of slag. The edges of these flows consist predominantly of a glassy matrix (grey) with small formations of fayalitic laths (lighter grey) and some precipitation of thin wüstite dendrites (light grey) where the two flows touch.

Within this group, four samples stand out, illustrating the fact that any proposed grouping is an arbitrary division along a continuum of possibilities. Sample E1 seems to have been tapped too early compared to the other tap slags. It is quite rich in first generation wüstite, but shows hardly any iron metal or hydroxide formations. This particular sample seems to lean more towards ‘raw material’ that has not been fully reduced. This is reflected by a high

iron oxide content (around 63 wt%), indicating that not enough iron oxide has yet been reduced to iron metal and remains trapped in this slag.

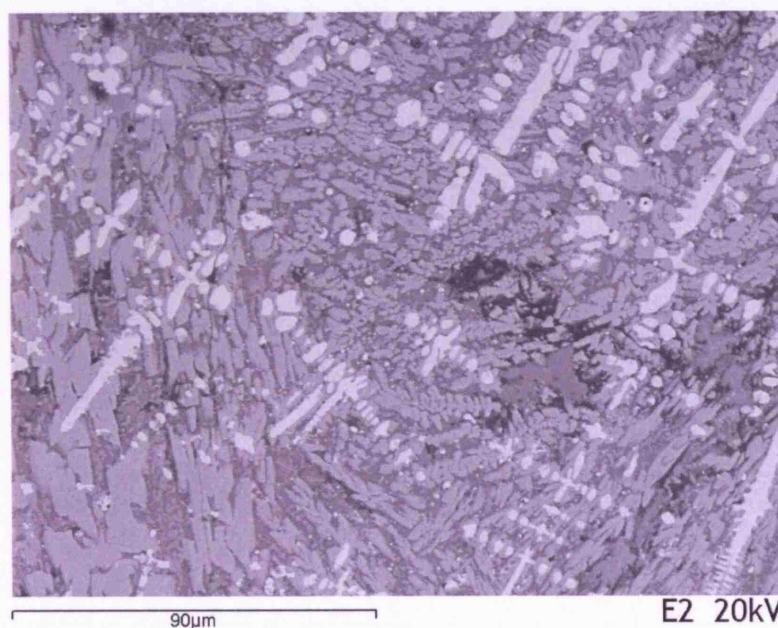


Figure 41. BSE micrograph of tap slag E2 showing skeletal fayalitic/olivine laths (mid-grey) in a glassy matrix (darker grey), with small dendritic wüstite (light grey). Tiny droplets of probable FeS (lightest grey) are interspersed between the laths.

Sample E3 turned out to be more ceramic in origin, and consists almost completely of an olivinic glassy matrix. It is extremely lean, with almost equal amounts of iron oxide and lime (20 wt% to 18 wt%). It presents a clear example of the aforementioned continuum, and as a transitional sample could also be classified with the ceramic-rich slags (discussed below). Therefore, these two

samples are not used for the calculation of the overall average bulk and trace composition of the tap slags (Table 25). Other samples can be considered to differ from the mean composition as well, i.e. A2 and C3. These samples, however, predominantly differ from the other tap slags in their chemistry and not in their external characteristics or microscopy. As they only marginally alter the averaged values, these have been retained in the calculations. It is likely that their divergent compositions are the result of similar relations to ore and ceramic respectively as samples E1 and E3.

The bulk chemical analysis of the Hammeh tap slags (Table 25) is consistent with a lean smelting slag. The CaO content (on average 10.9 wt%, up to 14 wt%) of the samples in this group is relatively high in comparison to ‘regular’ bloomery slag, whilst the iron oxide content is quite low, ranging from 40 to around 70 wt%, with an average around 52%. Regular fayalitic bloomery slag generally has between 1 and 4 wt% CaO, and 50 to 70 wt% FeO (e.g. compare bloomery slag from the Dietzhöhlztal, Germany Kronz 1998, 226-228).

Tap slags	SiO <sub>2</sub>	Al <sub>2</sub> O <sub>3</sub>	FeO	TiO <sub>2</sub>	MnO	CaO	MgO	K <sub>2</sub> O	P <sub>2</sub> O <sub>5</sub>	S
A1	24.55	5.67	52.68	0.35	1.29	10.85	2.17	0.99	1.14	0.31
A2	16.42	3.85	68.8	0.23	0.74	6.70	1.17	0.72	1.18	0.19
A3	20.09	5.22	61.61	0.31	1.24	7.27	1.34	0.89	1.33	0.70
A4	21.08	5.37	59.73	0.30	1.25	8.35	1.50	0.80	1.25	0.36
A5	20.7	4.75	59.8	0.26	1.01	9.54	1.44	1.19	1.10	0.21
C1	27.73	5.96	47.15	0.40	1.19	12.43	2.52	1.14	1.16	0.33
C2	23.03	5.77	55.72	0.33	1.30	9.36	1.94	1.00	1.32	0.23
C3	33.21	5.55	33.97	0.43	0.89	19.68	2.72	2.31	1.11	0.13
C4	27.08	4.76	49.73	0.29	1.12	12.55	1.81	1.13	1.33	0.21
C5	20.99	6.34	58.7	0.33	1.44	7.95	1.63	0.79	1.31	0.50
E1	17.78	2.98	58.28	0.17	1.71	13.81	3.09	0.59	1.44	0.15
E2	30.7	5.61	46.95	0.38	0.89	10.83	1.33	1.11	1.18	1.02
E3	45.67	6.61	21.11	0.47	0.87	19.01	2.88	2.17	0.79	0.43
E4	33.97	6.46	40.76	0.44	1.00	12.71	1.76	1.29	1.12	0.48
E5	27.6	5.43	47.1	0.39	1.21	13.51	2.07	1.20	1.08	0.40
average	25.17	5.44	52.52	0.34	1.12	10.9	1.80	1.12	1.20	0.39

Table 25. Bulk chemical composition (major elements) of the Hammeh tap slags. Note the progressive leanness from samples A to samples E. The overall tap slags average does not include samples E1 and E3. Analysis by (P)ED-XRF (slag fun calibration method, April 2005). Values are expressed in wt%, and normalised to 100%.



Tap slags	Ni	Cu	Zn	Rb	Sr	Y	Zr	Ba	Pb
A1	bdl	40	50	bdl	570	90	200	80	bdl
A2	bdl	20	160	bdl	460	80	130	bdl	bdl
A3	bdl	20	60	bdl	530	90	150	60	bdl
A4	bdl	50	70	bdl	530	90	170	50	bdl
A5	bdl	5	70	bdl	750	80	130	130	bdl
C1	bdl	20	40	bdl	590	90	240	90	bdl
C2	bdl	30	35	bdl	850	90	190	90	bdl
C3	bdl	40	30	10	1080	60	260	180	bdl
C4	bdl	45	100	bdl	590	90	200	140	bdl
C5	bdl	30	45	bdl	580	110	170	60	bdl
E1	bdl	35	25	bdl	710	70	120	50	bdl
E2	bdl	25	60	bdl	450	80	240	120	bdl
E3	bdl	10	20	20	820	80	330	150	bdl
E4	bdl	20	40	bdl	720	80	270	150	bdl
E5	bdl	25	35	bdl	640	70	230	160	bdl
average	bdl	28	61	10	642	85	198	109	bdl

Table 26. Bulk chemical composition (trace elements) of the Hammeh tap slags. The overall tap slags average does not include samples E1 and E3. Analysis by (P)ED-XRF (slag\_fun calibration method, April 2005). Values are expressed in ppm (parts per million).

The very low trace of copper in these samples (50 ppm and less; Table 26), clearly indicates that they cannot be related to copper smelting, but must be from iron production. Slags from a copper production process can be very similar to those of iron, but are characterised by larger amounts of Cu, from 0.3 wt% up to several percent. The trace of copper, present in all Hammeh slags, probably derives from the ore and technical ceramics in roughly equal measures, and is discussed in more detail on page 190.

This slag type as a whole is undoubtedly iron smelting tap slag, as evidenced by its morphology, chemistry, and microstructure. It does show a range of variation in the chemical and mineralogical constitution between samples and within individual samples themselves. This is quite common in early bloomery slag and is only to be expected in a highly complex process, where not all factors are necessarily under optimal control, and where conditions are not in equilibrium (see page 190). The presence of relatively large quantities of CaO in these slags further affects the solidification processes as well as the temperature range in which these slags form (Kronz 1998, 124).

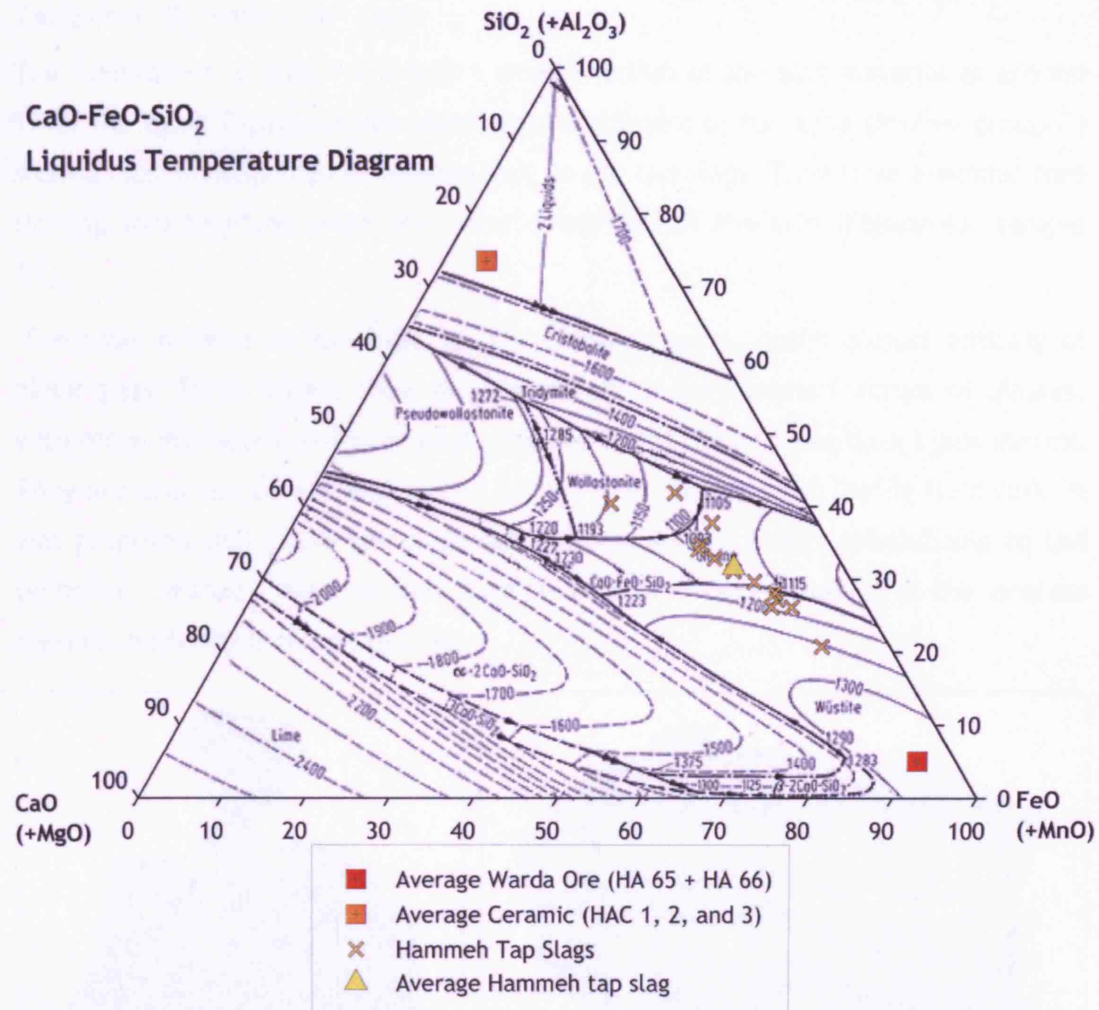


Figure 42. The tap slags plotted in the CaO (+MgO) - FeO (+MnO) - SiO<sub>2</sub> (+Al<sub>2</sub>O<sub>3</sub>) liquidus temperature diagram, indicating their solidification temperature. The linear spread of the samples illustrates that they form a continuum of compositions, ranging between ore like (FeO+MnO corner) and more ceramic like (SiO<sub>2</sub>+Al<sub>2</sub>O<sub>3</sub> corner). Most samples cluster in a (minimum) temperature area of between 1100 and 1150 °C.

The continuum of compositions is easily seen in Figure 42, which plots the main chemical compounds of these slags (together forming over 97 % of the total composition) in the CaO-FeO-SiO<sub>2</sub> ternary diagram. It is clearly visible how the samples range from iron oxide rich (FeO corner) to ceramic component rich (towards SiO<sub>2</sub>/CaO edge). What this range of compositions means in terms of relationships between the slags, the technical ceramics, and the Warda ore is discussed below (page 201, ff).

The ternary diagram indicates how the central cluster of the tap slag (and their average) concentrates in a temperature zone of between 1100-1150 °C. This temperature probably corresponds to (or is slightly below) the actual furnace operating temperature that created these slags.

### Technical ‘Ceramic-rich’ Slags

The ‘ceramic-rich’ slags form only a small fraction of the slag material at around 1% of the total. Especially the black glass specimens of this type (former group G) show a close morphological resemblance to the tap slags. They have a similar free flowing structure and even occasional ‘striation’ of the skin (Figure 43, sample G1).

The main difference, however, is that these samples consist almost entirely of black glass. Fresh breaks show the characteristic conchoidal fracture of glasses, with often distinctive swirls of pale green or ‘Delft’ blue in the dark black matrix. They are also less dense (less than 3 g/cm<sup>3</sup>) than the tap slag. During fieldwork, it was proposed that these samples could be slag with a closer relationship to the technical ceramics (tuyères and furnace wall or lining) involved in the process than to the furnace charge proper.



Figure 43. Samples G1 and H1, showing bottom of black glass ‘ceramic’ slag with flow patterns and impressions (G1), and black-green flows of ‘ceramic’ slag with attachment to ceramic material on one side (H1).

Some samples (e.g. G1) do appear to be tapped, and reveal impressions of tiny lumps at their bottom, whilst others may have remained inside the furnace (e.g. H1), and were attached to ceramic material. (Figure 43) Chemical and microscopic analysis makes clear that these samples are from a shared origin. Like the tap slag, differences between individual samples thus most likely reflect variations in the exact moment and location of their solidification, rather than fundamental differences that warrant further subdivision of this type.



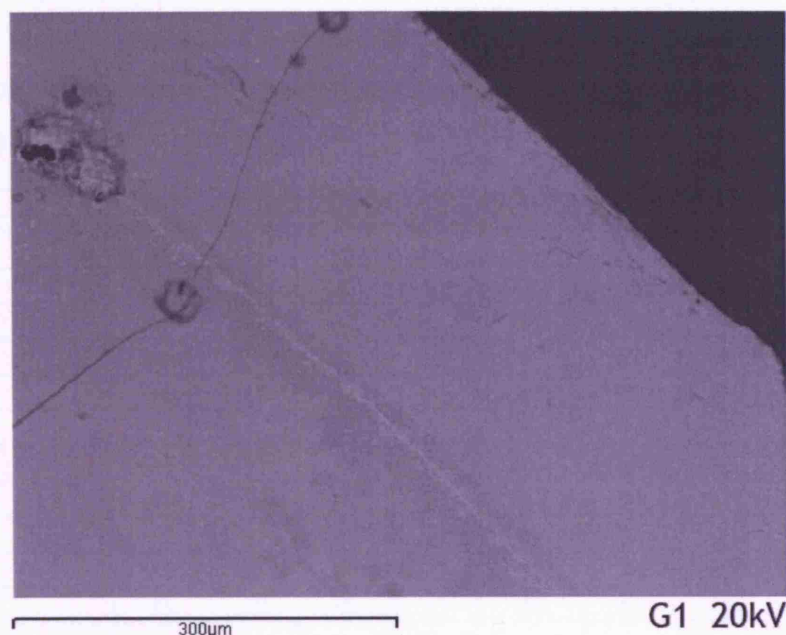


Figure 44. BSE micrograph of 'ceramic-rich' slag G1, showing an amorphous mass of glass and a thin tapping band of iron oxide or hydroxide (possibly wüstite) flanked by darker conglomerates of glass that is richer in  $\text{Al}_2\text{O}_3$  and  $\text{K}_2\text{O}$  than the matrix.

Microscopically, all samples show an almost clear glass matrix, with only sporadic precipitation of extremely thin wüstite dendrites and even rarer fayalitic/pyroxene laths, and a few almost completely dissolved grains of quartz. This microstructure represents a relatively high temperature during formation, a high level of absorption of ceramic material, and fast cooling on tapping.

Ceramic-rich slags	$\text{SiO}_2$	$\text{Al}_2\text{O}_3$	$\text{FeO}$	$\text{TiO}_2$	$\text{MnO}$	$\text{CaO}$	$\text{MgO}$	$\text{K}_2\text{O}$	$\text{P}_2\text{O}_5$	S
G1	38.2	6.01	27.1	0.44	0.93	20.6	3.54	1.86	1.11	0.17
G2	38.9	5.70	26.2	0.42	0.88	21.3	3.58	1.87	1.04	0.15
G3	38.1	6.43	32.1	0.50	1.08	17.0	2.25	1.57	0.88	0.13
G4	40.8	6.75	27.4	0.47	1.09	17.3	2.61	1.87	1.21	0.47
G5	36.3	5.06	29.6	0.43	0.54	23.3	2.53	1.25	0.81	0.15
H1	51.9	4.93	17.1	0.42	0.62	20.3	2.38	1.66	0.55	0.14
H2	55.1	5.82	17.3	0.51	0.51	16.7	1.86	1.63	0.53	0.10
H3	60.3	5.31	9.40	0.50	0.24	19.5	2.34	1.68	0.39	0.33
H4	48.4	6.13	19.6	0.49	0.60	19.9	2.40	1.68	0.64	0.14
H5	49.0	6.89	18.4	0.55	0.65	19.5	2.47	1.73	0.68	0.16
average	46.39	5.98	21.3	0.48	0.69	19.6	2.48	1.7	0.74	0.21

Table 27. Bulk chemical composition (major elements) of the ceramic-rich slags. Note how these samples contain far more silica and lime, and less iron oxide than the tap slags, which brings them closer to the average composition of the local clay and tuyères (see page 159). Analysis by (P)ED-XRF (slag\_fun calibration method, April 2005). Values are expressed in wt%, and normalised to 100%.

Chemically, the relation of these samples to the iron production is revealed by the presence of up to 25 wt% iron oxide, and their relation to the technical ceramics by a much higher silica and lime content than the tap slag (Table 27). They also contain a relatively large amount of barium (Table 28), a further indication to their origin in ceramic material.

Ceramic-rich slags	Ni	Cu	Zn	Rb	Sr	Y	Zr	Ba	Pb
G1	bdl	20	25	10	840	70	280	150	bdl
G2	bdl	20	20	10	820	60	270	150	bdl
G3	bdl	20	30	15	640	70	340	190	bdl
G4	bdl	20	20	15	780	90	300	150	bdl
G5	bdl	20	25	10	640	50	290	170	bdl
H1	10	35	35	20	580	50	350	150	bdl
H2	30	30	60	30	500	50	370	180	bdl
H3	30	30	35	30	510	30	370	160	bdl
H4	40	25	50	25	730	50	350	190	bdl
H5	15	20	40	25	680	60	370	200	bdl
average	25	24	34	19	672	58	329	169	bdl

Table 28. Bulk chemical composition (trace elements) of the Hammeh ceramic-rich slags. Analysis by (P)ED-XRF (slag\_fun calibration method, April 2005). Values are expressed in ppm (parts per million).

Some samples of this type (former group H) are more greenish black in colour and more foamy in structure. They are the least dense of all materials, and whether they should be termed 'slag' is debatable. However, they do share a free flowing structure similar to the tapped slag and chemically they do belong to the iron production assemblage. Their colour is very reminiscent of the vitrified nozzles of the tuyères (see below), and it is likely that they are closely related to these or the furnace wall or lining. Microscopically these samples do not reveal much, and are often difficult to study due to their foamy structure. They are less homogeneous than samples from (former) group G, and show many inclusions of thermally cracked and dissolving quartz grains and occasional clusters of tiny wüstite dendrites.

Chemically, these samples do indicate their relation to the metallurgical process in their iron oxide content, which lies around 10 to 18 wt%, which is considerably higher than that of the unvitrified tuyère ceramic or the local clay. An identification of this type of slags as technical 'ceramic-rich' slag, therefore, is justified, where the differences between the various samples once more show a continuum, now between a slightly more slag-like and a more ceramic-dominated origin. Concluding from the combination of characteristics described above, these



samples can be interpreted as the remains of vitrified or vitrifying furnace wall or tuyère nozzle, flowing down the inside of the shaft, and about to be absorbed into the reduction process, and sometimes tapped with the 'regular' tap slags before being absorbed.

### *Primary Smithing Slags*

The primary smithing slags are quite different from all other slag material, and form a minority (a few percent only) of the total assemblage. It consists of large and dense cakes of slag that are generally concavo-convex in section. Based on their macroscopic appearance, these samples (often referred to as plano-convex), are often interpreted as slag resulting from secondary smithing. However, such a shape can also result from bloom-smithing or further stages of primary smithing, and large concavo-convex shapes can also form at the bottom of a smelting furnace (see page 174).

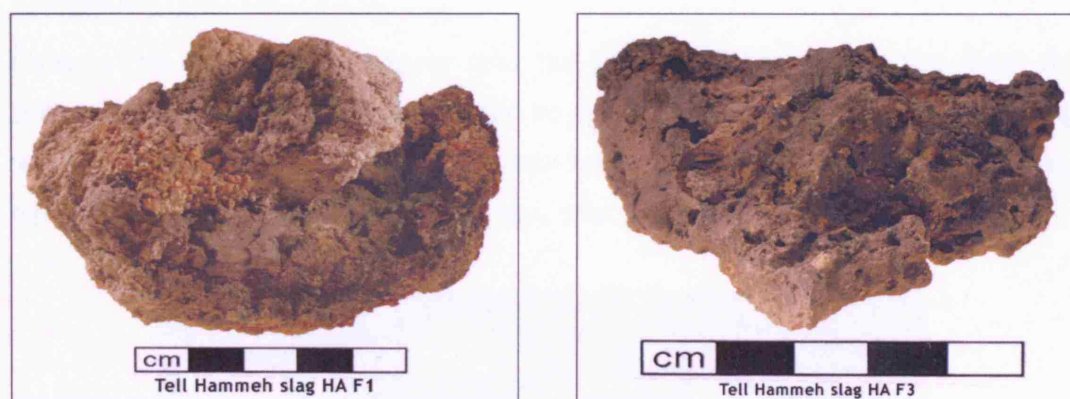


Figure 45. Primary smithing slag F1, showing a concavo-convex shape, soil embedded in the bottom and rust as well as remains of furnace/hearth ceramic on top; primary smithing slag F3, showing a more plano-convex shape, and revealing the internal vesicular structure of the slag.

It is difficult to fully exclude the possibility that these slags relate to secondary smithing, as secondary smithing samples can be quite similar in shape and chemical composition to primary smithing slags (Pleiner 2000, 255; compare the Beth-Shemesh smithing slags in chapter 9). However, several macroscopical factors as well as the find circumstances at Hammeh argue against such an interpretation. First, this type of the Hammeh slags is very different in size and shape from one individual specimen to the next, whereas secondary smithing slags often show a very narrow range in size and shape. Furthermore, the primary smithing slags at Hammeh do not reflect other possible indicators of an origin in secondary smithing such as a consistent round or oval shape (Serneels and Perret 2003). Another factor that argues against secondary smithing is the fact that these cakes only

appear in low numbers at Hammeh, in between much higher quantities of smelting and furnace slags. If secondary smithing had been performed at Hammeh, at a scale related to that suggested by the smelting slags, it is reasonable to expect that many more of these concavo-convex slags would have been recovered, and that they would form a consistent type with considerable homogeneity in their size, shape of their circumference, and section.

Microscopically, these samples are extremely heterogeneous, and show very unclear glassy matrices with equally unclear precipitations of phases. Near the top of the samples, glassy areas without any free iron oxide are found. Other areas show formations of two-phased particles. These started out as 'egg-shaped' wüstite, but after a change in redox conditions (more oxidising) grew on as magnetite; elsewhere magnetite spinel grows on as hercynite at the edges (Figure 46). This change in redox conditions, indicative of sudden and extensive contact with open air, opposes the idea that these slags may have formed at the bottom of a furnace.

Clusters rich in iron oxide appear near the bottom of the samples (i.e. near the soil) and some absorption of quartz can be observed there as well. Such a build-up within a slag is also opposed to what can be expected in a furnace bottom slag, where iron oxide concentrates at the top, near the bloom.

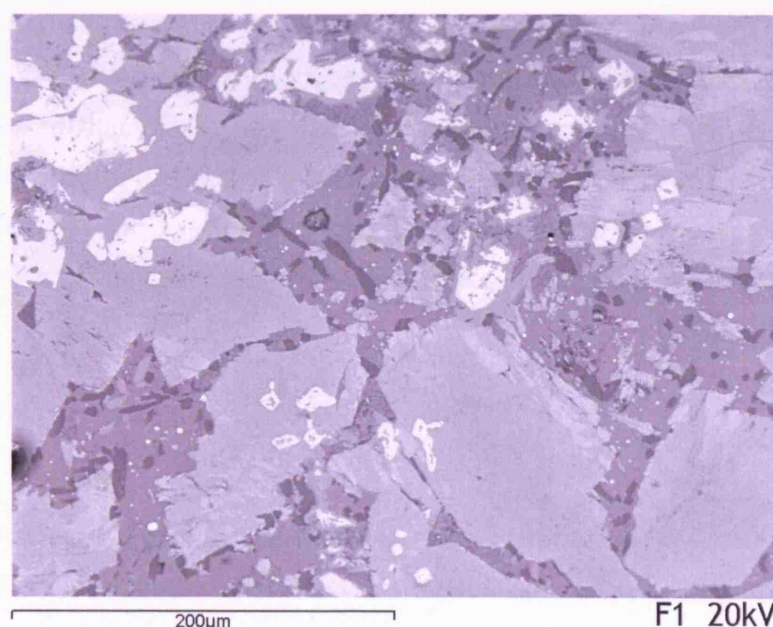


Figure 46. BSE micrograph of primary smithing slag F1, showing a calcio-olivinic glassy matrix, (mid-dark grey), with solid laths of leucite ( $\text{KAlSi}_2\text{O}_6$ ; dark grey), large 2-phased olivinic blocks (mid-grey, and slightly lighter), and precipitations of spinel with hercynitic (Al) and ulvitic ( $\text{TiO}_2$ ) components (whitish).

Chemically, the group is characterised by low iron oxide content (between 40 and 55 wt%) and a relatively high lime content of more than 14% (Table 29), which is similar to the composition of the tap slags.

Primary smithing slags	SiO <sub>2</sub>	Al <sub>2</sub> O <sub>3</sub>	FeO	TiO <sub>2</sub>	MnO	CaO	MgO	K <sub>2</sub> O	P <sub>2</sub> O <sub>5</sub>	S
F1	36.3	4.53	38.2	0.38	0.67	15.3	1.85	1.71	0.62	0.50
F3	38.2	5.00	33.6	0.41	0.75	16.5	2.19	1.91	0.85	0.53
F4	26.1	5.09	51.9	0.33	1.23	10.8	1.92	1.22	1.13	0.30
F5	32.4	6.77	38.6	0.42	1.23	14.9	1.64	1.83	1.39	0.77
average	33.3	5.35	40.6	0.39	0.97	14.4	1.90	1.67	1.00	0.52

Table 29. Bulk chemical composition (major elements) of the primary smithing slags. Note how these samples are quite similar to the tap slags. Analysis by (P)ED-XRF (slag\_fun calibration method, April 2005). Values are expressed in wt%, and normalised to 100%.

Primary smithing slags	Ni	Cu	Zn	Rb	Sr	Y	Zr	Ba	Pb
F1	100	30	25	bdl	520	50	280	130	bdl
F3	20	20	35	10	630	50	300	160	bdl
F4	bdl	25	25	bdl	620	80	220	100	bdl
F5	bdl	25	50	10	970	100	270	160	bdl
average	60	25	34	10	685	70	268	138	bdl

Table 30. Bulk chemical composition (trace elements) of the Hammeh primary smithing slags. Analysis by (P)ED-XRF (slag\_fun calibration method, April 2005). Values are expressed in ppm (parts per million).

The microstructure of these samples is often also similar to the tap slags, with formations of wüstite, but with a sudden boost of oxygen, these turned into magnetite. In my opinion, the combination of a concavo-convex morphology (somewhat similar to that of secondary smithing slag), a chemical composition that is close to that of the tap slags, a microstructure that again resembles the tap slag but with indications of a strong and sudden access to oxygen (as opposed to slag forming at the furnace bottom), and a large variation in size and shape (as opposed to secondary smithing slag), identifies these slags as primary smithing slag.

## Discussions

### *Sulphur in the Slag*

The tap, furnace, and primary smithing slags often show tiny droplets of iron sulphide (FeS) interspersed between the olivine and/or pyroxene laths, and the presence of sulphur is further confirmed by the bulk chemical analysis of these slags (ranging from ca. 0.2 to ca. 0.6 wt%). The presence of sulphur in an iron production process is undesirable, as the metal will become more brittle and

prone to cracking during smithing. The fresh surfaces of such cracks then oxidise rapidly, preventing rewelding (Rostoker and Bronson 1990, 21).

Experiments on modern industrial (blast furnace) slags describe the concept of a sulphide capacity for slag, from which in turn, when known, the distribution of sulphur between slag and metal can be calculated (Andersson *et al.* 2000, 287). The sulphide capacity of slag is a function of, primarily, the operating temperature and the  $\text{Al}_2\text{O}_3$  to CaO ratio of the slag (Andersson *et al.* 2000, 288-289), where a higher ratio of  $\text{Al}_2\text{O}_3$  to CaO correlates to a higher sulphide capacity. The average ratio of  $\text{Al}_2\text{O}_3$  wt%/CaO wt% in the Hammeh tap, furnace, and 'ceramic' slag is 0.36, which would point towards a high sulphide capacity for the slag (compare Andersson *et al.* 2000, 289, fig 2). As the experiments obviously involve very different and highly controlled equilibrium circumstances, a different technological process, and far higher temperatures (1500-1650 °C) than can be assumed at Tell Hammeh, direct comparison is not viable and actual sulphide capacity parameters will certainly differ.

The presence of FeS in the Hammeh slags may indicate a possible transfer of some sulphur to the iron metal, but from the fact that some of it is retained in the slag, one cannot deduce the quantity of that transfer. The  $\text{Al}_2\text{O}_3$  to CaO ratio of the Hammeh slags potentially helps to retain more sulphur in the slag, lowering the transfer to the iron produced. However, exact comparison of the sulphur content present in the Warda ore with that of Hammeh slags is not quantifiable, as some of the sulphur will vaporise (when  $\text{FeS}_2$  (pyrite) slowly breaks down to FeS around 700 °C), and the amount that was transferred to the metal is unknown. The presence of sulphur in the Hammeh slags and their sulphide capacity together seem to suggest that most of the sulphur may have been retained in the slag. The presence of sulphur in both the ore and the slags is a further indication of the fact that they are related.

It is furthermore interesting to note that ancient iron artefacts often contain levels of sulphur that would theoretically make them brittle and unforgeable, but clearly show that they were successfully forged (Rostoker and Bronson 1990, 21, fig 2.8, and the references therein). This observation implies that a relatively high level of transfer of sulphur into the metal that is produced does, in practise, not prevent the creation of proper artefacts.



### Trace Elements and Relations between Materials

Several trace elements were measured for the various slag types, and these are presented in the discussion of the various types. The levels of these traces present in the slag can be compared to those in the materials originally charged to the smelting furnace, i.e. the Warda ore and the charcoal. The trace element distribution in these materials can furthermore be compared to the technical ceramics, which in melting off contribute substantially to the formation and composition of the slags (see page 159 and 208). This comparison is shown in Table 31. In this table, the different slag types are arranged between the trace composition of the ore and that of the clay and tuyère ceramic, in such a way that they are nearest to the material they are most closely related to (as defined through the major element chemistry and microscopical characterisation described above). For example, the furnace slags are positioned immediately below the ore, and the ceramic-rich slags are positioned just above the ceramic. The trace element levels of the Hammeh charcoal and those of the Tel Beth-Shemesh secondary smithing slags are given at the bottom of the table.

Trace element comparison	S	Ni	Cu	Zn	Rb	Sr	Y	Zr	Ba	Pb
Warda ore average	0.28	bdl	25	65	bdl	bdl	25	70	bdl	bdl
furnace slags	0.62	bdl	45	45	bdl	340	60	120	45	bdl
furnace bottom slag	0.06	bdl	20	15	bdl	250	bdl	110	bdl	bdl
tap slags	0.39	bdl	30	60	bdl	640	80	200	100	bdl
primary smithing slags	0.52	30	25	35	bdl	690	70	270	140	bdl
ceramic-rich slags	0.21	10	25	35	20	670	60	330	170	bdl
Lisan clay + tuyères	0.33	45	25	90	60	270	30	410	170	bdl
Hammeh charcoal	0.10	10	20	10	bdl	790	bdl	bdl	bdl	bdl
Beth-Shemesh smithing slags	0.10	25	60	30	10	410	20	210	1290	bdl

Table 31. Comparison between the average trace element compositions of the Warda ore, the various Hammeh slag types, the local clay and Hammeh tuyères, and the Hammeh charcoal. In addition, the trace elements of the Tell Beth-Shemesh secondary smithing slags are shown. Analysis by (P)ED-XRF (slag\_fun calibration method, April 2005). Values are expressed in ppm (parts per million), except sulphur, which is expressed in wt%.

Several observations can be made from the comparison in Table 31. The first is that the trace of copper observed in all slags derives from the Warda ore as well as from the technical ceramics. Under normal circumstances, one would expect these small amounts of copper to pass straight into the metal. It seems possible to suggest that the presence of sulphur in the process, similarly deriving from both the ore and the technical ceramic, may have prevented this transfer.

Another observation is that traces of barium (which is not detected in the ore), are predominantly present in those slag types that were already assumed to have a larger absorption of technical ceramics (which do contain barium). To a slightly lesser extent, the same distribution is seen in zirconium. The influence of fuel ash on the process is indicated by the distribution of strontium in all slag materials. Overall, the comparison of the various trace elements is consistent with the assumed ceramic contribution to the Hammeh smelting process, as well as with the identification of Warda as the source of the ore used at Hammeh. The various distribution patterns of traces further underlines the range of compositions between ore-like and ceramic-like that was already observed with the major elements (see Figure 42).

Looking ahead to the description of the Beth-Shemesh material discussed in chapter 9, the trace element composition of the Beth-Shemesh smithing slag has been added to Table 31. A potential relation between these samples and the smelting material from Hammeh does not have to be excluded because of trace element comparison, but the Beth-Shemesh slags do indicate a far higher influence of a ceramic component, especially in the high level of barium. This is consistent with the expected formation of a smithing slag from a combination of sources, of which the hearth material forms a large contributor (see chapter 2 and chapter 9).

### ***Efficiency of the Process***

In the microscopical examination of the slags, one thing stands out. Several of the slags are microscopically speaking quite 'chaotic', and often show a very heterogeneous distribution and precipitation of phases. This is quite common in early iron metallurgy, and is not surprising considering how minute differences in furnace conditions such as temperature and redox conditions can have significant effects on the constitution of the materials in the furnace. To some extent, this microstructural heterogeneity of individual samples, as well as between samples, must relate to an occasionally less than complete control by the metalworkers over the technological process. Some tap slags, for example, appear to be 'mishaps', and were apparently tapped too early. These samples reveal a higher than desired level of free iron oxide still trapped in areas of the slag, which often oxidised to magnetite at the surface on contact with the outside air, as mentioned above.

To a much larger extent, however, sample heterogeneity simply reflects the fact that conditions in a smelting furnace are never in full equilibrium, with several processes going on simultaneously at different locations and at different temperature gradients. This, as indicated above, is to be expected in a bloomery process, and should not be interpreted as 'inefficient'. This is reflected, for example, by the observed continuum of compositions within the slag types, indicating that they are the result of an ongoing process. Another source of heterogeneity, again not to be interpreted as inefficiency, is seen in the furnace slags. These samples represent incompletely processed ore and slag from inside the furnace, which were probably left unfinished at the end of a smelt. Here, the incomplete stages of reduction result in a heterogeneous mass.

In contrast to these differences within and between individual samples, the various slags are chemically and especially macroscopically quite consistent when considering each type as well as the entire assemblage. The tap slags, for example, show clear and consistent characteristics of primary production, and are chemically equally consistent in revealing a low iron oxide and high lime content. This overall homogeneity rather indicates a well-established and relatively high efficiency of the process.

### ***Principal Component Analysis***

It is possible to test and explore the identification of the different slag types at Hammeh using the statistical tool of Principal Component Analysis (PCA; see chapter 6). This multivariate analysis is applied here with a non-model-based approach, i.e. it aims to illustrate and explore data structure rather than explain observed variation or correlation. The PCA plots shown in Figure 47 and Figure 48 clearly illustrate the various slag types identified through the analytical techniques as described above. The two graphs, each providing a different view of the same pattern of variation, furthermore visualise the continuum of compositions of the different types of material in the Hammeh system, which range from closely related to the Warda ore to more closely related to the technical ceramic from the sacrificial tuyères and furnace wall.

Distance and direction of the loading vectors from the origin show which elements influence the principal components axes most and to what magnitude, i.e. a longer distance indicates a stronger influence. The loading vectors in Figure 47 and Figure 48 show that the presumed ore-related slag types do cluster towards the ore and along ore-related elements such as FeO and MnO, whilst the more

ceramic-related slag types more closely correspond to ceramic-related elements such as  $\text{CaO}$  and  $\text{SiO}_2$ .

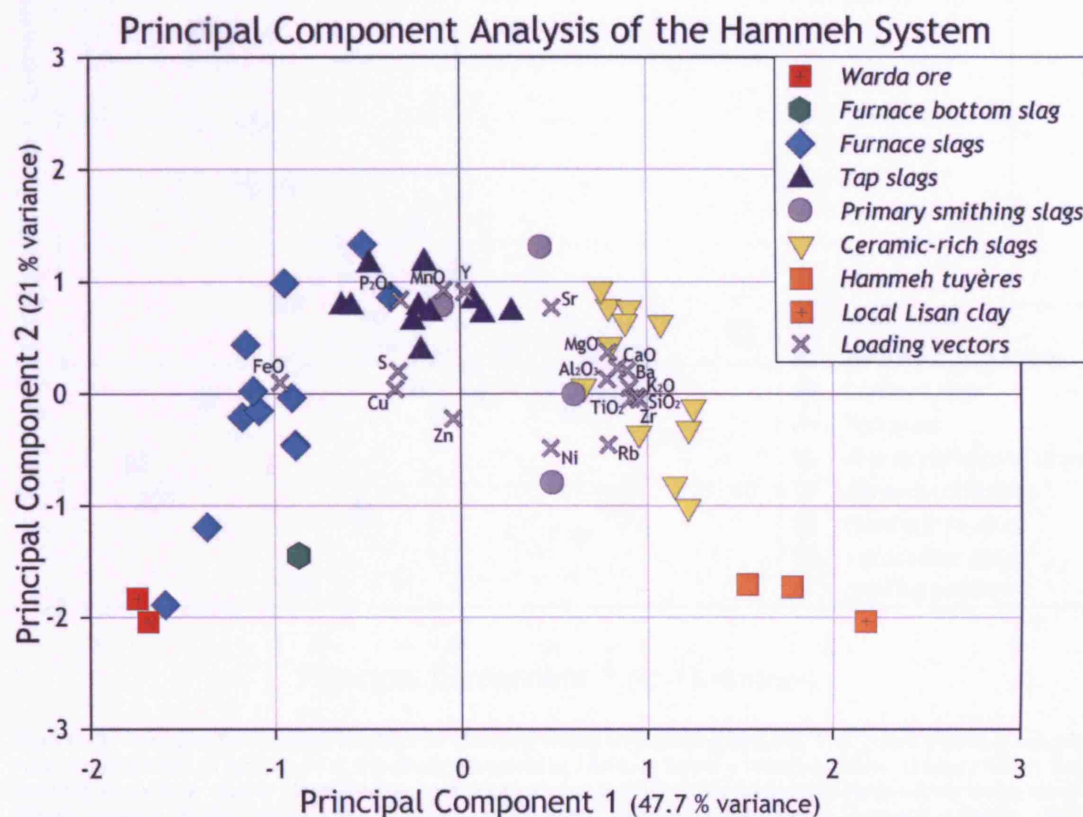


Figure 47. Principal Component Analysis of the Tell Hammeh Smelting System. The graph shows how each of the Hammeh smelting residues forms a relatively clear cluster, whilst the samples as a whole clearly illustrate the continuum of composition. This continuum ranges from being more closely related to the Warda ore, to being more closely related to the tuyère technical ceramic. The loading vectors of the original variables support this interpretation. The graph shows Principal Components 1 and 2. (The scores and loading vector values can be found in appendix 3).

Both plots show a clear clustering of each different slag type, and simultaneously underline how the various groups as a whole represent a continuum of compositions. This conveniently illustrates the macroscopical, microscopical, and chemical observations (see the PCA plot comparing the Hammeh tap and primary smithing slags with the Tel Beth-Shemesh secondary smithing slags in chapter 9, page 224). The PCA plots clearly illustrate and match the slag type identification as derived from macroscopical, microscopical, and chemical analysis.



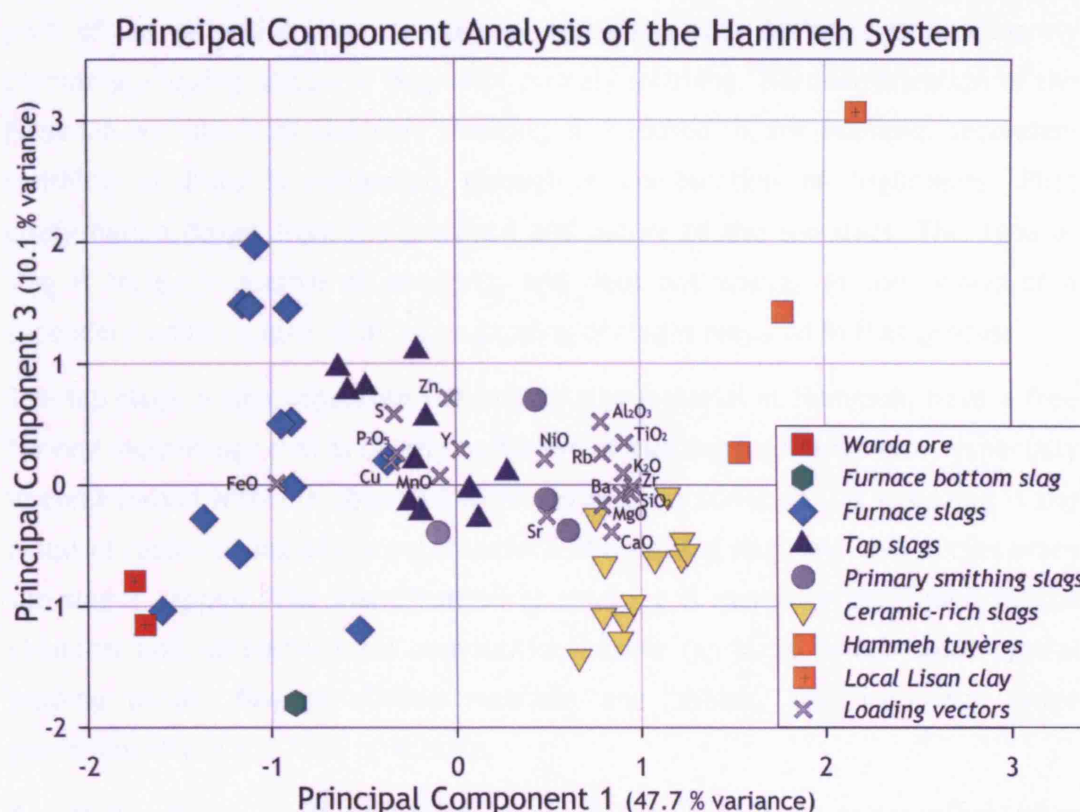


Figure 48. Principal Component Analysis of the Tell Hammeh Smelting System. The graph shows a second view (more linear) of how each of the Hammeh smelting residues forms a relatively clear cluster, whilst the samples as a whole clearly illustrate the continuum of composition. This continuum ranges from being more closely related to the Warda ore, to being more closely related to the tuyère technical ceramic. This corresponds with the loading vectors of the original variables. The graph shows Principal Component 1 and 3. (The scores and loading vector values can be found in appendix 3).

## Summary

The first aim of the slag analyses was to determine the nature of the metal processed at Hammeh. The chemical composition of all the different slags clearly supports an identification of the assemblage of slag types as belonging to iron metallurgy. None of the slags contains a significant amount of copper in its elemental composition. Although copper slags can be highly similar to iron slags in chemical composition as well as microstructure, with similar levels of iron oxide and fayalitic formations, slags related to copper are normally expected to contain at least some 0.3 wt%, or even up to 10 wt% CuO (Rostoker and Bronson 1990, 87), whereas the Hammeh slags only reveal traces. A relation of the Hammeh material to copper metallurgy is thus excluded.

With the metal now determined to be iron, the second aim was to establish what principal stages of the technological process of iron production (smelting, primary smithing, or secondary smithing) the Hammeh material represents. The overall characterisation of the Hammeh slags has shown that the different slag types form

part of an extensive iron production operation that includes predominantly bloomery smelting and some degree of primary smithing. The identification of the Hammeh operations as bloomery smelting, as opposed to, for example, secondary smithing of iron, is evidenced through a combination of arguments. First confirmation comes from the presence and nature of the tap slags. This type of slag is highly indicative of smelting, and does not appear in the debris of a secondary smithing operation, as no tapping of slag is required in that process.

The tap slags, which constitute the bulk of slag material at Hammeh, have a free flowing morphology that is clearly indicative of tapping from a furnace, especially in combination with the observed wrinkling of their surface. This wrinkling is the result of rapid cooling of the outer surface of a flowing slag, and only occurs when the slag is tapped. The identification of smelting is moreover confirmed by the chemical and microstructural composition of the tap slags, which show typical tapping bands, fayalitic-olivinic matrices and phases, and free iron oxide predominantly in the form of wüstite.

A certain amount of consolidation of the bloom must have taken place after smelting, as witnessed by the presence of primary smithing slags. Although unambiguous distinction of these slags from secondary smithing slags is often difficult, several factors combine in their identification. To begin with, the Hammeh primary smithing slags are highly inconsistent in their individual shapes and sizes, a fact that, in combination with the fact that they are morphologically quite thick and solid, clearly differs from what one would normally expect with secondary smithing slags (compare the Beth-Shemesh smithing slag and their features in chapter 9). A further issue is the low quantity of these smithing slags in the total assemblage. A secondary smithing process yields lower quantities of (usually smaller) slags than a primary smithing process, as there is less slag to be expelled than from a bloom. However, if secondary smithing had taken place at Hammeh in association with the bloomery smelting, the large scale of that smelting would suggest that secondary smithing would take place at a related scale, producing relatively large numbers of (secondary) smithing slags. Comparison with the assemblage of materials in the smithy context at Tel Beth-Shemesh suggests that more iron artefacts would have been present in the production context as well. A last diagnostic argument is found in the microstructure and chemical composition of these slags, which both resemble that of the tap slags, albeit with indications of a strong and sudden access to oxygen (on being expelled from the bloom). This close relationship to the tap slags, e.g.

in the continued presence of trace elements from the Warda ore, sets these samples apart from secondary smithing slags, which would be expected to show more of a clay component chemically, and more formation of magnetite due to prolonged oxidising circumstances.

With both the metal (iron) and the principal stages of the technology of that metal (smelting and primary smithing) now known, it is possible to relate the different slag types found at Tell Hammeh to different technological steps that constitute the principal stages, i.e. to reconstruct the technological *chaîne opératoire* of the Hammeh bloomery smelting operation. The furnace slags are the earliest stage of the smelting process represented at Hammeh. As described above, these slags contain varying quantities of haematite ore in various (progressive) stages of incomplete reduction. Some slags contain virtually unreduced fragments of ore, where others contain ore with cracks from lower temperature roasting effects (around 800 °C), i.e. the initial breaking up of the ore. Other furnace slags are more fully reduced, consisting of a fully reacted iron silicate slag phase that incorporates occasional remains of partly reacted ore. These samples represent an almost complete stage of reduction. This group of furnace slag samples clearly reflects a range of temperatures and reduction circumstances that ore travelling down a smelting furnace will encounter until full separation of slag and metallic iron in and near the combustion zone. The relation of these samples to the Warda ore (see page 148) is reflected in their iron oxide rich chemical composition, and a lower influence of ceramic components. The fact that roasting effects can be seen in some of these furnace slags does not suggest that roasting of the ore was performed prior to it being charged to the furnace, as these effects can form in the early stages of the smelting process within the furnace.

The furnace bottom slag represents a further step in the smelting process. Only one individual sample of this type was studied, as it was only recognised as a separate type during the examination of the primary smithing slags. Nonetheless, it is likely that more specimens of this type are present in the total Hammeh material. This slag formed at the bottom of the furnace, directly below the bloom. It resembles in its composition the more fully reacted of the furnace slags. It is the most iron-rich sample of the assemblage, but simultaneously reveals a much larger absorption of ceramic material (see the discussion on the ceramic contribution on page 208, ff) than the furnace slags.

The next stage of the smelting operation is represented by the tap slags, which in themselves are diagnostic for smelting activity. These slags were tapped from the furnace to prevent the process from halting, thus allowing more ore to be fully processed and more iron metal to be extracted from one smelt. Several conclusions can be drawn from this slag type and its characteristics. The large quantity of tap slags excavated at Hammeh clearly indicates that the smelting was a full-scale operation. Furthermore, compared to 'regular' bloomery smelting slags, the Hammeh slags are very lean, i.e. low in iron oxide content. This leanness is caused in part by the lime-richness of the ore, and in part by the absorption of considerable amounts of ceramic material into the slag formation process (both aspects are discussed in detail below).

Still related to the smelting furnace is the group of ceramic-rich slags. These slags unmistakably indicate that technical ceramics played a role in the Hammeh smelting process. Their highly glassy or even foamy structure relates to an origin in ceramic, where the complete melting and/or vitrification indicates the high (furnace) temperatures these samples were exposed to. That these samples do have an undoubted connection to the smelting of iron is shown in their high iron oxide content.

The last stage of the production process attested by the analysed assemblage is that of primary smithing. As discussed above, these samples are low in number, and vary widely in size and shape between individual smithing slags. An identification of these slags as primary smithing slag, i.e. remaining slag expelled from the bloom is supported by the apparent sudden change in oxidising conditions. Their morphological variation, chemical and mineralogical structure set these samples apart from secondary smithing, of which no evidence was found at Hammeh.

## The Charcoal

The iron production deposit at Hammeh contains a large amount of potential fuel remains, mostly in the form of fine black powdery ash mixed with soil, with lesser numbers of actual pieces of charcoal. Of this material, all charcoal fragments and most of the ash were found contained within the potential furnace structures of square A/B7, strengthening the idea that these materials, as well as the structures that contain them, are directly related to the metallurgical activities. All charcoal recovered at Hammeh within the context of the iron production debris is very small in size. As discussed before (see page 79), the size is likely related to the

origin of the wood, i.e. short-lived small branches or twigs that were obtained during the pruning of olive trees. None of the examined specimens seems to represent fragments of larger pieces, as might be the result of being trampled in antiquity, or other, postdepositional, processes.

The identification of the species as olive wood, as well as the likely pruning related specimen sizes, are important in archaeological terms, when one considers issues of deforestation and use of (locally available) resources. The (short-lived nature of) the Hammeh charcoal also provides an opportunity for accurate dating of the stratigraphy in which it is found, and it was used for AMS  $^{14}\text{C}$  dating of the production activities (see page 92). It is also interesting to note that the Hammeh smelters very likely used a self-renewing resource, as this supports the stratigraphically indicated seasonality of the smelting operations, and that they apparently chose not to exploit the quantities of oak that were still available on the surrounding hillsides during the Iron Age.

In technological terms, charcoal is an essential resource, both as the fuel that generates the heat necessary for the reduction process, and in acting as a reducing agent itself. Not only this dual function of the fuel is important, but also the contribution to the slag formation by ash derived from the charcoal. Chemical components in the fuel ash such as alkali and earth-alkali oxides are absorbed into the melt, and influence parameters of the reduction process and of the metal produced. It is therefore desirable to obtain insight into the chemical composition of the Hammeh charcoal.

However, only little data is available on the chemical composition of woods or their corresponding charcoal or ash (Stern and Gerber 2004, 140, table 1, which presents one analysis for fresh olive wood; Brill 1999, 482-486, table XXIVC). Wood is more often studied from an agro-economic perspective, e.g. in terms of growing-rates, properties as building material, or caloric values and quantities needed when used as fuel (Rostoker and Bronson 1990, 61-65). One thing that clearly emerges from the scarce wood-ash data is the wide compositional variability both between species and within the same species (Stern and Gerber 2004, 138), and the fact that the geochemical character of the soil will influence the wood that grows on it, e.g. lime-rich soils will produce lime-rich plants (Stern and Gerber 2004, 139). Looking at soil conditions in the Jordan Valley and Wadi Zarqa, this would certainly mean that charcoal from olive wood would contain a significant amount of lime.

Charcoal	SiO <sub>2</sub>	Al <sub>2</sub> O <sub>3</sub>	FeO	TiO <sub>2</sub>	MnO	CaO	MgO	K <sub>2</sub> O	P <sub>2</sub> O <sub>5</sub>	S	Sum
HA Ch1	0.4	n.d.	0.1	n.d.	0.0	8.4	2.1	2.5	0.1	0.1	13.9
normalised											

Table 32. Bulk chemical composition (major elements) of Hammeh charcoal. Analysis by (P)ED-XRF (slag\_fun calibration method, April 2005). Values are expressed in wt%. The difference to 100% is assumed to be predominantly carbon, undetectable under XRF. A normalised composition of the detected elements is provided as well.

In an attempt to characterise the Hammeh charcoal to compensate for the lack of comparable analyses of olive wood or olive charcoal, a handful of charcoal pieces (sampled from the furnace structure(s) in A/B7) were crushed, pulverised, dried, mixed with wax, and pressed into a pellet. This pellet was subsequently analysed by (P)ED-XRF using the 'slag\_fun' calibration method, in the same way as the slag, ore, and technical ceramic samples, to provide an indication of the composition of the Hammeh charcoal and its ash. This analysis both confirms the expected high lime content, and the presence of alkali and earth-alkali elements. As both the matrix of the pressed charcoal and its overall composition are very different from those of the materials the 'slag\_fun' calibration is designed for, the analysis should be considered qualitative.

Charcoal	Ni	Cu	Zn	Rb	Sr	Y	Zr	Ba	Pb
HA Ch1	10	20	10	bdl	790	bdl	bdl	bdl	bdl

Table 33. Bulk chemical composition (trace elements) of Hammeh charcoal. Analysis by (P)ED-XRF (slag\_fun calibration method, April 2005). Values are expressed in ppm (parts per million).

This qualitative chemical composition assists in the determination of the contribution of different materials to the formation of the Hammeh slag, as will be discussed in the mass balance calculations below.

## The Metal Artefacts

Metal artefacts are virtually absent at Hammeh. Only a handful of iron objects was excavated, and from some it could not even be identified what kind of artefact they were. None of the excavated artefacts is stratigraphically related to the iron production context. This scarcity of (iron) artefacts is illustrated by the fact that in the entire 2000 season of excavation, just one iron artefact (an arrowhead from trench part A/D7) was recovered, and this belongs to the younger phase immediately following the production layer.

It is nevertheless not impossible that some of the rare and apparently younger iron artefacts at Hammeh were produced at the site during the smelting phase that precedes them. The artefacts, for example, may have remained in use after

production ceased, and were discarded or deposited in a later phase. Another possibility is that later terrain modification by inhabitants of the tell or postdepositional processes may have changed the stratigraphical context where they were eventually excavated. Assuming that these rare artefacts do originate in the iron production activity at Hammeh, which is highly conjectural, their very low number would then still strengthen the interpretation of Hammeh as a production (i.e. smelting) rather than a consumption (i.e. secondary smithing) site.

Early on in the study of the Hammeh material, an attempt was made to examine these rare artefacts. However, X-Ray radiography at Yarmouk University in Jordan did not indicate a presence of any remaining metal, i.e. the artefacts were completely corroded. No (recognisable in the X-Ray radiograph) inclusions of slag were observed either. Further analysis of these artefacts was therefore abandoned. It is certainly desirable to perform a more widespread study of iron artefacts, the few from Hammeh, and especially those from sites in the surrounding and wider region. This might allow examination of the possibility that contemporaneous artefacts in the Jordan Valley, and perhaps beyond, are related to the Warda ore deposit and/or the Hammeh smelting operation, and may serve to establish trade or distribution patterns of iron metal in this region.

From a metallurgical viewpoint, a comprehensive study of iron metal artefacts from the region may furthermore help to determine what techniques were applied during secondary smithing, and as a result, what properties characterise these artefacts. Besides metallographic analyses, such a project could involve looking at ghost structures within corrosion, i.e. remaining structures of characteristics (e.g. carbon concentrations from a carburised edge) of the original corroded metal, that are retained in the corrosion product (Notis 2002; Knox 1963). Another possibility is the analysis of possible slag stringers (Buchwald and Wivel 1998) that often remain in artefacts after smithing. Such a study, however, clearly lies beyond the scope and aim of this research project.

In the context of the Hammeh iron production, it is important to note the find of a relatively large number of iron artefacts in a burial cave in the Baq'ah Valley, in the Umm ad-Dananir region. This cave is located just a few kilometres upstream from Hammeh, in a river valley that connects the Zarqa Valley to the 'Amman plateau. The burial cave was used from ca. 1250 to 1050 BC. In the cave, a group of 11 iron artefacts was found, eight bracelets and three rings, as well as forty



additional fragments. The excavators assume that these artefacts were made locally, as no imported items of any sort were recovered in this cave. An important characteristic of the Baq'ah artefacts is that they contained around 0.7 wt% carbon. The carbon was found not just on the surface of the artefacts, which could indicate carburising during secondary smithing, but was equally distributed throughout the entire objects from surface to surface, indicating that mild steel (with 0.3 - 0.6 % carbon; as opposed to 'proper' steel, which contains up to ca. 2 % of carbon) was produced during the smelting process (McGovern 1986; Pigott 1983; Pigott *et al.* 1982b).

With the dating of the Hammeh operations indicating that the production of iron there was active somewhere before 930 BC (see page 92), there is an obvious gap between that production site and the Baq'ah artefacts, which were deposited no later than 1050 BC. Therefore, a direct link between the iron smelting operations at Tell Hammeh artefacts cannot be made unless the Hammeh operations started significantly earlier than 930 BC. This is certainly not excluded by the  $^{14}\text{C}$  dating, which merely indicate that the smelting process was active around 930 BC, but there are no indicators in, for example, the archaeology that they did start considerably earlier than around that time.

With the lack of evidence for earlier activity in mind, it is still tempting to speculate that Hammeh, the only iron smelting site in the region attested thus far, might represent the local producer of the Baq'ah artefacts. The Baq'ah material was found just a few kilometres south of the iron ore deposit at Warda, ore from which site was used in the iron smelting operation Tell Hammeh, and only a few kilometres southeast of Hammeh itself. Considering the location of the Baq'ah iron artefacts, it seems possible to suggest that these artefacts were produced, if not at Hammeh itself, then perhaps at a similar production site that precedes the Hammeh activity and which may be located somewhere nearby.

## Technical Ceramics and Fuel Ash in the Formation of Slag

### Introduction

'Regular' bloomery slag is characterised predominantly by fayalite ( $\text{Fe}_2\text{SiO}_4$ ) in a glassy matrix, with varying amounts of free iron oxide in the form of wüstite. The total percentage of FeO usually ranges between 60 and 75 % (Kronz 1998, 225-226; Rostoker and Bronson 1990, 91, table 9.1a; Bachmann 1982, table 1; Sperl 1980, 45, table 13). Compared to this the tapped smelting slag from Hammeh is relatively low in FeO, with an average value of 52.5 wt%. Importantly, the

Hammeh slags contain more CaO than bloomery slags generally do (11 wt% average; usual values lie below 5%, often around 1 or 2 %). The high lime content of the Hammeh slags is consistent with the relatively low grade of fayalite formation visible in these samples.

If less FeO ends up in the slag, either more FeO must have been reduced to metallic iron, i.e. a low FeO percentage in slag indicates that a higher yield of metallic iron was achieved in the smelting process, or the slag must have been diluted by other contributions. During the formation of slag, iron oxide may be substituted by calcium oxide, enhancing the formation of pyroxenes (i.e.  $(\text{Fe,Ca})_2\text{Si}_2\text{O}_6$ ) and glass rather than fayalite. In addition,  $\text{Ca}^{2+}$  can replace part of the  $\text{Fe}^{2+}$  in olivines such as fayalite, resulting in, for example, kirschsteinite ( $(\text{Fe,Ca})_2\text{SiO}_4$ ); similarly  $\text{Mg}^{2+}$  and  $\text{Mn}^{2+}$  can replace part of  $\text{Fe}^{2+}$  in both spinels and olivines. These substitutions free additional iron oxide for reduction to metallic iron (Serneels 1993, 29-31). Both fuel ash (Crew 2000) and the melting of technical ceramics may contribute towards this, beyond the original presence of calcium, magnesium or manganese in the ore that is used (Serneels and Crew 1997). Absorption of fuel ash and technical ceramic by the liquid slag simultaneously dilutes the mixture, and components from the absorbed material, e.g. silica, may bind more iron oxide, thus lowering the yield again.

Contribution to the formation of slag by partial melting of furnace wall or furnace lining is a well known concept (Pleiner 2000, 257-259) and is, often implicitly, treated in studies concerning metallurgical slag (e.g. Joosten 2004, 60). A more active contribution of molten ceramic from the tuyères to the fluxing and formation of slag has been assumed previously, primarily with the ethnographically observed vertical tuyère smelting operation of the *Mafa* in Cameroon (David *et al.* 1989). Overall, however, little archaeometric data is available on this subject, besides the pioneering research on the contribution of technical ceramics and fuel ash to the formation of slag, and the role this contribution may play in enhancing the process, by Vincent Serneels and Peter Crew (Crew 2000, on clay-fuel ash-slag relations; Serneels and Crew 1997, on ore-slag relations).

As argued above, the Warda ore likely requires additional silica from other sources in order to allow the formation of a liquid slag and thus enable the reduction of iron metal. The large number of molten and vitrified tuyère nozzles does strongly suggest that they may have been 'sacrificed' to provide a considerable part if not most of that contribution. This idea is examined in the calculations below.

## Mass Balance Calculations

For a further interpretation of the technological *chaîne opératoire* at Hammeh, it is necessary to determine how the various materials involved contribute to the formation of the slag. The first step is to determine whether the Warda ore by itself could result in a slag of the particular composition of that found at Hammeh. In the characterisation of the Warda ore above (see page 147, ff), it was already discussed that, although the ore is suitable for smelting as far as its iron oxide content is concerned, it can be considered too low in silica to allow the formation of sufficient quantities of liquid slag, and in combination with the high lime component of the process, it may be difficult to actually achieve extraction of iron metal.

This leads to the hypothesis that other materials must have contributed to the process and the formation of the slag. From the heavily molten and vitrified state of the tuyère nozzles (see page 159), it is more than reasonable to propose that the technical ceramics, and in particular the tuyères, supplied the required silica. Such a contribution is quantifiable using the chemical composition of the ore, slag, and technical ceramic involved, and examining the compositional relation between them through mass balance calculations. A mass balance calculation is based on the physical law that, within a closed system, the total mass of components of that system is constant. Although there may be a movement of mass or a transformation of mass to different forms, nothing can be created or destroyed. The purpose of a mass balance is ‘balancing’ the inputs to an activity with the outputs of that activity.

In the context of iron smelting, a partially open system must be assumed, as the reduction of ore results in the withdrawal of iron metal from the system. This removal of metal results in a new balance of materials that represents the composition of the remaining material, which in the context of this discussion equals slag. As the system is presumed closed, apart from the removal of iron oxide to be reduced to metal, the remaining components that form the slag will increase proportionally to make up for the removed metal, i.e. the components are normalised to 100% again. This normalisation is done to reflect the fact that the remaining material, whilst only representing a certain percentage of the original mass, in itself forms a new mass of which the components add up to 100%. Other possible factors that in reality do play a role in slag formation and composition, such as redox conditions and the contribution and behaviour of fuel

ash are ignored here. It should furthermore be noted that the haematite ore is presented as FeO. Using this system of mass balances, the calculations discussed in this chapter will first examine the relation between the Warda ore and the Hammeh slag, and subsequently examine how the technical ceramics at Hammeh contribute substantially to the formation of that slag.

### Comparison of Warda Ore and Hammeh Slag

The first mass balance calculations presented here start with the composition of the two Warda ore samples, HA 65 and HA 66, as well as the average of their compositions. As discussed above, the two ore samples examined in this research are not identical in composition, predominantly differing in their lime content. As seen in the discussion of the various slags, it is particularly the high lime content of the Hammeh slags that sets them apart from 'regular' bloomery slags. It is therefore sought to determine which of these two ore compositions, or alternatively the average between the two, is closest to that presumably used by the Hammeh metalworkers.

To demonstrate how the method of mass balance described above is applied to the Hammeh ore samples, the calculation of a hypothetical slag from the first ore sample HA 65 is presented as a detailed example here. In these calculations, it is assumed that 100 kilograms of ore with the composition of HA 65 are processed in a smelting operation. Analogous to actual production of iron metal, more and more iron oxide is extracted from the system, in iterative steps, until the amount is reached where the balance of the remaining components, when normalised to 100%, contains the same amount of iron oxide as the actual Hammeh tap slags, i.e. 52.5 wt%. This normalised remainder of the original ore, after extraction of iron oxide to produce metal, reflects the hypothetical composition of a slag produced from that ore. If this specimen of Warda ore and the Hammeh (tap) slags are directly related, all other components of this hypothetical slag, besides the intentionally matching FeO, should now also match with those of the actual Hammeh slag. As demonstrated below, such a match does not occur and, therefore, other ore samples and/or a contribution to the system from other materials have to be explored.

A hundred kilograms of ore sample HA 65 contain 86.5 kilograms of iron oxide (when normalised and expressed as FeO, Table 34). In iterative steps, iron oxide is removed from the system until, at 71.5 kilograms, the FeO content of the hypothetical slag matches the actual Hammeh slags. In terms of the yield of iron

metal, 71.5 kilograms of iron oxide equal 55.6 kilograms of metallic iron (this is calculated stoichiometrically, i.e. the atomic weight of the oxygen in FeO is deducted to leave just Fe. In this case, 71.5 kg FeO times 0.773 equals 55.6 kg Fe).

After the removal of iron oxide, 28.5 kilograms of material remains, which is composed of the remaining iron oxide and all other gangue components of the original ore. These components are then proportionally increased (normalised to 100%) to compensate for that removal, thus creating a new mass balance that contains 52.5 wt% of FeO. As intended, this value almost completely matches the iron oxide content of the Hammeh slag. However, the remaining components of the hypothetical slag clearly do not match with the actual Hammeh slag values, as can be seen in Table 34. The hypothetical slag from HA 65 is too poor in SiO<sub>2</sub>, Al<sub>2</sub>O<sub>3</sub>, TiO<sub>2</sub>, MnO, MgO, K<sub>2</sub>O, and P<sub>2</sub>O<sub>5</sub>, and too rich in CaO and S.

Mass balance HA 65	SiO <sub>2</sub>	Al <sub>2</sub> O <sub>3</sub>	FeO	TiO <sub>2</sub>	MnO	CaO	MgO	K <sub>2</sub> O	P <sub>2</sub> O <sub>5</sub>	S
HA 65	4.45	0.00	86.5	0.01	0.03	8.45	0.16	0.00	0.06	0.38
Hypothetical slag HA 65	15.6	0.00	52.5	0.02	0.11	29.7	0.55	0.00	0.22	1.32
Actual Hammeh slag	25.2	5.44	52.5	0.34	1.12	10.90	1.80	1.12	1.20	0.39
Difference	10.75	5.44	0.00	0.33	1.09	21.25	1.64	1.12	1.14	-1.01

Table 34. Mass balances of ore sample HA 65, showing the differences in composition between a hypothetical slag calculated from that ore, and the actual Hammeh slag (average value of the tap slags). Results by (P)ED-XRF, using the 'slag\_fun' calibration method (April 2005). Values are expressed in wt% and normalised to 100%.

The discrepancies between the hypothetical and actual slag values as presented in Table 34 can be visualised in a graph (Figure 49). The first column at each component in the graph represents the elemental composition of ore sample HA 65, the second column shows the composition of the hypothetical slag after extraction of the iron metal, and the third column shows the average composition of the Hammeh tap slags.

A match between the hypothetical slag and the actual slag would be reflected in columns of identical height for each component. Figure 49 clearly shows that such a match does not occur. This is most clear in the considerable discrepancies between the values of SiO<sub>2</sub> (more than 9 wt% less than the actual slag) and CaO (almost 19 wt% more than the actual slag). With a clear mismatch between ore of the composition represented by sample HA 65, other options have to be considered. First, using the same method outlined above, it is examined whether a Warda ore of the composition of sample HA 66 would provide a better fit with the Hammeh slag.

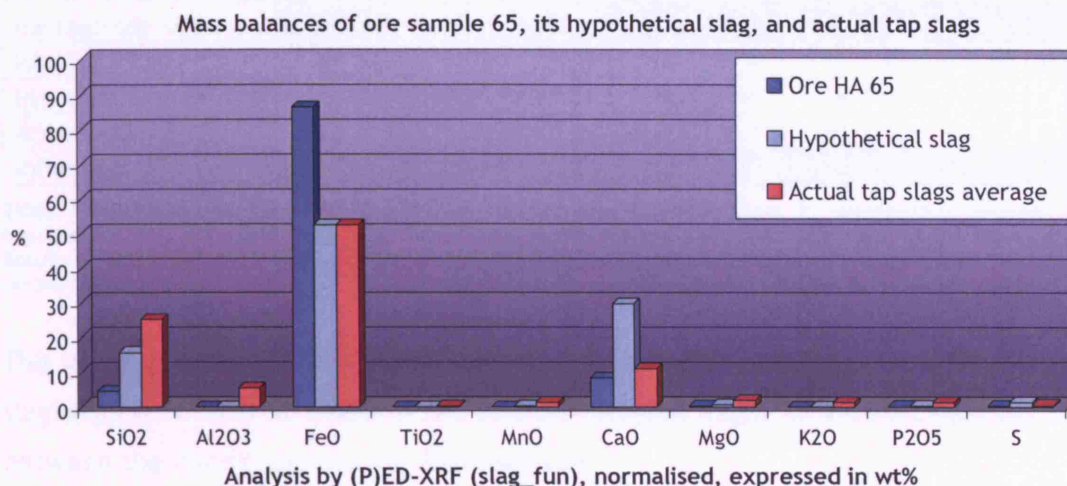


Figure 49. Mass balances of Mugharet al-Warda ore (sample HA 65), showing the composition of the hypothetical slag resulting from that ore, in comparison with the actual Hammeh slag. The graph clearly shows the large discrepancy in the major oxides SiO<sub>2</sub>, Al<sub>2</sub>O<sub>3</sub>, and CaO, as well as in the alkali and earth-alkali oxides. Results by (P)ED-XRF, using the 'slag\_fun' calibration method (April 2005). Values are expressed in wt% and normalised to 100%.

Processing 100 kg of ore of this composition is capable of a very high metal yield of almost 67 kg of iron metal (85.9 kg of iron oxide), and results in only ca. 14 kg of slag. However, once again the overall slag composition is incorrect (Table 35; Figure 50). The most striking observation about the hypothetical slag that is calculated from this iron oxide rich ore sample is a richness in SiO<sub>2</sub> (12.2 wt% more than the actual slag), combined with a lack of CaO (9 wt% less than the actual slag). This is the reverse of what was seen with sample HA 65.

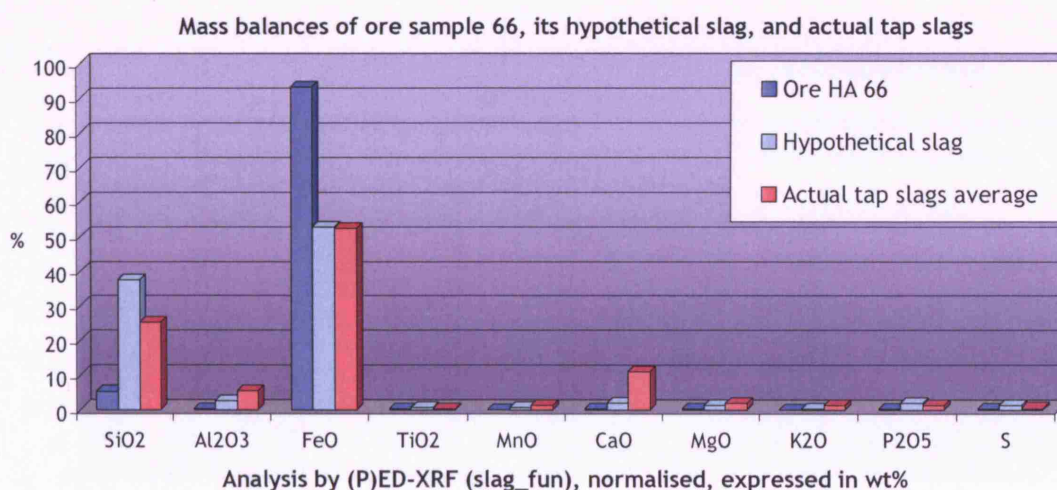


Figure 50. Mass balances of Mugharet al-Warda ore (sample HA 66), showing the composition of the hypothetical slag resulting from that ore, in comparison with the actual Hammeh slag. The graph clearly shows the large discrepancy in the major oxides SiO<sub>2</sub>, Al<sub>2</sub>O<sub>3</sub>, and CaO, as well as in the alkali and earth-alkali oxides. Results by (P)ED-XRF, using the 'slag\_fun' calibration method (April 2005). Values are expressed in wt% and normalised to 100%.



Mass balance HA 66	SiO <sub>2</sub>	Al <sub>2</sub> O <sub>3</sub>	FeO	TiO <sub>2</sub>	MnO	CaO	MgO	K <sub>2</sub> O	P <sub>2</sub> O <sub>5</sub>	S
HA 66	5.27	0.35	93.3	0.09	0.06	0.27	0.17	0.01	0.26	0.18
Hypothetical slag HA 66	37.4	2.45	52.6	0.65	0.43	1.95	1.24	0.10	1.88	1.29
Actual Hammeh slag	25.2	5.44	52.5	0.34	1.12	10.9	1.80	1.12	1.20	0.39
Difference	12.2	-2.99	0.11	0.31	-0.69	-8.95	-0.56	-1.02	0.68	0.90

Table 35. Mass balances of ore sample HA 66, showing the differences in composition between a hypothetical slag calculated from that ore, and the actual Hammeh slag (average value of the tap slags). Results by (P)ED-XRF, using the 'slag\_fun' calibration method (April 2005). Values are expressed in wt% and normalised to 100%.

This inverted nature of the discrepancies of each hypothetical slag with the actual slag suggests that an average of the two ore samples might provide a closer match between the Warda ore and the Hammeh slag.

In other words, a composition that is the average between samples HA 65 and HA 66 is probably more reflective of the Warda ore body as a whole, than the individual ore samples. This assumption should be reflected in the mass balance of that average, where the SiO<sub>2</sub> and CaO components should show a much closer match between a hypothetical slag and the actual slag.

Mass balance HA 65/66	SiO <sub>2</sub>	Al <sub>2</sub> O <sub>3</sub>	FeO	TiO <sub>2</sub>	MnO	CaO	MgO	K <sub>2</sub> O	P <sub>2</sub> O <sub>5</sub>	S
Average Warda ore	4.86	0.17	89.9	0.05	0.05	4.36	0.17	0.01	0.16	0.28
Hypothetical slag 65/66	22.8	0.81	52.5	0.23	0.21	20.5	0.78	0.03	0.77	1.31
Actual Hammeh slag	25.2	5.44	52.5	0.34	1.12	10.9	1.80	1.12	1.20	0.39
Difference	-2.34	-4.63	0.02	-0.11	-0.91	9.59	-1.02	-1.09	-0.43	0.92

Table 36. Mass balances of average composition of Mugharet al-Warda ore (average of samples HA 65 and HA 66), showing the differences in composition between a hypothetical slag calculated from that ore, and the actual Hammeh slag (average value of the tap slags). Results by (P)ED-XRF, using the 'slag\_fun' calibration method (April 2005). Values are expressed in wt% and normalised to 100%.

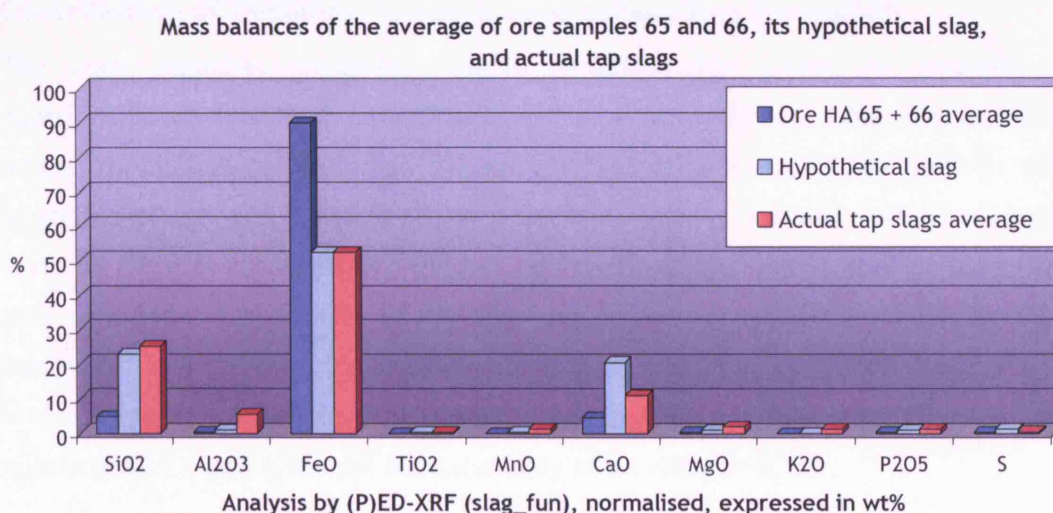


Figure 51. Mass balances of the average composition of Mugharet al-Warda ore (average of samples HA 65 and HA 66), a hypothetical slag based on this average, and the average Hammeh tapped smelting slag. The graph shows the remaining discrepancies between hypothetical and actual slag in the majors Al<sub>2</sub>O<sub>3</sub> and CaO, as well as in the alkali and earth-alkali oxides. Results by (P)ED-XRF, using the 'slag\_fun' calibration method. Values are expressed in wt% and normalised to 100%.



From the average of ore samples HA 65 and HA 66, more than 61 kg of metallic iron (78.7 kg of iron oxide) and some 21 kg of slag would be produced. Table 36 and Figure 51 do indeed demonstrate how the match between this hypothetical and the actual slag improves (compared to that from the individual ore samples) where  $\text{SiO}_2$  and to a lesser extent  $\text{CaO}$  are concerned. However, it is clear that the remaining components are still not balanced very well.

It clearly follows from the consistent mismatch presented above that the Warda ore by itself cannot result in the slag found at Tell Hammeh. One conclusion from this observation might be that the Hammeh slags are unrelated to the Warda ore, and that one has to consider a different ore source. However, as discussed above (see page 147), no other iron ore deposit is known in a radius of hundreds of kilometres from Tell Hammeh, which makes this option seem highly improbable.

Another, more likely conclusion would be that one has to consider other contributions to the process that explain this lack of correlation between the Warda ore and the Hammeh slags. From the mass balances presented above, it is clear that the remaining imbalance is particularly evident in the lack of alumina, which occurs consistently in all three calculations. This persistent mismatch in alumina, which is a typical clay component, suggests that this other contribution comes from the technical ceramics at Hammeh. This suggestion of a contribution by technical ceramics to the process is strongly supported by the observed highly molten state of the tuyères, as described above (see page 159).

### **Contribution of Technical Ceramic to Hammeh Slag Formation**

The mass balances presented below ascertain that when we consider a contribution of technical ceramics to the slag formation at Hammeh, we can adjust the imbalance between Warda ore and Hammeh slag. As before, 100 kilograms of ore are assumed to be processed, but varying amounts of ceramic material are now absorbed into the system as well. Based on the strong impression that considerable quantities of the Hammeh tuyères (made from the local clay) melted off into the smelting process, the technical ceramic composition used here is the average of a sample of the local Lisan clay (HAC1), a sample from a tuyère nozzle (HAC 2), and a sample from the body of a tuyère (HAC 3).

In practice, a smelting system will absorb as much ceramic material from the tuyères or furnace wall as necessary, as a function of the formation of fayalite ( $\text{Fe}_2\text{SiO}_4$ ). This lowers the metal yield per unit of ore, as more iron oxide is needed for the formation of that fayalite. This means that as more ceramic material

enters the system, less iron oxide can be reduced to iron metal (per unit of ore). In the context of the calculations, this addition of more ceramic material to the system changes the total mass involved in the balances. To calculate a hypothetical slag from Warda ore and Hammeh ceramic mixtures, a balance was therefore sought that contains an optimum iron oxide removal to ceramic addition ratio. To achieve this, the practice of a smelt was imitated, in trying to achieve a ceramic addition that is as low as possible. This was done by taking the ceramic-free calculations above as a starting point, and then iteratively adding ceramic (and consequently lowering the amount of iron oxide taken out) until the closest possible match was achieved between all components of the resulting hypothetical slag and the actual Hammeh tap slags.

The mass balances shown in Table 37 and Figure 52 show how the addition of technical ceramic leads to hypothetical slags for each of the ore samples that bear a much closer resemblance to the actual Hammeh slag. They indicate what hypothetical slag, based on the optimum ratio of ore to ceramic contribution, can be calculated for each ore sample as well as from their average. With a change in the ratio of materials contributing towards the slag formation, quantities of the end products (metal yield and slag) change as well. For example, ore sample HA 65, when processing 100 kg of ore together with 20 kg of ceramic, results in a metal yield of 40 kg (equalling 51.5 kg of iron oxide), and 68.5 kg of slag. To match the hypothetical slag of HA 66 with the actual tap slags found at Hammeh requires far more of the ceramic component. Here, 100 kg of ore and 29 kg of ceramic give a yield of almost 44 kg of iron metal, and leave some 72 kg of slag.

It is apparent from the graphs in Figure 52, which presents the mass balances of the three ore options with a ceramic contribution, that the hypothetical slag from the average of the two ore samples gives the best match with the actual Hammeh slag. Here, 100 kg of average ore and less than 19 kg of ceramic contribution yield approximately 47 kg of iron metal and 57.5 kg of slag. It is noteworthy that, due to the more silica-rich gangue component of the HA 66 ore and the more lime-rich HA 65 ore, the mix of the two actually yields more metal and less slag per unit ore than each on its own.

This 'best fit' of the average ore as opposed to the individual ore samples is quantified in the linear regression analysis for each ore option shown in Figure 53. As the various hypothetical slags are calculated towards a matching FeO content, this oxide is not included in the regression.

Mass balances of ore with ceramic contributions	SiO <sub>2</sub>	Al <sub>2</sub> O <sub>3</sub>	FeO	TiO <sub>2</sub>	MnO	CaO	MgO	K <sub>2</sub> O	P <sub>2</sub> O <sub>5</sub>	S
Average ceramic	57.2	13.15	4.78	0.96	0.07	17.5	2.96	2.84	0.22	0.33
HA 65	4.45	0.00	86.5	0.01	0.03	8.45	0.16	0.00	0.06	0.38
Hypothetical slag HA 65 with 20 kg ceramic	23.2	3.84	52.4	0.29	0.06	17.4	1.09	0.83	0.15	0.65
Actual Hammeh slag	25.2	5.44	52.5	0.34	1.12	10.9	1.80	1.12	1.20	0.39
Difference	-1.96	-1.60	-0.08	-0.05	-1.06	6.54	-0.71	-0.29	-1.05	0.26
HA 66	5.27	0.35	93.3	0.09	0.06	0.27	0.17	0.01	0.26	0.18
Hypothetical slag HA 66 with 29 kg ceramic	30.4	5.78	52.4	0.51	0.11	7.42	1.43	1.16	0.45	0.39
Actual Hammeh slag	25.2	5.44	52.5	0.34	1.12	10.9	1.80	1.12	1.20	0.39
Difference	5.20	0.34	-0.15	0.17	-1.01	-3.48	-0.37	0.04	-0.75	0.00
Average Warda ore	4.86	0.17	89.9	0.05	0.05	4.36	0.17	0.01	0.16	0.28
Hypothetical slag 65+66 with 18.3 kg ceramic	26.4	4.42	52.6	0.38	0.10	13.1	1.21	0.90	0.35	0.59
Actual Hammeh slag	25.2	5.44	52.5	0.34	1.12	10.9	1.80	1.12	1.20	0.39
Difference	1.20	-1.02	0.09	0.04	-1.02	2.16	-0.59	-0.22	-0.85	0.20

Table 37. Mass balances of the three ore samples (HA 65, HA 66, and their average, showing the differences in composition between a hypothetical slag with additions of technical ceramic, and the actual Hammeh slag (average value of the tap slags). Results by (P)ED-XRF, using the 'slag\_fun' calibration method (April 2005). Values are expressed in wt% and normalised to 100%.

The correlation coefficient (expressed as root square,  $R^2$ ), indicates the level to which all components of the relevant hypothetical slag are likely to match with the same components in the actual Hammeh slags, where an  $R^2$  value of 1 would mean that the two slags are identical. As seen in Table 37 and Figure 52, it is the average ore composition that, with a ceramic contribution, results in a hypothetical slag that, although not an exact match, does come very close to the actual composition of the Hammeh slag. The closeness of that match is confirmed in Figure 53 where the third regression line expresses the match between the hypothetical slag from the average and the Hammeh tap slags, which shows a high correlation coefficient of 0.9913.

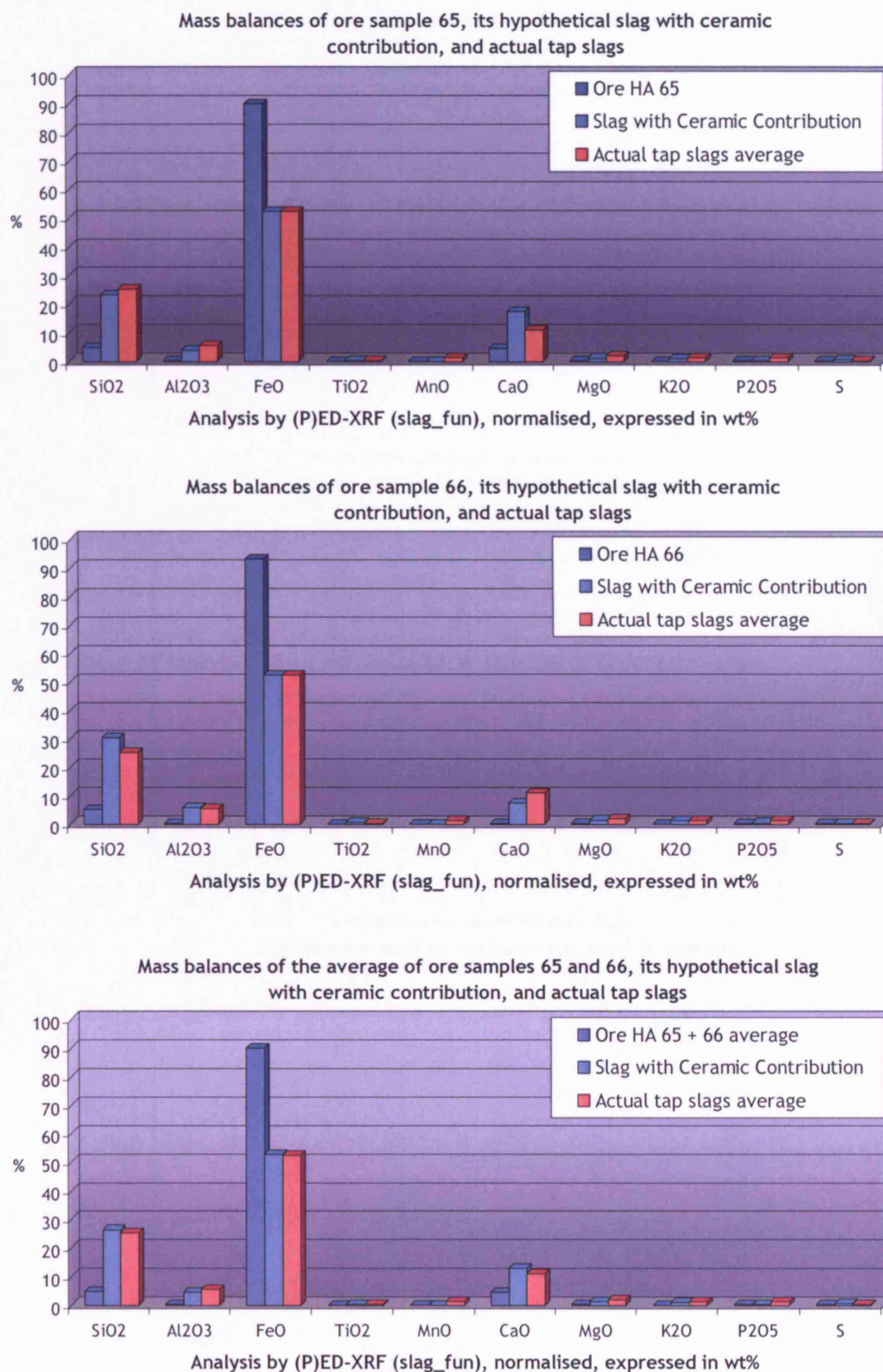


Figure 52. Mass balances of Mughareet al-Warda ore (HA 65, HA 66, and the average ore), showing the composition of a hypothetical slag resulting from each ore sample together with a ceramic contribution, in comparison with the actual Hammeh slag. The graph indicates an improved match in most components, with remaining discrepancies in predominantly Al<sub>2</sub>O<sub>3</sub> and CaO. Results by (P)ED-XRF, using the 'slag\_fun' calibration method (April 2005). Values are expressed in wt% and normalised to 100%.

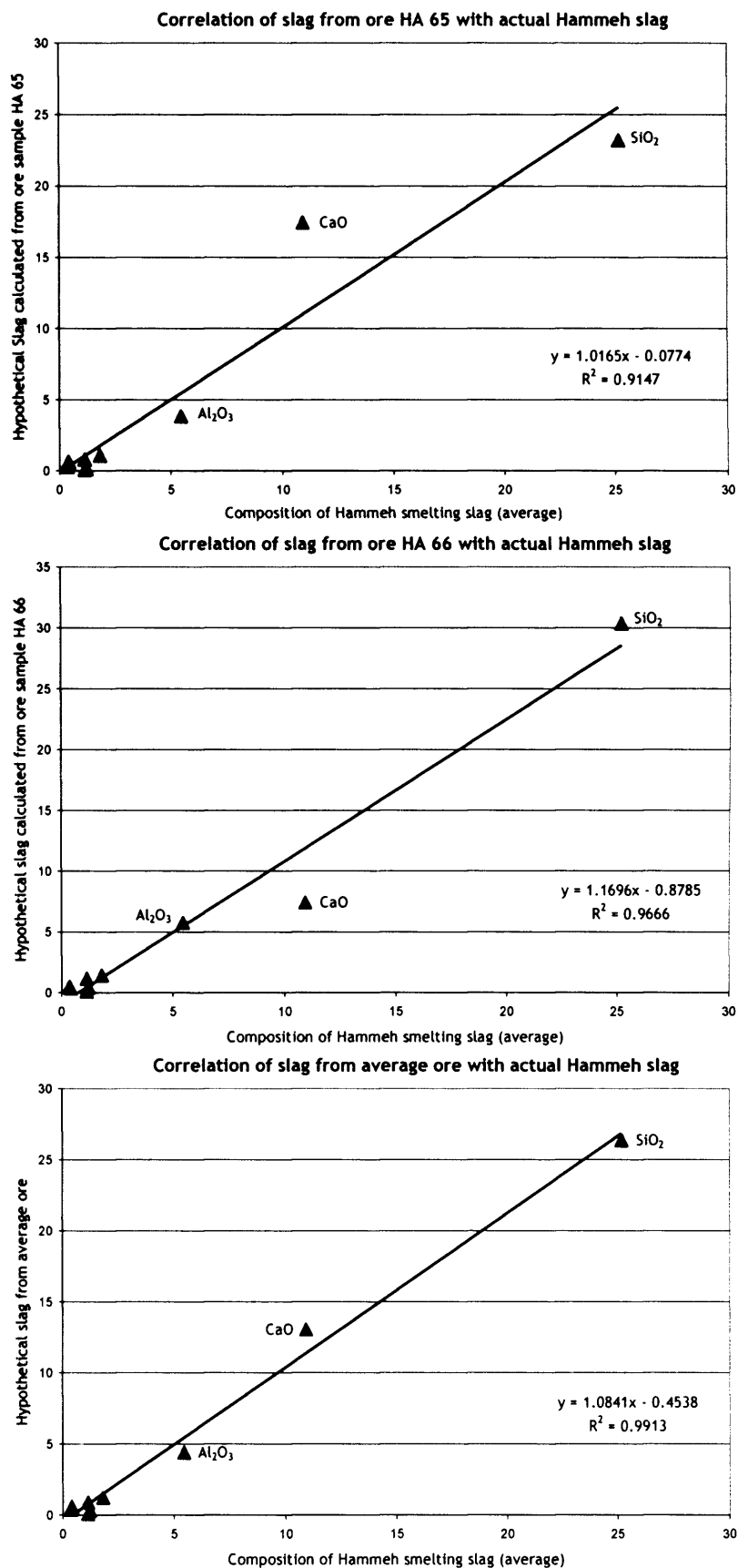


Figure 53. Regression line showing the correlation between the actual Hammeh slag compared with the hypothetical slags based on ore HA 65, HA 66, and the average of these two samples respectively. FeO is excluded from these analysis and values are expressed as wt%.

## Remaining Discrepancies

The remaining discrepancies mostly occur in MnO and CaO, and MgO, K<sub>2</sub>O and P<sub>2</sub>O<sub>5</sub> (Table 38). Especially these last, however, are typical fuel ash elements, and likely stem from there, as demonstrated by Serneels and Crew (Crew 2000; Serneels and Crew 1997). Because of the uncertainty of the exact lime content in the ore, and especially the quantitative nature of the charcoal analysis, the composition of the charcoal was not directly used in the mass balance calculations. Table 38 does indicate, nevertheless, which remaining discrepancies between the hypothetical slag and the actual slag the charcoal might compensate, and its contribution of alkali and earth alkali oxides to the slag formation is therefore assumed.

Remaining discrepancies	MnO	CaO	MgO	K <sub>2</sub> O	P <sub>2</sub> O <sub>5</sub>	S
Hypothetical slag to actual tap slags	1.03	-1.73	0.74	0.26	0.82	-0.23
Composition of Hammeh charcoal	0.05	58	15	5	0.7	1

**Table 38.** The remaining discrepancies between the hypothetical slag based on the average of ore samples HA 65 and HA 66 with ceramic contribution, compared to the amount of these samples present in the analysed charcoal from Hammeh. The charcoal values are normalised and all values are expressed in wt%. Analysis by (P)ED-XRF (slag\_fun calibration method, April 2005).

As demonstrated above through the mass balance calculation presented above, a contribution of technical ceramic from local clay clearly relates the Hammeh smelting operations to the Warda ore. The remaining discrepancies, to an extent, can be attributed to the -not calculated in the mass balances- contribution of fuel ash to the slag formation, as indicated in Table 38. Estimating a possible charcoal composition and related fuel ash contribution is very difficult when the actual fuel is not fully known. Hardly any chemical bulk analyses of woods and their charcoals are available, and where they are, olive wood is usually not among the species analysed.

Even so, most studies agree that the composition of wood is heavily influenced by the soil on which the tree grows. In a scenario of olive tree pruning in the areas surrounding Hammeh, and wood from that pruning ending up as charcoal for the iron production, the soil conditions in the Jordan and Zarqa Valleys would certainly dictate a lime rich charcoal. As shown below, that is born out by the screening analysis of Hammeh charcoal. When normalised for its ash components, this charcoal ash shows almost 60% of CaO, as well as quantities of the other alkali and earth-alkali (metal) oxides necessary for an even closer match of the Warda ore and Hammeh slag.

## Interpretations and Conclusions

From the above, it is reasonable to conclude that the two separate ore samples only represent two different compositions of a (perhaps wider) range of Warda ore composition. Without extensive further sampling at the site of the ore body, however, it is impossible to get a more precise picture of the nature of the Warda ore. Even with a larger range of compositions to process, that may still not fully represent the particular ore used by the Hammeh smelters.

The main problematic variable in the mass balances remains CaO. Differences of this component between the hypothetical slag and the actual slag are easily explained through the uncertainty about the ore composition used in antiquity. As mentioned by Bender (see page 147, ff, and Figure 21), the lens of haematite ore at Warda blends with surrounding limestone, and ore from early exploitation may well have been more  $\text{CaCO}_3$ -rich than  $\text{SiO}_2$ -rich. To smelt such an ore would only strengthen the need for sacrificial tuyères to act as a silica-rich flux. Another factor that was not reflected in the calculations above is variations in composition of the ore that was smelted in antiquity due to beneficiation or roasting for example. Whereas the presence of discarded 'ore' at Hammeh would suggest some degree of selection between material that is deemed more or less suitable, the sometimes unprocessed state of ore within some of the furnace slags suggest that roasting only took place as part of the smelting process proper.

It is clear that considerable amounts of technical ceramics were absorbed into the smelt. The physical appearance of the tuyères, with their heavily molten and vitrified nozzles, strongly supports the chemical data that indicate an important contribution of technical ceramics to the formation of the Hammeh slag.

From the combination of these physical and chemical data, it can be concluded that the Hammeh smelters purposefully applied *sacrificial tuyères* to facilitate and enhance the production of iron, in which the tuyères, and probably the furnace wall as well, act as a silica-rich flux. This sacrificial contribution of the tuyères plays a crucial role in the iron smelting operations on Tell Hammeh, as it strongly influences the temperature regime in the furnace.



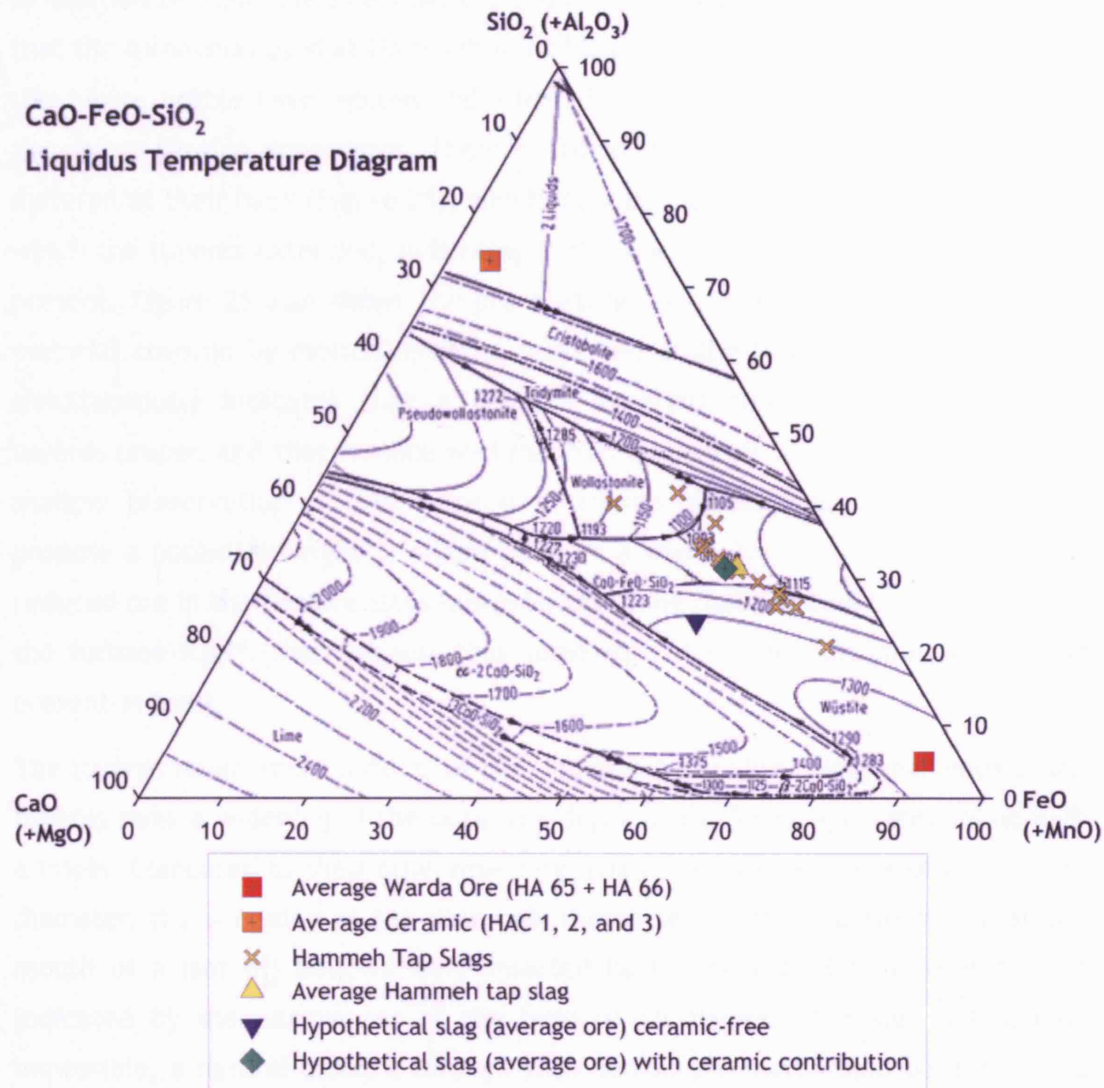


Figure 54. The average value of the Hammeh tap slags plotted in the CaO (+MgO)-FeO (+MnO)-SiO<sub>2</sub> (+Al<sub>2</sub>O<sub>3</sub>) liquidus temperature ternary diagram. This composition is compared to the hypothetical ceramic-free slag based on the average of the two ore samples, the average ore, and average ceramic composition. Comparing the actual slag with the ceramic-free slag shows how the ceramic contribution significantly affects the solidification temperature of the Hammeh slag, lowering it from around or above 1250 °C to around 1100 °C.

As can be seen in Figure 54, the absorption of technical ceramic in the formation process of the Hammeh slag exercises an important influence on the (liquidus) temperature of the Hammeh the tap slags. By shifting the balance of components in the system towards a more ceramic composition (towards the CaO and SiO<sub>2</sub> corners of the ternary diagram), the sacrificial tuyères change the liquidus temperature from around 1250 °C to around 1100 °C. This temperature represents or lies slightly below the operating temperature of the furnace. A temperature in the range of 1100 °C temperature would obviously be easier to achieve and to maintain by the Hammeh metalworkers.

In addition to their role as a flux, the physical appearance of the tuyères suggests that the furnace(s) used at Hammeh must have had some form of shaft. Several of the tuyère nozzle have molten and vitrified 'beards', i.e. material melting from the nozzle flowing downwards. These beards often incorporate unmolten ceramic material at their back (Figure 25), which must be part of the furnace wall through which the tuyères extended, indicating that some superstructure must have been present. Figure 25 also shows the preservation of a small fragment of unmolten material covered by molten material preserved at the top of the tuyère, which simultaneously indicates that a possible superstructure extended above the tuyères proper, and that furnace wall material melted off as well. Due to the very shallow preservation of the furnace structures themselves, it is difficult to propose a potential height or shape for such a shaft. The nature of the partially reduced ore in the furnace slags however, revealing that roasting took place inside the furnace itself, does suggest that some sort of filling shaft must have been present at least.

The tuyères reveal more aspects of the Hammeh technology. Most rear ends of the tuyères show a widening of the bore to a depth of ca. 5 cm, apparently done with a finger. Compared to their otherwise very narrow and straight bore of ca. 1 cm in diameter, the widening at the rear only makes sense when considering that the mouth of a (set of) bellows were inserted here. The use of bellows is further indicated by the narrowness of the bore of all tuyères. Although not strictly impossible, a natural draught through such narrow channels would be difficult to maintain, and might easily be disrupted by blockage of the bore by melting ceramic or slag at the nozzle end.

Finally, the large quantities and standardised size and shape of the tuyères together with the large quantities of smelting slag combine to create the impression of an iron smelting operation at Hammeh that functioned well beyond what might be considered an experimental stage of production. Using the estimated yield of metal and slag per unit of (the average) ore, as determined through the mass balance calculations, Hammeh must have produced some 10 tons of iron metal in less than 200 years of seasonal production.

## CHAPTER 9: ANALYSIS OF THE BETH-SHEMESH MATERIAL

### Introduction

The material excavated in the smithy at Beth-Shemesh falls into four or possibly five categories: slag, hammerscale (and slag prills), iron and copper artefacts, tuyères, and possible hearth structures or features. The tuyères, for now, remain in Israel and are currently being examined petrographically by Yuval Goren (see also chapter 5), in combination with a tuyère sample from Tell Hammeh. Analysis of the metal artefacts is outside the scope of this study. The analyses described here will therefore focus primarily on the slag and hammerscale/prills.

Analysis of these materials tries to answer several questions. First, the initial identification of the Beth-Shemesh activity as secondary smithing needs to be confirmed or denied. After determination of the nature of the metallurgical activity that took place at Beth-Shemesh, it can be attempted to reconstruct (parts of) the technological *chaîne opératoire* at Beth-Shemesh. Furthermore, by examining the spatial distribution and quantities of the various materials (and to a lesser extent the artefact finds) within the workshop, an interpretation can be made of the use of space, and possible activity areas.

### Formation and Analysis of the Slag

One factor in distinguishing smelting from (secondary) smithing, and thus in identifying the nature of the Beth-Shemesh metallurgy, is the composition and structure of the slag. Smithing slags are often very similar to bloomery smelting slags in general chemical and micro-structural composition. It is through analysis of microstructure and chemical composition of the slags together with their external shape and find circumstances that distinction between smelting and smithing is possible (Pleiner 2000, 255). The morphology, size, and uniformity of the Beth-Shemesh slag all point towards smithing. All the slags recovered at Beth-Shemesh are of one single type: round concavo-convex shapes, with a diameter of up to 10 cm, with rust adhering to the top and soil adhering to the bottom. Some of the more complete examples also reveal a shallow dip with a 'ridge' of slag on the top, as if the airflow from the tuyère pushed up the liquid material. These morphological features form a classic example of a smithing hearth bottom (SHB) or plano-convex bottom (PCB), where each specimen represents a single smithing operation (Serneels and Perret 2003, 473; see also chapter 5). An example of this typical SHB shape is shown by the section of E/T48 SF (a surface find from grid J2) in Figure 55. No slags with free flowing (tapped) structures, or any other type that

can be considered typical of a smelting operation (see chapter 8), were attested at Beth-Shemesh.



Figure 55. Section of SHB slag E/T48 SF. The SHB clearly shows a porous slag core of concavo-convex shape, with rust adhering to the top and soil embedded at the bottom.



Figure 56. Top view of SHB slag E/T48 2834.23, showing a depression at the centre, indicating where the airflow from the tuyère hit the forming slag. The approximately straight side at the bottom of the picture may be the place where the SHB was in contact with the hearth wall, indicating that the tuyère was located on this side of the SHB (Serneels and Perret 2003).

At least 65 individual SHBs have been excavated so far, together with more than 150 fragments. Much of what was recorded as ‘fragments’, however, are actually sample bags containing multiple pieces, so the actual total of fragments is considerably higher.

Smithing slag forms as a fusion of materials that collect at the bottom of the hearth. This fusion takes place in the hottest zone of the hearth, i.e. in front of the tuyère, after which the slag settles and solidifies just below that area. Shape, heterogeneity, and size of the slag is dependent on a range of factors, including strength of the air supply, temperature, and the nature of the materials that accumulate here (Serneels and Perret 2003, 470-471). An important contributor to the formation of smithing slag is the oxidation of the iron metal when exposed to oxygen at a high temperature. At prolonged heating, the surface of the iron metal will oxidise rapidly, forming a crust of iron oxide. This crust, or scale, in the shape of flakes as a result of the plastic deformation from the hammering, and in relation to shape and size of the metal worked, will eventually break away from the metal and part of it will end up in the hearth. Often the smith applies a flux (e.g. sand or clay) to cover the surface of the metal, both to protect the metal from oxidation, and to fuse with and liquefy the scale already present. A large proportion of these scales will further get detached and fly off as a result of hammering the metal on an anvil. Because of this, the scales are generally referred to as *hammerscales*, which are discussed below.

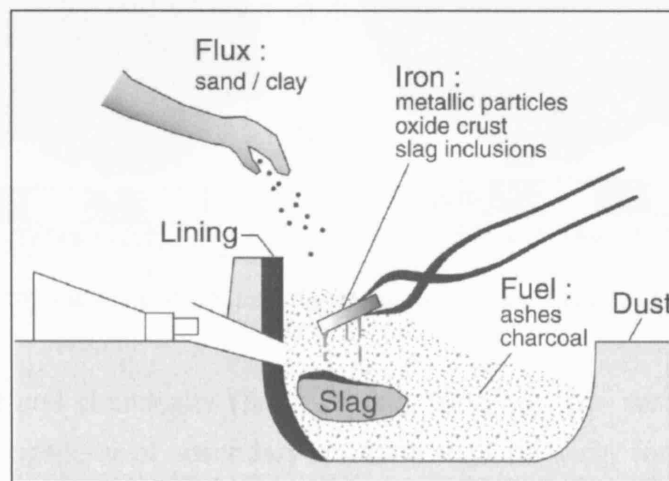


Figure 57. Schematic representation of contributions to the formation of a smithing hearth bottom slag (from Serneels and Perret 2003, 472)

There are several other contributions to the formation and composition of a smithing slag. The first is from smelting slag that remained trapped as inclusions



in the more or less consolidated piece of previously smelted metal. When this billet is fashioned into an object, the slag inclusions are remolten and will drip into the hearth. Other contributions come from the ceramic materials that form the hearth, dust from the surrounding workshop, and fuel ash and charcoal (Serneels and Perret 2003; Pleiner 2000, 254-255). A schematic representation of the formation of a smithing hearth bottom slag is given in Figure 57.

Five samples were selected for further analysis. They come from grid K10, unit 2 (sample TBS1), grid I15, unit 2 (sample TBS2), grid D13, unit 1 (sample TBS3), grid F10, unit 1 (sample TBS4), and grid K13, unit 1 (sample TBS5), all in square E/T48 (see Figure 13). Morphologically these samples do not retain their complete shape, but they reveal a clear SHB shape: they are concavo-convex, with rust on top and soil embedded in the bottom. The samples were sectioned and a part of this section, covering top, centre, and bottom, was mounted in resin, then ground and polished for microscopical examination. An additional part of each sample, adjacent to the mounted part, was crushed and milled, and pressed into a pellet for bulk chemical analysis by (P)ED-XRF.

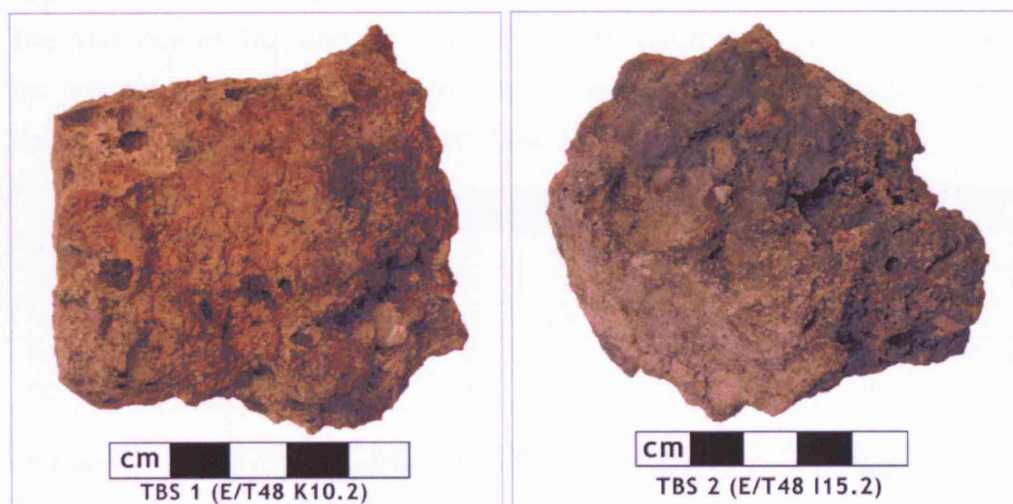


Figure 58. Samples TBS 1 (E/T48 grid K10, unit 2) seen from the top, and TBS 2 (E/T48 grid I15 unit 2) seen from the bottom.

Microscopically and chemically (Table 39 and Table 40), the samples reflect the expected heterogeneity of secondary smithing slag, showing, for example, some variation in their respective iron oxide, silica, and lime contents. This heterogeneity may partly be resolved by analysing a larger number of samples, which would, for example, counter possible sampling related variations and provide a slightly more balanced chemical characterisation. Performing a large range of analyses to reduce such statistical error lies outside the scope of this

thesis. Furthermore, it can be reasonably assumed that most of the observed variation is a function of the wide range of contributors to the formation of secondary smithing slags (see above).

Smithing slags	SiO <sub>2</sub>	Al <sub>2</sub> O <sub>3</sub>	FeO	TiO <sub>2</sub>	MnO	CaO	MgO	K <sub>2</sub> O	P <sub>2</sub> O <sub>5</sub>	S
TBS 1	21.0	3.27	59.1	0.20	0.06	12.7	1.05	1.71	0.86	0.07
TBS 2	30.6	4.97	34.8	0.41	0.18	24.5	1.87	2.05	0.53	0.06
TBS 3	28.7	4.62	44.5	0.33	0.07	17.8	1.57	1.68	0.81	0.05
TBS 4	20.7	3.22	57.6	0.19	0.05	13.3	1.51	2.03	1.26	0.08
TBS 5	23.2	3.64	54.1	0.25	0.06	14.9	1.18	1.77	0.81	0.04
Average	24.8	3.94	50.0	0.27	0.08	16.6	1.44	1.85	0.85	0.06

Table 39. Bulk chemical composition (major elements) of the Beth-Shemesh secondary smithing slags. Analysis by (P)ED-XRF (slag\_fun calibration method, April 2005). Analysis by (P)ED-XRF, normalised to 100% and expressed in wt%.

In their overall composition, these slags compare quite well to other smithing slags discussed in the literature (e.g. Kronz 1998, 225), except that their lime content is considerably higher (ca. 16 wt% compared to a more regular content between ca 0.5 and 5 wt%). Their average iron oxide content is also lower than might be considered regular (almost 50 wt% compared to between 50 and 80 wt%). The presence of TiO<sub>2</sub> and MnO in the Beth-Shemesh slags probably derives from the original ore, and thus indicates the presence of a contribution to the smithing slag from the smelting slag (Pleiner 2000, 255).

Smithing slags	Ni	Cu	Zn	Rb	Sr	Y	Zr	Ba	Pb
TBS 1	bdl	60	20	bdl	330	15	170	930	bdl
TBS 2	25	45	25	10	570	25	280	2130	bdl
TBS 3	bdl	50	40	bdl	430	30	230	1410	bdl
TBS 4	bdl	80	30	bdl	380	20	180	970	bdl
TBS 5	bdl	60	30	bdl	330	20	210	1030	bdl
Average	25	60	30	10	410	20	210	1290	bdl

Table 40. Bulk chemical composition (trace elements) of the Beth-Shemesh secondary smithing slags. Analysis by (P)ED-XRF (slag\_fun calibration method, April 2005). Values are expressed in ppm (parts per million), or as bdl (below detection limit).

The low level of iron oxide in the slags may also be the result of a carefully executed smithing cycle, where it is attempted to limit the loss of iron by oxidation, as one might expect in an early context, and/or a higher ceramic and fuel ash contribution instead. A higher contribution by ceramic material (than in the Hammeh smelting slags, compare chapter 8) seems to be illustrated by the considerable trace of barium in the Beth-Shemesh slags, with is ca. 10 times higher. Finally, virtually no copper is present in either sample, which is a clear indicator that the slags are related to ironworking only (Table 40).



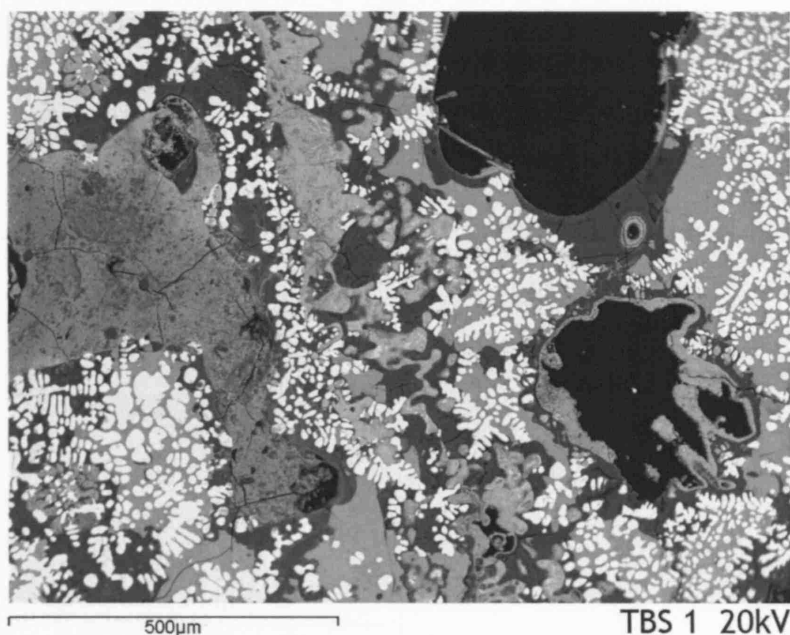


Figure 59. Back Scatter Electron (BSE) micrograph of sample TBS 1, showing the very heterogeneous microstructure of this sample. It consists of a heterogeneous glassy matrix (mid grey and dark grey), incorporating partly fused and thermally cracked quartz grains (dark grey), a large inclusion of iron rich ceramic material (left centre, with cracks), iron hydroxide (around holes), and wüstite (FeO) dendrites (whitish).

The Beth-Shemesh slags are quite similar in composition to the Hammeh smelting (tap) slags (see chapter 8), except that those contain more MnO (1.12 wt% average; related to the ore) and less CaO (ca. 11 wt% average; related to ceramic material). The earlier suggested contribution from smelting slag incorporated in the billet to the formation of the secondary smithing slags appears to be borne out by relatively large quantities of free iron oxide in the form of wüstite in the SHBs (Figure 59). This appears to be confirmed by the fact that all samples show only a low magnetism. Iron oxide contributing to the slag from the hot oxidation of the metal itself would most likely appear in the form of magnetite, which does occur as well (Figure 60), but less frequent, perhaps in relation to the aforementioned care taken to minimise loss of metal.

The very heterogeneous microscopic composition discussed here is matched by a heterogeneous chemical composition of several of the phases (see the SEM-EDS analyses in appendix 2). Whether this is related to the mixed origin of the slags, incorporating iron oxide from the billet, re-liquefied slag from the original smelt, and quartz grains and ceramic inclusions from the tuyère nozzle or hearth structure, in varying amounts, remains speculative.

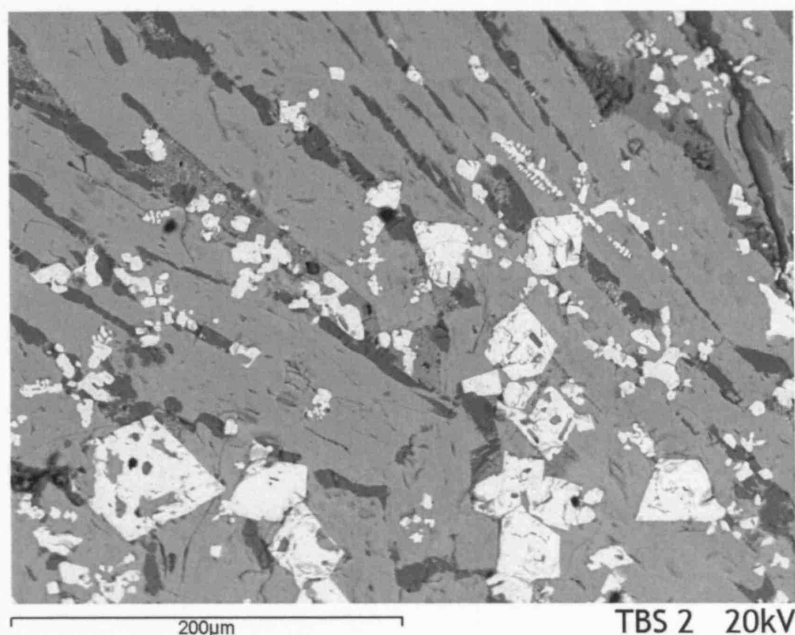


Figure 60. Back Scatter Electron (BSE) micrograph of sample TBS 2, showing a kalsilitic ( $\text{KAlSiO}_4$ ) glassy matrix (dark grey), large kirschsteinitic ( $\text{CaFeSiO}_4$ ) laths (mid grey), and precipitation of magnetite crystals (whitish).

The bulk chemical analyses of the Beth-Shemesh slags alone do not immediately allow an unquestionable identification of these slags as being the result of secondary smithing (as opposed to either smelting or primary smithing), but they do give some indications that support such an interpretation. The apparent stronger relation to ceramic material, as seen in elevated levels of lime and barium, combined with an apparent (but speculative) more distant relation to the original ore, as seen in the lower amounts of manganese (when compared to the Hammeh smelting and primary smithing slag; see chapter 8) do correspond with an origin in secondary smithing.

These observations are further illustrated by application of Principal Component Analysis (PCA; see chapter 6; compare chapter 8), comparing the chemical composition of the Beth-Shemesh slags to that of the tap slags and primary smithing slags of Tell Hammeh. Figure 61 shows how the Beth-Shemesh slags form a separate cluster away from the two Hammeh slag types. The loading vectors of the original variables illustrate how the variance of the Beth-Shemesh secondary smithing slags is more influenced by elements such as  $\text{K}_2\text{O}$ ,  $\text{CaO}$ , and  $\text{Ba}$ . This sets them apart from the Hammeh tap and primary smithing slags, whose variance is more strongly influenced by elements such as  $\text{FeO}$ ,  $\text{MnO}$ , and  $\text{MgO}$ . It should be noted that the PCA plot is used here as a non-model-based tool to illustrate patterns of variation, and does not provide an explanation of that variation.

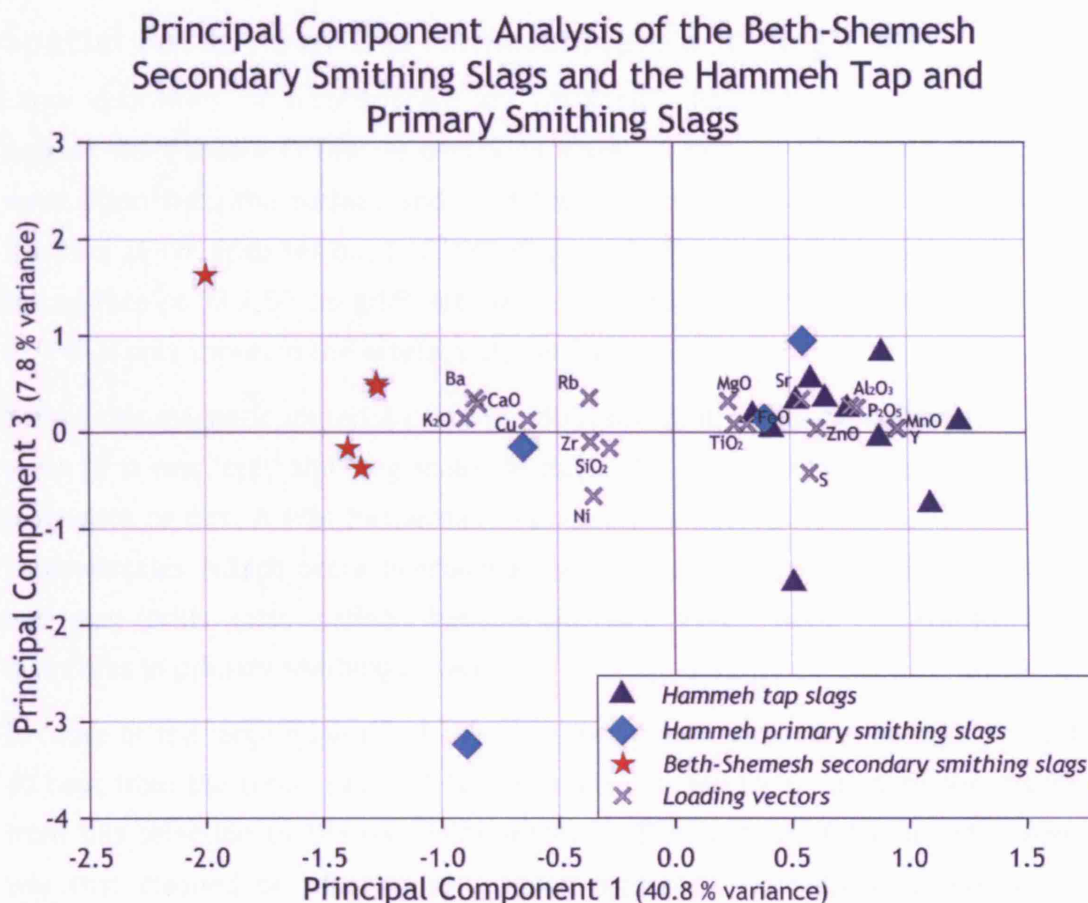


Figure 61. Principal Component Analysis of the Tel Beth-Shemesh secondary smithing slags, compared with the Hammeh tap and primary smithing slags. The graph illustrates how the Beth-Shemesh slags form a different group from the Hammeh slag types, and how their variance is more strongly influenced by  $K_2O$ ,  $CaO$ , and  $Ba$  than the Hammeh slags, whose variance is more strongly influenced by  $FeO$  and  $MnO$  for example. The plot uses Principal Component 1 and 3. (The PCA scores and loading vector values can be found in appendix 3).

Furthermore, the very singular and uniform morphology of the slags shows several details that do point towards secondary smithing, e.g. the depression of the top and concavo-convex shape, concentration of rust on the top of the samples, and embedded soil in the bottom of the slags. This uniformity together with the relatively low quantity of SHBs at Beth-Shemesh provides a further argument in favour of smithing. It stands in clear contrast to the large quantities of (morphologically and typologically more variable) slags at Hammeh. When combining this morphological homogeneity of the Beth-Shemesh slags with the heterogeneity observed in their microscopic constitution and phase chemistry, as well as the large quantities of hammerscale in the workshop as a whole (discussed below), an interpretation as secondary smithing slag (rather than smelting or primary smithing slag) is viable.

## Spatial Patterns of the Hammerscale and Slag Prills

Large quantities of hammerscale and magnetic material were recovered by magnet from square E/T48, as described above. A total of 322 separate batches were lifted from the surface and from the two units excavated separately from the 25 x 25 cm grids set out in E/T48 (Figure 13; Figure 63; Figure 64), and from the surface of 50 x 50 cm grids set out in the northern parts of E/T48 and E/T49 (E/T49 is only shown in the artefact plot in Figure 63).

Before this magnetic material could be interpreted, it had to be determined how much of it was 'real' smithing scales or slag prills, and how much was geological magnetite or dirt. It was furthermore necessary to determine the ratio between hammerscales (which occur predominantly from secondary smithing, see below) and slag prills (also called 'hammerspheres'; which occur in considerable quantities in primary smithing as well).

Because of the large quantity of this material, it was decided to randomly select 40 bags from the total, i.e. 12.5 %, for processing and to extrapolate the results from this selection to the remaining material. The content of the selected bags was first cleaned of adhering soil, which hindered examination of the actual magnetic material. A first attempt by sieving and then washing in industrial alcohol proved insufficient. This was replaced by using a solution of 10% HCl to dissolve the soil. As this process is quite corrosive, extreme care was taken to stop the reaction before the hammerscale could be affected, even if traces of soil then remained. Largely, determining when to stop is an intuitive decision. It is based on observing the reaction of the HCl with the soil, which creates an aggressively frothing layer of white foam. The frothing starts to slow as most of the reaction with the soil is complete, at which point the HCl will start to react with the now uncovered scales, which results in a yellowish colouring of the foam. Care was taken to stop the reaction when the frothing slowed down and whilst the foam was still white, by pouring away the HCl solution and adding water.

Microscopic inspection of the cleaned material showed that no geological magnetite was present. Therefore, it is assumed that all recovered magnetic material stems from the smithing process proper. It was further examined whether the quantities of slag prills (small, round or droplet shaped, slag globules dispersed during the hammering of an iron billet, or during the consolidation of a bloom during primary smithing) showed significant differences between individual batches. However, absolute quantities of slag prills were very low, and too evenly

distributed in all cleaned batches, to warrant any interpretation of spatial patterning. Almost all material in the cleaned samples is formed by hammerscale, indicating that the magnetic material stems from secondary smithing, as far larger quantities of slag prills could have been expected from primary smithing.

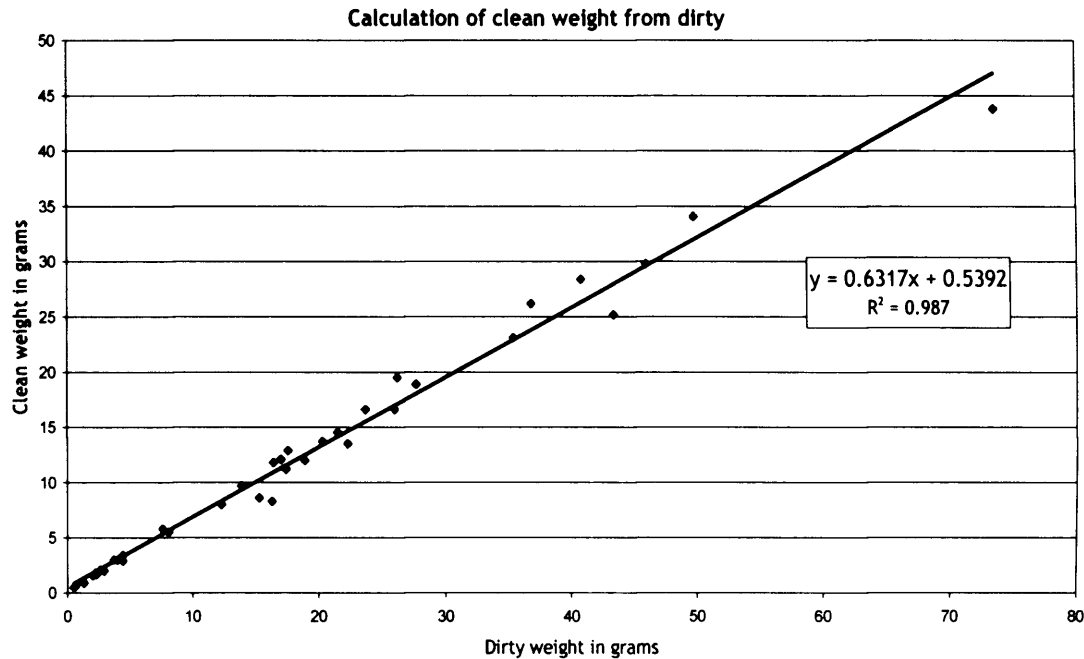


Figure 62. Regression analysis of dirty versus clean weight of the 40 processed batches.

Using the difference between the weight of the clean samples against their original 'dirty' weight, a correction could be calculated by establishing the root mean square of the two weights. Using this calculation ( $y$  (clean) =  $0.6317x$  (dirty) + 0.5392 gram, shown in Figure 62, the clean weight of all samples was subsequently established, and used in the plotting of the spatial pattern of the hammerscale.

From the high correlation between the 'dirty' and 'clean' samples it is clear that the dirty weight could have been used for further analysis just as well as the clean weight, but this is only valid for the particular circumstances at Beth-Shemesh (no geological dirt, little or no prills), and only became clear after the cleaning and examination of the 40 bags.



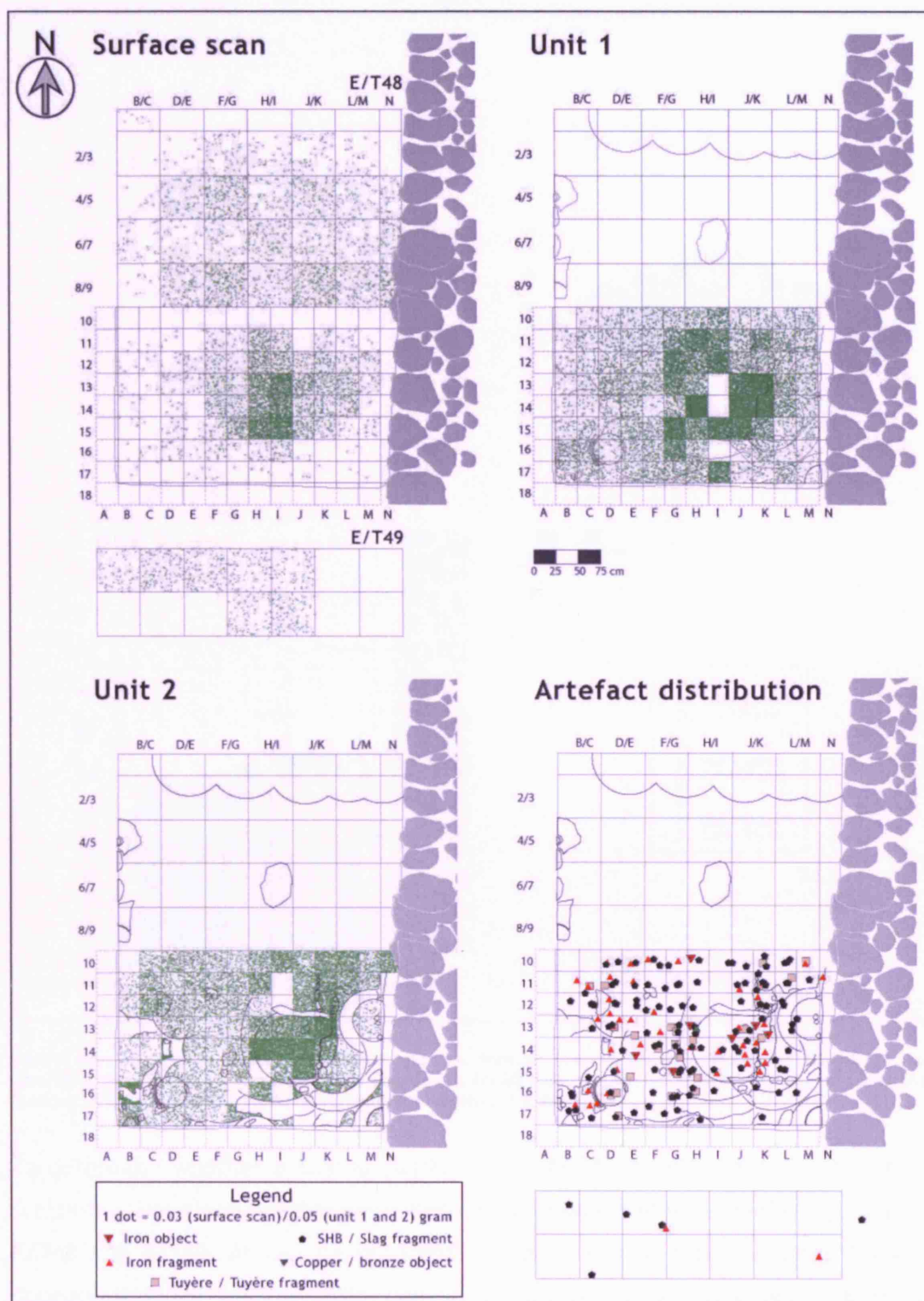


Figure 63. Distribution of hammerscale and artefacts in Square E/T48 (and surface of E/T49). The bottom of units 1 and 2 are 5 and 15 cm below the surface respectively. The remaining empty grids seen in unit 2 relate to a partially unexcavated intermediate baulk in rows H and I, and those in unit 1 to a few missing bags of hammerscale. The artefacts plotted in the lower right hand plan are from the 2003 season only, and have not been separated into the units excavated. Each dot represents a single artefact (SHB, metal object, or tuyère).

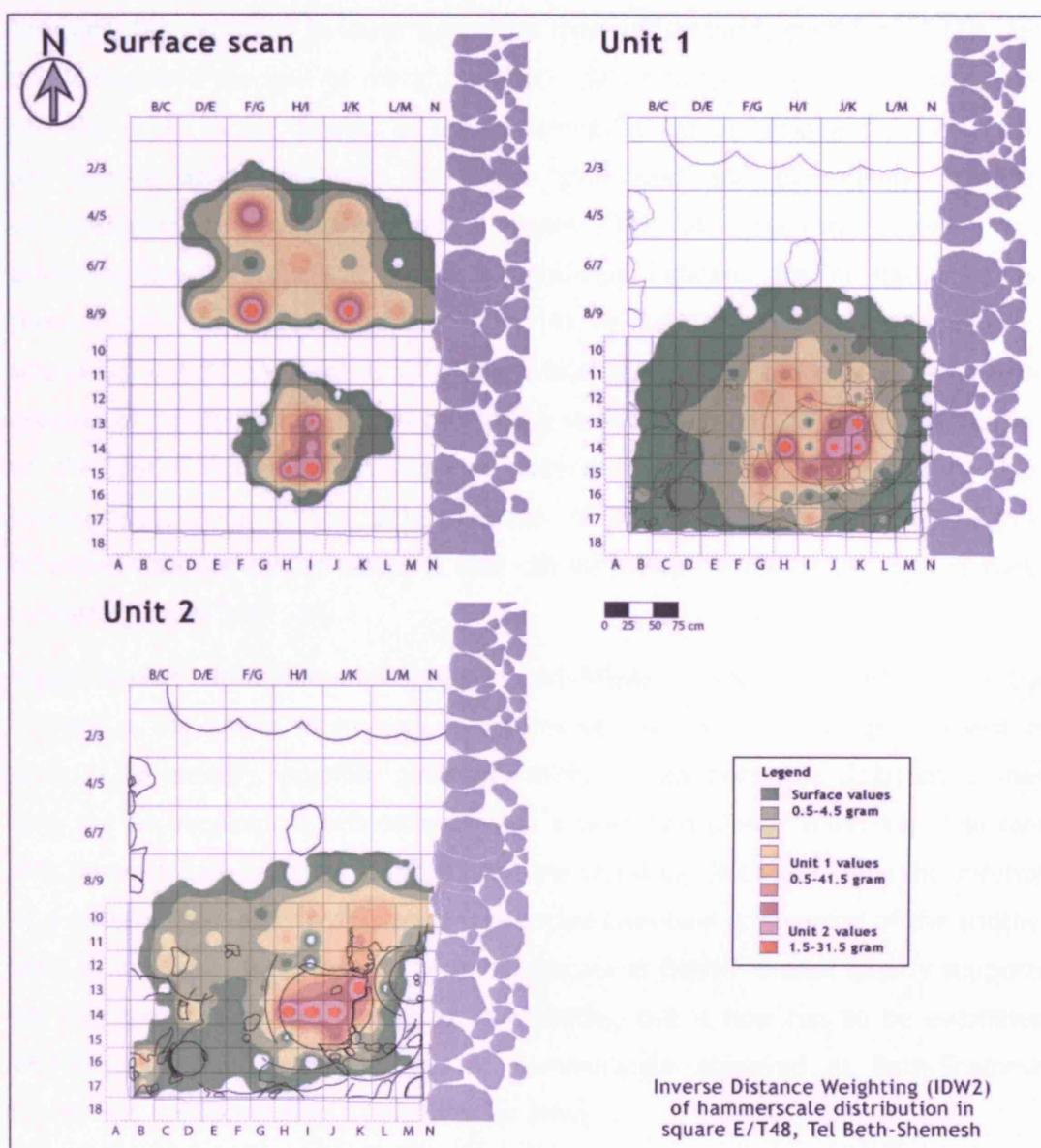


Figure 64. Distribution of hammerscale, presented through Inverse Distance Weighting (IDW2) of the hammerscale distribution in square E/T48 (created in ArcGIS 8.3 using Spatial Analyst). Please note that the plotting spills over into the empty grid row 8/9 for both unit 1 and 2.

To determine whether a spatial pattern could be discerned in the hammerscale scattering, the clean weights were plotted, per excavated unit, on the top-plan of E/T48 and E/T49. As can be observed in Figure 63 and Figure 64, the highest concentration of hammerscale coincides with the large ashy area observed archaeologically (see Figure 13), in all units excavated.

As mentioned above, the presence of hammerscale in an excavation, and its ratio to slag prills, carries several meanings. Slag prills are produced in relatively high quantity in a primary smithing context, by the expulsion of smelting slag during the consolidation of a bloom. Slag prills can also be produced during secondary



smithing, but generally in lower quantities than with primary smithing, as less slag is left enclosed per unit of metal. Magnetic debris in the shape of hammerscales can also occur in the context of primary smithing, but larger quantities of scales are usually associated with the more prolonged and extensively oxidising circumstances of secondary smithing (Jones 2001, 14). The ratio between slag prills and hammerscale is therefore a significant indicator for the nature of the process that they represent (Jones 2001, 14). As mentioned above, the number of slag prills at Beth-Shemesh is very low, whilst the bulk of the magnetic material consists of hammerscale, which provides a strong argument for the identification of the Beth-Shemesh metallurgy as secondary smithing. But not only does hammerscale help in the determination of the nature of the metallurgical activities that are taking place, it also can be indicative of the location of these activities (Jones 2001, 14).

Concentrations of hammerscale are found inside a smithing hearth or in the vicinity of the anvil. When such structures or objects are no longer present or difficult to identify, possible patterns within the hammerscale distribution may help the archaeological reconstruction of a workshop (Jones 2001, 14). The fact that hammerscale is easily trampled into the workshop floor can allow the survival of a pattern even after extensive or repetitive sweeping or cleaning of the smithy. Seen in this light, the presence of hammerscale at Beth-Shemesh clearly supports an interpretation of the workshop as a smithy, but it now has to be examined whether the main concentration of hammerscale observed at Beth-Shemesh represents the location of a hearth or an anvil.

The connection of the reconstructed highest concentration of hammerscale within its distribution (Figure 63 and Figure 64) to high concentrations of ash in the same location, suggests that this concentration reflects the (final) hearth structure rather than the location of an anvil. Rearrangement or rebuilding of the hearth structure, anvil, or storage facilities, and disturbance by (occasional or regular) cleaning of the workshop floor by the smith(s) can not be excluded, and may distort the archaeological picture. There may be slight indications for earlier hearth structures by slight rises in hammerscale quantities in the south-west corner of square E/T48. The distribution of tuyère fragments within E/T48 forms another potential but difficult to assess confirmation of the identification of the possible hearth locations. The location of an anvil cannot be determined at present.

## The Tuyères

A total of 28 fragments of tuyères were found at Beth-Shemesh. Most of these are very small pieces, often only just recognisable as being part of a tuyère. A few, however, are complete, in the sense that they preserve the entire circumference of the original tuyère, but not the full length. An important observation was that these tuyères, like the ones at Tell Hammeh, but unlike most other (bronze metallurgy) tuyères in the Levant, are square in section. They all measure around 5x5 cm in section (one is slightly smaller; Figure 65), and have a bore of 1 cm in diameter. They show a molten and partially vitrified surface at the nozzle. No rear ends survive, and all fragments are broken at a relatively short distance behind the nozzle.



Figure 65. One of (smaller) Beth-Shemesh tuyères, registration number 2319, which was excavated during the 2001 season. The tuyère clearly shows the narrow bore and square section, as well as the molten nozzle. This particular tuyère has a smaller cross section (3.5 x 3.5 cm) than the other Beth-Shemesh tuyères (After photograph by Zvi Lederman).

Because of the striking likeness between the Beth-Shemesh and Hammeh tuyères, it was decided to explore if there were more connections than just the shape. A small fragment of a tuyère from each site was sent to Yuval Goren at Tel Aviv University, who is currently performing petrographic analysis to determine the nature and origin of the clay. It has already emerged that both clays are identical, and do not resemble any clay within a reasonable distance from Beth-Shemesh, but rather the local clay of the Jordan and Zarqa Valleys. What this means for the interpretation of procurement of raw materials, or social, cultural, or economic links between the two sites is being studied.

## Iron and Copper (Alloy) Artefacts

Both iron (26 artefacts and some 100 fragments) and copper (alloy) (four artefacts and five fragments) objects were found in the context of the Beth-Shemesh smithy. These artefacts fall outside the scope of the research presented here. This means that a definite relation to the smithing activities cannot be attested, but such a relation is considered highly likely. With the analysed slags being identified as strictly connected to iron working (see above), the presence of both metals in the same workshop raises the possibility that copper (alloy) objects were being copied in the 'new' metal, or at least, and perhaps more likely, that the smith performed repair work on all metals at Beth-Shemesh, including copper and/or bronze. Several of these objects, including a potential iron billet found in E/T49, were examined by X-Ray photography, but no remains of metallic iron could be detected. More extensive analysis of these artefacts is planned for the near future.

## Interpretations and Conclusions

It is clear that the discovery of a smithy at Beth-Shemesh has opened several avenues of research. Spatial patterns within the workshop were examined, and the nature of the different materials found there was determined. Excavation of the smithy has not been fully completed thus far, and the potential hearth structures remain *in situ*. More excavation is thus certainly both possible and required, and might resolve the assumed but unproven sequence between those structures.

At Beth-Shemesh, an early example of a secondary smithing workshop has been excavated. The finds from the workshop were analysed using relevant archaeological science methods and techniques. From those analyses, a picture emerges of a well-established smithy that is operating in a craft/workshop area near public buildings and one of the city gates of the city of Beth-Shemesh. Through plotting of the magnetic remains recovered from the area under study, a quite clear picture has been created of the spatial lay-out of the workshop, where the likely position of the hearth (i.e. at least the last hearth in use) has been determined. The quantity of SHBs, 65 complete samples and over 150 fragments, where each specimen represents a separate smithing operation, cycle, or workday, clearly indicates that the smithing work at Beth-Shemesh must have been a regular operation, as opposed to an experimental or highly occasional one. In contrast to the smelting operations at Tell Hammeh, the choice of location of the

Beth-Shemesh smithy seems more determined by a desired closeness to the consumer, than by considerations such as the availability of raw materials. This is fully consistent with the, admittedly sparse, other smithing sites known from the region thus far (see chapter 2). From the number of SHBs excavated at Beth-Shemesh, it is difficult to ascertain the exact scale of the operation. Assuming that each SHB represents a single workday of smithing (Serneels and Perret 2003, 472), this would make the scale of operations considerably lower than that at Hammeh. This indicates that the Beth-Shemesh smithy was most probably a workshop for the creation and/or repair of iron (and perhaps bronze) artefacts for strictly local consumption, as opposed to a centre of secondary production for the wider area.

From the petrographic analyses that connect the tuyères from Hammeh and those from Beth-Shemesh, it seems as if the Beth-Shemesh smith either travelled far to collect desired materials, or that some form of exchange or contact between the two areas may have been present. The initial findings with regard to the origin of (the clay of) the Beth-Shemesh and Hammeh tuyères as well as their design characteristics is subject to further study, but might be indicative of possible cross-cultural contacts, shared technological characteristics or even a possible socio-ethnic link between two different, but related, technologies at two different sites. In the light of ethnographical observation from Sub-Saharan Africa (see chapter 2), it is tempting to speculate about smelters (seasonally) smelting on a site near the required resources (Hammeh), and then travelling around the surrounding area, smithing their product near the consumers, i.e. in settlement contexts such as Beth-Shemesh, or perhaps Tell Deir ʿAlla or Tell es-Saʿidiyeh (see chapter 2).

When comparing Hammeh and Beth-Shemesh, it is clear that the smithy at Beth-Shemesh is characterised by a very different material assemblage and spatial layout than the smelting operations at Tell Hammeh (az-Zarqa). As such, the analyses presented above (and in chapters 4, 5 and 8) provide a template for distinction between the primary and secondary stages of iron production technology, both during fieldwork and in subsequent analysis of the material. It also shows that a range of relatively cheap and easy (although quite time consuming) methods can be applied in the field, which further help the identification of the technology under study.

Future work on the Beth-Shemesh smithy, besides continuation of the excavation work in E/T48, could include the bulk chemical analysis of a larger random sampling of SHBs. This is desirable to create a more balanced and reliable interpretation of their composition, which will strengthen the interpretation of the Beth-Shemesh technological process as secondary smithing of iron, and might shed light on the possible repair activities on both iron and bronze. It will furthermore enhance the comparison with smelting slag (from Hammeh) or (potentially) material from other sites (see chapter 3), both currently known sites and others that may be discovered in the future. Finally, metallurgical study of the metal artefacts to examine the techniques used to produce them is certainly also desired, but lies outside the scope of the research presented here, and may be difficult due to the heavily corroded condition of the metal.

## CHAPTER 10: INTERPRETATIONS AND CONCLUSIONS

### Introduction

As set out in the introduction, research on the Tell Hammeh (az-Zarqa) iron smelting and the Tel Beth-Shemesh iron smithing materials covers three areas of interest. The principle objective is to identify the nature of the technologies at these two sites, to reconstruct their respective *chaînes opératoire*, and to determine how they differ from each other through comprehensive archaeological, macroscopical, microscopical, and chemical analyses. The second objective is to discuss the history of iron technology in the Levant in the light of these two new discoveries. The third objective is to reconstruct the context of social and economic organisation of the society in which these technologies operate.

The research has reached these objectives for the most part. It successfully determined the technological remains at Tell Hammeh (az-Zarqa) as belonging to iron smelting, and identified several stages of the *chaîne opératoire* of that technology. The research further identified and characterised the iron production debris at Tel Beth-Shemesh as the remains of secondary smithing of iron. The identifications of both technologies rests for a large part on accurate and precise determination of the chemical composition of the various materials involved. This prompted the development of a new tool for archaeometallurgy, a calibration model for quantitative (P)ED-XRF analysis of iron-rich materials. This so-called ‘method’ is specifically designed to solve problems with the quantification of lighter elements in an iron rich sample matrix. It is currently the most accurate calibration method available at UCL (where iron oxide rich samples are concerned), and has initiated and informed the ongoing development of specific calibration methods for other materials. Comparison of results obtained through the ‘slag\_fun’ calibration method with that of other analytical techniques on the same iron oxide rich slag (the Swedish slag W-25:R; see chapter 7) shows that this (P)ED-XRF on a pressed pellet using this method is as accurate as those other techniques.

The second and third objectives, placing the two technologies in their historical and socio-economic contexts was only partially successful, which is largely due to the lack of comparative material in the region. A discussion of interpretations and conclusions regarding the three objectives is presented in this chapter.

## Reconstruction of Technology

### Iron Smelting at Tell Hammeh (az-Zarqa)

Excavation at Hammeh in 2000 took place based on the hypothesis that the iron production layers presented an example of iron smelting technology. This hypothesis was examined from an archaeological and a metallurgical perspective.

The archaeological perspective leads to the identification of several interesting characteristics and choices. One issue is the distribution of the metallurgical debris on the site itself. No specific activity areas could be established. Possible furnace structures were found concentrating around the present-day eastern edge of the site, but no separate areas or structures for charcoal production or storage, roasting of ore, (primary) smithing, or similar activities that relate to a smelting operation were found. Together with the jumbled state of the material in all excavated areas, and the lack of clear-cut furnace structures, this leads to the interpretation that terrain levelling, possibly by the smelters themselves, must have eradicated traces of differential use of space.

A further issue is the choice of location for the smelting. The Hammeh metalworkers chose a site that is immediately adjacent to the resources of water and clay, but several kilometres away from the ore source of Mugharet al-Warda. This choice of location differs from the possibly Roman, possibly smelting, operations studied by Coughenour (Coughenour 1989; Coughenour 1976), who found furnaces and slag next to the Warda ore deposit. The choice at Hammeh is also unlike that of the (Greek or Byzantine) indications of iron metallurgy at Tellul ed Dhahab, that were surveyed by Robert Gordon (Gordon 1984; Gordon and Villiers 1983), where the activities took place in or next to an established settlement, based on surface finds of slag. At Hammeh, habitation apparently ceases prior to the metallurgical activity, and resumes only after smelting operations no longer take place. It should be noted that the technological activities at neither Warda nor Dhahab have received any metallurgical study so far, and that the nature of the metallurgy at those sites (i.e. primary or secondary) has not been established. These sites are therefore difficult to evaluate or compare further.

This choice of location relates to the political and economical situation in the Iron Age. With the collapse of the major Hittite and Egyptian empires during the Late Bronze Age came the consequent withdrawal of their control over this part of the Levant (see chapters 3 and 4). Although this leads to a partial collapse of the



existing city-system, many places show no cultural break. The indigenous population apparently formed decentralised local states. It is furthermore proposed that new (or previously less sedentary) groups arrive and settle in the area, which come from the east, i.e. from the Baq‘ah Valley or the ‘Amman plateau (van der Steen 2003; McGovern 1986). Both the indigenous and these incoming groups apparently prefer to settle along riverbanks and other easily accessible places, and previously existing settlements (van der Steen 2003; McGovern 1986). Locating the iron smelting activities at Hammeh, rather than up in the hills next to the ore deposit at Warda, may be related to this tendency. Possibly interrelated with this argument of accessibility is the idea that Hammeh was chosen because it is easy to reach from a neighbouring site that may have instigated or controlled the production. Such political or economical factors and considerations are, thus far, impossible to retrieve from the archaeological record. Nevertheless, the fact that smelting took place at such a distance from the ore body does indicate that the metalworkers at Hammeh must have had unhindered access to this resource.

It is equally viable to assign a large role in the choice of location to the smelters themselves, who may simply have deemed this place to strike the right balance between procurement and transport of raw materials, availability of resources, and closeness or distance to their own habitation and/or the ‘consumer’. The noted absence of habitation and related material culture during the smelting operations makes outside control likely. At the same time, no indications for ‘foreign’ involvement, e.g. from the Assyrians or Philistines, have been found.

It is clear that several major powers had knowledge of iron, e.g. the Hittites, Assyrians, and Philistines, based on the artefactual and textual evidence, but there is no direct evidence for production by any of them. At Hammeh, the smelting of iron coincides with a significant rise in the number of iron artefacts in the archaeological record of the southern Levant. However, the Hammeh production appears to be independent from influences of the major powers. In fact, it only starts after the collapse of the Hittite and Egyptian empires, and it ends before the arrival of the Assyrians in the Jordan Valley around 720 BC. Analogous to the authors’ interpretation concerning the iron artefacts excavated at Taanach (Stech-Wheeler *et al.* 1981, see also chapter 3), which are roughly contemporaneous to the Hammeh smelting (see chapter 4, page 92), it seems as if the political fragmentation of the Iron Age I and II provides a socio-economic climate in which local industries can develop, which are based on the exploitation

of local raw materials. In my opinion, it is the local group or groups of people that are monopolising production of the new metal from local resources (smelting at Hammeh), and travel around the region smithing objects where required (e.g. secondary smithing at Beth-Shemesh and other sites).

From a metallurgical perspective, it is clear that the Hammeh smelters were more or less bound to use the local Mugharet al-Warda ore. Not only is this the only or only viable ore deposit in a very large area, the large scale of the operation (as witnessed by the large quantities of slag and calculated potential yield) together with the presumed socio-political situation make abundant and coordinated transport of raw materials from further away unlikely. This assumption is confirmed by the ore analyses, which show the Warda ore as suitable but difficult to smelt by the bloomery process, and almost certainly related to the Hammeh slag, as attested through the presence of matching trace elements in both, and the mass balance calculations (see chapter 8).

With the use of this particular ore came two important characteristics that the smelters had to deal with: a considerable presence of calcium, and a relatively low amount of silica. These factors play an important role in the constitution of the technological process at Hammeh. The low amount of silica, together with the high amount of calcium, makes the formation of a workable slag, and thereby the reduction of the iron oxides to metal, difficult. As the mass balance calculations examining the relationship between the chemical compositions of the Warda ore, the Hammeh slag, and the Hammeh technical ceramics have shown, the solution to this problem was found in the use of 'sacrificial' tuyères (see chapter 8).

The chemical composition of the technical ceramics (tuyères, furnace wall, and perhaps furnace lining) makes up for the deficient silica in the ore. As shown through mass balance calculations, it is only with a ceramic contribution to the smelting process that the Warda ore produces a slag that melts at reasonable temperatures of around 1100 °C, such as found at Hammeh. The large number of recovered tuyères, together with their molten state and probably considerable reduction in length, suggests that a large part of this ceramic contribution must be due to the tuyères in particular. The furnace structure was likely of the same or similar material, and will have contributed to the process as well. In my opinion, it is highly unlikely that the Hammeh smelters were unaware of this essential factor in their process.

The technical ceramics at Hammeh were produced using the ubiquitous lime-rich local clay. The composition of that clay, besides providing the required extra silica to allow the formation of a functional slag, also feeds additional lime into the smelting system. The bulk of ceramic added to the furnace charge and the role of the silica from that addition (binding with free iron oxide to form fayalite or kirschsteinite) lowers the output of the process in terms of metal yield per quantity of ore, but the added silica helps to lower the operational temperature by ca. 100 °C (see chapter 8, tap slags).

This loss of yield is partially counterbalanced by the calcium present in the ore and the technical ceramics. By replacing some of the iron oxide in several slag phases, it frees more iron oxide for reduction to iron metal. In this way, it actively fluxes the ore and potentially raises the yield. That this presence of lime, deriving in part from the Warda ore and in part from the technical ceramics, had an effect on the Hammeh technology is clearly observed in the lime-rich and iron-oxide-poor Hammeh slag, and the related yield calculations. Whether the Hammeh smelters were actively aware of the balance between the detrimental (more material, specifically silica, in the process, i.e. less metal per unit of ore) and the beneficial (lower operating temperature due to the silica and less loss of yield due to the calcium) effects of their sacrificial use of tuyères, is difficult to determine.

A further interesting observation is that the charcoal used at Hammeh exclusively consists of olive wood. The intrinsic economic value of olive trees and the consistently small size of the charcoal recovered suggest that the wood used was derived from pruning of the olive trees rather than the cutting down of entire trees. This strongly suggests that the Hammeh smelters were dependent on the seasonal nature of pruning, and would perform their smelting seasonally as well. This corresponds with the multi-layered structure of the smelting debris stratigraphy at Hammeh, which indicates (large scale and regular) seasonality rather than continuous production.

Analysis of the Hammeh slag and Warda ore has further shown that the initial subdivisions of slag types defined in the field needed revision, as these were far too elaborate. Besides the technical ceramics, Warda ore, and charcoal, the material at Hammeh consists of three main slag types: tapped smelting slag, furnace slags (partially reduced ore), and primary smithing (bloomsmithing) slag. Additional material is formed by a rare furnace bottom slag and 'ceramic-rich slag'.

The chemical composition of all slag materials reflects the important role of technical ceramics in the Hammeh process, and confirms that they are the result of predominantly smelting and to a lesser extent primary smithing. The microscopic structure of the slag indicates that the technology may not have been fully streamlined at all times, showing a sometimes less than perfect control over temperature and occasionally incorrect timing of slag tapping. Nevertheless, the material, in its overall quality and quantity, reflects a regular, large scale operation and opposes an interpretation as experimental stage of an emergent technology.

The tuyères also forward the assumption of an organised rather than experimental nature of the Hammeh smelting process. The relative uniformity of their size and shape shows a level of standardisation that may well reflect a considerable level of organisation of the production. Remarkably, the tuyère design further incorporates potential cultural elements unrelated to technological necessity. Their particular square section may be building on local pyro-technological traditions, as witnessed by the presence of the same design in 1600 BC bronze reworking at Tell Abu al Kharaz, at 700 BC Tell Deir 'Alla (no production context), and not in the least at Tel Beth-Shemesh in the approximately contemporaneous 9<sup>th</sup> century secondary smithing activity.

To summarise, a picture emerges at Hammeh of local people adapting their technology to the constraints and demands of locally available materials in order to produce both the iron metal they needed and more for export or exchange. The estimated total production at Hammeh, up to ca. 12 tons of metal in a period of some 150 years, i.e. at ca. 80 kilograms per annum, must be considered substantial for this time. The socio-economic context of the site in the early Iron Age II remains more elusive, but seems to suggest control of the production by a nearby site. As mentioned above, the political fragmentation of the Iron Age I and II in the Levant apparently stimulated local industries that exploit locally available raw materials. In my opinion, such a scenario is very likely reflective of the activities at Hammeh.

### **Iron Smithing at Tel Beth-Shemesh**

Comparison of the metallurgical debris found at Tel Beth-Shemesh with that at Hammeh results in a very different picture. Here, a metallurgical activity is taking place in what is likely the craft area near the gate of a larger city. In a workshop of limited dimensions, bloomery smelted iron was forged into objects. In choosing

this location for metallurgical activity, one may assume that the smith is clearly motivated by proximity to customers rather than the availability of resources.

Within the smithy, several structures can be observed that perhaps served as storage containers, although some may represent smithing hearths that went out of use. There is an apparent sequence between these structures, as some apparently intersect others, but a high similarity in their construction material as well as an absence of clear stratigraphy prevents untangling their history. Four main groups of metallurgical debris were recovered at Beth-Shemesh: concavo-convex smithing hearth bottom slags (SHBs), tuyères, metal artefacts, and large quantities of magnetic material, i.e. hammerscale and slag prills. This thesis focused primarily on the characterisation of the slag, and detailed spatial analysis of the hammerscale.

Analysis of the uniform SHBs reveals a highly heterogeneous composition, with formations of wüstite as well as magnetite. Their chemical composition is quite similar to the smelting slag of Hammeh, but together with their microstructure and especially their highly uniform concavo-convex shape, the Beth-Shemesh slags clearly relate to secondary smithing. The interpretation of secondary smithing is further confirmed by the high quantity of hammerscale found throughout the smithy, in combination with very low quantities of slag prills.

The fieldwork experiences at Hammeh informed the development and application of specific excavation techniques for the workshop at Beth-Shemesh. A detailed spatial patterning of the distribution of the hammerscale within the smithy was established through these techniques, which in turn enabled the reconstruction of the use of space. From this distribution pattern, the likely location of what is probably the last hearth in use could be determined.

The metal artefacts, which are largely outside the scope of this research, consist of fragments of iron objects, generally arrowheads and possible fragments of knives. The chemical composition of the production debris does not indicate working or reworking of copper or bronze, nevertheless a few copper/bronze artefacts were also found in the smithy. This raises the possibility that the Beth-Shemesh smith, besides producing iron objects, may have reworked or repaired bronze. Another possible explanation for the presence of bronze objects, although highly conjectural, may be that the smith was copying existing shapes from one metal in the other.

The tuyères found at Beth-Shemesh provide a very interesting range of ideas. Whereas it is clear that Hammeh and Beth-Shemesh each represent a different part of the *chaîne opératoire* of producing iron metal, which is reflected in different choices of location, different organisation, and last but not least a different assemblage of technological remains, the tuyères at Beth-Shemesh are identical in size and shape to those at Hammeh. More importantly, preliminary petrographic analysis of both sets of tuyères, prompted by their similarity, has shown that both are made from the same clay, and that this is most likely the clay local to Hammeh rather than Beth-Shemesh.

These petrographic analyses are not yet completed, and more detailed analyses of the tuyères are certainly required, before speculating about possible relations between the two sites is really possible. Nevertheless, it seems inescapable to assume that some form of contact existed between the two operations. Several interpretations are imaginable, ranging from simple sharing of preferred clay to actual social, cultural, ethnic, or economic links between the smelter at Hammeh and the smith at Beth-Shemesh. The fact that the tuyères not only share the provenance of their clay, but also their particular square section design certainly points towards the latter. One can imagine a situation where, in the fragmented socio-economic context of the Iron Age Levant, smelter and smith are the same (group), seasonally smelting at Hammeh, and then smithing or trading their own product at various settlements and cities in the region. Perhaps 'old' bronze weaponry or tools were exchanged for the same artefact made in the 'new' metal.

A picture emerges from the study of the Beth-Shemesh material of a smithing workshop that is operated regularly and at considerable (local) scale within the confines of one of the larger cities in the Iron Age Levant, which caters to the needs and wants of that settlement. In terms of the site itself, the quantity of smithing at Beth-Shemesh (some 200 SHBs) is quite considerable, in comparison to the large scale smelting at Hammeh the operations are of a more local nature, probably catering only for the city itself.

### Comparing Smelting and Smithing

Comparison between the two sites reveals clear differences between the primary and secondary stages of iron production, both in the way they are organised and laid-out, and in the material they leave behind. The nature of these differences can assist field interpretation of future metallurgical finds. The smelting at Tell Hammeh is located away from the settlement that likely coordinates these

operations, but is next or close to the various resources needed for production, especially ore, clay, and water. The metallurgical debris at Hammeh comprises of a wide variety of slags and technical ceramics materials, with a marked dominance of tap slags and large numbers of tuyère segments, whereas iron objects are virtually absent.

The smithing at Beth-Shemesh shows a quite different choice of location, as it takes place within the confines of a large city, which corresponds with the other finds identified as smithing in the region (see chapter 3). Here the choice of location likely reflects a desire to be close to the consumer, rather than being close to resources. The metallurgical assemblage at Beth-Shemesh also differs from that at Hammeh, in that it is dominated by one type of uniform smithing hearth bottom slag and large amounts of hammer scale. Numerous iron objects were found within the production context, but only a few tuyères. I suggest that these clear differences in material, as well as those in choice of location and layout of the workshop can guide distinction between smelting or smithing activities, both in the re-evaluation of 'older' evidence and in the interpretation of future finds.

An important discovery concerning both sites is the connection between Hammeh and Beth-Shemesh evidenced by the tuyères. Petrographic analysis shows that the tuyères from either site are made of identical clay, and that this clay is locally available near Hammeh, but not near Beth-Shemesh. Beyond sharing the same clay, the tuyères of both sites also share the particular square section design, discussed above. The combination of these factors leads me to propose that contact between Hammeh and Beth-Shemesh goes beyond a simple sharing of a preferred resource, and may signify extensive contact between the smelters and the smiths, if not a direct relation. Both sites seem to reflect a clear level of specialisation (see chapter 2), as well as a separation between the production and the working of this new metal. If the smelters at Hammeh and the smiths at Beth-Shemesh are not the same groups, this separation of processes further reflects a division of labour.

With all necessary caveats concerning the use of ethnographic or ethnoarchaeological comparison, especially across so much space and time, the suggested scenario of seasonal smelters travelling around to smith their metal near the consumer, exchanging it for other artefacts or desired goods does have parallels in Sub-Saharan ethnography. An important example are the ca. AD 1000



metal workers of the Njanja, in the Wedza area of East Central Zimbabwe. These metalworkers travelled a long distance to the ore source of their preference, smelted there, and smithed their blooms to artefacts (in exchange for other commodities) at the various settlements they passed on their way back home (MacKenzie 1975, and current research by Shadreck Chirikure, UCL, personal communication).

## **The Place of Hammeh and Beth-Shemesh in the History of Iron**

The second objective of this study was to examine the history of iron production in the Near East in the light of these new discoveries. This proved extremely difficult. Although the Near East is generally considered to be the origin of iron metallurgy, early finds (pre 500 BC) of smelting processes are absent, and of smithing operations they remain extremely scarce. Existing reconstructions of the invention or development and spread of early iron production technology are therefore generally informed by artefactual or textual evidence rather than actual production remains.

The absence of any comparable production material, especially when considering smelting, prevents the determination of patterns or developments within the wider region at this time. Evidence for contact with, or influence from, known or supposed centres of metallurgical activity such as Anatolia, Cyprus, Assyria, or the Aegean is clearly absent from Tell Hammeh, nor can it be attested in the Beth-Shemesh evidence. In this light, the case studies of both Hammeh and Beth-Shemesh provide important contributions to the existing knowledge of early iron production, and present a first comprehensive set of data that can form the basis for comparison of future finds.

It is viable to suggest that both Hammeh and Beth-Shemesh represent a local industry, using locally existing knowledge and being embedded in the local economy and society, rather than operations coordinated by outside forces, performed by foreign people, or largely based on external knowledge. Such external influences cannot be excluded, however, on the basis of our current understanding of the organisation of production at either site. This issue needs to be addressed when more production evidence becomes available for comparison.

Neither the Beth-Shemesh smithing nor the Hammeh smelting shows any sign of innovation or development of the technology practised. Both sites represent well-established technological processes, in the case of Hammeh of a considerable

scale and with indications of standardisation. This clearly suggests that iron production and working were known and practised in the region prior to the start of iron smelting at Hammeh around 930 BC, and the smithing at Beth-Shemesh in ca. 900-850 BC.

## Organisation of Production and Technological Choices

It has been equally difficult to interpret the findings at either site within the context of theoretical thought about technology. A basic level of interpretation can be achieved, when looking at the social and economic context of the metallurgical activities. The likely absence at Hammeh of habitation contemporaneous with the smelting must indicate some form of external coordination of the smelting operations, but simultaneously prevents a closer look at the nature of such coordination. Some degree of social or economic organisation must certainly be assumed, if only because of the scale of the operations, where the potential yield of metal is clearly larger than the consumption needs of a single site.

At Beth-Shemesh, the situation is slightly more straightforward, as we clearly see a metallurgical activity embedded in the social and economic context of a city. This certainly suggests some relation between the production that is taking place there with the local inhabitants or rulers of the settlement. It is difficult to ascertain the actual scale of the operations here. If each of the ca. 200 excavated SHBs represents a full working day, this would mean that the operations at Beth-Shemesh are of distinctly smaller scale than those at Hammeh. The smithy is confined itself to 5 by 5 metre square E/T48 and its immediate surroundings. This reinforces the proposition made above of a regional production centre (Hammeh) supplying (itself or through exchange or trade) the metal for secondary smithing in smaller, settlement oriented, workshops around the region.

However, without further evidence for iron production and working elsewhere, it is impossible to establish whether the activities at Hammeh or Beth-Shemesh show any distinct characteristics in terms of social and cultural issues such as ethnic movements, diffusion of knowledge, and the control of resources and technological knowledge. With regard to the reconstructed technologies, most choices seem to be shaped by practical and technological considerations rather than cultural ones.

A significant exception to the last statement is formed by the Hammeh and Beth-Shemesh tuyères. These show design characteristics that very likely go beyond

purely technological considerations. Whilst their square section may (also) serve a practical purpose (e.g. efficient packing for transport, or not rolling away during production or when fitting into a furnace or hearth), their shape is certainly not a technological requirement for their use. The square shape may therefore represent what Heather Lechtman would term a *technological choice*, i.e. a choice not guided by technological constraints, but one made by the person performing the technological activity based on, for example, social or cultural considerations, perceived requirements, or local traditions. More data is needed to attempt to identify the underlying reason(s) for the square section design, but the fact that this shape transcends metals, technological stages, and time periods in my opinion strongly suggest that the shape is a cultural choice or local metallurgical tradition.

To summarise, a full understanding and reconstruction of the social and economic organisation of the Tell Hammeh smelting and its possible relation with the Beth-Shemesh smithing (and perhaps that at other sites) is not possible until more data becomes available for comparison. The first indications suggest a technology at either site that operates within the local economy and society, is locally managed or organised, executed by indigenous people, and likely informed by locally existing metallurgical traditions.

## Original Contributions and Suggestions for Future Research

The research at Hammeh and Beth-Shemesh provides several original contributions to the interpretation and understanding of early iron technology in the Levant. On the archaeological side, it has positively identified and comprehensively characterised and interpreted the thus far only known instance of iron smelting technology in the Near East, as well as one of the earliest known instances of iron smithing in the same region. Dissemination of the results of these identifications will allow other excavations to properly identify iron metallurgy in the field and formulate a starting hypothesis about what stage of technology may be represented.

The specific metallurgical excavation techniques applied to and developed on Hammeh and in particular Beth-Shemesh can inform future excavation of metallurgical debris, thus stimulating a uniform approach and creating comparable data. In particular the grid based excavation method for hammerscale

recovery provides a relatively easy and cheap (although time consuming) field method to track the use of space in metallurgical activities.

The identification by petrographic analysis of the tuyères at Hammeh and Beth-Shemesh as sharing a particular clay, in combination with their shared square section design provides a basis for future research into both organisation of production and relations between smelters and smiths, as well as for determinations of technological style.

An important feature of the research presented here is that debris from primary production (smelting and primary smithing) and secondary production (smithing, production of objects) were studied together for the first time. This provided a first insight into possible technological, social, and economical relationships between the two processes. It has hinted at previously unknown, (cross-)cultural, direct social and/or economic relations between the two sites, which may reflect a wider structure of the organisation of iron production and working in the southern Levant during the Iron Age II.

On the metallurgical side, the development of a more precise and accurate calibration for bulk chemical analyses of iron-rich samples by (P)ED-XRF has created a tool that enhances the characterisation of archaeological materials in general, and iron rich slags in particular. This makes the data extracted from such finds more reliable, quantifiable, as well as more comparable with data from other sites and other analytical techniques. Using this method, the particular lean, i.e. lime-rich and iron-oxide-poor, nature of the Hammeh smelting slag could be analysed. This has shown how the Hammeh slags reflect the particularities of the locally available ore. It further revealed how the sacrificial use of tuyères in the smelting process exerted an extensive influence on production parameters such as operating temperature and yield of metal per unit of ore.

Besides answers, this research has also provided a whole new range of questions, which may be used to formulate suggestions for future research. With regard to Hammeh and Beth-Shemesh themselves, a study of the iron and copper/bronze artefacts from these sites is desirable, as this will potentially reveal information about, for example, the carbon content of the metal smelted, and smithing techniques used in the creation of objects.

Expanding on the research presented in this study, a reconstruction of iron production in the Levant as a whole is desirable. In order to do so, it is necessary to revisit the 'old' data from sites such as Kamid el-Loz in Lebanon (see chapter

3), as well as studying more recently excavated sites. Besides Tell Hammeh and Tel Beth-Shemesh, this might involve recently reported instances of iron production or working at Tel Hamid in Israel, and Tell Siukh Fawqani and Tell Afis in Syria. Re-evaluation of 'old' and more recent data from more sites can certainly build on the data provided by Hammeh and Beth-Shemesh. Such data should be evaluated with regard to their metallurgical characteristics, as well as in terms of social and cultural issues. When more data is available, issues like social organisation, ethnic movements or diffusion of knowledge, and the control of resources and technological knowledge can be addressed on a regional rather than case-study scale.

Evidence for early iron technology in the Levant remains extremely scarce. Much more research is needed to clarify the 'coming of the age of iron' (Craddock 1995; Maddin 1988; Wertime and Muhly 1980). No comprehensive overarching picture exists of early production in the Near East in general, nor of its characteristics, and it is hoped that the data on Hammeh and Beth-Shemesh presented here will provide a basis for further research.

Such future research should not focus exclusively on slag material but examine the role played by technical ceramics as well. The research presented here has shown that tuyères and furnace wall material can play a crucial role in smelting technology and that it is these same materials that form a possible connection between the Hammeh smelting and Beth-Shemesh smithing. Technical ceramics also seem ideally suited to reveal a lot of information when iron production technology is placed in its socio-cultural context. It seems that tuyères may reflect choices and changes that, in turn, reflect social and cultural aspects of the society that produced the metal, rather than technological requirements or constraints.

Clearly, future archaeometallurgical research needs to be comprehensive enough to cover all these aspects of the sites and materials to be studied. Such study is bound to eventually change and enhance the picture of iron production in the Levant. Furthermore, it will allow for meaningful comparison to, and refinement of, the current historical views that are largely based on artefactual evidence, because information derived from studying production finds is far less susceptible to problems of 'movement'. Whereas artefacts can travel over long distances, local production leads to local remains, making a historical view based on iron production remains far more reliable.

## APPENDIX 1. BULK CHEMICAL ANALYSES

Sample	Material type	Date	SiO <sub>2</sub>	Al <sub>2</sub> O <sub>3</sub>	Fe <sub>2</sub> O <sub>3</sub>	MgO	K <sub>2</sub> O	TiO <sub>2</sub>	MnO	CaO	V <sub>2</sub> O <sub>5</sub>	Cr <sub>2</sub> O <sub>3</sub>	P <sub>2</sub> O <sub>5</sub>	SO <sub>3</sub>	Na <sub>2</sub> O	Sum
<b>Tell Hammeh Slags</b>																
A1	tap slag	28/03/2005	24.57	5.67	58.56	2.21	0.98	0.35	1.29	10.86	bdl	0.01	1.14	0.78	0.55	106.97
A1_r01	tap slag	28/03/2005	24.45	5.64	58.35	2.13	0.99	0.35	1.28	10.83	bdl	0.01	1.13	0.78	0.73	106.67
A1_r02	tap slag	28/03/2005	24.6	5.69	58.65	2.15	0.99	0.35	1.29	10.85	bdl	0.01	1.14	0.77	0.28	106.77
A2	furnace slag	28/03/2005	16.93	3.98	79.19	1.28	0.74	0.24	0.77	6.93	bdl	0.01	1.21	0.49	0.66	112.43
A2_r01	furnace slag	28/03/2005	17.23	4.06	80.2	1.15	0.75	0.24	0.78	7.02	bdl	0.01	1.25	0.49	0.46	113.64
A2_r02	furnace slag	28/03/2005	17.03	3.97	78.95	1.22	0.74	0.24	0.77	6.94	bdl	0.01	1.21	0.5	0.28	111.86
A3	tap slag	28/03/2005	20.36	5.26	69.45	1.37	0.89	0.31	1.26	7.36	bdl	0.01	1.36	1.77	0.26	109.66
A3_r01	tap slag	28/03/2005	20.41	5.3	69.31	1.27	0.9	0.31	1.26	7.4	bdl	0.01	1.34	1.78	0.14	109.43
A3_r02	tap slag	28/03/2005	20.43	5.36	69.83	1.44	0.9	0.31	1.26	7.4	bdl	0.01	1.36	1.79	0.13	110.22
A4	tap slag	28/03/2005	21.73	5.62	68.69	1.53	0.83	0.32	1.3	8.65	bdl	0.01	1.34	0.95	0.36	111.33
A4_r01	tap slag	28/03/2005	21.87	5.57	68.81	1.59	0.82	0.31	1.29	8.65	bdl	0.01	1.34	0.93	0.34	111.53
A4_r02	tap slag	28/03/2005	21.81	5.48	68.42	1.53	0.83	0.31	1.29	8.61	bdl	0.01	1.19	0.94	0.49	110.91
A5	tap slag	28/03/2005	21.87	5.01	70.21	1.48	1.25	0.27	1.07	10.07	bdl	0.01	1.17	0.56	0.47	113.44
A5_r01	tap slag	28/03/2005	21.99	4.99	70.29	1.56	1.26	0.27	1.07	10.11	bdl	0.01	1.17	0.55	0.55	113.82
A5_r02	tap slag	28/03/2005	21.84	5.07	70.39	1.54	1.26	0.27	1.07	10.09	bdl	0.01	1.16	0.56	0.63	113.89
B1	furnace slag	28/03/2005	11.52	2.37	78.76	0.86	0.71	0.17	0.89	4.36	bdl	0.01	0.92	0.64	0.37	101.58
B1_r01	furnace slag	28/03/2005	11.49	2.38	78.86	0.79	0.7	0.17	0.89	4.36	bdl	0.01	0.92	0.66	bdl	101.23
B1_r02	furnace slag	28/03/2005	11.45	2.41	78.66	0.78	0.7	0.17	0.89	4.35	bdl	0.01	0.91	0.65	0.36	101.34
B2	furnace slag	28/03/2005	13.93	4.27	70.39	0.37	1.24	0.3	0.3	1.65	bdl	0.01	1.66	1.01	0.93	96.06
B2_r01	furnace slag	28/03/2005	13.73	4.28	69.48	0.34	1.23	0.29	0.3	1.63	bdl	0.01	1.6	1	0.95	94.84
B2_r02	furnace slag	28/03/2005	13.88	4.33	70.01	0.35	1.24	0.3	0.3	1.65	bdl	0.01	1.65	1.02	0.71	95.45
B3	furnace slag	28/03/2005	13.32	3.69	71.8	0.71	0.86	0.22	1.1	3.4	bdl	0.01	1.76	1.91	0.37	99.15
B3_r01	furnace slag	28/03/2005	13.43	3.65	71.94	0.74	0.87	0.22	1.11	3.43	bdl	0.01	1.78	1.9	0.44	99.52
B3_r02	furnace slag	28/03/2005	13.35	3.63	71.92	0.64	0.87	0.22	1.1	3.41	bdl	0.01	1.75	1.89	0.28	99.07



Sample	Material type	Date	SiO <sub>2</sub>	Al <sub>2</sub> O <sub>3</sub>	Fe <sub>2</sub> O <sub>3</sub>	MgO	K <sub>2</sub> O	TiO <sub>2</sub>	MnO	CaO	V <sub>2</sub> O <sub>5</sub>	Cr <sub>2</sub> O <sub>3</sub>	P <sub>2</sub> O <sub>5</sub>	SO <sub>3</sub>	Na <sub>2</sub> O	Sum
B4	furnace slag	28/03/2005	9.2	0.74	79.72	bdL	0.39	0.07	0.04	0.97	bdL	0.01	0.08	1.07	0.13	92.42
B4_r01	furnace slag	28/03/2005	9.19	0.72	80.26	0.29	0.4	0.07	0.04	0.97	bdL	0.01	0.08	1.08	0.22	93.33
B4_r02	furnace slag	28/03/2005	9.11	0.76	79.58	0.25	0.4	0.07	0.04	0.97	bdL	0.01	0.08	1.07	bdL	92.34
B5	furnace slag	28/03/2005	19.49	4.29	53.94	1.28	1.46	0.27	0.98	8.3	bdL	0.01	1.48	1.56	0.51	93.57
B5_r01	furnace slag	28/03/2005	19.4	4.37	54.14	1.24	1.46	0.28	0.98	8.29	bdL	0.01	1.45	1.53	0.46	93.61
B5_r02	furnace slag	28/03/2005	19.5	4.3	53.97	1.25	1.46	0.28	0.98	8.31	bdL	0.01	1.46	1.55	0.84	93.91
C1	tap slag	28/03/2005	27.55	5.84	52.09	2.49	1.14	0.4	1.18	12.34	bdL	0.01	1.14	0.8	0.41	105.39
C1_r01	tap slag	28/03/2005	27.45	5.92	51.85	2.49	1.13	0.39	1.17	12.31	bdL	0.01	1.15	0.82	0.61	105.30
C1_r02	tap slag	28/03/2005	27.49	5.98	51.95	2.51	1.14	0.39	1.17	12.32	bdL	0.01	1.17	0.81	0.6	105.54
C2	tap slag	28/03/2005	23.01	5.79	62	2.01	0.99	0.33	1.3	9.37	bdL	0.01	1.34	0.58	0.57	107.30
C2_r01	tap slag	28/03/2005	23.34	5.88	62.97	1.93	1.02	0.34	1.32	9.53	bdL	0.01	1.33	0.59	0.53	108.79
C2_r02	tap slag	28/03/2005	23.64	5.86	63.23	1.96	1.02	0.33	1.33	9.55	bdL	0.01	1.34	0.59	0.6	109.46
C3	ceramic-rich slag	28/03/2005	30.99	5.12	35.23	2.53	2.15	0.4	0.83	18.35	bdL	0.01	1.04	0.3	0.76	97.71
C3_r01	ceramic-rich slag	28/03/2005	31.33	5.25	35.72	2.59	2.19	0.41	0.84	18.63	bdL	0.01	1.07	0.31	0.69	99.04
C3_r02	ceramic-rich slag	28/03/2005	31.49	5.29	35.68	2.55	2.18	0.41	0.84	18.62	bdL	0.01	1.04	0.32	0.58	99.01
C4	tap slag	28/03/2005	27.25	4.78	55.52	1.92	1.13	0.29	1.13	12.62	bdL	0.01	1.35	0.54	0.76	107.30
C4_r01	tap slag	28/03/2005	27.11	4.82	55.3	1.74	1.13	0.29	1.12	12.54	bdL	0.01	1.34	0.52	0.58	106.50
C4_r02	tap slag	28/03/2005	27.07	4.72	55.4	1.78	1.13	0.29	1.13	12.59	bdL	0.01	1.31	0.53	0.72	106.68
C5	tap slag	28/03/2005	21.73	6.59	67.47	1.76	0.82	0.34	1.49	8.23	bdL	0.01	1.34	1.31	0.55	111.64
C5_r01	tap slag	28/03/2005	21.8	6.51	67.54	1.61	0.82	0.35	1.49	8.23	bdL	0.01	1.37	1.3	0.39	111.42
C5_r02	tap slag	28/03/2005	21.64	6.59	67.54	1.7	0.82	0.35	1.49	8.23	bdL	0.01	1.36	1.29	0.45	111.47
D1	furnace slag	20/04/2005	16.99	4.98	69.2	0.7	1.15	0.28	0.81	3.27	bdL	0.01	1.12	2.88	0.58	101.97
D1_r01	furnace slag	20/04/2005	16.97	5.07	69.02	0.62	1.15	0.27	0.81	3.3	bdL	0.01	1.1	2.89	0.34	101.55
D1_r02	furnace slag	20/04/2005	17	4.97	68.75	0.7	1.14	0.28	0.81	3.27	bdL	0.01	1.09	2.87	0.26	101.15
D2	furnace slag	20/04/2005	15.63	4.59	80.21	0.83	0.89	0.27	0.54	3.15	bdL	0.01	1.31	1.99	0.65	110.07
D2_r01	furnace slag	20/04/2005	15.62	4.51	79.61	0.71	0.88	0.27	0.54	3.14	bdL	0.01	1.31	1.99	0.37	108.96
D2_r02	furnace slag	20/04/2005	15.72	4.61	80.19	0.81	0.89	0.27	0.55	3.18	0	0.01	1.33	2.01	0.54	110.11

Sample	Material type	Date	SiO <sub>2</sub>	Al <sub>2</sub> O <sub>3</sub>	Fe <sub>2</sub> O <sub>3</sub>	MgO	K <sub>2</sub> O	TiO <sub>2</sub>	MnO	CaO	V <sub>2</sub> O <sub>5</sub>	Cr <sub>2</sub> O <sub>3</sub>	P <sub>2</sub> O <sub>5</sub>	SO <sub>3</sub>	Na <sub>2</sub> O	Sum
D3	furnace slag	20/04/2005	16.79	3.27	62.82	0.52	1.05	0.23	0.21	3.2	bdl	0.01	1.01	1.07	0.14	90.32
D3_r01	furnace slag	20/04/2005	16.8	3.31	62.75	0.6	1.05	0.23	0.21	3.2	bdl	0.01	1.02	1.07	0.29	90.54
D3_r02	furnace slag	20/04/2005	16.98	3.33	63.2	0.64	1.05	0.23	0.21	3.23	bdl	0.01	1.02	1.07	0.35	91.32
D4	furnace slag	20/04/2005	15.46	1.66	66.36	0.6	0.5	0.14	0.2	2.48	bdl	0.01	0.96	0.79	0.13	89.29
D4_r01	furnace slag	20/04/2005	15.2	1.58	65.73	0.53	0.5	0.13	0.19	2.44	bdl	0.01	0.96	0.79	0.29	88.35
D4_r02	furnace slag	20/04/2005	15.36	1.6	66.27	0.55	0.5	0.14	0.2	2.47	bdl	0.01	0.96	0.78	0.15	88.99
D5	furnace slag	20/04/2005	15.46	4.35	74.27	1.2	0.8	0.22	1.55	7.91	bdl	0.01	1.52	1.13	0.26	108.68
D5_r01	furnace slag	20/04/2005	15.49	4.37	74.75	1.14	0.81	0.22	1.56	7.92	bdl	0.01	1.54	1.13	0.42	109.36
D5_r02	furnace slag	20/04/2005	15.51	4.3	74.12	1.02	0.8	0.22	1.55	7.89	bdl	0.01	1.56	1.12	0.54	108.64
E1	furnace slag	30/03/2005	18.77	3.11	68.19	3.29	0.62	0.18	1.8	14.52	bdl	0.01	1.53	0.4	0.67	113.09
E1_r01	furnace slag	30/03/2005	18.58	3.14	67.96	3.35	0.61	0.19	1.79	14.47	bdl	0.01	1.51	0.4	0.55	112.56
E1_r02	furnace slag	30/03/2005	18.56	3.11	67.52	3.09	0.61	0.18	1.78	14.43	bdl	0.01	1.5	0.4	0.54	111.73
E2	tap slag	30/03/2005	29.36	5.33	50.16	1.23	1.06	0.37	0.85	10.38	bdl	0.01	1.14	2.45	0.59	102.93
E2_r01	tap slag	30/03/2005	29.8	5.46	50.34	1.31	1.08	0.37	0.86	10.49	bdl	0.01	1.15	2.46	0.62	103.95
E2_r02	tap slag	30/03/2005	29.3	5.37	49.86	1.3	1.06	0.36	0.85	10.35	bdl	0.01	1.12	2.44	0.39	102.41
E3	ceramic-rich slag	31/03/2005	43.53	6.24	22.34	2.74	2.07	0.45	0.83	18.09	bdl	0.01	0.8	1.02	0.6	98.72
E3_r01	ceramic-rich slag	31/03/2005	43.71	6.33	22.48	2.79	2.07	0.46	0.84	18.18	bdl	0.01	0.63	1.03	0.8	99.33
E3_r02	ceramic-rich slag	31/03/2005	43.3	6.31	22.25	2.69	2.07	0.45	0.83	18.06	bdl	0.01	0.82	1	0.29	98.08
E4	tap slag	30/03/2005	33.1	6.25	44.09	1.76	1.25	0.42	0.98	12.35	bdl	0.01	1.09	1.16	0.69	103.15
E4_r01	tap slag	30/03/2005	33.31	6.3	44.41	1.64	1.26	0.43	0.98	12.44	bdl	0.01	1.09	1.17	0.55	103.59
E4_r02	tap slag	30/03/2005	33.38	6.42	44.57	1.78	1.28	0.43	0.99	12.55	bdl	0.01	1.1	1.17	0.57	104.25
E5	tap slag	31/03/2005	27.46	5.41	52.12	2.13	1.2	0.39	1.21	13.44	bdl	0.01	1.08	1	0.41	105.86
E5_r01	tap slag	31/03/2005	27.48	5.41	52.1	2.05	1.19	0.39	1.21	13.46	bdl	0.01	1.08	1	0.41	105.79
E5_r02	tap slag	31/03/2005	27.47	5.38	52.07	2.02	1.21	0.39	1.21	13.44	bdl	0.01	1.06	1	0.63	105.89
F1	primary smithing slag	25/03/2005	33.14	4.17	38.91	1.62	1.56	0.35	0.62	13.99	bdl	0.01	0.68	1.15	0.69	96.89
F1_r01	primary smithing slag	25/03/2005	33.41	4.17	39.02	1.79	1.57	0.36	0.62	14.03	bdl	0.01	0.53	1.16	0.54	97.21
F1_r02	primary smithing slag	25/03/2005	33.23	4.12	38.91	1.69	1.57	0.35	0.62	13.98	bdl	0.01	0.51	1.15	0.49	96.63

Sample	Material type	Date	SiO <sub>2</sub>	Al <sub>2</sub> O <sub>3</sub>	Fe <sub>2</sub> O <sub>3</sub>	MgO	K <sub>2</sub> O	TiO <sub>2</sub>	MnO	CaO	V <sub>2</sub> O <sub>5</sub>	Cr <sub>2</sub> O <sub>3</sub>	P <sub>2</sub> O <sub>5</sub>	SO <sub>3</sub>	Na <sub>2</sub> O	Sum
F2	furnace bottom slag	25/03/2005	19.03	2.3	83.6	1.09	1.14	0.14	0.07	8.75	bdl	0.01	0.21	0.16	0.53	117.03
F2_r01	furnace bottom slag	25/03/2005	18.98	2.39	83.37	1.05	1.15	0.14	0.07	8.74	bdl	0.01	0.23	0.17	0.66	116.96
F2_r02	furnace bottom slag	25/03/2005	19.01	2.36	83.65	1.08	1.14	0.14	0.07	8.75	bdl	0.01	0.24	0.16	0.35	116.96
F3	primary smithing slag	25/03/2005	36.4	4.72	35.63	1.98	1.81	0.39	0.71	15.71	bdl	0.01	0.81	1.24	0.47	99.88
F3_r01	primary smithing slag	25/03/2005	35.96	4.77	35.14	2.1	1.8	0.39	0.7	15.49	bdl	0.01	0.8	1.25	0.65	99.06
F3_r02	primary smithing slag	25/03/2005	35.97	4.69	35.13	2.14	1.78	0.39	0.7	15.49	bdl	0.01	0.79	1.24	0.85	99.18
F4	primary smithing slag	25/03/2005	26.79	5.27	59.14	1.96	1.25	0.34	1.27	11.14	bdl	0.01	1.16	0.78	0.53	109.64
F4_r01	primary smithing slag	25/03/2005	27.04	5.29	59.69	1.98	1.26	0.35	1.27	11.2	bdl	0.01	1.17	0.77	0.54	110.57
F4_r02	primary smithing slag	25/03/2005	27.22	5.23	60.15	2.02	1.27	0.34	1.29	11.28	bdl	0.01	1.19	0.77	0.49	111.26
F5	primary smithing slag	25/03/2005	31.4	6.54	41.6	1.57	1.78	0.41	1.19	14.47	bdl	0.01	1.36	1.84	0.67	102.84
F5_r01	primary smithing slag	25/03/2005	31.17	6.61	41.33	1.61	1.76	0.41	1.18	14.37	bdl	0.01	1.33	1.84	0.48	102.10
F5_r02	primary smithing slag	25/03/2005	31.25	6.47	41.38	1.56	1.77	0.41	1.19	14.4	bdl	0.01	1.34	1.85	0.74	102.37
G1	ceramic-rich slag	30/03/2005	36.11	5.71	28.73	3.36	1.76	0.41	0.88	19.49	bdl	0.01	1.06	0.41	0.49	98.42
G1_r01	ceramic-rich slag	30/03/2005	36.04	5.7	28.68	3.29	1.76	0.42	0.88	19.44	bdl	0.01	1.04	0.4	0.59	98.25
G1_r02	ceramic-rich slag	30/03/2005	37.97	5.91	29.24	3.53	1.84	0.43	0.92	20.43	bdl	0.01	1.1	0.42	0.53	102.33
G2	ceramic-rich slag	30/03/2005	36.91	5.36	27.65	3.44	1.78	0.4	0.84	20.18	bdl	0.01	0.99	0.35	0.71	98.62
G2_r01	ceramic-rich slag	30/03/2005	37	5.39	27.7	3.45	1.77	0.4	0.84	20.25	bdl	0.01	0.98	0.35	0.47	98.61
G2_r02	ceramic-rich slag	30/03/2005	36.94	5.51	27.77	3.34	1.77	0.4	0.84	20.29	bdl	0.01	1	0.36	0.55	98.78
G3	ceramic-rich slag	30/03/2005	36.61	6.22	34.24	2.13	1.51	0.48	1.04	16.31	bdl	0.01	0.9	0.32	0.58	100.35
G3_r01	ceramic-rich slag	30/03/2005	36.8	6.18	34.45	2.24	1.52	0.48	1.04	16.33	bdl	0.01	0.91	0.32	0.65	100.93
G3_r02	ceramic-rich slag	30/03/2005	36.56	6.15	34.24	2.14	1.5	0.48	1.04	16.26	bdl	0.01	0.73	0.32	0.66	100.9
G4	ceramic-rich slag	30/03/2005	38.08	6.29	28.49	2.43	1.75	0.44	1.02	16.13	bdl	0.01	1.14	1.08	0.16	97.02
G4_r01	ceramic-rich slag	30/03/2005	38.3	6.35	28.5	2.37	1.75	0.43	1.02	16.14	bdl	0.01	1.14	1.09	0.36	97.46
G4_r02	ceramic-rich slag	30/03/2005	38.55	6.37	28.86	2.55	1.77	0.44	1.03	16.34	bdl	0.01	1.14	1.1	0.81	98.97
G5	ceramic-rich slag	30/03/2005	34.6	4.89	31.32	2.44	1.2	0.41	0.52	22.26	bdl	0.01	0.77	0.36	0.5	99.28
G5_r01	ceramic-rich slag	30/03/2005	34.79	4.81	31.45	2.47	1.2	0.41	0.52	22.35	bdl	0.01	0.76	0.36	0.61	99.74
G5_r02	ceramic-rich slag	30/03/2005	34.68	4.81	31.39	2.33	1.19	0.41	0.52	22.26	bdl	0.01	0.78	0.36	0.1	98.84

Sample	Material type	Date	SiO <sub>2</sub>	Al <sub>2</sub> O <sub>3</sub>	Fe <sub>2</sub> O <sub>3</sub>	MgO	K <sub>2</sub> O	TiO <sub>2</sub>	MnO	CaO	V <sub>2</sub> O <sub>5</sub>	Cr <sub>2</sub> O <sub>3</sub>	P <sub>2</sub> O <sub>5</sub>	SO <sub>3</sub>	Na <sub>2</sub> O	Sum
G6	ceramic-rich slag	30/03/2005	44.41	6.62	17.96	2.37	2.03	0.54	0.72	20.91	bdl	0.01	0.74	0.79	0.67	97.77
G6_r01	ceramic-rich slag	30/03/2005	44.49	6.61	17.83	2.3	2.02	0.53	0.71	20.83	bdl	0.01	0.6	0.8	0.58	97.31
G6_r02	ceramic-rich slag	30/03/2005	44.16	6.55	17.75	2.25	2.02	0.53	0.71	20.66	bdl	0.01	0.59	0.8	0.43	96.46
H1	ceramic-rich slag	30/03/2005	50.1	4.72	18.26	2.28	1.6	0.4	0.6	19.57	bdl	0.01	0.54	0.34	0.32	98.74
H1_r01	ceramic-rich slag	30/03/2005	50.2	4.79	18.44	2.26	1.6	0.41	0.6	19.72	bdl	0.01	0.54	0.34	0.8	99.71
H1_r02	ceramic-rich slag	30/03/2005	49.64	4.74	18.18	2.32	1.59	0.4	0.59	19.5	bdl	0.01	0.52	0.34	0.19	98.02
H2	ceramic-rich slag	30/03/2005	53.19	5.58	18.61	1.77	1.58	0.5	0.5	16.17	bdl	0.02	0.53	0.25	0.24	98.94
H2_r01	ceramic-rich slag	30/03/2005	53.55	5.66	18.7	1.74	1.59	0.5	0.5	16.25	bdl	0.02	0.5	0.25	0.11	99.37
H2_r02	ceramic-rich slag	30/03/2005	53.68	5.72	18.67	1.9	1.58	0.5	0.5	16.24	bdl	0.02	0.53	0.25	0.6	100.19
H3	ceramic-rich slag	30/03/2005	57.23	5.09	9.87	2.25	1.6	0.48	0.23	18.55	bdl	0.01	0.37	0.79	bdl	96.47
H3_r01	ceramic-rich slag	30/03/2005	57.13	4.97	9.84	2.18	1.59	0.47	0.23	18.44	bdl	0.01	0.39	0.79	0.19	96.23
H3_r02	ceramic-rich slag	30/03/2005	57.26	5.04	9.88	2.22	1.6	0.48	0.23	18.51	bdl	0.01	0.36	0.78	0.1	96.47
H4	ceramic-rich slag	30/03/2005	47.14	5.98	21.17	2.33	1.63	0.49	0.58	19.3	bdl	0.01	0.55	0.34	bdl	99.52
H4_r01	ceramic-rich slag	30/03/2005	47.03	5.93	21.14	2.31	1.63	0.49	0.58	19.24	bdl	0.01	0.56	0.33	0.16	99.41
H4_r02	ceramic-rich slag	30/03/2005	47.05	5.97	21.25	2.35	1.64	0.47	0.57	19.35	bdl	0.01	0.76	0.33	0.38	100.13
H5	ceramic-rich slag	30/03/2005	46.25	6.57	19.31	2.39	1.63	0.54	0.63	18.43	bdl	0.01	0.59	0.37	0.78	97.50
H5_r01	ceramic-rich slag	30/03/2005	46.45	6.51	19.38	2.31	1.65	0.51	0.61	18.5	bdl	0.01	0.59	0.37	0.11	97.00
H5_r02	ceramic-rich slag	30/03/2005	46.41	6.49	19.39	2.32	1.64	0.51	0.62	18.47	bdl	0.01	0.76	0.36	0.19	97.17
<b>Ore samples</b>																
HA 97 64	discarded ore	25/03/2005	67.56	1.78	30.69	bdl	0.25	0.16	0.01	0.14	bdl	0.02	bdl	0.71	0.54	101.86
HA 97 64_r01	discarded ore	25/03/2005	67.75	1.79	30.78	bdl	0.25	0.16	0.01	0.15	bdl	0.02	bdl	0.72	0.6	102.23
HA 97 64_r02	discarded ore	25/03/2005	67.4	1.75	30.62	bdl	0.25	0.16	0.01	0.15	bdl	0.02	bdl	0.71	0.47	101.54
HA 97 65	Warda ore	25/03/2005	4	bdl	86.39	0.16	bdl	0.01	0.03	7.59	bdl	0.01	0.06	0.84	bdl	99.09
HA 97 65_r01	Warda ore	25/03/2005	4	bdl	86.42	0.17	bdl	0.01	0.03	7.61	bdl	0.01	0.04	0.85	bdl	99.14
HA 97 65_r02	Warda ore	25/03/2005	4.01	bdl	86.35	0.09	bdl	0.01	0.03	7.6	bdl	0.01	0.06	0.85	bdl	99.01

Sample	Material type	Date	SiO <sub>2</sub>	Al <sub>2</sub> O <sub>3</sub>	Fe <sub>2</sub> O <sub>3</sub>	MgO	K <sub>2</sub> O	TiO <sub>2</sub>	MnO	CaO	V <sub>2</sub> O <sub>5</sub>	Cr <sub>2</sub> O <sub>3</sub>	P <sub>2</sub> O <sub>5</sub>	SO <sub>3</sub>	Na <sub>2</sub> O	Sum
HA 97 66	Warda ore	25/03/2005	4.66	0.32	91.49	0.07	0.01	0.08	0.05	0.24	0.03	0.01	0.23	0.39	bdl	97.58
HA 97 66_r01	Warda ore	25/03/2005	4.61	0.32	91.01	0.24	0.01	0.08	0.05	0.24	0.03	0.01	0.23	0.4	bdl	97.23
HA 97 66_r02	Warda ore	25/03/2005	4.67	0.28	91.63	0.15	0.01	0.08	0.05	0.24	0.03	0.01	0.24	0.41	0.15	97.95
Charcoal																
HA Ch1	charcoal	25/03/2005	0.44	bdl	0.12	2.09	2.46	bdl	0.01	8.27	bdl	bdl	0.1	0.35	0.69	14.53
HA Ch1_r01	charcoal	25/03/2005	0.44	bdl	0.12	2.16	2.53	bdl	0.01	8.5	bdl	bdl	0.11	0.36	0.7	14.93
HA Ch1_r02	charcoal	25/03/2005	0.45	bdl	0.12	2.18	2.55	bdl	0.01	8.53	bdl	bdl	0.11	0.36	0.75	15.06
Clay/Tuyère																
HAC 1	Lisan clay	25/03/2005	43.32	14.01	5.61	3.14	2.28	0.96	0.07	9.82	bdl	0.01	0.11	0.55	1.19	81.07
HAC 1_r01	Lisan clay	25/03/2005	43.54	14.11	5.65	3.24	2.31	0.97	0.07	9.91	bdl	0.02	0.12	0.56	1.16	81.66
HAC 02	tuyère nozzle	25/03/2005	50.49	7.39	3.08	1.47	2.03	0.6	0.04	16.45	bdl	0.01	0.23	0.26	0.44	82.49
HAC 02_r01	tuyère nozzle	25/03/2005	50.78	7.54	3.12	1.49	2.06	0.62	0.05	16.72	bdl	0.01	0.24	0.25	0.32	83.20
HAC 03	tuyère body	25/03/2005	41.51	9.46	3.82	2.27	2.35	0.69	0.04	14.89	bdl	0.02	0.17	1.11	0.36	76.69
HAC 03_r01	tuyère body	25/03/2005	41.61	9.55	3.81	2.33	2.36	0.69	0.04	14.9	bdl	0.02	0.15	1.13	0.5	77.09
Beth-Shemesh slags																
TBS 1	secondary smithing slag	25/03/2005	21.66	3.39	67.65	1.16	1.76	0.21	0.06	13.12	bdl	0.01	0.89	0.17	0.57	110.65
TBS 1_r01	secondary smithing slag	25/03/2005	22.22	3.44	69.55	1.12	1.81	0.21	0.06	13.51	bdl	0.01	0.9	0.18	0.38	113.39
TBS 1_r02	secondary smithing slag	25/03/2005	22.28	3.47	69.51	1.03	1.81	0.21	0.06	13.51	bdl	0.01	0.91	0.19	0.72	113.71
TBS 2	secondary smithing slag	25/03/2005	30.51	4.98	38.58	1.87	2.05	0.4	0.18	24.4	bdl	0.01	0.62	0.15	1.09	104.84
TBS 2_r01	secondary smithing slag	25/03/2005	30.53	4.92	38.47	1.85	2.04	0.41	0.18	24.36	bdl	0.01	0.48	0.15	0.37	103.77
TBS 2_r02	secondary smithing slag	25/03/2005	30.41	4.94	38.48	1.86	2.04	0.4	0.18	24.33	bdl	0.01	0.49	0.14	0.61	103.89
TBS 3	secondary smithing slag	20/04/2005	29.34	4.72	50.53	1.6	1.71	0.33	0.07	18.13	bdl	0.01	0.82	0.13	0.66	108.05
TBS 3_r01	secondary smithing slag	20/04/2005	29.3	4.67	50.69	1.58	1.73	0.34	0.07	18.2	bdl	0.01	0.84	0.12	0.74	108.29
TBS 3_r02	secondary smithing slag	20/04/2005	29.22	4.79	50.29	1.64	1.7	0.33	0.07	18.13	bdl	0.01	0.82	0.12	0.73	107.85
TBS 4	secondary smithing slag	20/04/2005	21.55	3.39	66.74	1.6	2.11	0.2	0.06	13.83	bdl	0.01	1.32	0.21	0.53	111.55
TBS 4_r01	secondary smithing slag	20/04/2005	21.67	3.39	66.96	1.56	2.12	0.2	0.06	13.93	bdl	0.01	1.34	0.21	0.5	111.95
TBS 4_r02	secondary smithing slag	20/04/2005	21.8	3.32	67.39	1.59	2.15	0.2	0.06	13.98	bdl	0.01	1.3	0.2	0.38	112.38

Sample	Material type	Date	SiO <sub>2</sub>	Al <sub>2</sub> O <sub>3</sub>	Fe <sub>2</sub> O <sub>3</sub>	MgO	K <sub>2</sub> O	TiO <sub>2</sub>	MnO	CaO	V <sub>2</sub> O <sub>5</sub>	Cr <sub>2</sub> O <sub>3</sub>	P <sub>2</sub> O <sub>5</sub>	SO <sub>3</sub>	Na <sub>2</sub> O	Sum
TBS 5	secondary smithing slag	20/04/2005	24.46	3.85	63.11	1.22	1.86	0.26	0.07	15.67	bdl	0.01	0.86	0.11	0.47	111.95
TBS 5	secondary smithing slag	21/04/2005	24.2	3.73	62.67	1.21	1.85	0.26	0.07	15.55	bdl	0.01	0.86	0.11	0.38	110.90
TBS 5_r01	secondary smithing slag	21/04/2005	23.93	3.81	62.33	1.27	1.83	0.25	0.07	15.42	bdl	0.01	0.83	0.11	0.36	110.22
<b>Standards</b>																
BCS-CRM 381	Basic Slag	25/03/2005	8.6	bdl	18.72	bdl	0.04	0.25	2.81	48.51	0.83	0.32	15.03	0.61	0.85	96.57
BCS-CRM 381	Basic Slag 2	25/03/2005	8.35	bdl	18.79	bdl	0.05	0.26	2.82	48.1	0.82	0.32	14.58	0.61	0.72	95.42
BCS-CRM 381	Basic Slag 3	28/03/2005	8.43	bdl	18.72	bdl	0.05	0.25	2.83	48.35	0.82	0.32	14.68	0.6	0.82	95.87
BCS-CRM 381	Basic Slag 4	30/03/2005	8.42	bdl	18.71	bdl	0.05	0.25	2.83	48.44	0.83	0.32	14.78	0.6	0.75	95.98
BCS-CRM 381	Basic Slag 5	31/03/2005	8.37	bdl	18.79	bdl	0.05	0.26	2.85	48.45	0.82	0.32	14.65	0.61	0.95	96.12
BCS-CRM 381	Basic Slag 5	20/04/2005	8.22	bdl	18.61	bdl	0.04	0.25	2.81	47.77	0.82	0.32	14.3	0.59	0.53	94.26
BCS-CRM 381_r01	Basic Slag 6	25/03/2005	8.55	bdl	18.75	bdl	0.05	0.26	2.83	48.57	0.83	0.32	14.91	0.62	0.75	96.44
BCS-CRM 381_r01	Basic Slag 2	25/03/2005	8.34	bdl	18.74	bdl	0.04	0.25	2.82	48.04	0.82	0.32	14.49	0.6	0.8	95.26
BCS-CRM 381_r01	Basic Slag 3	28/03/2005	8.44	bdl	18.73	bdl	0.05	0.26	2.84	48.47	0.82	0.32	14.64	0.61	0.77	95.95
BCS-CRM 381_r01	Basic Slag 4	30/03/2005	8.49	bdl	18.67	bdl	0.04	0.25	2.82	48.32	0.84	0.32	14.7	0.62	0.75	95.82
BCS-CRM 381_r01	Basic Slag 5	31/03/2005	8.39	bdl	18.7	bdl	0.05	0.25	2.83	48.21	0.82	0.32	14.65	0.62	0.87	95.71
BCS-CRM 381_r01	Basic Slag 6	20/04/2005	8.25	bdl	18.66	bdl	0.04	0.25	2.8	47.64	0.82	0.32	14.34	0.59	0.59	94.30
BCS-CRM 381_r02	Basic Slag 2	25/03/2005	8.33	bdl	18.76	bdl	0.05	0.25	2.82	48.08	0.83	0.32	14.55	0.61	0.94	95.54
BCS-CRM 381_r02	Basic Slag 3	28/03/2005	8.41	bdl	18.65	bdl	0.04	0.25	2.82	48.15	0.83	0.32	14.65	0.61	0.56	95.29
BCS-CRM 381_r02	Basic Slag 4	30/03/2005	8.46	bdl	18.78	bdl	0.05	0.26	2.83	48.61	0.84	0.32	14.81	0.62	0.79	96.37
BCS-CRM 381_r02	Basic Slag 5	31/03/2005	8.44	bdl	18.7	bdl	0.04	0.25	2.84	48.38	0.82	0.32	14.67	0.62	0.6	95.68
USGS BHVO-2	Basalt Hawaiian Volcanic	25/03/2005	46.42	15.02	12.12	5.66	0.5	2.4	0.15	11.02	0.03	0.03	0.08	0.09	2.25	95.77
USGS BHVO-2	Basalt Hawaiian Volcanic 2	25/03/2005	46.15	14.84	12.18	5.5	0.51	2.41	0.15	11.03	0.02	0.03	0.09	0.09	2.03	95.03
USGS BHVO-2	Basalt Hawaiian Volcanic 3	28/03/2005	46.56	15.02	12.16	5.71	0.5	2.4	0.15	11.06	0.02	0.03	0.09	0.08	2.17	95.95
USGS BHVO-2	Basalt Hawaiian Volcanic 4	30/03/2005	46.42	15.03	12.15	5.69	0.51	2.39	0.15	11.04	0.02	0.04	0.09	0.09	2.17	95.79
USGS BHVO-2	Basalt Hawaiian Volcanic 5	31/03/2005	46.49	14.92	12.13	5.59	0.5	2.4	0.15	11.05	0.02	0.04	0.09	0.09	2.26	95.73
USGS BHVO-2	Basalt Hawaiian Volcanic 6	20/04/2005	45.31	14.69	12.1	5.44	0.5	2.37	0.15	10.93	0.02	0.03	0.08	0.08	1.86	93.56
USGS BHVO-2	Basalt Hawaiian Volcanic 7	21/04/2005	45.94	14.8	12.13	5.61	0.5	2.39	0.15	10.95	0.03	0.03	0.07	0.08	2.1	94.78
USGS BHVO-2_r01	Basalt Hawaiian Volcanic	25/03/2005	46.48	14.87	12.1	5.65	0.49	2.39	0.15	10.97	0.02	0.03	0.09	0.09	1.89	95.22
USGS BHVO-2_r01	Basalt Hawaiian Volcanic 2	25/03/2005	46.04	14.86	12.13	5.57	0.5	2.4	0.15	11	0.02	0.03	0.09	0.09	2.19	95.07
USGS BHVO-2_r01	Basalt Hawaiian Volcanic 4	30/03/2005	46.27	14.87	12.09	5.66	0.5	2.39	0.15	11.01	0.02	0.03	0.08	0.09	1.94	95.10
USGS BHVO-2_r01	Basalt Hawaiian Volcanic 5	31/03/2005	46.45	14.82	12.13	5.65	0.5	2.39	0.15	11	0.02	0.04	0.08	0.09	2.16	95.48
USGS BHVO-2_r01	Basalt Hawaiian Volcanic 6	20/04/2005	45.53	14.57	12.13	5.44	0.49	2.39	0.15	10.96	0.02	0.03	0.09	0.08	2.08	93.96
USGS BHVO-2_r01	Basalt Hawaiian Volcanic 7	21/04/2005	45.76	14.82	12.13	5.53	0.49	2.4	0.15	10.96	0.02	0.03	0.09	0.08	2.2	94.66

Sample	Material type	Date	SiO <sub>2</sub>	Al <sub>2</sub> O <sub>3</sub>	Fe <sub>2</sub> O <sub>3</sub>	MgO	K <sub>2</sub> O	TiO <sub>2</sub>	MnO	CaO	V <sub>2</sub> O <sub>5</sub>	Cr <sub>2</sub> O <sub>3</sub>	P <sub>2</sub> O <sub>5</sub>	SO <sub>3</sub>	Na <sub>2</sub> O	Sum
USGS BHVO-2_r02	Basalt Hawaiian Volcanic 2	25/03/2005	45.82	14.68	12.11	5.54	0.5	2.39	0.15	10.98	0.02	0.03	0.08	0.09	2.08	94.47
USGS BHVO-2_r02	Basalt Hawaiian Volcanic 3	28/03/2005	46.56	15.01	12.15	5.75	0.5	2.4	0.15	11.05	0.02	0.03	0.1	0.09	2.28	96.09
USGS BHVO-2_r02	Basalt Hawaiian Volcanic 4	30/03/2005	46.64	14.99	12.13	5.66	0.5	2.4	0.15	11.03	0.02	0.03	0.1	0.09	2.04	95.78
USGS BHVO-2_r02	Basalt Hawaiian Volcanic 5	31/03/2005	46.59	14.98	12.14	5.77	0.51	2.41	0.15	11.02	0.02	0.04	0.09	0.09	2.1	95.91
Swedish Slag_r01	Reference slag W-25:R	20/04/2005	24.51	7.59	68.41	0.32	1.08	0.22	2.74	1.44	bdl	0.01	0.14	0.19	0.95	107.60
Swedish Slag_r02	Reference slag W-25:R	20/04/2005	24.08	7.58	67.04	0.19	1.08	0.22	2.69	1.4	bdl	0.01	0.16	0.18	1.02	105.65

Table 41. Bulk chemical analysis (main elements) of the Tell Hammeh and Tel Beth-Shemesh slags, the Warda and discarded Hammeh Ore, Hammeh charcoal, Lisan clay and tuyère ceramic. Sodium is presented here in *italics*, to indicate that it is not fully quantifiable (see chapter 7). Results of the CRMs run in parallel with the samples are grouped at the bottom of the table. Analysis by (P)ED-XRF, slag\_fun calibration method, at the given date.



Sample	Material Type	Date	NiO	CuO	ZnO	Rb2O	SrO	Y	ZrO2	Ba	PbO
Tell Hammeh Slags											
A1	tap slag	28/03/2005	bdl	21	51	bdl	573	87	210	83	bdl
A1_r01	tap slag	28/03/2005	bdl	48	51	bdl	563	88	193	77	bdl
A1_r02	tap slag	28/03/2005	bdl	43	51	bdl	568	88	200	75	bdl
A2	furnace slag	28/03/2005	bdl	18	166	bdl	460	83	111	bdl	bdl
A2_r01	furnace slag	28/03/2005	bdl	24	156	bdl	465	86	135	bdl	bdl
A2_r02	furnace slag	28/03/2005	bdl	25	150	bdl	458	83	138	bdl	bdl
A3	tap slag	28/03/2005	bdl	39	56	bdl	526	90	151	54	bdl
A3_r01	tap slag	28/03/2005	bdl	11	58	bdl	520	93	148	57	bdl
A3_r02	tap slag	28/03/2005	bdl	9	62	bdl	533	88	156	54	bdl
A4	tap slag	28/03/2005	bdl	52	69	bdl	529	97	154	57	bdl
A4_r01	tap slag	28/03/2005	bdl	45	66	bdl	535	95	167	55	bdl
A4_r02	tap slag	28/03/2005	bdl	47	60	bdl	527	92	186	53	bdl
A5	tap slag	28/03/2005	bdl	10	69	bdl	756	76	133	140	bdl
A5_r01	tap slag	28/03/2005	bdl	bdl	70	bdl	758	76	115	128	bdl
A5_r02	tap slag	28/03/2005	bdl	7	66	bdl	750	76	134	123	bdl
B1	furnace slag	28/03/2005	bdl	72	35	bdl	447	48	99	29	bdl
B1_r01	furnace slag	28/03/2005	bdl	49	27	bdl	449	47	104	23	bdl
B1_r02	furnace slag	28/03/2005	bdl	10	30	bdl	447	50	98	26	bdl
B2	furnace slag	28/03/2005	bdl	28	66	bdl	404	30	119	55	bdl
B2_r01	furnace slag	28/03/2005	bdl	bdl	59	bdl	400	30	106	58	bdl
B2_r02	furnace slag	28/03/2005	bdl	14	62	bdl	407	30	126	49	bdl
B3	furnace slag	28/03/2005	bdl	43	64	bdl	277	83	97	45	bdl
B3_r01	furnace slag	28/03/2005	bdl	25	65	bdl	278	83	118	55	bdl
B3_r02	furnace slag	28/03/2005	37	51	68	bdl	282	86	94	39	bdl

Sample	Material Type	Date	SiO <sub>2</sub>	Al <sub>2</sub> O <sub>3</sub>	FeO	MnO	P <sub>2</sub> O <sub>5</sub>	TiO <sub>2</sub>	NiO	CuO	ZnO	Rb <sub>2</sub> O	SrO	Y	ZrO <sub>2</sub>	Ba	PbO
B4	furnace slag	28/03/2005	55	15	10	0.1	0.1	0.1	bdl	44	25	bdl	30	5	70	bdl	bdl
B4_r01	furnace slag	28/03/2005	55	15	10	0.1	0.1	0.1	bdl	38	21	bdl	31	5	64	bdl	bdl
B4_r02	furnace slag	28/03/2005	55	15	10	0.1	0.1	0.1	bdl	18	20	bdl	31	4	62	bdl	bdl
B5	furnace slag	28/03/2005	55	15	10	0.1	0.1	0.1	bdl	41	21	bdl	552	90	162	159	bdl
B5_r01	furnace slag	28/03/2005	55	15	10	0.1	0.1	0.1	bdl	34	18	bdl	552	91	145	173	bdl
B5_r02	furnace slag	28/03/2005	55	15	10	0.1	0.1	0.1	bdl	34	20	bdl	547	91	152	164	bdl
C1	tap slag	28/03/2005	55	15	10	0.1	0.1	0.1	bdl	18	45	bdl	596	89	251	96	bdl
C1_r01	tap slag	28/03/2005	55	15	10	0.1	0.1	0.1	bdl	26	44	bdl	590	88	234	90	bdl
C1_r02	tap slag	28/03/2005	55	15	10	0.1	0.1	0.1	bdl	23	38	bdl	596	91	241	99	bdl
C2	tap slag	28/03/2005	55	15	10	0.1	0.1	0.1	bdl	28	37	bdl	841	90	199	96	bdl
C2_r01	tap slag	28/03/2005	55	15	10	0.1	0.1	0.1	bdl	23	28	bdl	851	93	179	86	bdl
C2_r02	tap slag	28/03/2005	55	15	10	0.1	0.1	0.1	bdl	32	34	bdl	862	94	193	99	bdl
C3	ceramic-rich slag	28/03/2005	55	15	10	0.1	0.1	0.1	bdl	41	29	11	1069	55	251	181	bdl
C3_r01	ceramic-rich	28/03/2005	55	15	10	0.1	0.1	0.1	bdl	44	29	12	1083	58	260	189	bdl
C3_r02	ceramic-rich	28/03/2005	55	15	10	0.1	0.1	0.1	bdl	40	27	10	1082	58	271	181	bdl
C4	tap slag	28/03/2005	55	15	10	0.1	0.1	0.1	bdl	53	100	bdl	594	90	206	129	bdl
C4_r01	tap slag	28/03/2005	55	15	10	0.1	0.1	0.1	bdl	39	95	bdl	593	90	205	135	bdl
C4_r02	tap slag	28/03/2005	55	15	10	0.1	0.1	0.1	bdl	41	93	bdl	596	86	198	161	bdl
C5	tap slag	28/03/2005	55	15	10	0.1	0.1	0.1	bdl	41	43	bdl	572	105	167	67	bdl
C5_r01	tap slag	28/03/2005	55	15	10	0.1	0.1	0.1	bdl	42	51	bdl	579	105	177	52	bdl
C5_r02	tap slag	28/03/2005	55	15	10	0.1	0.1	0.1	bdl	14	38	bdl	581	113	151	54	bdl
D1	furnace slag	20/04/2005	55	15	10	0.1	0.1	0.1	bdl	38	71	bdl	236	55	123	29	bdl
D1_r01	furnace slag	20/04/2005	55	15	10	0.1	0.1	0.1	bdl	64	62	bdl	235	58	99	25	bdl
D1_r02	furnace slag	20/04/2005	55	15	10	0.1	0.1	0.1	bdl	54	75	bdl	237	55	105	20	bdl
D2	furnace slag	20/04/2005	55	15	10	0.1	0.1	0.1	bdl	25	67	bdl	292	87	116	bdl	bdl
D2_r01	furnace slag	20/04/2005	55	15	10	0.1	0.1	0.1	bdl	27	63	bdl	294	83	117	bdl	bdl
D2_r02	furnace slag	20/04/2005	55	15	10	0.1	0.1	0.1	bdl	57	72	bdl	292	85	128	26	bdl

Sample	Material Type	Date	NiO	CuO	ZnO	Rb2O	SiO	Y	ZrO2	Ba	PbO
D3	furnace slag	20/04/2005	bdl	46	32	bdl	431	52	162	52	bdl
D3_r01	furnace slag	20/04/2005	bdl	47	36	bdl	431	53	172	72	bdl
D3_r02	furnace slag	20/04/2005	bdl	55	33	bdl	438	55	152	44	bdl
D4	furnace slag	20/04/2005	bdl	74	29	bdl	201	19	125	bdl	bdl
D4_r01	furnace slag	20/04/2005	bdl	66	25	bdl	191	21	109	bdl	bdl
D4_r02	furnace slag	20/04/2005	63	112	24	bdl	193	20	114	bdl	bdl
D5	furnace slag	20/04/2005	bdl	63	32	bdl	500	83	112	95	bdl
D5_r01	furnace slag	20/04/2005	bdl	81	39	bdl	497	87	114	91	bdl
D5_r02	furnace slag	20/04/2005	bdl	69	40	bdl	506	81	98	87	bdl
E1	furnace slag	30/03/2005	bdl	34	22	bdl	714	71	122	46	bdl
E1_r01	furnace slag	30/03/2005	bdl	37	25	bdl	711	69	133	47	bdl
E1_r02	furnace slag	30/03/2005	bdl	30	21	bdl	712	69	109	50	bdl
E2	tap slag	30/03/2005	bdl	26	53	bdl	453	74	260	130	bdl
E2_r01	tap slag	30/03/2005	bdl	18	63	bdl	451	77	223	113	bdl
E2_r02	tap slag	30/03/2005	bdl	25	59	bdl	447	78	238	119	bdl
E3	ceramic-rich slag	31/03/2005	bdl	10	19	17	817	83	322	150	bdl
E3_r01	ceramic-rich slag	31/03/2005	bdl	11	21	17	825	85	335	151	bdl
E3_r02	ceramic-rich slag	31/03/2005	bdl	16	20	18	812	84	327	153	bdl
E4	tap slag	30/03/2005	bdl	29	41	4	711	84	278	150	bdl
E4_r01	tap slag	30/03/2005	bdl	9	39	bdl	721	84	252	144	bdl
E4_r02	tap slag	30/03/2005	bdl	21	40	bdl	720	83	267	146	bdl
E5	tap slag	31/03/2005	bdl	14	36	bdl	636	70	237	163	bdl
E5_r01	tap slag	31/03/2005	bdl	26	37	bdl	638	70	213	143	bdl
E5_r02	tap slag	31/03/2005	bdl	30	37	bdl	640	67	226	177	bdl
F1	primary smithing slag	25/03/2005	109	22	25	bdl	522	49	291	128	bdl
F1_r01	primary smithing slag	25/03/2005	95	31	24	bdl	517	51	285	139	bdl
F1_r02	primary smithing slag	25/03/2005	95	39	24	bdl	518	50	271	131	bdl

Sample	Material Type	Date	NiO	CuO	ZnO	Rb2O	SrO	Y	ZrO2	Ba	PbO
F2	primary smithing slag	25/03/2005	bdl	17	11	bdl	249	8	114	bdl	bdl
F2_r01	primary smithing slag	25/03/2005	bdl	32	11	bdl	256	8	123	bdl	bdl
F2_r02	primary smithing slag	25/03/2005	bdl	18	21	bdl	250	6	106	8	bdl
F3	primary smithing slag	25/03/2005	20	24	36	9	642	53	308	162	bdl
F3_r01	primary smithing slag	25/03/2005	20	21	33	10	628	49	300	165	bdl
F3_r02	primary smithing slag	25/03/2005	14	19	33	11	627	51	304	167	bdl
F4	primary smithing slag	25/03/2005	bdl	28	23	bdl	615	75	220	100	bdl
F4_r01	primary smithing slag	25/03/2005	bdl	30	25	bdl	623	78	216	100	bdl
F4_r02	primary smithing slag	25/03/2005	bdl	17	25	bdl	636	77	214	96	bdl
F5	primary smithing slag	25/03/2005	bdl	23	49	7	977	97	292	168	bdl
F5_r01	primary smithing slag	25/03/2005	bdl	25	49	8	973	94	269	168	bdl
F5_r02	primary smithing slag	25/03/2005	bdl	22	52	8	970	98	261	158	bdl
G1	ceramic-rich slag	30/03/2005	bdl	18	24	11	841	68	290	153	bdl
G1_r01	ceramic-rich slag	30/03/2005	bdl	16	24	13	842	65	267	137	bdl
G1_r02	ceramic-rich slag	30/03/2005	bdl	21	24	12	837	67	286	152	bdl
G2	ceramic-rich slag	30/03/2005	bdl	22	22	13	816	63	279	155	bdl
G2_r01	ceramic-rich slag	30/03/2005	bdl	17	20	12	816	63	269	140	bdl
G2_r02	ceramic-rich slag	30/03/2005	bdl	25	23	11	816	62	273	149	bdl
G3	ceramic-rich slag	30/03/2005	bdl	19	30	13	640	71	339	193	bdl
G3_r01	ceramic-rich slag	30/03/2005	bdl	20	29	14	642	73	346	193	bdl
G3_r02	ceramic-rich slag	30/03/2005	bdl	25	29	14	634	71	329	195	bdl
G4	ceramic-rich slag	30/03/2005	bdl	21	19	13	778	88	302	148	bdl
G4_r01	ceramic-rich slag	30/03/2005	bdl	22	21	14	772	89	297	154	bdl
G4_r02	ceramic-rich slag	30/03/2005	bdl	23	21	14	787	92	301	160	bdl
G5	ceramic-rich slag	30/03/2005	bdl	23	23	9	643	54	268	157	bdl
G5_r01	ceramic-rich slag	30/03/2005	bdl	18	22	9	645	53	296	169	bdl
G5_r02	ceramic-rich slag	30/03/2005	bdl	22	26	10	642	53	299	171	bdl

Sample	Material Type	Date	NiO	CuO	ZnO	Rb2O	SrO	Y	ZrO2	Ba	PbO
G6	ceramic-rich slag	30/03/2005	16	12	30	32	677	55	362	213	bdl
G6_r01	ceramic-rich slag	30/03/2005	17	17	31	31	675	56	378	214	bdl
G6_r02	ceramic-rich slag	30/03/2005	15	18	28	32	669	54	368	221	bdl
H1	ceramic-rich slag	30/03/2005	11	35	34	20	579	49	340	138	bdl
H1_r01	ceramic-rich slag	30/03/2005	14	37	34	21	587	50	375	163	bdl
H1_r02	ceramic-rich slag	30/03/2005	11	36	36	21	575	48	344	146	bdl
H2	ceramic-rich slag	30/03/2005	34	36	60	31	499	48	375	179	bdl
H2_r01	ceramic-rich slag	30/03/2005	25	27	62	31	501	48	359	170	bdl
H2_r02	ceramic-rich slag	30/03/2005	30	30	61	32	499	48	375	183	bdl
H3	ceramic-rich slag	30/03/2005	29	27	36	28	511	32	379	151	bdl
H3_r01	ceramic-rich slag	30/03/2005	33	29	36	29	512	31	332	144	bdl
H3_r02	ceramic-rich slag	30/03/2005	33	25	35	29	510	32	406	176	bdl
H4	ceramic-rich slag	30/03/2005	37	27	46	23	731	55	368	207	bdl
H4_r01	ceramic-rich slag	30/03/2005	34	27	48	24	732	54	346	180	bdl
H4_r02	ceramic-rich slag	30/03/2005	42	22	52	23	732	55	336	168	bdl
H5	ceramic-rich slag	30/03/2005	17	21	39	26	681	60	372	199	bdl
H5_r01	ceramic-rich slag	30/03/2005	13	16	36	27	682	60	364	198	bdl
H5_r02	ceramic-rich slag	30/03/2005	11	21	38	27	681	59	365	199	bdl
Ore samples											
HA 64	discarded ore	25/03/2005	bdl	12	66	bdl	22	7	221	bdl	bdl
HA 64_r01	discarded ore	25/03/2005	bdl	15	62	bdl	21	7	195	9	bdl
HA 64_r02	discarded ore	25/03/2005	bdl	7	68	bdl	22	7	205	5	bdl
HA 65	Warda ore	25/03/2005	bdl	bdl	65	bdl	bdl	bdl	26	bdl	bdl
HA 65_r01	Warda ore	25/03/2005	bdl	bdl	65	bdl	bdl	bdl	bdl	bdl	bdl
HA 65_r02	Warda ore	25/03/2005	bdl	15	69	bdl	bdl	bdl	bdl	bdl	bdl

Sample	Material Type	Date	NiO	CuO	ZnO	Rb2O	SrO	Y	ZrO2	Ba	PbO
HA 66	Warda ore	25/03/2005	bdl	32	59	bdl	bdl	21	65	bdl	bdl
HA 66_r01	Warda ore	25/03/2005	bdl	11	62	bdl	bdl	22	72	bdl	bdl
HA 66_r02	Warda ore	25/03/2005	bdl	36	53	bdl	bdl	23	63	bdl	bdl
<b>Charcoal</b>											
HA Ch1	charcoal	25/03/2005									
HA Ch1_r01	charcoal	25/03/2005	9	17	11	5	777	1	bdl	bdl	2
HA Ch1_r02	charcoal	25/03/2005	9	20	10	5	799	1	bdl	bdl	2
	charcoal	25/03/2005	10	19	10	6	800	1	bdl	bdl	2
<b>Clay/Tuyère</b>											
HAC 1	Lisan clay	25/03/2005	61	30	114	75	226	31	328	163	7
HAC 1_r01	Lisan clay	25/03/2005	62	28	114	76	226	31	344	163	7
HAC 02	tuyère nozzle	25/03/2005	36	21	64	40	325	22	449	162	7
HAC 02_r01	tuyère nozzle	25/03/2005	34	20	67	41	328	23	456	161	8
HAC 03	tuyère body	25/03/2005	38	20	77	57	272	24	444	189	7
HAC 03_r01	tuyère body	25/03/2005	37	19	77	56	271	24	444	184	7
<b>Beth-Shemesh slags</b>											
TBS 1	secondary smithing slag	25/03/2005	bdl	64	17	bdl	325	18	170	895	bdl
TBS 1_r01	secondary smithing slag	25/03/2005	bdl	65	21	bdl	335	14	158	929	bdl
TBS 1_r02	secondary smithing slag	25/03/2005	bdl	60	19	bdl	333	15	172	962	bdl
TBS 2	secondary smithing slag	25/03/2005	21	50	24	11	570	25	288	2120	bdl
TBS 2_r01	secondary smithing slag	25/03/2005	21	36	24	11	562	25	276	2150	bdl
TBS 2_r02	secondary smithing slag	25/03/2005	30	47	25	13	572	27	267	2110	bdl
TBS 3	secondary smithing slag	20/04/2005	bdl	54	33	bdl	428	30	226	1389	bdl
TBS 3_r01	secondary smithing slag	20/04/2005	bdl	36	38	bdl	430	26	232	1414	bdl
TBS 3_r02	secondary smithing slag	20/04/2005	bdl	55	39	bdl	429	26	225	1419	bdl
TBS 4	secondary smithing slag	20/04/2005	bdl	71	27	bdl	380	17	177	900	bdl
TBS 4_r01	secondary smithing slag	20/04/2005	bdl	81	30	bdl	385	17	163	877	bdl
TBS 4_r02	secondary smithing slag	20/04/2005	bdl	76	24	bdl	384	19	202	1127	bdl

Sample	Material Type	Date	NiO	CuO	ZnO	Rb2O	SrO	Y	ZrO2	Ba	PbO
TBS 5	secondary smithing slag	20/04/2005	bdL	57	30	bdL	328	17	208	1015	bdL
TBS 5_r01	secondary smithing slag	21/04/2005	bdL	56	28	bdL	328	16	223	1030	bdL
TBS 5_r02	secondary smithing slag	21/04/2005	bdL	57	27	bdL	329	18	202	1029	bdL
Standards											
BCS-CRM 381	Basic Slag	25/03/2005	bdL	5	13	bdL	362	6	29	416	bdL
BCS-CRM 381	Basic Slag 2	25/03/2005	bdL	5	17	bdL	367	6	21	423	bdL
BCS-CRM 381	Basic Slag 3	28/03/2005	bdL	3	16	bdL	367	7	20	412	bdL
BCS-CRM 381	Basic Slag 4	30/03/2005	bdL	8	15	bdL	362	5	23	423	bdL
BCS-CRM 381	Basic Slag 5	31/03/2005	bdL	5	17	bdL	364	6	17	468	bdL
BCS-CRM 381	Basic Slag 5	20/04/2005	bdL	22	24	bdL	363	5.9	19	414	bdL
BCS-CRM 381_r01	Basic Slag 6	25/03/2005	bdL	9	15	bdL	363	7	26	410	bdL
BCS-CRM 381_r01	Basic Slag 2	25/03/2005	bdL	7	16	bdL	366	6	29	417	bdL
BCS-CRM 381_r01	Basic Slag 3	28/03/2005	bdL	4	17	bdL	366	6	23	399	bdL
BCS-CRM 381_r01	Basic Slag 4	30/03/2005	bdL	7	16	bdL	364	6	18	416	bdL
BCS-CRM 381_r01	Basic Slag 5	31/03/2005	bdL	4	17	bdL	364	6	23	415	bdL
BCS-CRM 381_r01	Basic Slag 6	20/04/2005	bdL	24	24	bdL	364	6	24	405	bdL
BCS-CRM 381_r02	Basic Slag 2	25/03/2005	bdL	4	18	bdL	367	6	20	428	bdL
BCS-CRM 381_r02	Basic Slag 3	28/03/2005	bdL	3	16	bdL	364	6	15	404	bdL
BCS-CRM 381_r02	Basic Slag 4	30/03/2005	bdL	5	16	bdL	365	7	18	426	bdL
BCS-CRM 381_r02	Basic Slag 5	31/03/2005	bdL	4	15	bdL	366	6	28	417	bdL
USGS BHVO-2	Basalt Hawaiian Volcanic	25/03/2005	115	167	106	9	452	24	221	113	bdL
USGS BHVO-2	Basalt Hawaiian Volcanic 2	25/03/2005	122	167	107	9	457	24	227	114	bdL
USGS BHVO-2	Basalt Hawaiian Volcanic 3	28/03/2005	121	171	108	8	455	24	223	117	bdL
USGS BHVO-2	Basalt Hawaiian Volcanic 4	30/03/2005	118	170	105	8	451	24	207	117	bdL
USGS BHVO-2	Basalt Hawaiian Volcanic 5	31/03/2005	120	168	106	8	454	25	221	114	bdL
USGS BHVO-2	Basalt Hawaiian Volcanic 6	20/04/2005	126	178	109	8	455	25	254	140	bdL
USGS BHVO-2	Basalt Hawaiian Volcanic 7	21/04/2005	118	174	112	9	454	24	228	119	bdL
USGS BHVO-2_r01	Basalt Hawaiian Volcanic	25/03/2005	119	170	102	9	451	24	221	115	bdL
USGS BHVO-2_r01	Basalt Hawaiian Volcanic 2	25/03/2005	113	165	107	9	456	24	219	118	bdL
USGS BHVO-2_r01	Basalt Hawaiian Volcanic 4	30/03/2005	119	176	106	8	452	24	265	149	bdL
USGS BHVO-2_r01	Basalt Hawaiian Volcanic 5	31/03/2005	119	168	106	9	456	24	215	116	bdL
USGS BHVO-2_r01	Basalt Hawaiian Volcanic 6	20/04/2005	114	178	109	9	455	24	221	121	bdL
USGS BHVO-2_r01	Basalt Hawaiian Volcanic 7	21/04/2005	122	186	109	8	455	24	224	126	bdL
USGS BHVO-2_r02	Basalt Hawaiian Volcanic 2	25/03/2005	118	173	106	9	454	24	216	118	bdL



Sample	Material Type	Date	NiO	CuO	ZnO	Rb2O	SrO	Y	ZrO2	Ba	PbO
USGS BHVO-2_r02	Basalt Hawaiian Volcanic 3	28/03/2005	122	168	104	9	456	25	229	116	bdl
USGS BHVO-2_r02	Basalt Hawaiian Volcanic 4	30/03/2005	123	175	106	8	454	24	220	116	bdl
USGS BHVO-2_r02	Basalt Hawaiian Volcanic 5	31/03/2005	116	164	104	8	452	24	234	123	bdl
Swedish Slag_r01	Reference slag W-25:R	20/04/2005	bdl	29	36	bdl	88	132	160	1059	bdl
Swedish Slag_r02	Reference slag W-25:R	20/04/2005	bdl	20	35	bdl	87	125	119	948	bdl

Table 42. Bulk chemical analysis (trace elements) of the Tell Hammeh and Tel Beth-Shemesh slags, the Warda and discarded Hammeh Ore, Hammeh charcoal, Lisan clay and tuyère ceramic. Results of the CRMs ran in parallel with the samples are grouped at the bottom of the table. Analysis by (P)ED-XRF, slag\_fun calibration method, at the given date.

## APPENDIX 2. SEM-EDS ANALYSES

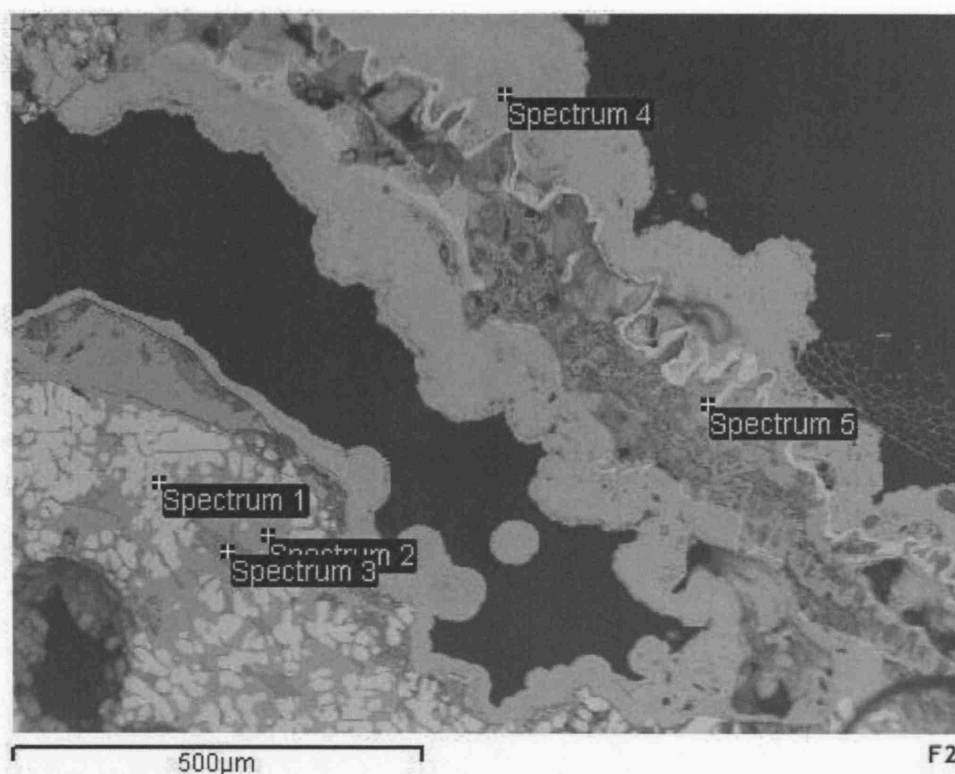


Figure 66. BSE micrograph of sample F2, showing a glassy matrix, (mid-dark grey), with olivine laths (mid grey), and thick dendritic wüstite in the left bottom corner, and a skin of mostly various iron hydroxides (FeOOH) that has partly separated from the slag. The dark areas are voids, and a small piece of attached charcoal can be seen in the centre right of the picture.

Sample: F2	ID: furnace bottom slag										
	SiO <sub>2</sub>	Al <sub>2</sub> O <sub>3</sub>	FeO	TiO <sub>2</sub>	CaO	MgO	K <sub>2</sub> O	P <sub>2</sub> O <sub>5</sub>	S	Na <sub>2</sub> O	Total
Spectrum 1		0.70	98.9	0.42							100
Spectrum 2	32.2		38.7		26.8	2.32					100
Spectrum 3	39.1	14.2	24.9	0.54	9.34		8.48	0.85	0.71	1.79	100
Spectrum 4	1.14		98.9								100
Spectrum 5			100								100

Table 43. SEM-EDS analyses of furnace bottom slag F2. Values are presented as compounds, and are normalised to 100%.

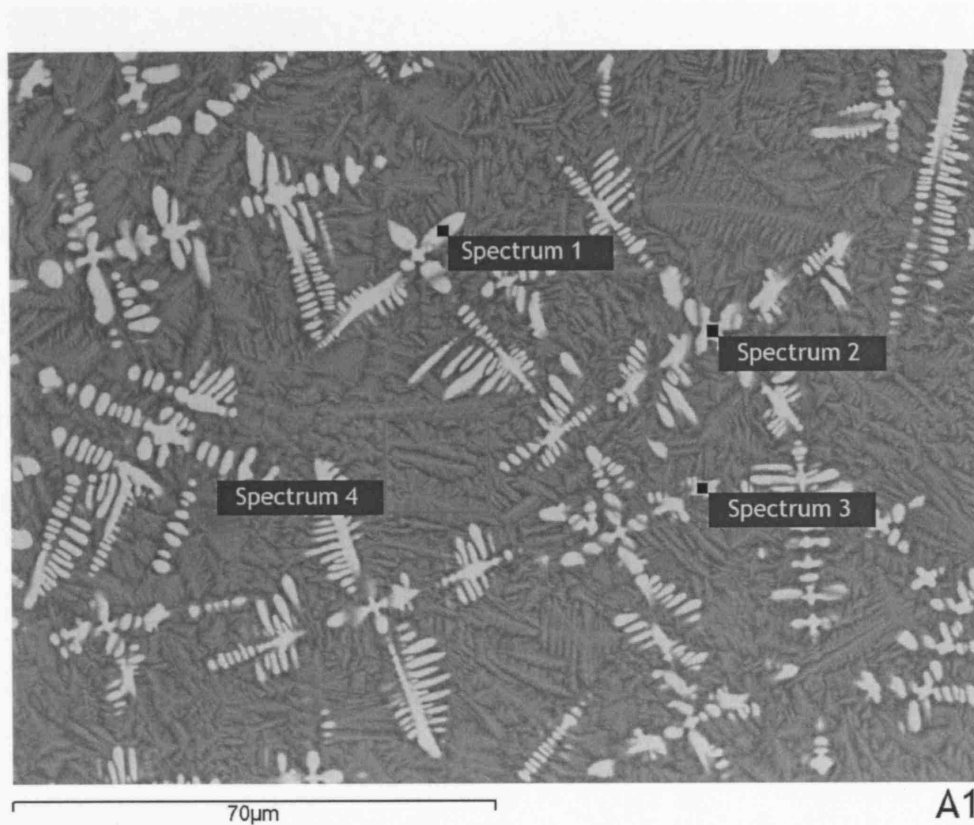


Figure 67. BSE micrograph of tap slag A1, showing a glassy matrix (dark grey), with feathery devitrification (mid-grey) and wüstite dendrites (light grey).

Sample: A1	ID: tap slag											
	SiO <sub>2</sub>	Al <sub>2</sub> O <sub>3</sub>	FeO	TiO <sub>2</sub>	MnO	CaO	MgO	K <sub>2</sub> O	P <sub>2</sub> O <sub>5</sub>	S	Na <sub>2</sub> O	Total
Spectrum 1	26.8	5.23	52.2		1.17	10.3	2.49	0.74	1.05			100
Spectrum 2	33.4	6.84	38.9		1.50	13.1	2.58	1.39	1.18	1.03		100
Spectrum 3	25.6	4.54	55.8		1.18	7.62	3.24	0.91	1.13			100
Spectrum 4	35.5	7.16	34.2	0.60	1.48	14.2	2.62	1.30	1.72	0.68	0.56	100

Table 44. SEM-EDS analyses of tap slag A1. Values are presented as compounds, and are normalised to 100%.

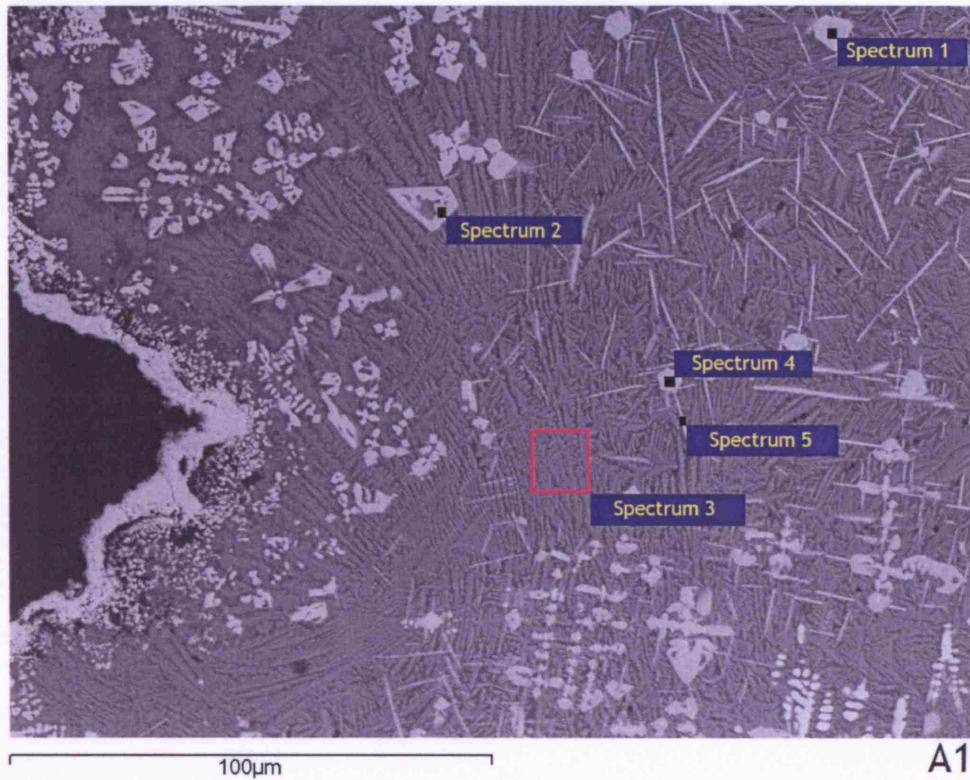


Figure 68. BSE Micrograph of tap slag A1. Showing a glassy matrix (dark-grey), with feathery devitrification (mid-grey), wüstite dendrites ( $\text{FeO}$ , white), magnetite from oxygen penetration near the surface (light grey), and possible iscorite ( $\text{Fe}_7\text{SiO}_{10}$ , needle-shaped), the black area is the edge of the sample and shows a band of iron hydroxide ( $\text{FeOOH}$ ).

Sample: A1	ID: tap slag										
	$\text{SiO}_2$	$\text{Al}_2\text{O}_3$	$\text{FeO}$	$\text{TiO}_2$	$\text{MnO}$	$\text{CaO}$	$\text{MgO}$	$\text{K}_2\text{O}$	$\text{P}_2\text{O}_5$	$\text{S}$	Total
Spectrum 1	37.6	5.62	35.0		1.60	14.2	2.24	1.36	1.56	0.77	100
Spectrum 2	0.96	9.83	84.9	2.06	0.67	0.46	1.17				100
Spectrum 3	34.8	5.83	36.8		1.65	14.5	2.58	1.33	1.44	1.09	100
Spectrum 4	30.1	9.32	41.8	0.90	0.58	12.2	2.65	0.72	1.07	0.66	100
Spectrum 5	35.3	4.63	41.1		1.86	10.6	3.63	1.12	1.68		100

Table 45. SEM-EDS analyses of tap slag A1. Values are presented as compounds, and are normalised to 100%



Figure 69. BSE micrograph of tap slag C1, showing a tapping band between two flows of slag. The edges of these flows consist predominantly of a glassy matrix (grey) with small formations of fayalitic laths (lighter grey) and some precipitation of thin wüstite dendrites (light grey) where the two flows touch.

Sample: C1	ID: tap slag											
	SiO <sub>2</sub>	Al <sub>2</sub> O <sub>3</sub>	FeO	TiO <sub>2</sub>	MnO	CaO	MgO	K <sub>2</sub> O	P <sub>2</sub> O <sub>5</sub>	S	Na <sub>2</sub> O	Total
Spectrum 1	37.9	6.13	34.9	0.67	1.19	13.6	1.83	1.23	1.28	0.85	0.44	100
Spectrum 2	37.0	6.24	35.3	0.54	1.23	14.1	2.00	1.30	1.23	0.62	0.44	100
Spectrum 3	37.1	6.36	35.5	0.49	1.19	13.4	2.22	1.21	1.37	0.69	0.43	100

Table 46. SEM-EDS analyses of tap slag C1. Values are presented as compounds, and are normalised to 100%.



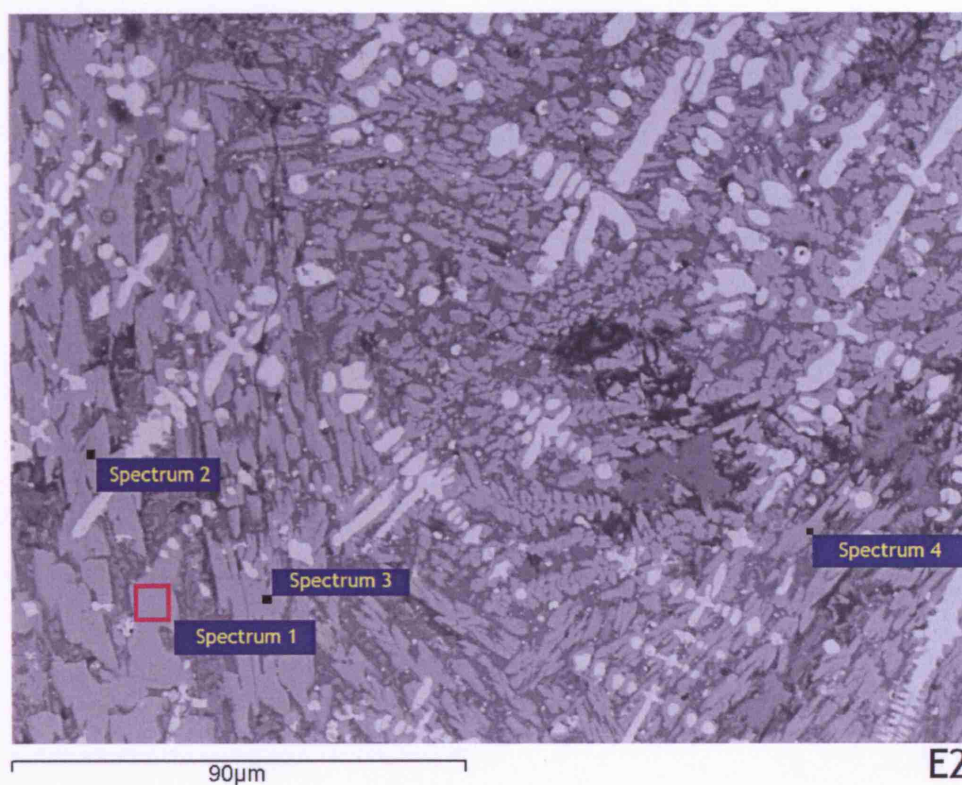


Figure 70. BSE micrograph of tap slag E2 showing skeletal fayalitic/olivine laths (mid-grey) in a glassy matrix (darker grey), with small dendritic wüstite (light grey). Tiny droplets of probable FeS (lightest grey) are interspersed between the laths.

Sample: E2	ID: tap slag											
	SiO <sub>2</sub>	Al <sub>2</sub> O <sub>3</sub>	FeO	MnO	CaO	MgO	K <sub>2</sub> O	P <sub>2</sub> O <sub>5</sub>	S	Na <sub>2</sub> O	WO <sub>3</sub>	Total
Spectrum 1	36.3	1.49	47.5	1.69	7.67	4.45			0.88			100
Spectrum 2	36.8		48.8	1.97	6.70	5.74						100
Spectrum 3	36.4		49.0	2.22	7.00	5.46						100
Spectrum 4	35.2	16.6	20.4		16.0		3.02	2.52	2.57	0.78	2.90	100

Table 47. SEM-EDS analyses of tap slag E2. Values are presented as compounds, and are normalised to 100%.



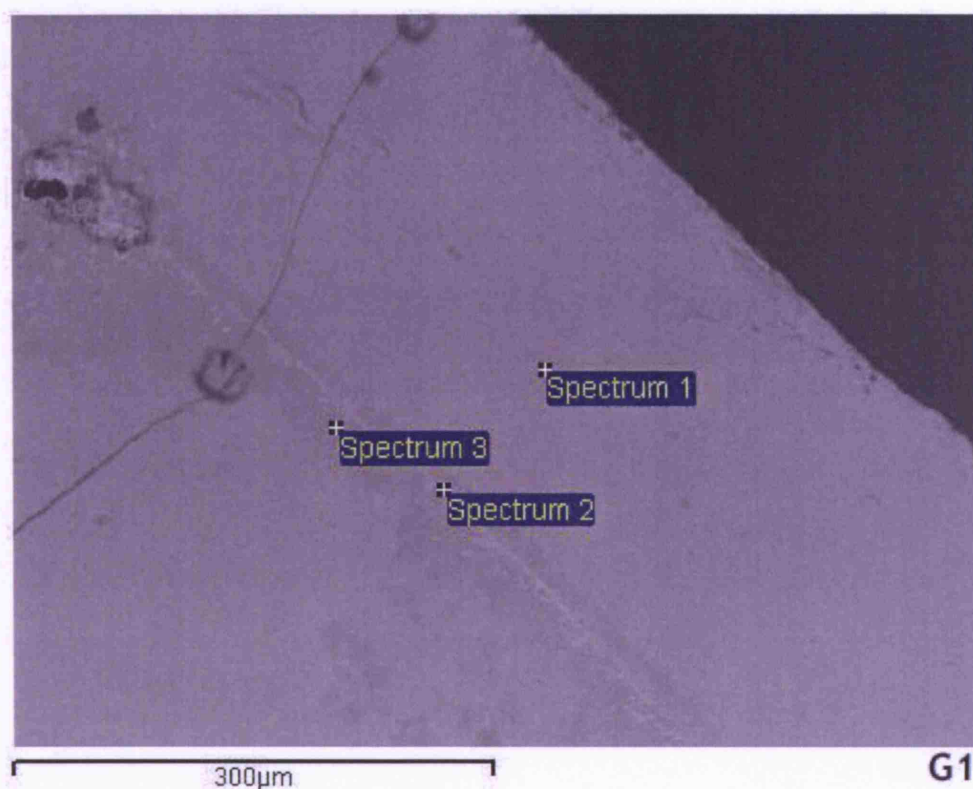


Figure 71. BSE micrograph of 'ceramic-rich' slag G1, showing an amorphous mass of glass and a thin tapping band of iron oxide or hydroxide (possibly wüstite) flanked by darker conglomerates of glass that is richer in  $\text{Al}_2\text{O}_3$  and  $\text{K}_2\text{O}$  than the matrix.

Sample: G1	ID: ceramic-rich slag										
	<b><math>\text{SiO}_2</math></b>	<b><math>\text{Al}_2\text{O}_3</math></b>	<b>FeO</b>	<b>TiO<sub>2</sub></b>	<b>MnO</b>	<b>CaO</b>	<b>MgO</b>	<b><math>\text{K}_2\text{O}</math></b>	<b><math>\text{P}_2\text{O}_5</math></b>	<b><math>\text{Na}_2\text{O}</math></b>	<b>Total</b>
Spectrum 1	40.5	5.72	24.9	0.63	1.05	19.9	3.63	1.86	1.29	0.49	100
Spectrum 2	30.0	4.82	36.8		0.69	21.6	4.14	0.87	1.01		100
Spectrum 3	43.0	6.49	22.6		0.92	20.5	3.21	1.93	1.35		100

Table 48. SEM-EDS analyses of ceramic-rich slag G1. Values are presented as compounds, and are normalised to 100%.

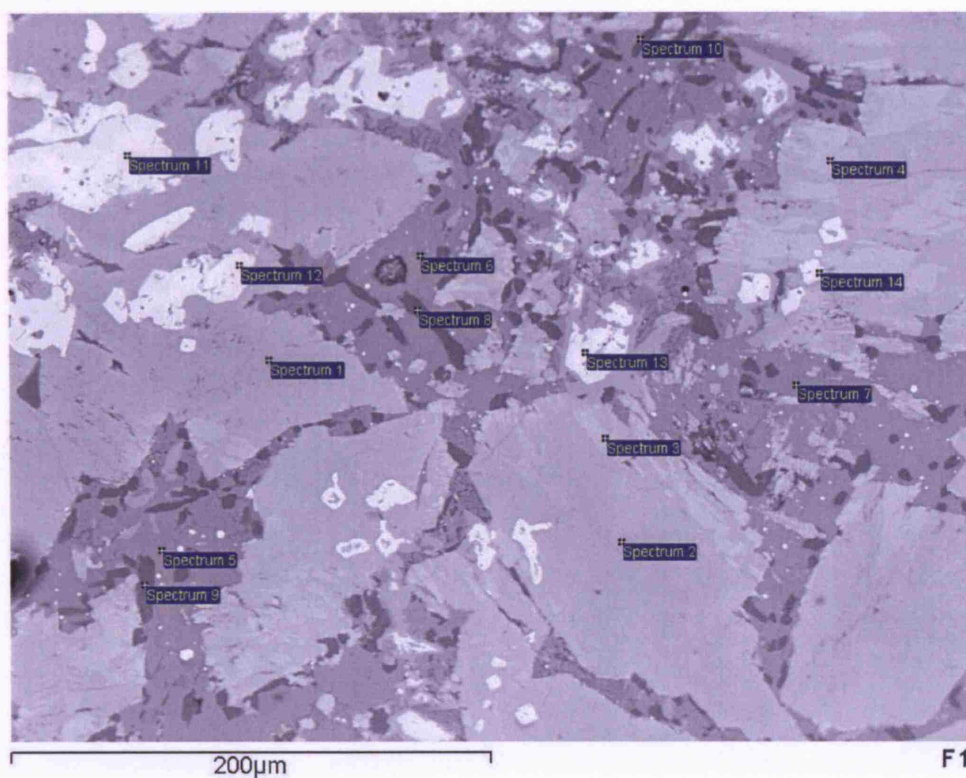


Figure 72. BSE micrograph of primary smithing slag F1, showing a calcio-olivinic glassy matrix, (mid-dark grey), with solid laths of leucite ( $\text{KAlSi}_2\text{O}_6$ ; dark grey), large 2-phased olivinic blocks (mid-grey, and slightly lighter), and precipitations of spinel with hercynitic (Al) and ulvitic ( $\text{TiO}_2$ ) components (whitish).

Sample: F1		ID: primary smithing slag											
	$\text{SiO}_2$	$\text{Al}_2\text{O}_3$	$\text{FeO}$	$\text{TiO}_2$	$\text{MnO}$	$\text{CaO}$	$\text{MgO}$	$\text{K}_2\text{O}$	$\text{P}_2\text{O}_5$	$\text{S}$	$\text{Cr}_2\text{O}_3$	$\text{Na}_2\text{O}$	Total
Spectrum 1	31.9		41.2		1.59	20.4	4.86						100
Spectrum 2	31.4		39.6		1.63	23.1	4.26						100
Spectrum 3	30.2		56.8		1.88	8.09	3.10						100
Spectrum 4	30.8		55.6		1.71	7.37	4.51						100
Spectrum 5	37.9	9.49	22.3	0.84		24.7	0.85		3.95				100
Spectrum 6	39.1	11.2	23.0		0.55	20.0		0.98	3.12	0.78		1.40	100
Spectrum 7	38.5	11.9	23.4	0.76		18.8		0.89	2.78	1.70		1.23	100
Spectrum 8	55.7	20.5	1.93			1.55		19.7				0.67	100
Spectrum 9	55.9	20.5	3.18					19.6				0.82	100
Spectrum 10	53.6	20.0	5.31			4.39		15.8				0.99	100
Spectrum 11	1.07		98.0		0.58	0.36							100
Spectrum 12		3.49	93.1	1.96		0.70					0.74		100
Spectrum 13		2.88	95.4	1.74									100
Spectrum 14	20.5	7.90	56.2	3.30	0.59	9.77	1.21				0.50		100

Table 49. SEM-EDS analyses of primary smithing slag F1. Values are presented as compounds, and are normalised to 100%.



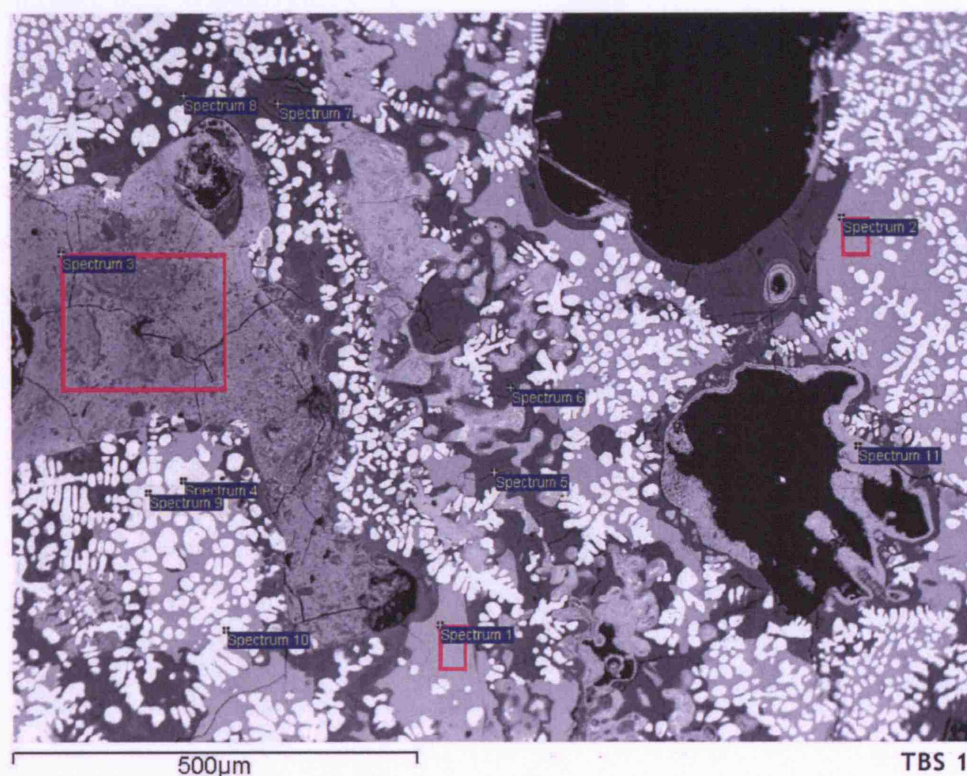


Figure 73. Back Scatter Electron (BSE) micrograph of sample TBS 1, showing the very heterogeneous microstructure of this sample. It consists of a heterogeneous glassy matrix (mid grey and dark grey), incorporating partly fused and thermally cracked quartz grains (dark grey), a large inclusion of iron rich ceramic material (left centre, with cracks), iron hydroxide (around holes), and wüstite (FeO) dendrites (whitish).

Sample: TBS 1	ID: secondary smelting slag									
	SiO <sub>2</sub>	Al <sub>2</sub> O <sub>3</sub>	FeO	TiO <sub>2</sub>	CaO	MgO	K <sub>2</sub> O	P <sub>2</sub> O <sub>5</sub>	Na <sub>2</sub> O	Total
Spectrum 1	33.9	6.23	39.1		14.7	0.77	3.52	0.89	0.95	100
Spectrum 2	33.5	5.96	37.3		17.8		3.37	1.00	1.10	100
Spectrum 3	27.5	1.21	52.9		8.48	0.80	1.29	7.86		100
Spectrum 4			100							100
Spectrum 5	69.4	13.4	4.84		3.04	0.68	6.61	2.01		100
Spectrum 6	68.4	12.3	4.19		3.80		9.12	2.25		100
Spectrum 7	68.4	12.4	6.40	0.69	2.87	0.59	7.62	1.06		100
Spectrum 8	69.0	13.4	5.81	0.73	2.17		8.97			100
Spectrum 9			99.1			0.92				100
Spectrum 10			100							100
Spectrum 11	13.6	0.92	82.7		1.21			1.51		100

Table 50. SEM-EDS analyses of secondary smelting slag TBS 1. Values are presented as compounds, and are normalised to 100%.

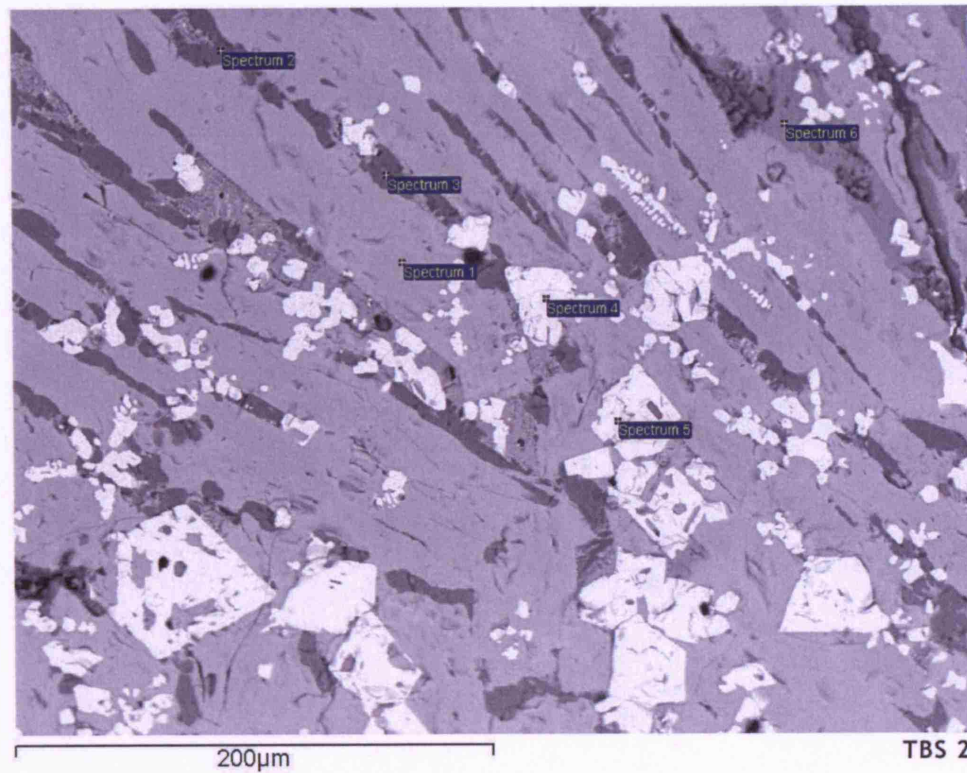


Figure 74. Back Scatter Electron (BSE) micrograph of sample TBS 2, showing a kalsilitic ( $\text{KAlSiO}_4$ ) glassy matrix (dark grey), large kirschsteinitic ( $\text{CaFeSiO}_4$ ) laths (mid grey), and precipitation of magnetite crystals (whitish).

Sample: TBS 2	ID: secondary smithing slag								
	<b>SiO<sub>2</sub></b>	<b>Al<sub>2</sub>O<sub>3</sub></b>	<b>FeO</b>	<b>TiO<sub>2</sub></b>	<b>CaO</b>	<b>MgO</b>	<b>K<sub>2</sub>O</b>	<b>Na<sub>2</sub>O</b>	<b>Total</b>
Spectrum 1	32.6		33.3		32.2	1.97			100
Spectrum 2	40.7	29.1	2.01	0.69			25.2	2.21	100
Spectrum 3	41.0	30.4	1.35				24.4	2.90	100
Spectrum 4		5.23	93.5	1.27					100
Spectrum 5		5.61	93.7	0.65					100
Spectrum 6	38.5	7.89	16.17		34.5	0.84	0.52	1.59	100

Table 51. SEM-EDS analyses of secondary smithing slag TBS 2. Values are presented as compounds, and are normalised to 100%.

## **APPENDIX 3. PRINCIPAL COMPONENT ANALYSES**



## PCA Scores and Loading Vector Values of the Hammeh System

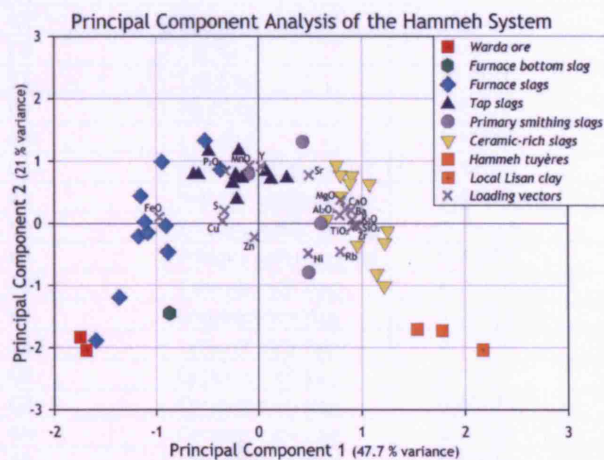


Figure 75. PCA plot of the Hammeh System, using PC1 and PC2.

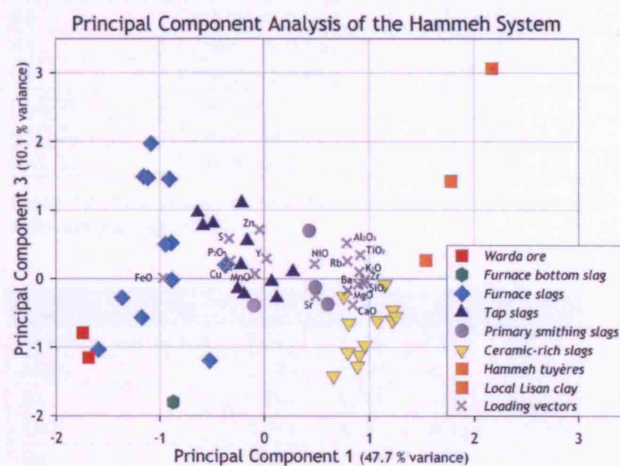


Figure 76. PCA plot of the Hammeh System, using PC1 and PC3.

Principal Component Scores					
Sample	Type	PC01	PC02	PC03	PC04
HA 65	Ore	-1.6877	-2.04164	-1.15487	-2.04269
HA 66	Ore	-1.74403	-1.83155	-0.79109	-1.01449
F2	Furnace bottom slag	-0.87181	-1.44663	-1.80142	-0.46186
A2	Furnace slag	-0.90611	-0.03561	1.45244	-2.78538
B1	Furnace slag	-1.17353	-0.21027	-0.57122	0.50763
B2	Furnace slag	-0.88754	-0.45625	0.51979	-1.02136
B3	Furnace slag	-1.15326	0.43767	1.48882	0.54747
B4	Furnace slag	-1.59331	-1.88893	-1.03694	0.30017
B5	Furnace slag	-0.37041	0.86312	0.19827	0.99825
D1	Furnace slag	-1.08321	-0.15277	1.97062	1.25055
D2	Furnace slag	-1.11353	0.02367	1.47037	0.02838
D3	Furnace slag	-0.88513	-0.46806	-0.01893	1.08804
D4	Furnace slag	-1.36436	-1.19174	-0.27995	3.07025
D5	Furnace slag	-0.94335	0.98651	0.50154	1.93814
E1	Furnace slag	-0.52285	1.32815	-1.19816	-0.08868
A1	Tap slag	-0.22195	0.7742	0.20003	-0.09229
A3	Tap slag	-0.63568	0.77862	0.96209	-0.69094

A4	Tap slag	-0.58502	0.77498	0.77045	0.20181
A5	Tap slag	-0.25357	0.64063	-0.14671	-1.9253
C1	Tap slag	0.07131	0.82951	-0.0399	-0.59451
C2	Tap slag	-0.19197	1.16601	-0.22777	-0.30663
C4	Tap slag	-0.16242	0.72017	0.55267	-0.38121
C5	Tap slag	-0.48748	1.15098	0.80458	-0.10767
E2	Tap slag	-0.2121	0.38151	1.10421	0.02331
E4	Tap slag	0.27378	0.72426	0.10034	-0.36423
E5	Tap slag	0.11848	0.7068	-0.2822	-0.25058
F1	Primary smithing slag	0.48926	-0.79905	-0.12779	2.14359
F3	Primary smithing slag	0.60902	-0.01099	-0.38197	0.31991
F4	Primary smithing slag	-0.09514	0.7821	-0.40061	-0.11534
F5	Primary smithing slag	0.43321	1.30154	0.69239	0.00474
C3	Ceramic-rich slag	0.79478	0.77604	-1.07741	0.65492
E3	Ceramic-rich slag	1.07531	0.63007	-0.61151	-0.32267
G1	Ceramic-rich slag	0.90433	0.75981	-1.11359	-0.45513
G2	Ceramic-rich slag	0.88535	0.64136	-1.27968	-0.27723
G3	Ceramic-rich slag	0.80231	0.43638	-0.65328	-0.33757
G4	Ceramic-rich slag	0.75509	0.93348	-0.25914	0.13023
G5	Ceramic-rich slag	0.65926	0.06305	-1.42109	-0.34185
H1	Ceramic-rich slag	0.95513	-0.3538	-0.97055	0.607
H2	Ceramic-rich slag	1.14572	-0.81223	-0.08516	0.24839
H3	Ceramic-rich slag	1.21718	-1.01041	-0.60477	0.74579
H4	Ceramic-rich slag	1.22197	-0.31429	-0.45725	0.20543
H5	Ceramic-rich slag	1.2499	-0.11941	-0.55146	-0.24976
HAC 01	Lisan Clay	2.17038	-2.03638	3.06608	-0.51218
HAC 02	Tuyère nozzle	1.53651	-1.7045	0.26762	-0.13418
HAC 03	Tuyère body	1.77718	-1.7261	1.4221	-0.14026

Table 52. PCA scores of the Hammeh Smelting System, PC1 - PC4. Scores were calculated with statistical software package SPSS 12.

Loading Vectors				
Original variables	PC01	PC02	PC03	PC04
Al <sub>2</sub> O <sub>3</sub>	0.784	0.131	0.52	-0.079
Ba	0.894	0.209	-0.082	0.064
CaO	0.841	0.23	-0.386	-0.046
Cu	-0.35	0.041	0.19	0.765
FeO	-0.968	0.099	0.013	-0.131
K <sub>2</sub> O	0.905	0.053	0.1	0.092
MgO	0.792	0.372	-0.169	-0.077
MnO	-0.088	0.927	0.075	0.013
Ni	0.48	-0.486	0.214	0.336
P <sub>2</sub> O <sub>5</sub>	-0.321	0.839	0.264	0.076
Rb	0.79	-0.457	0.256	-0.031
SiO <sub>2</sub>	0.944	-0.026	-0.07	0.083
S	-0.333	0.199	0.584	0.256
Sr	0.489	0.771	-0.255	-0.026
TiO <sub>2</sub>	0.914	-0.042	0.348	-0.03
Y	0.022	0.909	0.293	-0.052
Zn	-0.042	-0.221	0.715	-0.484
Zr	0.957	-0.05	-0.013	0.082

Table 53. Loading vector values for the Hammeh Smelting System, PC1 - PC4. Values were calculated with statistical software package SPSS 12.



## PCA Scores and Loading Vector Values of the Beth-Shemesh Secondary Smithing Slags Compared with the Hammeh Tap and Primary Smithing Slags

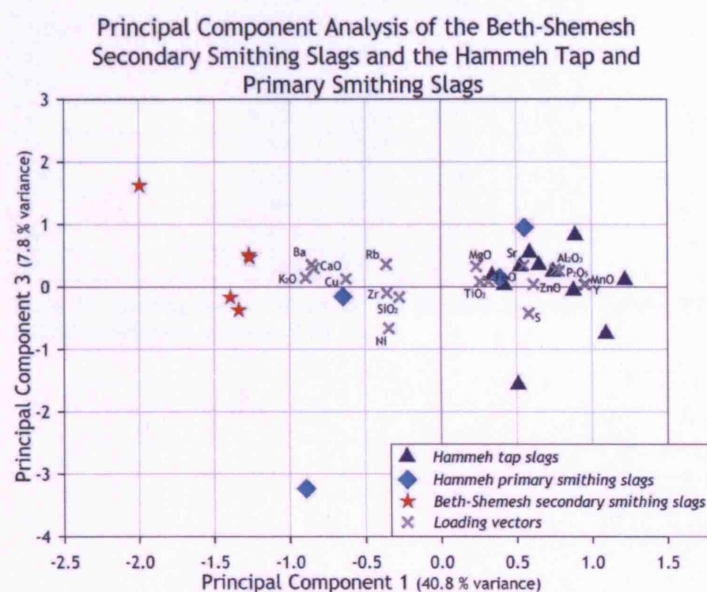


Figure 77. PCA plot of the Beth-Shemesh smithing slags, compared to the Hammeh tap and primary smithing slags, using PC1 and PC3.

Principal Component Scores					
Sample	Type	PC01	PC02	PC03	PC04
A1	Tap slag	0.65044	-0.07172	0.34721	-1.18051
A3	Tap slag	1.09184	-0.84168	-0.74676	1.04145
A4	Tap slag	0.8784	-0.86444	-0.05893	0.17634
A5	Tap slag	0.74418	-0.80851	0.24365	0.27509
C1	Tap slag	0.58875	0.62494	0.54533	-1.68877
C2	Tap slag	0.89069	-0.1421	0.82281	-1.07953
C4	Tap slag	0.52592	-0.40707	0.32611	0.3308
C5	Tap slag	1.21827	-0.4658	0.11004	-0.14167
E2	Tap slag	0.50962	0.26038	-1.56313	1.96036
E4	Tap slag	0.41929	1.11744	0.0321	0.29255
E5	Tap slag	0.34007	0.45335	0.17803	-0.87699
F1	Primary smithing slag	-0.89271	1.06207	-3.23409	-1.26408
F3	Primary smithing slag	-0.64744	1.72747	-0.15549	0.3367
F4	Primary smithing slag	0.39114	0.07012	0.14238	-1.09169
F5	Primary smithing slag	0.55498	1.47203	0.95029	2.10281
TBS 1	Secondary smithing slag	-1.33697	-1.6537	-0.37326	0.32232
TBS 2	Secondary smithing slag	-1.99535	1.30847	1.62352	0.22818
TBS 3	Secondary smithing slag	-1.27257	-0.13391	0.50921	-0.04797
TBS 4	Secondary smithing slag	-1.26541	-1.63338	0.46942	0.00916
TBS 5	Secondary smithing slag	-1.39314	-1.07398	-0.16844	0.29544

Table 54. Table 55. PCA scores of the Hammeh Smelting System, PC1 - PC4. Scores were calculated with statistical software package SPSS 12.

Loading Vectors				
Original variables	1	2	3	4
Al <sub>2</sub> O <sub>3</sub>	0.759	0.464	0.274	0.041
Ba	-0.854	-0.085	0.354	0.099
CaO	-0.839	0.398	0.295	0.037

Cu	-0.627	-0.549	0.127	-0.016
FeO	0.316	-0.922	0.087	-0.064
K <sub>2</sub> O	-0.894	0.113	0.144	0.18
MgO	0.235	0.521	0.323	-0.677
MnO	0.951	0.188	0.039	-0.144
Ni	-0.344	0.389	-0.662	-0.265
P <sub>2</sub> O <sub>5</sub>	0.786	-0.376	0.254	0.162
Rb	-0.361	0.659	0.358	0.328
SiO <sub>2</sub>	-0.275	0.89	-0.167	0.071
S	0.581	0.393	-0.423	0.466
Sr	0.549	0.544	0.341	0.046
TiO <sub>2</sub>	0.259	0.91	0.083	-0.036
Y	0.96	0.208	0.044	-0.013
Zn	0.614	-0.126	0.042	0.335
Zr	-0.358	0.882	-0.101	0.023

Table 56. Loading vector values for the Hammeh Smelting System, PC1 - PC4. Values were calculated with statistical software package SPSS 12.

## APPENDIX 4. GLOSSARY OF THE MATERIAL SCIENCE OF IRON

This glossary is based on those presented by Rostoker and Bronson (Rostoker and Bronson 1990, 211-217), Tylecote (Tylecote 1987, xix-xv), Pleiner (Pleiner 2000, 287-302) and that available on the Materials Science on CD-ROM version 2.1 (MATTER 2000). It has been adjusted and expanded where necessary.

### A

#### Air Blast

In most kinds of smelting furnaces the air necessary for combustion must be forced into the combustion zone under pressure. This pressurised air, supplied by bellows or other blowing devices, is called the air blast. See also *hot blast*.

#### Accuracy

The degree of conformity of a measured or calculated value to its actual or specified value.

##### *Related entries:*

Precision

#### Alloy

A metal-like substance produced by mixing two or more metals or non-metals. Ceramics can also be mixed to form alloys.

A binary alloy contains two components.

A ternary alloy contains three.

##### *Related entries:*

Component

#### Annealing

A heat treatment designed to soften a metal or alloy. Microstructurally, annealing is associated with recovery, recrystallisation and/or grain growth.

##### *Related entries:*

Grain growth

Recovery (Microstructure)

Recrystallisation

#### Atomic Absorption Spectrometry

##### (AAS)

Laboratory analysis used to define the constituents of an ore or slag. In

AAS, the sample is atomised - *ie* converted into ground state free atoms in the vapour state - and a beam of electromagnetic radiation emitted from excited lead atoms is passed through the vaporised sample. Some of the radiation is absorbed by the atoms in the sample.

The greater the number of atoms there is in the vapour, the more radiation is absorbed. The amount of light absorbed is proportional to the number of lead atoms. A calibration curve is constructed by running several samples of known lead concentration under the same conditions as the unknown. The amount the standard absorbs is compared with the calibration curve and this enables the calculation of the lead concentration in the unknown sample.

Consequently an **atomic absorption** spectrometer needs the following three components: a light source; a sample cell to produce gaseous atoms; and a means of measuring the specific light absorbed.

#### Auger electron

An Auger electron has characteristic energy related to the electronic transitions within the atom which have caused it to be emitted. Emission of an Auger electron is an alternative to the emission of a characteristic X-ray. The energy of an Auger electron,  $E_A$ , is given by  $E_A = E_1 - E_2 - E_3$ , where  $E_1$  = energy of atom with inner-shell vacancy,  $E_2$  = energy of atom with outer-shell vacancy, and  $E_3$  = binding energy of emitted (Auger) electron.

##### *Related entries:*

Auger emission example

Binding energy

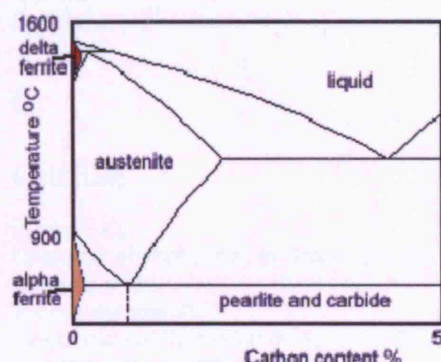
Characteristic X-ray

Inner-shell

#### Austenite

One of the allotropes of iron, also known as gamma iron. It is formed when iron is between 912 °C and 1,394 °C and has a face-centred

cubic structure. Also found in carbon steel. Austenite is a component of stainless steel used for making cutlery, hospital and food-service equipment, and tableware.



**Related entries:**

Allotropy  
Austempering  
Ferrite

## B

### Backscattered electron

A backscattered electron is a high energy primary electron which suffers large angle (> 90°) scattering and re-emerges from the entry surface of a specimen. Backscattered electrons usually have energies close to that of the primary electron beam. They are of greatest interest to SEM users, giving surface sensitive information.

**Related entries:**

Primary electron  
Secondary electron

### Bainite

A non-equilibrium phase, usually in steel, which is formed by quenching from the austenite phase. The rate of quenching required is slower than that necessary to form martensite but faster than that which produce the equilibrium phase of pearlite. The mechanism of formation is a displacive i.e. diffusionless transformation. Two types of bainite are recognised; upper and lower. Upper bainite forms at higher temperature and consequently the carbon present has sufficient to diffuse out forming carbides outside the bainite laths. Lower bainite forms at lower temperature and contains carbides within the laths as the carbon cannot diffuse out rapidly enough.

**Related entries:**

Martensite  
Pearlite  
Steel

### Billet

A well-consolidated iron bloom, suitable for making a bar.

### Bloom

Note the very different use of these terms in modern metallurgy!!

An ingot is rolled to produce a bloom, about 250 mm square, but much longer and slimmer than a slab. It would be the intermediate product for a much longer rolled product.

**Related entries:**

Bar  
Billet  
Ingot  
Rod  
Slab

### Bog Ore

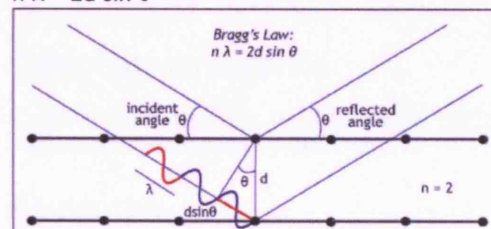
A limonite ore formed in swamps.

### Bond

As applied to atoms, the mechanism by which two (or more) atoms are held together. The mechanism is always reliant on some electron process. Common types include covalent, ionic, metallic and van der Waals.

### Bragg's law

$$n \lambda = 2d \sin \theta$$



Where  $n$  = number of wavelengths in the path length,  $\lambda$  = the wavelength,  $d$  = interatomic distance,  $\theta$  = the reflected (and incident) angle.

**Related entries:**

Diffraction

### Bremsstrahlung

This is the name given to background X-rays in any electron-generated X-ray spectrum. (German for braking radiation.)

### Brittle

A brittle material has a tendency to fracture by brittle fracture, in which there is no significant plastic deformation and where fracture occurs

by crack propagation. A brittle material has a low fracture toughness.

**Related entries:**

Cleavage  
Ductile

## C

### Calcium

Symbol: Ca

Chemical element, Ca, in Group II of the periodic table.

Atomic number 20

Electronic configuration is:  $1s^2 2s^2 2p^6 3s^2 3p^4 4s^2$

It is the most abundant metallic element in the human body (2%) and the fifth most abundant element in the Earth's crust (3.64%).

In ferrous metallurgy used as a deoxidiser and desulphuriser.

**Related entries:**

Desulphurization

### Carbide

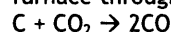
A compound of carbon and one or more metals.

### Carbon monoxide

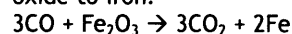
Symbol: CO

A highly toxic, colourless, and odourless gas, CO.

In ferrous metallurgy produced in the blast furnace through the reaction:



and acts as reducing agent converting iron(III) oxide to iron.



### Carburisation

By heating a ferrous material in a carbon rich atmosphere such as carbon dioxide or methane, the carbon potential can be sufficient to cause adsorption of carbon at the surface of the material, making the surface harder.

Decarburisation is the reverse, when the material is heated in a carbon depleted atmosphere in order to remove carbon from the material

### Cast

To give a shape to a metal/alloy by pouring in liquid form into a mould and letting solidify.

**Related entries:**

Casting

### Cast iron

Iron containing 2-4% carbon. As its name suggests, cast iron has excellent casting properties. It can be strong, but brittle compared to most steels.

**Related entries:**

Grey cast iron

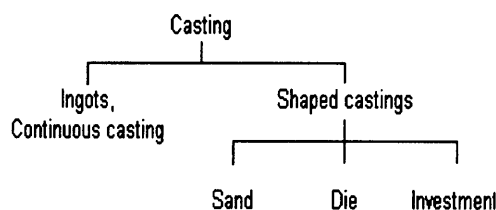
Steel

White cast iron

### Casting

Fabrication technique in which a molten material is poured into a mould cavity. **Shaped castings** provide finished or nearly-finished products. **Ingots** and **continuous castings** are subsequently processed. Shaped castings are often used for complicated shapes:

- where quality and strength are not critical;
- for low-ductility materials;
- as an economical alternative to other fabrication processes.



**Related entries:**

Ductility

### Cathodoluminescence

Cathodoluminescence is the emission of light in response to irradiation by electrons

### Cementite

Iron carbide,  $Fe_3C$ . Harder and stronger than ferrite, but not as malleable

### Ceramic

A predominantly ionic bonded material made up of metallic anions and non-metallic cations. Commonly have very high melting temperatures due to the strong ionic bonds, and high stiffness due to a strong resistance to dislocation movement. However, also have a low toughness and are therefore brittle.

**Related entries:**

Brittle

Melting point

## Chalcedony

Formula:  $\text{SiO}_2$

Hardness: 7

A variety of Quartz

A fibrous cryptocrystalline variety of Quartz.

When it is concentrically banded (often in rather wild patterns) it is called by the subvariety name "agate." When it is in flat layers/bands it is called by the subvariety name "onyx."

## Characteristic X-ray

A characteristic X-ray can be emitted from an excited atom when an outer-shell (e.g. L) electron jumps in to fill an inner-shell (e.g. K) vacancy. It has an energy characteristic of the atom and can therefore be used for analytical purposes. Its energy is the difference between the energies of the atom with an inner-shell vacancy and the same atom with an outer-shell vacancy.

The emission of the excess energy when an atom de-excites (decays or relaxes) can alternatively be achieved by the production of an Auger electron.

### *Related entries:*

Auger electron

Decay

Excited

Inner-shell

## Chill zone

A region formed during the solidification of a metal. The chill zone is the outer zone that solidifies first, and consists of fine, randomly oriented grains.

### *Related entries:*

Grain

## Cleavage

Fracture of a crystal along certain crystallographically determined planes, resulting in a smooth and shiny fracture surface, although the cleavage plane may change over the fracture surface.

### *Related entries:*

Brittle

Cleavage plane

## Cleavage plane

A plane through a material along which it splits most easily. Usually requires some form of lattice, with relatively few bonds across that particular plane.

### *Related entries:*

Cleavage

## Coherent radiation

Radiation is said to be coherent if its photons are in phase. This concept can be applied to any radiation and thus to any particles, such as electrons, which show wave properties.

### *Related entries:*

Photon

## Component

Also Constituent.

The individual chemical substances (elements or compounds) present in an alloy system.

The components in carbon steel are Fe and C. In bronze they are Cu and Sn.

### *Related entries:*

Alloy

Constituent

## Composite material

A solid material which consist of a combination of two or more constituents, in which the individual components retain their separate identities. The term composite often implies that the physical properties are improved since the main interest technologically is in obtaining materials with superior physical (usually mechanical) properties to those of the composite's component materials

## Composition

The nature and proportions of individual elements present in a system (alloy, phase, etc.). The units of composition vary depending on the situation, and include:

- mole fraction
- atomic fraction
- weight/mass fraction
- weight/mass percentage

It is important therefore to include units when quoting compositions.

### *Related entries:*

Alloy

Phase

## Conchoidal fracture

A mineral's habit of fracturing to produce curved surfaces like the interior of a shell (conch). This is typical of glass and quartz.



## Constituent

Component of an alloy or other chemical substance.

### Related entries:

Alloy  
Component

## Constitution

The constitution of an alloy is described by three parameters:

- (a) The phases present
- (b) The composition of each phase
- (c) The proportion of each phase

The properties of a material are determined to a large extent by its constitution. The other important features are the scale and morphology of the phases.

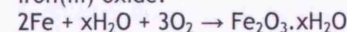
### Related entries:

Alloy  
Composition  
Phase  
Phase morphology  
Proportion of phases  
Scale of microstructure

## Corrosion

The gradual wearing away by chemical action, usually of a metal.

Iron corrodes by forming red-brown hydrated iron(III) oxide.



The corrosion of iron is known as **rusting**.

## Crystal

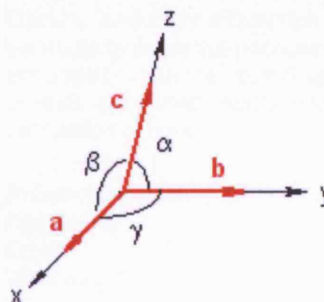
A crystal consists of identical structural units, consisting of one or more atoms, which are regularly arranged with respect to each other in space.

### Related entries:

Crystal axes  
Crystal plane  
Crystal system  
Crystallinity

## Crystal axes

The unit vectors which define the unit cell for a lattice give the x, y and z axes of the crystal, using a right handed rotation. The x-axis points in the direction of the **a** vector, the y-axis points in the direction of the **b** vector and the z-axis point in the direction of the **c** vector. The angles between the axes are  $\gamma$ ,  $\alpha$ , and  $\beta$ . The set of axes is not necessarily orthogonal.



### Related entries:

Crystal  
Lattice  
Unit cell  
Unit vector

## Crystal system

Every crystal belongs to one of seven crystal systems. Each system is defined in terms of the relative lengths of the unit vectors **a**, **b** and **c** of the lattice unit cell, as well as the angles between the vectors (see crystal axes).

The seven crystal systems are cubic, tetragonal, orthorhombic, trigonal, hexagonal, monoclinic and triclinic.

### Related entries:

Crystal  
Crystal axes  
Lattice  
Unit cell  
Unit vector

## Crystallinity

Non-polymeric solids are essentially 100% crystalline, whereas polymers only crystallise if the molecules have regular structures and then only do so to a limited extent. The extent of crystallinity is often called the degree of crystallinity and is typically 30-80%. The remaining material is amorphous.

Crystallinity has a profound effect on mechanical properties of polymers. As degree of crystallinity increases, so do the modulus, yield and tensile strength, hardness and softening point.

### Related entries:

Amorphous polymer  
Hardness  
Polymer  
Strength  
Young modulus

## Crystallization

Crystallization occurs when a saturated solution is cooled.



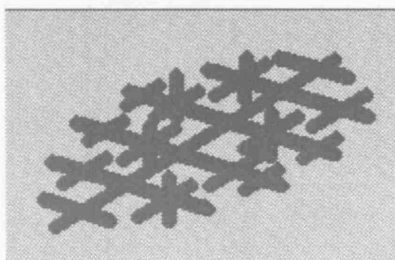
If the solution contained two solutes the one which is least soluble will crystallize first leaving the other in solution.

Slow cooling produces the largest and purest crystals. Often seeding is employed to enhance the crystallization process

## D

### Dendrite

When metallic phases form during solidification, they often do so along certain preferred directions that relate to their crystal structure. The resultant tree-like structures are called dendrites.



#### Related entries:

Crystal  
Phase

### Density

Symbol:  $\rho$

Units:  $\text{kg/m}^3$  or  $\text{g/cm}^3$

A material property giving the ratio of mass to volume. Typical densities of a range of engineering materials are given below:

Material	$\rho$ ( $\text{kg m}^{-3}$ )
Copper	8960
Nickel	8900
Iron	7870
Zinc	7140
Aluminium	2700
Glass	2500
Concrete	2400
UPVC	1700
Wood	750

### Diffraction

Diffraction is an interference effect which leads to the scattering of strong beams of radiation in specific directions. Diffraction from crystals is described by the Bragg Law:  $n\lambda = 2d \sin \theta$

- where  $n$  is an integer (the order of scattering),
- $\lambda$  is the wavelength of the radiation,
- $d$  is the spacing between the scattering entities (e.g. planes of atoms in the crystal)
- and  $\theta$  is the angle of scattering.

Electron and X-ray diffraction are both particularly powerful because their wavelengths are smaller than the typical spacings of atoms in crystals and strong, easily measurable, diffraction occurs.

#### Related entries:

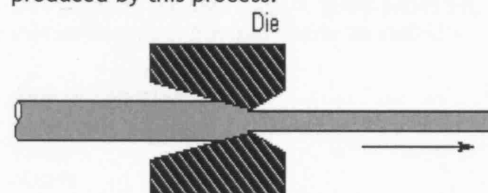
Bragg's law  
Crystal  
Wavelength

### Diffraction pattern

A diffraction pattern is the recording, usually on film, of the diffracted beams from a sample

### Drawing

A metal-forming operation in which a piece of metal is pulled through a die in order to reduce the cross-section. Rod, wire and tubing are all produced by this process.



### Ductile

A ductile material is capable of undergoing large plastic (permanent) strains before fracture.

#### Related entries:

Brittle  
Diffraction pattern

### Ductility

The degree to which a material can be **plastically** deformed before failure. The two most important measures of ductility are percentage elongation (%el) and percentage reduction in area (%RA).

#### Related entries:

% elongation  
Ductile  
Ductile failure  
Plastic deformation

## E

### Elastic deformation

Change in shape of a material subject to an applied stress in which the initial shape is completely recoverable with negligible time delay when the stress is removed. The work

done in elastically deforming a material is completely recoverable.

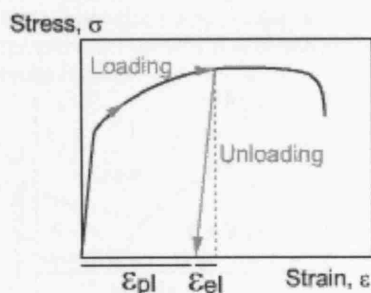
**Related entries:**

Elastic strain  
Plastic deformation

## Elastic strain

Symbol:  $\epsilon_{el}$

The portion of the overall strain that is recovered when an applied load causing the strain is removed.



**Related entries:**

Elastic deformation  
Plastic strain  
Strain

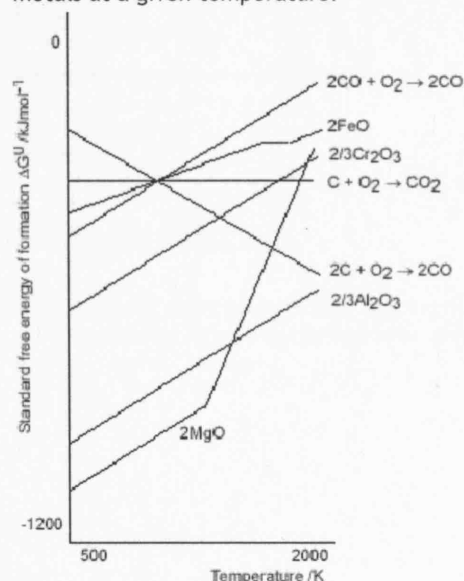
## Electron volt

Abbrev: eV

Unit of energy, value  $1.602 \times 10^{-19}$  J.

## Ellingham diagram

A plot of temperature against free energy of formation of oxides. Used to predict whether a certain redox reaction will occur in extraction of metals at a given temperature.



## Epoxy

A thermoset polymer made from epichlorhydrin and bisphenol-A. Properties include a low shrinkage on polymerisation, good adhesion, chemical resistance and mechanical and electrical strength. Useful as a structural material, surface coatings, adhesives, and for non-electrical parts of electronic components.

**Related entries:**

Epoxy resins  
Polymer  
Thermoset

## Epoxy resins

Thermosetting polymers derived from epichlorhydrin and bisphenol-A. Widely used as structural plastics, and as the matrix for composite materials. Characterised by low shrinkage on polymerization, good adhesion, mechanical strength and chemical stability.

**Related entries:**

Composite material  
Epoxy  
Matrix  
Polymer  
Strength  
Thermoset

## Equilibrium

Equilibrium is said to exist when, at a given, constant temperature (and pressure), THERE IS NO FURTHER TENDENCY FOR A REACTION TO TAKE PLACE (phase, chemical, etc.), i.e. the driving force for the reaction,  $\Delta G = 0$ .

In the case of phase diagrams, the equilibrium constitution is that which is stable for the particular combination of alloy composition and temperature.

**Related entries:**

Composition  
Constitution  
Phase

## Etching

Used in micrography, etching is the attack of a highly polished surface with a chemical that has a differential effect on different areas of the sample. Different chemicals are used for different samples.

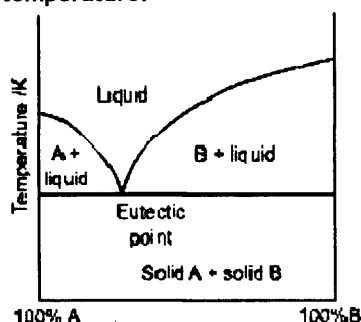
Removing coatings from a surface in preparation for the deposition of another coating, eg paint.

## Eutectic

The mixture of a two or more substances which liquefies at the lowest temperature of all such mixtures.

Whenever a liquid mixture of 2 miscible substances is cooled, one component will begin to separate in its solid form.

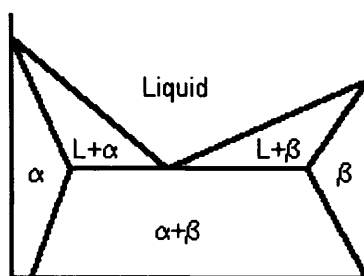
As this component separates, the remaining liquid continuously becomes richer in the other component, until, eventually, the composition of the liquid reaches a value at which both substances begin to separate simultaneously as an intimate mixture of solids. This composition is the **eutectic composition** and the temperature at which it solidifies is the **eutectic temperature**.



## Eutectic reaction

A three-phase reaction in which, upon cooling, a liquid transforms to give two solid phases.

e.g:  $L \rightarrow \alpha + \beta$



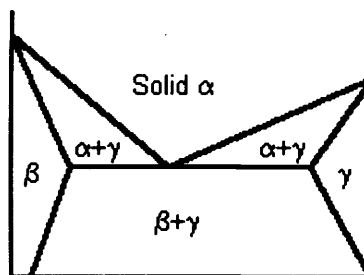
**Related entries:**

Phase

## Eutectoid reaction

A three-phase reaction in which, upon cooling, a solid transforms to give two other solid phases,

e.g:  $\alpha \rightarrow \beta + \gamma$



**Related entries:**

Phase

## Excited

An atom or electron is said to be excited if it has an energy greater than its ground state. When an electron is promoted from a low energy to a higher energy state or band the atom becomes excited.

**Related entries:**

Ground state

## F

### Feldspar

A group of aluminosilicate minerals, usually containing potassium, sodium or calcium. Feldspars constitute the most common type of mineral in the earth's crust. Most Feldspars have monoclinic or triclinic crystal structures. Solid solution series exist between several members.

**Related entries:**

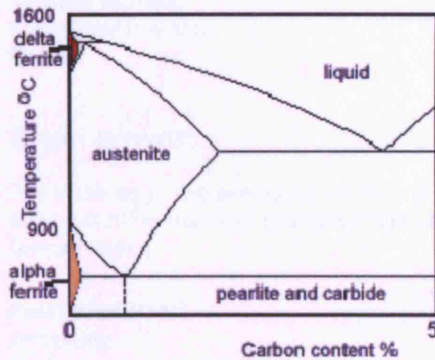
Crystal

Monoclinic

Solid solution

### Ferrite

Pure iron up to 912 °C has a bcc structure and is known as alpha ferrite. Between 1394 °C and the melting point of iron the bcc structure is now known as delta ferrite. Also found in carbon steel.



## Ferrites

Brittle, polycrystalline, ceramic-like materials, usually gray or black with magnetic properties that are useful in many types of electronic devices. Ferrites have the formula  $M(Fe_xO_y)$  where M could be a divalent metal such as barium, cobalt, copper, iron, manganese, magnesium or nickel. The most common ferrite is magnetite (lodestone, or ferrous ferrite),  $Fe(Fe_2O_4)$ .

Ferrites exhibit ferrimagnetism, which is weaker than the ferromagnetism found in iron, cobalt, and nickel. In ferrites the magnetic moments of constituent atoms align themselves in two or three different directions.

The most important properties of ferrites include high magnetic permeability (useful in antennae) and high electrical resistance (for use in transformer cores).

## Ferrous

Being or containing divalent iron, e.g. ferrous sulphate, also called iron(II) sulphate. Ferrous metallurgy refers to the metallurgy of iron whereas non ferrous metallurgy would include the metallurgy of copper, aluminium, etc.

## Flux

In metallurgy, a flux is any substance introduced in the smelting of ores to promote fluidity, to remove objectionable impurities in the form of slag, and to lower the melting point of metals and minerals. Examples are siliceous or calciferous components that, according to the composition of the ore, may be added to the charge. Intentional lime fluxes were exceptional in bloomery technology, silica could be added in case of high grade iron ores.

Old bloomery slag with a high FeO content can potentially be used as a flux as well.

Sand flux (fine quartz) was used to remove hammerscale during forging by melting to fayalitic slag.

### Related entries:

Slag

## Forging

A metal-forming operation in which the workpiece is deformed between a hammer and an anvil.

## Fusion welding

Fusion welding involves the melting of metal by the application of heat.

Gas (oxy-acetylene process) welding, arc welding, and resistance (spot) welding all appeared at the end of the 19th century. More recent developments are: electron-beam welding, laser welding, and several solid-phase processes such as diffusion bonding, friction welding, and ultrasonic joining.

### Related entries:

Acetylene

Arc welding

Friction welding

Spot welding

## G

### Glass

An amorphous, non-equilibrium or metastable, structure of a material, characterised as having a transition temperature which is altered by changes in the cooling rate of the liquid. Glasses lack the long range order of a crystal. They effectively retain the disorder of the liquid from which they were obtained.

### Grain

In metallurgy this refers to any of the small randomly distributed crystals of varying sizes that compose a solid metal. The grains contact each other at surfaces called grain boundaries. The structure and size of the grains determine important physical properties of the solid metal. Forming modifies the grains of a metal ingot to improve the mechanical properties in the direction of grain length. Internal stresses at grain boundaries may be relieved by annealing to restore ductility in certain alloys or to harden other alloys.

### Related entries:

Annealing

Forming

Grain growth

### Grain boundary

Zone formed at the junction of individual crystals in a polycrystalline material. Impurities tend to accumulate here by being excluded from normal growth of each crystal.



**Related entries:**

Anti-phase boundary  
Crystal

**Grain growth**

The increase in the average grain size of a polycrystalline material that occurs at elevated temperatures.

**Related entries:**

Annealing  
Grain  
Recovery (Microstructure)  
Recrystallisation

**Grey cast iron**

Cast iron that contains more than 4.3wt% carbon equivalent. This results in the formation of graphite flakes in the resultant microstructure. The combination of these with the lighter coloured remainder of the casting results in an observed grey colour. Grey cast irons are generally brittle due to the presence of the graphite flakes which act as cracks.

**Related entries:**

Cast iron  
White cast iron

**Ground state**

The ground state of an atom is the state in which all the localised electrons adopt the states of lowest possible energy. The ground state is usually considered to be the lowest energy stable reference state compared with which higher energy atoms are said to be excited.

**Related entries:**

Excited  
Localised electron

**H****Heat treatment**

This is the way to produce particular microstructures and properties in steel. The temperatures, holding times, and heating and cooling rates are chosen according to the chemical composition, size, and shape of the steel.

Steel is first heated, then quenched (cooled) and finally tempered (re-heated at a lower temperature). Common quenching media are air, oil, water and salt brine.

Each part of the process is carried out in a uniform manner in order to avoid warping, disortion and residual stresses in the steel

**Hydrogen**

Symbol: H

Colourless, odourless, tasteless, flammable gas.

It contains only one proton and one electron.

Atomic number 1

Electronic configuration is: 1s

Although hydrogen is the most abundant element in the Galaxy, the earth's crust is about 0.14 percent hydrogen by mass. It is present in water, petroleum and all animal and vegetable matter.

The main uses of hydrogen are in the manufacture of ammonia and in the hydrogenation of carbon monoxide and organic compounds.

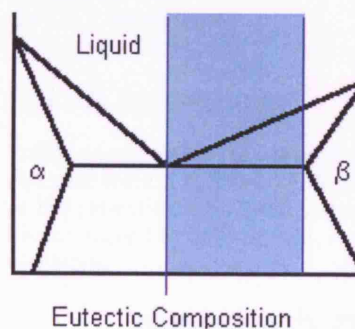
Deuterium (with one neutron) making 0.0156 percent of normal hydrogen; and tritium (with two neutrons) (radioactive but of negligible amounts) are isotopes of hydrogen.

**Related entries:**

Ammonia  
Carbon monoxide

**Hypereutectic**

Alloys having a composition GREATER than that of the eutectic alloy are described as hypereutectic.



(Compare Hypoeutectic.)

**Related entries:**

Alloy  
Composition  
Hypoeutectic

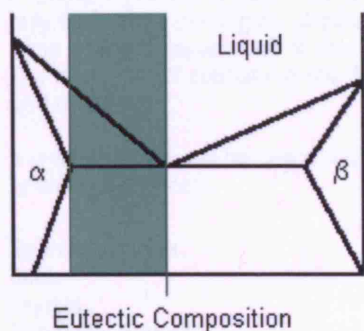
**Hypereutectoid**

Alloys having a composition greater than that of the eutectoid alloy are described as hypereutectoid. Note the difference between eutectic and eutectoid: eutectoid applies to solid state transformations whereas eutectic applies to liquid - solid transformations.

**Related entries:**  
Hypoeutectoid

## Hypoeutectic

Alloys having a composition less than that of the eutectic alloy are described as hypoeutectic.



**Related entries:**  
Alloy  
Composition  
Hypereutectic

## Hypoeutectoid

Alloys having a composition less than that of the eutectoid alloy are described as hypoeutectoid.

**Related entries:**  
Hypereutectoid

## I

### Ingot

Conveniently sized lump cast from molten metal. The shape varies according to practice.

**Related entries:**  
Bar  
Billet  
Bloom

### Interstitial

A crystal lattice is composed of approximately spherical atoms or ions between which there are holes. Another smaller atom or ion fitting into these holes would be described as an interstitial atom or ion.

### Isopach

Geological term, indicating a contour that connects points of equal thickness. Commonly, the isopachs, or contours that make up an isopach map, display the stratigraphic thickness of a rock unit as opposed to the true vertical

thickness. Isopachs are true stratigraphic thicknesses; i.e., perpendicular to bedding surfaces.

### Isotropic

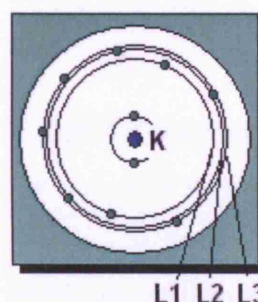
Having uniform physical properties, such as elastic constants, in all directions.

**Related entries:**  
Anisotropic

## K

### K, L, M details

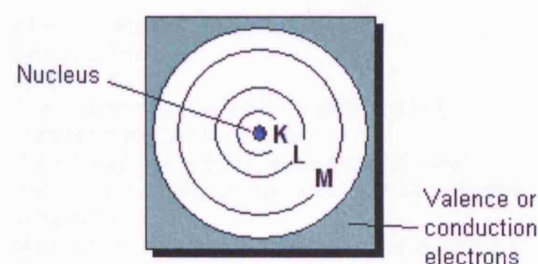
Each L, M or higher shell contains several electron states. These are called L1, L2, L3, M1, M2... etc. It is better in many ways to use the spdf terminology for these states.



**Related entries:**  
s, p, d, f terminology

### K, L, M terminology

This is a well-established way of referring to the electron states localised on an atom. At the simplest level, the K, L and M shells can be considered to hold up to 2, 8 and 18 electrons.



**Related entries:**  
K, L, M details  
Localised electron

## L

### Lattice

A lattice is an array of points in space, in which the environment of each point is identical.

A lattice is the set of points upon which a crystal may be built by placing an identical basis, in the same orientation, on each of the lattice points. The lattice itself consists of nothing other than a grid of points.

A crystal lattice can be described in terms of its symmetry elements.

**Related entries:**

Basis  
Crystal  
Symmetry element

### Lime

The common name for calcium oxide, CaO

### Limestone

The common name for a rock composed of calcium carbonate, CaCO<sub>3</sub> of organic origin such as shells.

In a furnace it is decomposed by heat into calcium oxide (lime).



**Related entries:**

Lime

### Liquidus

The liquidus is the phase boundary which limits the bottom of the liquid phase field.

In other words, at each composition above the liquidus line, the alloy is completely liquid.

**Related entries:**

Alloy  
Composition  
Liquidus temperature

### Liquidus temperature

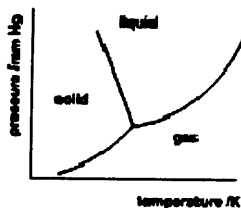
Symbol:  $T_{\text{liq}}$

Units: K (or °C, °F)

The temperature ABOVE which a substance is completely LIQUID.

**Related entries:**

Liquidus  
Solidus temperature



## M

### Martensite

Very rapid cooling (quenching) of steel (at about 1,000° C per minute) produces a new microstructure, martensite. It is the hardest and most brittle form of steel. Subsequent reheating to about 400° C and holding it for a time (tempering) produces a strong and tough steel with lower hardness and brittleness.

**Related entries:**

Bainite  
Pearlite  
Steel

### Materials Science

The study of the properties of solid materials and how those properties are determined by a material's composition and structure. It grew out of an amalgam of solid-state physics, metallurgy, and chemistry.

### Matrix

The component of a composite material in which the fibres are embedded.

**Related entries:**

Composite material  
Stress

### Melting point

Also: Melting temperature

Symbol:  $T_m$

Units: K, °C

The temperature at which a solid starts to transform to the liquid state.

Pure crystalline metals, eutectic alloys and many intermetallic compounds melt at a specific temperature.

Most alloys melt over a range of temperatures. Glasses have no well-defined melting temperature.

**Related entries:**

Alloy  
Intermetallic compound



## Metallurgy

Looks at the extraction of metals from their ores and how properties of metals are modified for everyday use. It includes the chemical, physical, and atomic properties and structures of metals and studies how metals are mixed to form alloys.

## Metastable

An equilibrium state which is a local minimum only. Upon excitation a system may transform to a lower energy state which may be a global minimum (or may be another metastable state).

## Micron

Also: Micrometre  
 $10^{-6}$  m

## Mineral

A naturally occurring inorganic solid that possesses an orderly internal structure and a definite chemical composition.

## Miscibility of components

The extent to which alloy components are miscible in the solid state depends on the interaction between the two atoms:

- Species that repel each other tend to form separate phases with limited miscibility.
- Conversely, those with strong mutual attraction will order themselves into intermetallic compounds.
- Components which are indifferent to one another will mix freely and this leads to a wide range of compositions over which solid solutions are formed.

### Related entries:

Component  
 Composition  
 Intermetallic compound  
 Solid solution  
 Two-phase alloy

## N

## Noise

Noise is the unpredictable varying background on which a signal is superimposed.

### Related entries:

Signal

## Non-ferrous

Those industries and processes using metals other than iron, e.g. the aluminium, copper, tin, zinc industries.

## O

## Olivine

Group of minerals of the basic structure  $X_2SiO_4$ , where X can be Mg, Fe or Ca. Different olivine minerals are:

- Olivine,  $(Mg, Fe)_2SiO_4$ ,
- Forsterite  $Mg_2SiO_4$ ,
- Calcio-Olivine  $(Mg, Ca)_2SiO_4$

## Ore

A mineral containing, e.g. a metal, for which it is mined and worked. Common ores are haematite, magnetite.

## Oxide

Formed by reaction of an element with oxygen. In steelmaking oxides are often referred to, e.g.

- many ores of iron contain iron(III) oxide as the essential chemical;
- stainless steel has a protective coating of chromium(III) oxide;
- carbon monoxide reduces iron(III) oxide;
- calcium oxide (lime) and silicon dioxide (silica) combine to form slag;

### Related entries:

Slag

## Oxygen

A nonmetallic chemical element of Group VI of the periodic table.

Atomic number 8

Electronic configuration is:  $1s^2 2s^2 2p^4$

Gaseous oxygen,  $O_2$ , is a colourless, odourless, tasteless gas. It is the most abundant element in the Earth's crust; it occupies 20.8% by volume of the atmosphere. It is essential for combustion and breathing. It forms oxides when reacting with both metallic and non-metallic elements.

## P

## Pearlite

When steel is cooled at the rate of about 400° C per minute austenite crystals change into pearlite (a fine lamellar structure of alternating platelets of ferrite and iron carbide) at about 727° C. Faster cooling produces martensite.

**Related entries:**

Austenite  
Bainite  
Ferrite  
Martensite  
Steel

**Phase**

A homogeneous, physically distinct portion of matter which can be mechanically separated from a mixture containing it.

Thus in a beaker of melting ice a solid phase (ice) and a liquid phase (water) can be seen.

**Phase 2**

A phase is a portion of a (alloy) system that is homogeneous in both its PHYSICAL and CHEMICAL properties.

A single phase can be made up of more than one component. Cu-Ni alloys for example solidify to give a single phase (solid solution).

Conversely, it is possible for a single component to exist as two phases - e.g. liquid and solid phases are in equilibrium at the melting temperature.

(Compare Phase Region.)

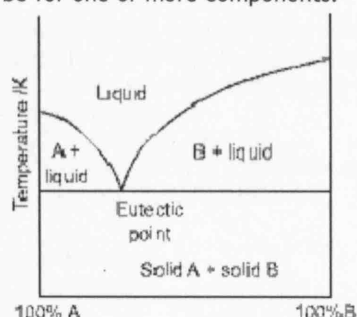
**Related entries:**

Alloy  
Component  
Equilibrium  
Phase region  
Solid solution

**Phase diagram**

A phase diagram shows the limiting conditions of temperature and pressure or solubility and temperature under which two phases are in equilibrium with one another. In each area of the graph only one phase exists.

At the conditions indicated by the lines two phases are in equilibrium. Phase diagrams may be for one or more components.



A two component phase diagram is shown right. The regions A+liquid, B+liquid and solid show the conditions under which those components are stable.

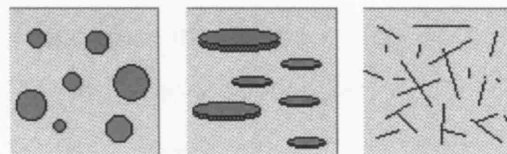
Complex mixtures may require 3D diagrams to adequately express all phases and their equilibria.

**Related entries:**

Eutectic  
Phase

**Phase morphology**

The shape of phases in a material. Together with constitution and scale, the phase morphology (globular, plate-like, rod-like, etc.) of a material is critical in determining its properties.

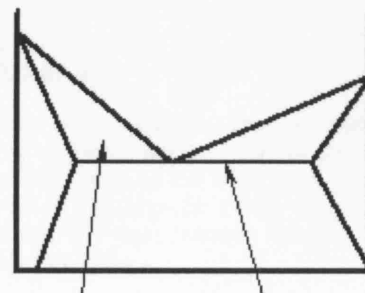
**Related entries:**

Constitution  
Scale of microstructure

**Phase region**

Also: Phase Field

An area of a phase diagram in which the same phase or phases are in equilibrium - in other words, the different regions between phase boundaries.



Phase Region      Phase Boundary

**Related entries:**

Equilibrium  
Phase

**Phosphorus**

Symbol: P

Phosphorus is a nonmetallic element of the nitrogen family (Group V of the periodic table).

Valency = 3.

Atomic number 15

Electronic configuration is:  $1s^2 2s^2 2p^6 3s^2 3p^3$

Its compounds are called phosphates, e.g. calcium phosphate..

It is a vital element in cell chemistry in the body, e.g. energy storage in adenosine triphosphate (ATP). Calcium phosphate is the principal inorganic constituent of teeth and bones.

In steelmaking phosphorus, having been converted into the acidic oxide  $P_4O_{10}$ , then combines with basic calcium oxide to form one of the ingredients of slag.

**Related entries:**

Slag

## Photon

A photon is a quantum of electromagnetic radiation - e.g. light or X-ray. It has no charge and zero rest mass.

Photons of light have energies in the range 1eV (infra red) to 4eV (ultra violet), while X-ray photons can have energies from a few eV (soft) to many tens of keV (hard).

**Related entries:**

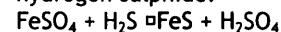
Light

## Porosity

Porosity is the presence of holes, space, or gaps inside a solid. Two main sources of porosity during casting are shrinkage and gas porosity. The first of these arises due to the volume contraction between solid and liquid, if additional liquid is not supplied to compensate then porosity will appear in the casting. Gas porosity occurs due to dissolved gas coming out of solution as the metal is cooled resulting in pockets of gas and consequently porosity in the solid. Porosity is generally undesirable as pores can act as crack nucleation points.

## Precipitation

Precipitation is the process in which an insoluble compound is formed by a chemical reaction, e.g. iron(II) sulphide from iron(II) sulphate and hydrogen sulphide.



For the separation of a soluble substance from solution see crystallization.

**Related entries:**

Crystallization

## Precision:

1. The degree of mutual agreement among a series of individual measurements, values,

or results; often, but not necessarily, expressed by the standard deviation.

2. With respect to a set of independent devices of the same design, the ability of these devices to produce the same value or result, given the same input conditions and operating in the same environment.
3. With respect to a single device, put into operation repeatedly without adjustments, the ability to produce the same value or result, given the same input conditions and operating in the same environment.  
**Synonym (1,2, and 3):** reproducibility.
4. The degree of discrimination with which a quantity is stated; for example, a three-digit numeral to the base 10 discriminates among 1000 possibilities

## Proportion of phases

The mass % of phase  $\alpha$  is given by:

$$M_{\alpha} = \frac{\text{mass of } \alpha \text{ phase}}{\sum \text{mass of each phase}} \times 100\%$$

NB. It is not possible to express the proportion of a phase in atomic %. This is because a phase, unlike a component, does not have an atomic mass. For this reason, many people prefer phase diagrams which have composition axes labelled in mass or weight percentage.

**Related entries:**

Component

Composition

Phase

## Pyroxenes

Group of silicate minerals that are closely related to each other in chemical composition and crystal form, of the basic form  $XYZ_2O_6$ , where X, Y and Z can be a wide range of elements. The most common form is  $(Ca,Mg,Fe)_2Si_2O_6$ .

## Q

### Quenching

Quenching is part of the heat treatment of steel. It is done by cooling the hot steel with one of a variety of cooling agents, such as oil, water, air, brine.

## R

### Radiation

- A. the process by which energy is emitted from a source and propagated through the surrounding medium, or

- B. the energy involved in this process.
- C. Radiant energy described in wave terms include sound; and light, a form of electromagnetic radiation. Differing from light only in wavelength are X-rays (from machines and deep space) and gamma rays from radioactive elements.
- D. Other types of radiation from radioactive elements include alpha and beta rays which are particles.

## Raw materials

These are the starting materials for an industrial process.

In some cases the term refers to substances obtained from the natural world, e.g. air, mineral ores, natural gas, petroleum, trees, and water.

In other cases the term refers to materials already processed from the above materials, e.g. iron as a raw material for the steel industry; ethene as starting material to make polyethene.

## Refractory

This is material which is not deformed or damaged by high temperatures. Thus it is used in various forms to line crucibles, incinerators and furnaces, or make insulation.

Depending on its use refractories are selected as acid, basic, or neutral. The most commonly used are magnesite and dolomite (basic) in open-hearth steel furnaces while fireclay (a mixture of silica and alumina) is acidic. Neutral carbon is used as the hearth of a blast furnace.

## S

### S, p, d, f terminology

The subshell descriptors s, p, d, f .. correspond to values of the orbital quantum number ( *l* ) of 0, 1, 2, 3 ... The correspondence between K, L, M terminology and spdf is thus:

K	1s (where 1 is the principal quantum number)
L1	2s
L2, L3	2p
M1	3s
M2, M3	3p
M4, M5	3d etc.

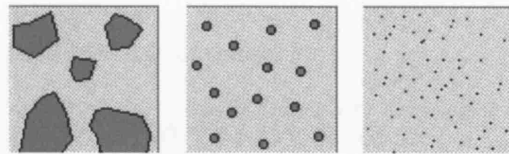
#### Related entries:

K, L, M terminology  
Orbital  
Quantum numbers

## Scale of microstructure

The scale of microstructure (nm,  $\mu$ m, mm, etc.) is one of the three most important factors that determine a material's properties.

The other two are constitution and phase morphology.



#### Related entries:

Constitution  
Phase morphology

## Scanning Electron Microscope

Also: SEM

A microscope in which a high energy, focused beam of electrons is used to scan the sample surface, ejecting secondary electrons that form the picture of the sample.

## Secondary electron

A secondary electron arises as a result of the interaction of a primary electron with a specimen. In principle the term refers to all electrons emitted from a specimen after it has been bombarded with primary electrons, X-rays or other radiation. In practice the phrase most commonly refers to low-energy electrons (kinetic energy less than 50eV) emitted from the specimen in a scanning electron microscope (SEM).

#### Related entries:

Auger electron  
Backscattered electron  
Primary electron

## Sintering

The process by which small particles coalesce to form larger masses, usually at high temperature. Occurs by a variety of mechanisms. Used for ceramics, powdered metals, and ores and concentrates.

## Slag

A by-product formed in smelting, welding, and other metallurgical and combustion processes from impurities in the metals or ores being treated. Slag consists mostly of salts formed by combination of basic oxides like calcium oxide (e.g. lime from limestone, ash, aluminium oxide) and acidic oxides of elements such as silicon, sulphur, and phosphorus.

Slag is less dense than metals so it floats on the surface of the molten metal, protecting it from oxidation by the atmosphere and keeping it clean.

Slag can be used to make certain concretes; is used as a road material and ballast and as a source of available phosphate fertilizer.

**Related entries:**

Lime  
Limestone  
Phosphorus  
Sulphur

## Solidus

The solidus is the phase boundary which limits the top of the solid phase field(s).

## Solidus temperature

Symbol:  $T_{sol}$   
Units: K (or °C, °F)  
Temperature BELOW which a substance is completely SOLID. (Values of  $T_{sol}$  are often better obtained from heating curves).

**Related entries:**

Liquidus temperature  
Solidus

## Spinel

Spinel is the name given to  $MgAl_2O_4$ , and is also the name given to the structure type of that mineral. Almost any can assume a spinel structure, important examples for iron metallurgy are  $Fe^{+3}[Fe^{+2}Fe^{+3}]O_4$ , or magnetite, and  $FeAl_2O_4$ , or hercynite.

## Steel

An alloy of iron, carbon and often several other elements. The amount of carbon is below 2% by mass - materials with higher levels are termed 'cast irons'. Steels in which carbon is the main alloying element are termed **carbon steels**. Those with significant concentrations of other elements are termed **alloy steels**.

**Related entries:**

Bainite  
Cast iron  
Martensite  
Pearlite

## Strength

A measure of a material's resistance to failure. It depends of details on how it is measured, specimen geometry and, for brittle materials, on the presence of flaws.

**Tensile Strength**, the maximum tensile force in the test divided by the original cross-sectional area.

**Shear Strength and Compressive Strength**, are equivalents of tensile strength in their respective loading modes.

## Sulphur

Symbol: S  
Element of atomic number 16.  
Its electronic configuration is:  $1s^2 2s^2 2p^6 3s^2 3p^4$   
Semi-metallic chemical element in the oxygen family (Group VI of the periodic table).

A small quantity of sulphur forms inclusions with e.g. manganese. These cause the steel to have decreased toughness perpendicular to the direction of rolling.

In steelmaking sulphur is removed from the blast furnace when its oxide combines with calcium oxide.

## Stringers

Small quantities of impurity that align into long threads (stringers) on rolling. These threads restrict grain movement so providing improved creep-strength.

## T

### Technical Ceramic

The term technical ceramic is used to describe ceramic material used for a technical purpose, e.g. furnace wall or tuyère material, as opposed to domestic pottery or other kinds of ware.

### Topography

Topography is the description of the surface features of a specimen.

### Toughness

The energy absorbed in tearing the metal. Toughness can be increased by heat treatment which produces more grain boundaries or fine precipitates. Cold working the metal, and alloying can also increase toughness.

### Transformation

The change of a phase into one or more different phases that are thermodynamically stable as governed by the phase diagram of the relevant system. Several general categories of phase transformation are recognised such as eutectic, eutectoid, peritectic, etc. which share common characteristics in all alloy systems.

## V

### Viscosity

Units:  $\text{N m}^{-2} \text{ s}$  or  $\text{Pa s}$ .

A measure of a material's resistance to flow when a mechanical stress is applied. Viscosity is quantitatively defined in terms of shear stress ( $\tau$ ) and shear rate ( $dy/dt$ ). The coefficient of viscosity ( $\eta$ ) is defined by:

$$\eta = \frac{\tau}{\left(\frac{dy}{dt}\right)}$$

**Related entries:**

Shear stress  
Stress

## W

### Wavelength

Symbol:  $\lambda$

Units:  $\text{m}$

The electron wavelength,  $\lambda$ , is related to electron energy via the de Broglie relationship. High-energy electrons have wavelengths which are a small fraction of interatomic spacings.

**Related entries:**

De Broglie equation

### White cast iron

A cast iron contains between 2 and 4 wt% carbon equivalent. This results in the carbon precipitating primarily as cementite, resulting in a microstructure consisting of cementite and pearlite. Cast irons are hard and brittle.

**Related entries:**

Cast iron  
Grey cast iron

### Work-hardening

The increase in strength and hardness (ie resistance to plastic deformation) produced by plastic deformation of metals at temperature below about  $0.5 T_m$ . It results from increasing numbers of dislocations and their entanglement and is accompanied by reduction in ductility.

**Related entries:**

Dislocation  
Plastic deformation  
Strength

## Wrought

Lit. "worked". (Material or product) shaped by one of a number of forming operations, including forging, rolling, extrusion and drawing. Such processes can be carried out at high temperatures ("hot-working") or low temperatures ("cold-working"), relative to the recrystallisation temperature. In addition to shape, the properties of the material can also be significantly altered. (c.f. casting)

**Related entries:**

Casting  
Drawing  
Forging  
Recrystallisation  
Rolling

## Wrought iron

Wrought iron contains less than 0.035 percent carbon. This high purity ensures good corrosion resistance. In structure it is classed as ferrite, but contains a little slag elongated into stringers by rolling. This reduces its strength and malleability.

**Related entries:**

Ferrite  
Stringers

## Wüstite

Iron monoxide  $\text{FeO}$  ( $\text{Fe}_x - 10$  or  $\text{Fe}_n\text{O}$ ). Can contain some  $\text{MnO}$ ,  $\text{MgO}$  or  $\text{NiO}$  as well. Wüstite is a phase in the reduction of iron ore, forming subsequently, combined with  $\text{SiO}_2$ , the fayalite. Excess wüstite appears in bloomery slags and slag inclusions, in carbon-poor parts of iron/steel as light crystals, also arranged as dendrites. Besides magnetite, it can also be a component in hammerscale.

- first generation wüstite: free  $\text{FeO}$  present in the original melt, in excess of that which will combine with silica to form fayalite, often precipitates as egg-shaped blobs
- second generation wüstite: remaining free  $\text{FeO}$  precipitating near the end of the slag solidification after formation of fayalite, usually forms in dendritic shapes.

Thinness of both generations of wüstite relates to initial temperature and cooling speed of the slag.

## X

### X-ray

Electromagnetic radiation of very short wavelength (0.01 to 100 nm) produced when an

electron hits a piece of metal in an evacuated tube.

## **X-ray diffraction**

Also: XRD

The atomic planes of a crystal cause an incident beam of X-rays (if wavelength is approximately the magnitude of the interatomic distance) to interfere with one another as they leave the crystal. The phenomenon is called X-ray diffraction.

(See Roentgen, von Laue)

### ***Related entries:***

X-ray



## REFERENCES

- al-Amri, Y.A.e.S. (1998) *Early Metallurgy in the Jordan Valley: a Case Study from Wadi Hamah*, Irbid, Jordan: Unpublished MA Thesis, Yarmouk University.
- Andersson, M.A.T., Jönsson, P.G. and Hallberg, M. (2000) Optimisation of Ladle Slag Composition by Application of Sulphide Capacity Model. *Ironmaking and Steelmaking* 27 (4), 286-293.
- Anguilano, L. (2002) *Analisi di Scorie di Smelting del Piombo Rinvenute in Laurium (Grecia) e Copa Hill (Galles)*, Milano: Università degli Studi di Milano, unpublished MSc thesis.
- Bachmann, H.-G. (1982) *The Identification of Slags from Archaeological Sites*, London: Institute of Archaeology; Occasional Publication 6.
- Barndon, R. (1996) Fipa Ironworking and its Technological Style. In: Schmidt, P.R. (Ed.) *The Culture and Technology of African Iron Production*, 58-73.
- de Barros, P.F.L. (1986) Bassar: A Quantified, Chronologically Controlled, Regional Approach to a Traditional Iron Production Centre in West Africa. *Africa* 56 (2), 148-174.
- de Barros, P.F.L. (1997) Ironworking in Its Cultural Context. In: Vogel, J.O. (Ed.) *Encyclopedia of Precolonial Africa (Archaeology, History, Languages, Cultures and Environments)*, 135-148.
- Begin, Z.B., Erlich, A. and Nathan, Y. (1974) Lake Lisan - The Pleistocene Precursor of the Dead Sea. *Geological Survey of Israel Bulletin* 63, 1-30.
- Bender, F.K. (1968) *Geologie Von Jordanien (Beiträge Zur Regionalen Geologie Der Erde, Band 7)*, Berlin: Gebrüder Borntraeger Verlagsbuchhandlung.
- Benedict, R. (1948) Anthropology and the Humanities. *American Anthropologist* 50 (4, Part 1), 585-593.
- Bienkowski, P. (2000) Transjordan and Assyria. In: Stager, L.E., Greene, J.A., and Coogan, M.D. (Eds) *The Archaeology of Jordan and Beyond; Essays in Memory of James A. Sauer*, 44-58. Winona Lake, Indiana: Harvard Semitic Museum/Eisenbrauns.
- Blanckenhorn, M. (1912) *Naturwissenschaftliche Studien Am Toten Meer Und Im Jordantal*, Berlin: Friedländer.
- Boas, F. (1940) *Race, Language, and Culture*, New York: MacMillan.
- van den Boom, G. and Lahloub, M. (1962) *The Iron-Ore Deposit 'Warda' in the Southern Ajlun District*, Hannover/Amman: Unpublished report, Federal Institute of Geoscience and Natural Resources, Hannover (Unveröffentlichte Bericht Deutsche Geologische Mission Jordanien, Archiv Bundesanstalt für Bodenforschung)/National Resources Authority, Amman.
- Brill, R.H. (1999) *Chemical Analyses of Early Glasses*, New York: The Corning Museum of Glass, New York.
- Buchwald, V.F. (1976) *Handbook of Iron Meteorites: Their History, Distribution, Composition and Structure*, Berkeley; London: University of California Press (for the Center for Meteorite Studies, Arizona State University).

- Buchwald, V.F. (1992) On the Use of Iron by the Eskimos in Greenland. *Materials Characterization* 29 (2), 139-176.
- Buchwald, V.F. (2001) *Ancient Iron and Slags in Greenland*.
- Buchwald, V.F. (2005) *Iron and Steel in Ancient Times*, Copenhagen: Det Kongelige Danske Videnskabernes Selskab.
- Buchwald, V.F. and Mosdal, G. (1985) *Meteoritic Iron, Telluric Iron and Wrought Iron in Greenland*.
- Buchwald, V.F. and Wivel, H. (1998) Slag Analysis As a Method for the Characterization and Provenancing of Ancient Iron Objects. *Materials Characterization* 40 (2), 73-96.
- Buhrke, V.E., Jenkins, R., and Smith, D.K. (1998) *Preparation of Specimens for XRF and XRD Analysis*, New York: Wiley/VCH.
- Bunimovitz, S. and Lederman, Z. (2003) Tel Beth Shemesh, 2001-2003. *Israel Exploration Journal* 53 (2), 233-237.
- Calvocoressi, D. and David, N. (1979) A New Survey of Radiocarbon and Thermoluminescence Dates for West Africa. *Journal of African History* 20 (1), 1-29.
- Childe, V.G. (1929) *The Danube in Prehistory*, Oxford: Oxford University Press.
- Childe, V.G. (1944) Archaeological Ages As Technological Stages. *Journal of the Royal Anthropological Institute* 74, 7-24.
- Childs, S.T. (1991) Iron As Utility or Expression: Reforging Function in Africa. In: Ehrenreich, R.M. (Ed.) *Metals in Society: Theory Beyond Analysis*, 57-67. Philadelphia: MASCA Research Papers in Science and Archaeology 8 (2), University of Pennsylvania Museum.
- Childs, S.T. (1994) Society, Culture, and Technology in Africa: An Introduction. In: Childs, S.T. (Ed.) *Society, Culture, and Technology in Africa*, 6-14. Philadelphia: MASCA Research Papers In Science and Archaeology 11, University of Pennsylvania Museum.
- Childs, S.T. and Herbert, E.W. (2005) Metallurgy and Its Consequences. In: Stahl, A.B. (Ed.) *African Archaeology: a Critical Introduction*, 276-301. Oxford: Blackwell.
- Childs, S.T. and Killick, D.J. (1993) Indigenous African Metallurgy: Nature and Culture. *Annual Review of Anthropology* 22, 317-337.
- Chirikure, S. (2002) *A Metallurgical Investigation of Iron Processing Remains From Nyanga, Northeastern Zimbabwe*, London: University College London, Institute of Archaeology, unpublished MA thesis.
- Chirikure, S. and Rehren, T. (2004) Ores, Furnaces, Slags, and Prehistoric Societies: Aspects of Iron Working in the Nyanga Agricultural Complex, AD 1300-1900. *African Archaeological Review* 21 (3), 135-152.
- Cleere, H.F. and Crossley, D.W. (1995) *The Iron Industry of the Weald*, Leicester: Leicester University Press.
- Coghlan, H.H. (1977) *Notes on Prehistoric and Early Iron in the Old World*, 2 edn. Oxford: Pitt Rivers Museum, Occasional Papers on Technology 8.

- Costin, C.L. (1991) Craft Specialization: Issues in Defining, Documenting, and Explaining the Organization of Production. In: Schiffer, M.B. (Ed.) *Archaeological Method and Theory*, 1-56. Tucson: University of Arizona Press.
- Costin, C.L. (1998) Introduction: Craft and Social Identity. In: Costin, C.L. and Wright, R.P. (Eds) *Craft and Social Identity*, 3-16. Arlington, VA: American Anthropological Association.
- Costin, C.L. (2001) Craft Production Systems. In: Feinman, G.M. and Price, T.D. (Eds) *Archaeology at the Millennium: A Sourcebook*, 273-327. New York: Kluwer Academic/Plenum Publishers.
- Costin, C.L. and Hagstrum, M.B. (1995) Standardization, Labor Investment, Skill, and the Organization of Ceramic Production in Late Prehispanic Highland Peru. *American Antiquity* 60 (4), 619-639.
- Costin, C.L. and Wright, R.P. (1998) *Craft and Social Identity*, Arlington, VA: American Anthropological Association.
- Coughenour, R.A. (1976) Preliminary Report on the Exploration and Excavation of Mugharet El Wardeh and Abu Thawab. *Annual of the Department of Antiquities of Jordan* XXI, 71-78.
- Coughenour, R.A. (1989) A Search for Manahaim. *Bulletin of the American Schools for Oriental Research* 273, 57-66.
- Craddock, P.T. (1995) *Early Metal Mining and Production*, Edinburgh: Edinburgh University Press.
- Craddock, P.T. and Hughes, M.J. (1992) *Furnaces and Smelting Technology in Antiquity*, London: British Museum.
- Crew, P. (2000) The Influence of Clay and Charcoal Ash on Bloomery Slags. In: Tizzoni, C.C. and Tizzoni, M. (Eds) *Il Ferro Nelle Alpi. Atti Del Convegno/Iron in the Alps. Proceedings of the Conference*, 38-48.
- Curtis, J.E., Stech-Wheeler, T., Muhly, J.D. and Maddin, R. (1979) Neo-Assyrian Ironworking Technology. *Proceedings of the American Philosophical Society* 123 (6), 369-390.
- David, N., Heimann, R.B., Killick, D.J. and Wayman, M.L. (1989) Between Bloomery and Blast Furnace: Mafa Iron-Smelting Technology in North Cameroon. *The African Archaeological Review* 7, 183-208.
- Dobres, M.-A. (2000) *Technology and Social Agency: Outlining a Practice Framework for Archaeology*, Oxford: Blackwell Publishers.
- Dobres, M.-A. and Hoffman, C.R. (1994) Social Agency and the Dynamics of Prehistoric Technology. *Journal of Archaeological Method and Theory* 1 (3), 211-258.
- Dobres, M.-A. and Hoffman, C.R. (1999) *The Social Dynamics of Technology: Practice, Politics, and World Views*, Washington D.C.: Smithsonian Institution Press.
- Dobres, M.-A. and Robb, J.E. (2000) *Agency in Archaeology*, London: Routledge.
- Docter, R.F. (2002) Carthage Bir Massouda: Excavations by the Universiteit Van Amsterdam (UVA) in 2000 and 2001. *Centre d'Etudes et de Documentation Archéologique de la Conservation de Carthage (CEDAC Carthage)* 21, 29-34.

- Docter, R.F. (in press) *Carthage. The Excavations at the Bir Massouda Site 2 Volume I*, Ghent: ARGU. Archaeological Reports Ghent University 4.
- Docter, R.F., Chelbi, F. and Telmini, B.M. (2003) Carthage Bir Massouda: Preliminary Report on the First Bilateral Excavations of Ghent University and the Institut National du Patrimoine (2002-2003). *BABesch. Annual Papers on Mediterranean Archaeology* 78, 43-70.
- Dornemann, R.H. (1983) *The Archaeology of Transjordan in the Bronze and Iron Ages*, Milwaukee, Wisconsin: Milwaukee Public Museum.
- Échard, N. (1983) *Métallurgies Africaines, Nouvelles Contributions*, Paris: Mémoires de la Société des Africanistes.
- Ehrenreich, R.M. (1985) *Trade, Technology and the Ironworking Community in the Iron Age of Southern Britain*, Oxford: BAR (British Series 144).
- Ehrenreich, R.M. (1991) Metalworking in Iron Age Britain: Hierarchy or Heterarchy? In: Ehrenreich, R.M. (Ed.) *Metals in Society: Theory Beyond Analysis*, 69-80. Philadelphia: MASCA Research Papers in Science and Archaeology 8 (2), University of Pennsylvania Museum.
- Finkelstein, I. (1998) The Great Transformation: the 'Conquest' of the Highlands Frontiers and the Rise of the Territorial States. In: Levy, T.E. (Ed.) *The Archaeology of Society in the Holy Land*, 2nd edn., 349-398. London: Leicester University Press.
- Finkelstein, I. (1999) State Formation in Israel and Judah - a Contrast in Context, a Contrast in Trajectory (Middle-Eastern Biblical Archaeology). *Near Eastern Archaeology* 62 (1), 35-52.
- Finkelstein, I. (2003) City-States to States: Polity Dynamics in the 10th-9th Centuries B.C.E. In: Dever, W.G. and Gitin, S. (Eds) *Symbiosis, Symbolism, and the Power of the Past: Canaan, Ancient Israel, and Their Neighbors From the Late Bronze Age Through Roman Palaestina. (Proceedings of the Centennial Symposium, W. F. Albright Institute of Archaeological Research and American Schools of Oriental Research, Jerusalem, May 29-31, 2000)*, 75-83. Winona Lake, Indiana: Eisenbrauns.
- Forbes, R.J. (1940-1963) *Bibliographia Antiqua: Philosophia Naturalis (10 Volumes)*, Leiden: E. J. Brill.
- Forbes, R.J. (1950) *Metallurgy in Antiquity*, Leiden: E. J. Brill.
- Forbes, R.J. (1964-1972) *Studies in Ancient Technology (9 Volumes)*, Leiden: E. J. Brill.
- Franken, H.J. (1969) *Excavations at Tell Deir 'Alla I: Stratigraphical and Analytical Study of the Early Iron Age Pottery*, Leiden: E. J. Brill.
- Friedman, E.S. (1995) *Technological Style in Early Bronze Age Anatolia*, Chicago: The Department of Near Eastern Languages and Civilizations, The University of Chicago, Unpublished PhD thesis.
- Frisch, B., Mansfeld, G., and Thiele, W.-R. (1985) *Kamid El-Loz 6, Die Werkstätten Der Spätbronzezeitlichen Paläste*, Bonn: Dr. Rudolf Habelt.
- Gardner, A. (2004) *Agency Uncovered: Archaeological Perspectives on Social Agency, Power, and Being Human*, London: UCL Press.
- Geselowitz, M.N. (1993) Archaeology and the Social Study of Technological Innovation. *Science, Technology, and Human Values* 18 (2), 231-246.

- Gille, B. (1978) *Histoire des Techniques*, Paris: Gallimard.
- Glueck, N. (1933) The Archaeological Exploration of El-Hammeh on the Yarmuk. *Bulletin of the American Schools for Oriental Research* 49, 22-23.
- Glueck, N. (1935) Tell El-Hammeh. *American Journal of Archaeology* 39 (3), 321-330.
- Glueck, N. (1951) *Explorations in Eastern Palestine IV*, New Haven: American Schools of Oriental Research.
- González de Canales Cerisola, F., Serrano Pichardo, L., and Llompart Gomez, J. (2004) *El Emporio Fenicio Precolonial De Huelva. Ca. 900-770 a.C.*, Madrid: Biblioteca Nueva, S.L.
- Gordon, R.B. and Killick, D.J. (1993) Adaptation of Technology to Culture and Environment: Bloomery Iron Smelting in America and Africa. *Technology and Culture* 34 (2), 243-270.
- Gordon, R.L. (1984) Telul Edh Dhahab Survey (Jordan) 1980 and 1982. *Mitteilungen der deutschen Orient-Gesellschaft zu Berlin [MDOG]* 116, 131-187.
- Gordon, R.L. and Villiers, L.E. (1983) Telul Edh Dhahab and Its Environs Surveys of 1980 and 1982. A Preliminary Report. *Annual of the Department of Antiquities of Jordan [ADAJ]* XXVII, 275-289.
- Goucher, C.L. and Herbert, E.W. (1996) The Blooms of Bandjeli: Technology and Gender in West-African Iron Making. In: Schmidt, P.R. (Ed.) *The Culture and Technology of African Iron Production*, 40-57. Gainesville, Florida.
- Grant, E. and Wright, G.E. (1939) *Ain Shems Excavations (Palestine): Part V (Text)*, Haverford, Pennsylvania: Haverford College.
- van Grieken, R. and Markowicz, A. (2002) *Handbook of X-Ray Spectrometry*, 2nd rev. and expanded edn. New York: Marcel Dekker.
- Hamilton, E.G. (1996) *Technology and Social Change in Belgic Gaul: Copper Working at the Titelberg, Luxembourg, 125 B.C.-A.D. 300*, Pennsylvania: MASCA research papers in science and archaeology 13, University of Pennsylvania Museum.
- Haudricourt, A.-G. (1962) Domestication des Animaux, Culture des Plantes et Traitement a'Autrui. *L'Homme* 2, 40-50.
- Haudricourt, A.-G. (1988) *La Technologie, Science Humaine: Recherche D'Histoire et d'Etnologie des Techniques*, Paris: Editions de la Maison des Sciences de l'Homme.
- Hegmon, M. (1992) Archaeological Research on Style. *Annual Review of Anthropology* 21, 517-536.
- Hegmon, M. (1998) Technology, Style, and Social Practices: Archaeological Approaches. In: Stark, M.T. (Ed.) *The Archaeology of Social Boundaries*, 264-279. Washington, London: Smithsonian Institution Press.
- Herbert, E.W. (1988) *Iron. Gender, and Power. Rituals of Transformation in African Societies. African Systems of Thought*, Bloomington, Indiana: Indiana University Press.
- Hjärthner-Holdar, E. and Risberg, C. (2003) The Introduction of Iron in Sweden and Greece. In: Nørbach, L.C. (Ed.) *Prehistoric and Medieval Direct Iron Smelting in Scandinavia and Europe. Aspects of Technology and Society: Proceedings of the*

- Sandbjerg Conference 16th to 20th September 1999*, 83-86. Aarhus: Aarhus University Press.
- Hosler, D. (1988) Ancient West Mexican Metallurgy: South and Central American Origins and West Mexican Transformations. *American Anthropologist* 90 (4), 832-855.
- Hosler, D. (1994) *The Sounds and Colors of Power: the Sacred Metallurgical Technology of Ancient West Mexico*, Cambridge, MA; London: MIT Press.
- Hughes, T.P. (1986) The Seamless Web: Technology, Science, Etcetera, Etcetera. *Social Studies of Science* 16 (2), 281-292.
- Hughes, T.P. (1987) The Evolution of Large Technological Systems. In: Bijker, W.E., Hughes, T.P., and Pinch, T.J. (Eds) *The Social Construction of Technological Systems: New Directions in the Sociology and History of Technology*, 51-82. Cambridge, MA: MIT Press.
- Humphris, J. (2004) *Reconstructing a Forgotten Industry: an Investigation of Iron Smelting in Buganda*, London: University College London, Institute of Archaeology, unpublished MA thesis.
- Ige, A. and Rehren, T. (2003) Black Sand and Iron Stone: Iron Smelting in Modakeke, Ife, South Western Nigeria. *IAMS journal* 23, 15-20.
- Ingo, G.M. and Scoppio, L. (1992) Small-Area XPS and XAES Study of Early Iron Metallurgy Slags. *Surface and Interface Analysis* 18 (7), 551-554.
- Ingo, G.M., Scoppio, L., Bruno, R. and Bultrini, G. (1992a) Microchemical Investigation of Early Iron Metallurgy Slags. *Mikrochimica Acta* 109 (5-6), 269-280.
- Ingo, G.M., Scoppio, L., Mazzoni, S., Mattogno, G. and Scandurra, A. (1992b) Application of Surface and Bulk Analytical Techniques for the Study of Iron Metallurgy Slags at Tell Afis (N/W Syria). In: Vandiver, P.B., Druzik, J.R., Wheeler, G.S., and Freestone, I.C. (Eds) *Material Issues in Art and Archaeology III*, 285-290. Pittsburgh, Pennsylvania: Materials Research Society.
- Joffe, A.H. (2002) The Rise of Secondary States in the Iron Age Levant. *JESHO* 45 (4), 425-467.
- Jones, D.M. (2001) *Archaeometallurgy*, Swindon: English Heritage Publications.
- Joosten, I. (2004) *Technology of Early Historical Iron Production in the Netherlands*, Amsterdam: Institute for Geo- and Bioarchaeology, Vrije Universiteit.
- Juleff, G. (1996) An Ancient Wind-Powered Iron Smelting Technology in Sri Lanka. *Nature* 379 (6560), 60-63.
- Juleff, G. (1998) *Early Iron and Steel in Sri Lanka: a Study of the Samanlawewa Area*, Mainz am Rhein: Zabern.
- Kense, F.J. (1985) The Initial Diffusion of Iron to Africa. In: Haaland, R. and Shinnie, P.L. (Eds) *African Iron Working: Ancient and Traditional*, 11-27. Oslo; New York; Oxford: Norwegian University Press; Oxford University Press.
- Khakutaishvili, N. (1976) A Contribution of the Kartvelian Tribes to the Mastery of Metallurgy in the Ancient Near East. In: Harmatta, J. and Komoroczy, G. (Eds) *Wirtschaft Und Gesellschaft in Vorderasien*, 337-348. Budapest: Akademiai Kiado.
- Khakutaishvili, N. (2001) Alte Eisenproduktion an Der Östlichen Schwarzmeerküste. In:

- Gambaschidze, I., Hauptmann, A., Slotta, R., and Yalçin, Ü. (Eds) *Georgien. Schätze Aus Dem Land Des Goldenen Vlies*, 182-185. Bochum: Deutsches Bergbau-Museum.
- Khouri, R.G. (1981) *The Jordan Valley: Life and Society Below Sea Level*, London, New York: Longman.
- Killick, D.J. (2004a) Social Constructionist Approaches to the Study of Technology. *World Archaeology* 36 (4), 571-578.
- Killick, D.J. (2004b) What Do We Know About African Iron Working? *Journal of African Archaeology* 2 (1), 97-112.
- Kingery, W.D. (1986) *Ceramics and Civilization: Technology and Style*, Columbus, Ohio: American Ceramic Society (Vol. 2).
- Knox, R. (1963) Detection of Iron Carbide Structure in the Oxide Remains of Ancient Steel. *Archaeometry* 6, 43-45.
- van der Kooij, G. and Ibrahim, M.M. (1989) *Picking Up the Threads: a Continuing Review of Excavations at Deir 'Alla, Jordan*, Leiden: Leiden University, Archaeological Centre.
- Košak, S. (1982) *Hittite Inventory Texts (Catalogue des Textes Hittites CTH) 241-250*, Heidelberg: Carl Winter Verlag.
- Košak, S. (1986) The Gospel of Iron. In: Hoffner, H.A. and Beckman, G.M. (Eds) *Kaniššuar. A Tribute to Hans G. Güterbock on His Seventy-Fifth Birthday, May 27, 1983*, 125-135. Chicago: The Oriental Institute.
- Kresten, P. and Hjärthner-Holdar, E. (2001) Analyses of the Swedish Ancient Iron Reference Slag W-25:R. *Historical Metallurgy* 35 (1), 48-51.
- Kronz, A. (1998) *Phasenbeziehungen Und Kristallisationsmechanismen in Fayalitischen Schmelzsystemen. Untersuchungen an Eisen- Und Buntmetallschlacken*, Bielefeld: Friedland.
- Kuhn, S.L. (2004) Evolutionary Perspectives on Technology and Technological Change. *World Archaeology* 36 (4), 561-570.
- Kusimba, C.M. (1996) The Social Context of Iron Forging on the Kenya Coast. *Africa* 66 (3), 386-410.
- LaBianca, Ø.S. and Younger, R.W. (1998) The Kingdoms of Ammon, Moab and Edom: the Archaeology of Society in Late Bronze/Iron Age Transjordan (Ca. 1400-500 BCE). In: Levy, T.E. (Ed.) *The Archaeology of Society in the Holy Land*, 2nd edn., 399-415. London: Leicester University Press.
- Landmann, G., Abu Qudaira, G.M., Shawabkeh, K., Wrede, V. and Kempe, S. (2002) Geochemistry of the Lisan and Damya Formation in Jordan, and Implications for Paleoclimate. *Quaternary International* 89 (1), 45-57.
- Lechtman, H. (1977) Style in Technology -- Some Early Thoughts. In: Lechtman, H. and Merrill, R.S. (Eds) *Material Culture: Styles, Organization, and Dynamics*, 3-20. St Paul: American Ethnological Society/West Publishing.
- Lechtman, H. (1988) Traditions and Style in Central Andean Metalworking. In: Maddin, R. (Ed.) *The Beginning of the Use of Metals and Alloys*, 344-378. Cambridge, MA: MIT Press.



- Lechtman, H. and Steinberg, A. (1979) The History of Technology: An Anthropological Point of View. In: Bugliarello, G. and Doner, D.B. (Eds) *The History and Philosophy of Science*, 135-162. Urbana, Illinois: University of Illinois Press.
- Lemonnier, P. (1986) The Study of Material Culture Today: Toward an Anthropology of Technical Systems. *Journal of Anthropological Archaeology* 5, 147-186.
- Lemonnier, P. (1989a) Bark Capes, Arrowheads and Concorde: On Social Representations of Technology. In: Hodder, I. (Ed.) *The Meaning of Things. Material Culture and Symbolic Expression*, 156-171. Boston, Massachusetts: Unwin Hyman.
- Lemonnier, P. (1989b) Towards an Anthropology of Technology. *Man* 24 (3), 526-527.
- Lemonnier, P. (1990) Topsy Turvy Techniques: Remarks on the Social Representation of Techniques. *Archaeological Review from Cambridge* 9 (1), 27-37.
- Lemonnier, P. (1992) *Elements for an Anthropology of Technology*, Ann Arbor, Michigan: University of Michigan; Anthropological Paper 88.
- Lemonnier, P. (1993a) Introduction. In: Lemonnier, P. (Ed.) *Technological Choices: Transformation in Material Cultures Since the Neolithic*, 1-35. London: Routledge.
- Lemonnier, P. (1993b) *Technological Choices: Transformation in Material Cultures Since the Neolithic*, London: Routledge.
- Lemonnier, P. and Pfaffenberger, B. (1989) Towards an Anthropology of Technology. *Man* 24 (3), 526-527.
- Leroi-Gourhan, A. (1957) Le Comportement Technique Chez l'Animal et Chez l'Homme. In: Leroi-Gourhan, A. (Ed.) *L'Evolution Humaine*, Paris: Flammarion.
- Lévi-Strauss, C. (1966) *The Savage Mind*, Chicago: University of Chicago Press.
- Lévi-Strauss, C. (1976) *Structural Anthropology (Vol. II)*, New York, New York: Basic Books.
- Lévi-Strauss, C. (1983) *Le Regard Éloigné*, Paris: Plon.
- Levy, J. (1991) Metalworking Technology and Craft Specialization in Bronze Age Denmark. *Archaeomaterials* 5 (1), 55-74.
- Liebowitz, H. (1981) Excavations at Tel Yin'Am: The 1976 and 1977 Seasons. Preliminary Report. *Bulletin of the American Schools of Oriental Research* 243, 79-94.
- Liebowitz, H. (1983) Reply to Beno Rothenberg. *Bulletin of the American Schools of Oriental Research* 252, 71-72.
- Liebowitz, H. and Folk, R.L. (1980) Archeological Geology of Tel Yin'Am, Galilee, Israel. *Journal of Field Archaeology* 7 (1), 23-42.
- Liebowitz, H. and Folk, R.L. (1984) The Dawn of Iron Smelting in Palestine: The Late Bronze Age Smelter at Tel Yin'Am, Preliminary Report. *Journal of Field Archaeology* 11 (3), 265-280.
- Loud, G. (1936) *Khorsabad I: Excavations in the Palace and at a City Gate*, Chicago: Oriental Institute Publications 38.
- Lucas-Tooth, H.J. and Pyne, C. (1964) The Accurate Determination of Major Constituents by X-Ray Fluorescence Analysis in the Presence of Large Inter-element Effects. *Advanced X-Ray Analysis* 7, 523-541.

- Luciani, M., Zaghis, F., Salviulo, G., Calliari, I., and Ramous, E. (2003), *Iron Age metallurgy: A Preliminary Study of Slags from Tell Shiukh Fawqani (Northern Syria)*. In: *Archaeometallurgy in Europe*. Vol. 2, 499-505. Milan: Associazione Italiana di Metallurgia.
- Maandag, F.L.A. and Macksoud, S.W. (1969) Annex C: Soils and Drainage. In: Maandag, F.L.A. and Macksoud, S.W. (Eds) *Jordan Valley Project: Agro- and Socio-Economic Study, Final Report*, 1-43. Amman, Jordan: The Hashemite Kingdom of Jordan - Jordan River and Tributaries Regional Corporation/Dar al-Handasah Consulting Engineers/Netherlands Engineering Consultants (NEDECO).
- MacKenzie, D. (1914) *Excavations at Ain Shems (Beth-Shemesh)*, London: Harrison and Sons.
- MacKenzie, J.M. (1975) Pre-Colonial Industry: the Njanja and the Iron Trade. *NADA* 11 (2), 200-220.
- Maddin, R. (1988) *The Beginning of the Use of Metals and Alloys*, Cambridge, MA: MIT Press.
- Mahé-le Carlier, C., Dieudonné-Glad, N. and Ploquin, A. (1998) Des Laitiers Obtenus dans un Bas-Fourneau? Études Chimiques et Minéralogiques des Scories du Site D'Oulches (Indre). *Revue d'Archéométrie* 22, 91-101.
- Mascelloni, M.L. (2004) *Testing the Evidence for Local Metalworking. Metals, Slag and Vitriified Materials From Tell Es-Sa'ldiyeh, Jordan*, London: University College London, Institute of Archaeology, unpublished MA thesis.
- Materials Science on CD-ROM version 2.1. MATTER ( 2000) 2.1. Liverpool: The University of Liverpool.
- Mauss, M. (1923) Essai sur le Don. *Sociologie et Anthropologie*, 150-151.
- Mauss, M. (1935) Les Techniques du Corps. *Journal de Psychology* 32, 271-293.
- McDonnell, G. (1983) Tap Slags and Hearth Bottoms, or, How to Identify Slags. *Current Archaeology* 86, 81-83.
- McGovern, P.E. (1986) *The Late Bronze and Early Iron Ages of Central Transjordan: The Baq'Ah Valley Project, 1977-1981*, Philadelphia, Pennsylvania: The University Museum, University of Pennsylvania.
- McGovern, P.E. (1989) Ancient Ceramic Technology and Stylistic Change. In: Henderson, J. (Ed.) *Scientific Analysis in Archaeology and Its Interpretation*, 63-81. Oxford; Los Angeles, CA: Oxford University Committee for Archaeology, Monograph 19; UCLA, Institute of Archaeology; Archaeological Research Tools 5.
- Merkel, J.F. and Barrett, K. (2000) 'The Adventitious Production of Iron in the Smelting of Copper' Revisited: Metallographic Evidence Against a Tempting Model. *Historical Metallurgy* 34 (2), 59-66.
- Merrill, R.S. (1968) The Study of Technology. In: Sills, D.L. (Ed.) *International Encyclopedia of the Social Sciences; Vol 15*, New York: MacMillan/Free Press.
- Merrill, S. (1881) *East of the Jordan: a Record of Travel and Observation in the Countries of Moab, Gilead and Bashan*, London.
- van der Merwe, N.J. and Scully, R.T.K. (1971) The Phalaborwa Story: Archaeological and Ethnographic Investigations of a South African Iron Age Group. *World Archaeology*

- 3 (2, Archaeology and Ethnography), 178-196.
- Miller, D.E. and van der Merwe, N.J. (1994) Early Metal Working in Sub-Saharan Africa: A Review of Recent Research. *Journal of African History* 35 (1), 1-36.
- Miller, D.E., Killick, D.J. and van der Merwe, N.J. (2001-2002) Metal Working in the Northern Lowveld, South Africa, A.D. 1000-1890. *Journal of Field Archaeology* 28 (3/4), 401-417.
- Morton, G.R. and Wingrove, J. (1969) Constitution of Bloomery Slags: Part I-Roman. *Journal of the Iron and Steel Institute* 207, 1556-1564.
- Morton, G.R. and Wingrove, J. (1972) Constitution of Bloomery Slags: Part II-Medieval. *Journal of the Iron and Steel Institute* 210, 478-488.
- Muhly, J.D. (1980) The Bronze Age Setting. In: Wertime, T.A. and Muhly, J.D. (Eds) *The Coming of the Age of Iron*, 25-67. New Haven; London: Yale University Press.
- Muhly, J.D. and Maddin, R. (1981) The Role of Cyprus in the Development of Iron Technology, Ca. 1200-900 BC. *American Journal of Archaeology* 85 (2), 208
- Muhly, J.D., Maddin, R., and Karageorghis, V. (1982) *Early Metallurgy in Cyprus. 4000-500 BC*, Larnaca.
- Notis, M.R. (2002) A Ghost Story: Remnant Structures in Corroded Ancient Iron Objects. In: Vandiver, P.B., Goodway, M., and Mass, J.L. (Eds) *Materials Issues in Art and Archaeology VI*, 259-267. Warrendale, PA: Materials Research Society Symposium Series on Materials Issues in Art & Archaeology, 712.
- Ortner, S.B. (1984) Theory in Anthropology Since the Sixties. *Comparative Studies in Society and History* 26 (1), 126-166.
- Orton, C. (2000) *Sampling in Archaeology*, Cambridge: Cambridge University Press.
- Paynter, S. (2005) Regional Variations in Bloomery Smelting Slag of the Iron Age and Romano-British Periods. *Archaeometry* (In Press).
- Pétrequin, P., Fluzin, P., Thiriot, J., and Benoit, P. (2000) *Arts du Feu et Productions Artisanales (XXe Rencontres Internationales D'Archéologie et D'Histoire D'Antibes)*, Antibes: Editions APDCA.
- Pfaffenberger, B. (1988b) Fetishised Objects and Humanised Nature: Towards an Anthropology of Technology. *Man* 23 (2), 236-252.
- Pfaffenberger, B. (1992) Social Anthropology of Technology. *Annual Review of Anthropology* 21, 491-516.
- Pigott, V.C. (1977) The Question of the Presence of Iron in the Iron I Period in Western Iran. In: Levine, L.D. and Young, Jr.T.C. (Eds) *Mountains and Lowlands. Essays in the Archaeology of Greater Mesopotamia*, 209-234. Malibu.
- Pigott, V.C. (1980) The Iron Age in Western Iran. In: Wertime, T.A. and Muhly, J.D. (Eds) *The Coming of the Age of Iron*, 417-461. New Haven; London: Yale University Press.
- Pigott, V.C. (1983) The Innovation of Iron (As Steel) in Palestine. *American Journal of Archaeology* 87 (2), 252
- Pigott, V.C. (1989a) Archaeo-Metallurgical Investigations at Bronze Age Tappeh Hesar,

1976. In: Dyson, R.H. and Howard, S.M. (Eds) *Tappeh Hesar. Reports of the Restudy Project, 1976*, 25-34. Florence.
- Pigott, V.C. (1989b) The Emergence of Iron Use at Hasanlu. *Expedition* 31 (2-3), 67-79.
- Pigott, V.C. (2003) Iron and Pyrotechnology at 13th Century -Late Bronze Age- Tel Yin'Am (Israel): a Reinterpretation. In: Stöllner, Th., Körlin, G., Steffens, G., and Cierny, J. (Eds) *Man and Mining - Mensch Und Bergbau. Studies in Honour of Gerd Weisgerber, on Occasion of His 65th Birthday*, 365-375. Bochum: Deutsches Bergbau Museum.
- Pigott, V.C., Howard, S.M. and Epstein, S.M. (1982a) Pyrotechnology and Culture Change at Bronze Age Tepe Hissar (Iran). In: Wertime, T.A. and Wertime, S.F. (Eds) *Early Pyrotechnology. The Evolution of the First Fire-Using Industries*, 215-236. Washington D.C.: Smithsonian Institution Press.
- Pigott, V.C., McGovern, P.E. and Notis, M.R. (1982b) The Earliest Steel From Transjordan. *Journal of the Museum Applied Science Center for Archaeology* 2 (2), 35-39.
- Pleiner, R. (1969) *Iron Working in Ancient Greece*, Praha: Archeologický Ústav Av Cr.
- Pleiner, R. (2000) *Iron in Archaeology. The European Bloomery Smelters*, Praha: Archeologický Ústav Av Cr.
- Pleiner, R. and Bjorkman, J.K. (1974) The Assyrian Iron Age: The History of Iron in the Assyrian Civilization. *Proceedings of the American Philosophical Society* 118 (3), 283-313.
- Pleiner, R., Fluzin, P., Mangin, M., Dillmann, P., Billon, M. and Rabeisen, E. (2002) Lingots et Couteaux en Fer d'Alésia: Études Archéométriques. *Revue archéologique de l'Est*
- Ploquin, A. (1993) A Propos des Scories Légères et Laitiers Associés aux Déchets Paléosidéurgiques en France: Quelques Apports de la Base de Données Artémise-Scories. In: Espelund, A. (Ed.) *Bloomery and Ironmaking During 2000 Years. Seminar "in Honorem Ole Evenstand". III. International Contributions. Smelting and Excavation in Budalen*, 91-103. Budalen, Sor-Trondelag: Comité pour la Sidérurgie Ancienne de l'UISPP.
- Posnansky, M. and McIntosh, R.J. (1976) New Radiocarbon Dates for Northern and Western Africa. *Journal of African History* 17 (2), 161-195.
- Reber, S.C. and Smith, M.R. (1986) Contextual Contrasts: Recent Trends in the History of Technology. In: Kingery, W.D. (Ed.) *Technology and Style. Ceramics and Civilization: Ancient Technology to Modern Science*, 1-15. Columbus, Ohio: American Ceramic Society (Vol. 2).
- Reed-Hill, R.E. (1973) *Physical Metallurgy Principles*, 2 edn. Monterey, CA: Brooks/Cole, University Series in Basic Engineering.
- Reifenberg, A. and Whittles, C.A. (1947) *The Soils of Palestine*, London: Thomas Murby Co.
- Rice, P.M. (1981) The Evolution of Specialized Pottery Production: A Trial Model. *Current Anthropology* 22 (3), 219-240.
- Rostoker, W. and Bronson, B. (1990) *Pre-Industrial Iron, Its Technology and Ethnology*, Philadelphia, Pennsylvania: Archeomaterials Monograph 1, Rostoker Inc. (privately published).
- Rothenberg, B. (1983) Corrections on Timna and Tel Yin'am in the Bulletin. *Bulletin of the*

*American Schools of Oriental Research* 252, 69-70.

- Rothenberg, B. (1990) Copper Smelting Furnaces, Tuyeres, Slags, Ingot-Moulds and Ingots in the Arabah: The Archaeological Data. In: Rothenberg, B. (Ed.) *The Ancient Metallurgy of Copper. Archaeology-Experiment-Theory*, 1-77. London: Institute for Archaeo-Metallurgical Studies, Institute of Archaeology, University College London.
- Rothenberg, B. and Tylecote, R.F. (1991) A Unique Assyrian Iron Smithy in the Northern Negev (Israel). *IAMS* 17, 11-14.
- Routledge, B. (2000) The Politics of Mesha: Segmented Identities and State Formation in Iron Age Moab. *Journal of the Social and Economic History of the Orient* 43 (3), 221-256.
- Routledge, B. (2004) *Moab in the Iron Age: Hegemony, Polity, Archaeology*, Philadelphia: University of Pennsylvania.
- Rowlands, M.J. (1971) The Archaeological Interpretation of Prehistoric Metalworking. *World Archaeology* 3, 210-223.
- Schiffer, M.B. (2001) Toward an Anthropology of Technology. In: Schiffer, M.B. (Ed.) *Anthropological Perspectives on Technology*, 1-15. Albuquerque: University of New Mexico Press.
- Schiffer, M.B. (2004) Studying Technological Change: a Behavioral Perspective. *World Archaeology* 36 (4), 579-585.
- Schiffer, M.B. and Skibo, J.M. (1987) Theory and Experiment in the Study of Technological Change. *Current Anthropology* 28 (5), 595-622.
- Schramm, R. (1998) *Chemometrische Und Gerätetechnische Weiterentwicklungen in Der Energiedispersiven Röntgenfluoreszenzanalyse Mit Polarisierter Röntgenstrahlung ED(P)RFA*, Duisburg: Gerhard Mercator Universität, Dissertation.
- Schramm, R. (undated a) *Why Using XRF for Analysis?* Kleve: Spectro Analytical Instruments (instrument documentation).
- Schramm, R. (undated b) *XRF Fundamentals*, Kleve: Spectro Analytical Instruments (instrument documentation).
- Scott, D.A. (1991) *Metallography and Microstructure of Ancient and Historic Metals*, Marina del Rey, California: The Getty Conservation Institute.
- Serneels, V. (1993) *Archéométrie des Scories de Fer. Recherches sur la Sidérurgie Ancienne en Suisse Occidentale*, Lausanne: Cahiers d'archéologie romande 61.
- Serneels, V. and Crew, P. (1997) Ore-Slag Relationships from Experimentally Smelted Bog-Iron Ore. In: Crew, P. and Crew, S. (Eds) *Early Ironworking in Europe: Archaeology and Experiment*, 78-82. Maentwrog: Plas Tan y Bwlch Occasional Paper 3.
- Serneels, V. and Perret, S. (2003), *Quantification of Smithing Activities based on the Investigation of Slag and Other Material Remains*. In: Proceedings of the International Conference Archaeometallurgy in Europe. Vol. 1, 469-479. Milano: Associazione Italiana di Metallurgia.
- Shennan, S. (1997) *Quantifying Archaeology*, 2nd edn. Iowa City: University of Iowa Press.
- Sherratt, S. (1994), *Commerce, iron and ideology: Metallurgical innovation in 12th-11th century Cyprus*. In: Karageorghis, V., (Ed.) Proceedings of the International

- Symposium Cyprus in the 11th Century B.C., 30-31 October 1993, Nicosia. Nicosia: University of Cyprus.
- Siegelová, J. (1984) Gewinnung Und Verarbeitung Von Eisen Im Hethitischen Reich Im 2. Jahrtausend V. U. Z. *Annals of the Náprstek Museum* 12, 71-168.
- Siegelová, J. (2005) Metalle in Hethitischen Texten. In: Yalçin, Ü. (Ed.) *Anatolian Metal III*, 35-40. Bochum: Deutsches Bergbau-Museum.
- Sillar, B. and Tite, M.S. (2000) The Challenge of 'Technological Choices' for Materials Science Approaches in Archaeology. *Archaeometry* 42, 2-20.
- Singer, C.J., Holmyard, E.J., Hall, M.R., and Williams, T.I. (1954-1958) *A History of Technology (5 Volumes)*, Oxford: Clarendon Press.
- Smith, R.H., Maddin, R., Muhly, J.D. and Stech-Wheeler, T. (1984) Bronze-Age Steel From Pella, Jordan. *Current Anthropology* 25 (2), 234-236.
- Snodgrass, A.M. (1980) Iron and Early Metallurgy in the Mediterranean. In: Wertime, T.A. and Muhly, J.D. (Eds) *The Coming of the Age of Iron*, 335-374. New Haven; London: Yale University Press.
- Spectro Analytical Instruments (undated) *Spectro Calibration Manual*, Kleve: Spectro Analytical Instruments.
- Sperl, G. (1980) *Über Die Typologie Urzeitlicher, Frühgeschichtlicher Und Mittelalterlicher Eisenhüttenschlacken*, Wien: Österreichische Akademie der Wissenschaften.
- Stanway, T. (2003) *An Analysis of the Experimental Smelts XP90 and XP91 From Plas Tan Y Bwlch, Using Reflected Light Microscopy and XRF Analysis*, London: University College London, Institute of Archaeology, unpublished MSc Thesis.
- Staudenmaier, J.M. (1985) *Technology's Storytellers: Reweaving the Human Fabric*, Cambridge: The Society for the History of Technology and The MIT Press.
- Stech-Wheeler, T., Muhly, J.D., Maxwell-Hyslop, K.R. and Maddin, R. (1981) Iron at Taanach and Early Iron Metallurgy in the Eastern Mediterranean. *American Journal of Archaeology* 85 (3), 245-268.
- van der Steen, E.J. (2003) *Tribes and Territories in Transition: the Central East Jordan Valley and Surrounding Regions in the Late Bronze and Early Iron Ages: a Study of the Sources.*, Groningen: Rijksuniversiteit Groningen.
- Stein, M., Starinsky, A., Katz, A., Goldstein, S.L., Machlus, M. and Schramm, A. (1997) Strontium Isotopic, Chemical, and Sedimentological Evidence for the Evolution of Lake Lisan and the Dead Sea. *Geochimica et Cosmochimica Acta* 61, 3975-3992.
- Stenvik, L.F. (2003) Iron Production in Scandinavian Archaeology. *Norwegian Archaeological Review* 36 (2), 119-134.
- Stern, W.B. and Gerber, Y. (2004) Potassium-Calcium Glass: New Data and Experiments. *Archaeometry* 46 (1), 137-156.
- Steuernagel, D.C. (1925) Der 'Adschlun. Nach Den Aufzeichnungen Von Dr. G. Schumacher. *ZDPV* 48, 201-392.
- van Strydonck, M., Nelson, D.E., Crombé, P., Bronk Ramsey, C., Scott, E.M., van der Plicht, J., and Hedges, R.E.M. (1999), *What's in a 14C Date*. In: 14C et

- Archéologie. Actes du 3e congrès international (Lyon 6-10 avril 1998). Vol. Rapport du Groupe de travail: Les limites de méthode du carbone 14 appliquée à l'archéologie, 433-440. Rennes: Mémoires de la Société Préhistorique Française, XXVI, 1999 et Supplément 1999 de la Revue d'Archéométrie.
- Stuiver, M. and van der Plicht, J. (1998) INTCAL98 Editorial Comment. *Radiocarbon (INTCAL98, Calibration Issue)* 40 (3), xii -xiii
- Stuiver, M., Reimer, P.J., Bard, E., Beck, J.W., Burr, G.S., Hughen, K.A., Kromer, B., McCormac, G., van der Plicht, J. and Spurk, M. (1998) INTCAL98 Radiocarbon Age Calibration, 24,000-0 Cal BP. *Radiocarbon (INTCAL98, Calibration Issue)* 40 (3), 1041-1084.
- Tabor, G.R., Molinari, D. and Juleff, G. (2005) Computational Simulation of Air Flows Through a Sri Lankan Wind-Driven Furnace. *Journal of Archaeological Science* 32 (5), 753-766.
- Tarawneh, M.F. (in press) *Rural Capitalist Development in the Jordan Valley: the Case of Deir 'Alla (the Rise and Demise of Social Groups)*, Leiden: CNWS.
- Trigger, B.G. (1986) The Role of Technology in V. Gordon Childe's Archaeology. *Norwegian Archaeological Review* 19 (1), 1-14.
- Trigger, B.G. (1989) *A History of Archaeological Thought*, Cambridge: Cambridge University Press.
- Tylecote, R.F. (1976) *A History of Metallurgy*, London: The Metals Society.
- Tylecote, R.F. (1987) *The Early History of Metallurgy in Europe*, London: Longman.
- Tylecote, R.F. (1992) *A History of Metallurgy*, London: Institute of Materials.
- Tylecote, R.F., Austin, J.N. and Wraith, A.E. (1971) The Mechanism of the Bloomery Process in Shaft Furnaces. *Journal of the Iron and Steel Institute* 209 (5), 342-363.
- Tylecote, R.F. and Merkel, J.F. (1992) Experimental Smelting Techniques: Achievements and Future. In: Craddock, P.T. and Hughes, M.J. (Eds) *Furnaces and Smelting Technology in Antiquity*, 3-20. London: British Museum.
- Veldhuijzen, H.A. (1998) *Early Iron Smelting. Analysis and Interpretation of Late Iron Age Iron Smelting Remains From Tell Hammeh Az-Zarqa, Jordan*, Leiden: Leiden University, Faculty of Archaeology, unpublished M.A. Thesis.
- Veldhuijzen, H.A. (2002) *Ethnography of Ironsmelting* [online]. Available from: <<http://www.ironsmelting.net/www/smelting/index.html>> Accessed July 01, 2005.
- Wade, J.A. (1989) The Context of Adoption of Brass Technology in Northeastern Nigeria and Its Effects on the Elaboration of Culture. In: van der Leeuw, S.E. and Torrence, R. (Eds) *What's New? A Closer Look at the Process of Innovation*, 225-244. London: Allen and Unwin.
- Waldbaum, J.C. (1978) *From Bronze to Iron, the Transition From the Bronze Age to the Iron Age in the Eastern Mediterranean*, Goteborg: Paul Astroms Forlag.
- Waldbaum, J.C. (1980) The First Archaeological Appearance of Iron and the Transition to the Iron Age. In: Wertime, T.A. and Muhly, J.D. (Eds) *The Coming of the Age of Iron*, 69-98. New Haven; London: Yale University press.



- Waldbaum, J.C. (1989) Copper, Iron, Tin, Wood, the Start of the Iron Age in the Eastern Mediterranean. *Archeomaterials* 3, 111-122.
- Waldbaum, J.C. (1999) The Coming of Iron in the Eastern Mediterranean. Thirty Years of Archaeological and Technological Research. In: Pigott, V.C. (Ed.) *The Archaeometallurgy of the Asian Old World*, 27-57. Pennsylvania: MASCA Research Papers in Science and Archaeology 16, University of Pennsylvania Museum.
- Wembah-Rashid, J.A.R. (1967) Iron Working in Ufipa. Dar-es-Salaam: National Museum of Tanzania. Film.
- Wembah-Rashid, J.A.R. (1969) Iron Workers in Ufipa. *Bulletin of the International Committee of Urgent Anthropological Research* 37, 425-452.
- Wembah-Rashid, J.A.R. (1973) *Iron Working in Ufipa. A Record of Traditional Processes of Iron Smelting and Forging Among the Fipa of Tanzania*, Dar-es-Salaam: National Museum of Tanzania.
- Wertime, T.A. and Muhly, J.D. (1980) *The Coming of the Age of Iron*, New Haven; London: Yale University Press.
- White, L.A. (1949) *The Science of Culture*, New York: Farrar Straus and Cudahy.
- White, L.A. (1962) *Medieval Technology and Social Change*, Oxford: Clarendon Press.
- Wise, R. (1958a) Iron Smelting in Ufipa. *Tanganyika Notes and Records* 51, 106-111.
- Wise, R. (1958b) Some Rituals of Iron Making in Ufipa. *Tanganyika Notes and Records* 51
- Worssam, B. and Gibson-Hill, J. (1976) Analyses of Wealden Iron Ores. *Historical Metallurgy* 10 (2), 77-82.
- Wright, G.E. (1939) Iron, the Date of Its Introduction to Palestine. *American Journal of Archaeology* 43, 458-463.
- Wright, R.A. (1985) Technology and Style in Ancient Ceramics. In: Kingery, W.D. (Ed.) *Ceramics and Civilization: Ancient Technology to Modern Science*, 5-26. Columbus, Ohio: American Ceramic Society (Vol. 1).
- Wright, R.A. (1986) The Boundaries of Technology and Stylistic Change. In: Kingery, W.D. (Ed.) *Ceramics and Civilization: Technology and Style*, 1-20. Columbus, Ohio: American Ceramic Society (Vol. 2).
- Yalçın, Ü. (1998) Frühe Eisenverwendung in Anatolien. *Istanbuler Mitteilungen* 48, 79-95.
- Yunker, R.W. (1997) Moabite Social Structure. *Biblical Archaeologist* 60 (4), 237-248.
- Zitzmann, A. (1977) *The Iron Ore Deposits of Europe and Adjacent Areas*, Hannover; Stuttgart: Bundesanstalt für Geowissenschaften und Rohstoffe.
- Zwicker, W. (1996) Pnuel. *Biblische Notizen* 85, 38-43.